

AD/A-001 738

ARL PRELIMINARY DATA ANALYSIS FROM
ACODAC SYSTEM ANALYSIS OF THE BLAKE
TEST ACODAC DATA

Glen E. Ellis, et al

Texas University at Austin

Prepared for:

Office of Naval Research

15 October 1974

DISTRIBUTED BY:

NTIS

National Technical Information Service
U. S. DEPARTMENT OF COMMERCE

Best Available Copy

AD/A 001 738

20 JULY 1973
REVISED 15 OCTOBER 1974

ARL-TM-73-11 ARL PRELIMINARY DATA ANALYSIS FROM ACODAC SYSTEM
ARL-TM-73-12 ANALYSIS OF THE BLAKE TEST ACODAC DATA

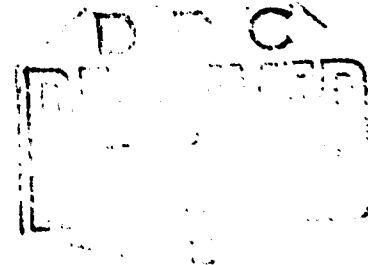
Glen E. Ellis, Terry D. Plemons
Loyd D. Hampton, Jack A. Shooter

OFFICE OF NAVAL RESEARCH
Contract N00014-70-A-0166, Task 0016

Reproduced by
NATIONAL TECHNICAL
INFORMATION SERVICE
U.S. Department of Commerce
Springfield, VA. 22151

APPLIED RESEARCH LABORATORIES
THE UNIVERSITY OF TEXAS AT AUSTIN
AUSTIN, TEXAS 78712

This Document Contains
Missing Page/s That Are
Unavailable In The
Original Document



ABSTRACT

These technical memoranda (ARL-TM-73-11 and ARL-TM-73-12) describe two analyses of ACODAC data tapes. The first memorandum contains the initial or preliminary analysis of an ACODAC performed at ARL. Data generated by four types of sources--ambient noise, cw source, vibroseis source, and shot (explosive) source--were analyzed. The second memorandum describes the analysis performed and results obtained at ARL in support of the Test Director for the Blake Test to evaluate ACODAC system self-noise effects on system performance.

Preceding page blank

TABLE OF CONTENTS

	<u>Page</u>
ABSTRACT	iii
LIST OF ILLUSTRATIONS	vii
LIST OF TABLES	x
I. ARL PRELIMINARY DATA ANALYSIS FROM ACODAC SYSTEM (ARL-TM-73-11)	1
A. Introduction	1
B. Playback System and Procedures	1
C. Ambient Noise	4
D. Calibration	8
E. Vibroseis	8
F. cw Sources	12
1. Spectral Analysis	12
2. Adaptive Spectra Estimation	19
G. Validation of Data	19
H. Digitization and Analysis of Shot Data	21
I. Intensity Spectrum of Shot Data	30
J. Estimation of Signal-to-Noise Ratio	30
II. ANALYSIS OF THE BLAKE TEST ACODAC DATA (ARL-TM-73-12)	1
A. Blake Test Analysis	1
1. Introduction	1
2. Data Reduction Procedures	1
3. Analysis Constraints	1
4. Data Tape Quality	2
B. ACODAC Calibration Analysis	3
1. Purpose	3
2. Data Reduction Procedures	3
3. Spectral Analysis	3

Preceding page blank

TABLE OF CONTENTS (Cont'd)

	<u>Page</u>
C. Ambient Noise Analysis	13
1. Data Analyzed	13
2. Data Reduction Procedures	13
3. Spectra	15
D. Strumming Analysis	15
1. Purpose	15
2. Data Reduction Procedures	15
3. Results	26
E. Shot Data Analysis	26
1. Introduction	26
2. Multipath Structure of Signals	32
3. Signal-to-Noise Ratio	32
4. Spectrum	48
APPENDIX A	51
APPENDIX B	61

LIST OF ILLUSTRATIONS

I. ARL PRELIMINARY DATA ANALYSIS FROM ACODAC SYSTEM (ARL-TM-73-11)

<u>Figure</u>	<u>Title</u>	<u>Page</u>
1	Applied Research Laboratories CDC 3200 Computer Configuration	2
2	ARL Data Reduction Facility	3
3	Ambient Noise Spectra	5
4	Ambient Noise Spectra	6
5	Ambient Noise Spectra	7
6	Ambient Noise Time Varying Spectra	9
7	ACODAC Calibration Signal Spectra	10
8	Vibroseis Source Time Varying Spectra	11
9	Vibroseis Source Time Varying Spectra	13
10	cw Source Spectra	14
11	cw Source Spectra	15
12	cw Source Spectra	16
13	cw Source Spectra	17
14	cw Source Time Varying Spectra	18
15	cw Source Adaptive Spectral Estimation	20
16	Test for Homogeneity Ambient and cw Source	22
17	Representative Computer Plots of Digital Shot Data	23
18	Representative Computer Plots of Digital Shot Data	24
19	Comparison of Structures of Received Shot Signals from Beginning and End of Data Sets	26
20	Detailed Comparison of Two Primary Arrivals from Shot Sources	27
21	Effect of Reduction in Sample Rate on Preservation of Waveform Structure	28
22	Comparison of the Waveform Structures of the Second Arrivals of the First Four Shots	29
23	Intensity Spectrum of the First Arrival of the Fourth Shot Sequence	31

LIST OF ILLUSTRATIONS (Cont'd)

<u>Figure</u>	<u>Title</u>	<u>Page</u>
24	Estimation of Shot Signal-to-Noise Ratio, S/N	33
25	Signal-to-Noise Ratio Estimates as Functions of Averaging Time of Noise	34

II. ANALYSIS OF THE BLAKE TEST ACODAC DATA (ARL-TM-73-12)

<u>Figure</u>	<u>Title</u>	<u>Page</u>
1	Calibration Spectra for WHOI Array - Hydrophone 1	4
2	Calibration Spectra for WHOI Array - Hydrophone 2	5
3	Calibration Spectra for WHOI Array - Hydrophone 3	6
4	Calibration Spectra for WHOI Array - Hydrophone 4	7
5	Calibration Spectra for WHOI Array - Hydrophone 5	8
6	Calibration Spectra for WHOI Array - Hydrophone 6	9
7	Calibration Spectra for UM Array - Hydrophone 6	10
8	Ambient Noise Spectra for WHOI Array - Hydrophone 1	16
9	1/3 Octave Spectra of Ambient Noise for WHOI Array - Hydrophone 1	17
10	Ambient Noise Spectra for WHOI Array - Hydrophone 2	18
11	Ambient Noise Spectra for WHOI Array - Hydrophone 3	19
12	Ambient Noise Spectra for WHOI Array - Hydrophone 4	20
13	Ambient Noise Spectra for WHOI Array - Hydrophone 5	21
14	Ambient Noise Spectra for WHOI Array - Hydrophone 6	22
15	Ambient Noise Spectra for UM Array - Hydrophone 6	23
16	Time Varying Spectra for WHOI Hydrophone 1	26
17	Time Varying Spectra for WHOI Hydrophone 2	27
18	Time Varying Spectra for WHOI Hydrophone 3	28
19	Time Varying Spectra for WHOI Hydrophone 4	29
20	Time Varying Spectra for WHOI Hydrophone 5	30

LIST OF ILLUSTRATIONS (Cont'd)

<u>Figure</u>	<u>Title</u>	<u>Page</u>
21	Time Varying Spectra for WHOI Hydrophone 6	31
22	Amplitude versus Time, Digitized Record 4-Shot Sequence, 10 mile Range, 300 ft Shot Depth, WHOI Hydrophone 1, First Half	33
23	Amplitude versus Time, Digitized Record 4-Shot Sequence, 10 mile Range, 300 ft Shot Depth, WHOI Hydrophone 1, First Half	34
24	Amplitude versus Time Record of Two Shots Showing Multipath Arrivals, 10 mile Range, WHOI Hydrophone 1	35
25	Estimation of Shot Signal-to-Noise Ratio (S/N)	36
26	Shot Signal and Signal-to-Noise Ratio	39
27	Signal-to-Noise Ratio of Shot Data as a Function of WHOI Hydrophone Number	40
28	Signal-to-Noise Ratio of Shot Data as a Function of WHOI Hydrophone Number	41
29	Signal-to-Noise Ratio of Shot Data as a Function of WHOI Hydrophone Number	42
30	Signal-to-Noise Ratio of Shot Data as a Function of WHOI Hydrophone Number	43
31	Variation of S/N with Range of Shot	44
32	Variation of S/N with Range of Shot	45
33	Variation of S/N with Range of Shot	46
34	Comparison of WHOI and Miami Hydrophone 6 Shot S/N	47
35	Shot Spectrum	49
36	Shot Spectrum	50

LIST OF TABLES

II. ANALYSIS OF THE BLAKE TEST ACODAC DATA (ARL-TM-73-12)

<u>Table</u>	<u>Title</u>	<u>Page</u>
I	Signal Level Check for the ACODAC Tapes	2
II	Calibration Spectra Labels	11
III	Calibration Spectral Levels in decibels	12
IV	Calibration Spectra Labels	14
V	Ambient Noise, Relative Spectral Levels in decibels	24
VI	Shot Pattern	26
VII	Signal-to-Noise Ratios: Shot Data	38

I. ARL PRELIMINARY DATA ANALYSIS FROM ACODAC SYSTEM (ARL-TM-73-11)

A. Introduction

The duplicate data tape from the ACODAC System used during the Church Gabbro Exercise was received at Applied Research Laboratories (ARL), The University of Texas at Austin, early on 11 June 1973. A preliminary analysis was conducted to demonstrate ARL's capabilities to handle data analysis of this type. The analysis was constrained by limited time, inability to read time code information and amplifier gain changes, and no log or record of the content of the data tape.

After examining the tape, the decision was made to isolate and analyze four different data segments containing ambient noise, continuous wave (cw) sources, shots, and the vibroseis source. Time permitted only the analysis of data from hydrophone number 3.

B. Playback System and Procedures

Figures 1 and 2 are block diagrams of the ARL computer and data reduction facility.

Since no log was provided with the data tape, it was necessary to search the tape to locate four different types of data for analysis. The analog data was played back at a speedup of 80:1 to locate different data segments for analysis. Simultaneous visual observations of the output of hydrophones 2 and 3, with an audio presentation of the output of hydrophone 3, enabled the operator to locate the data segments.

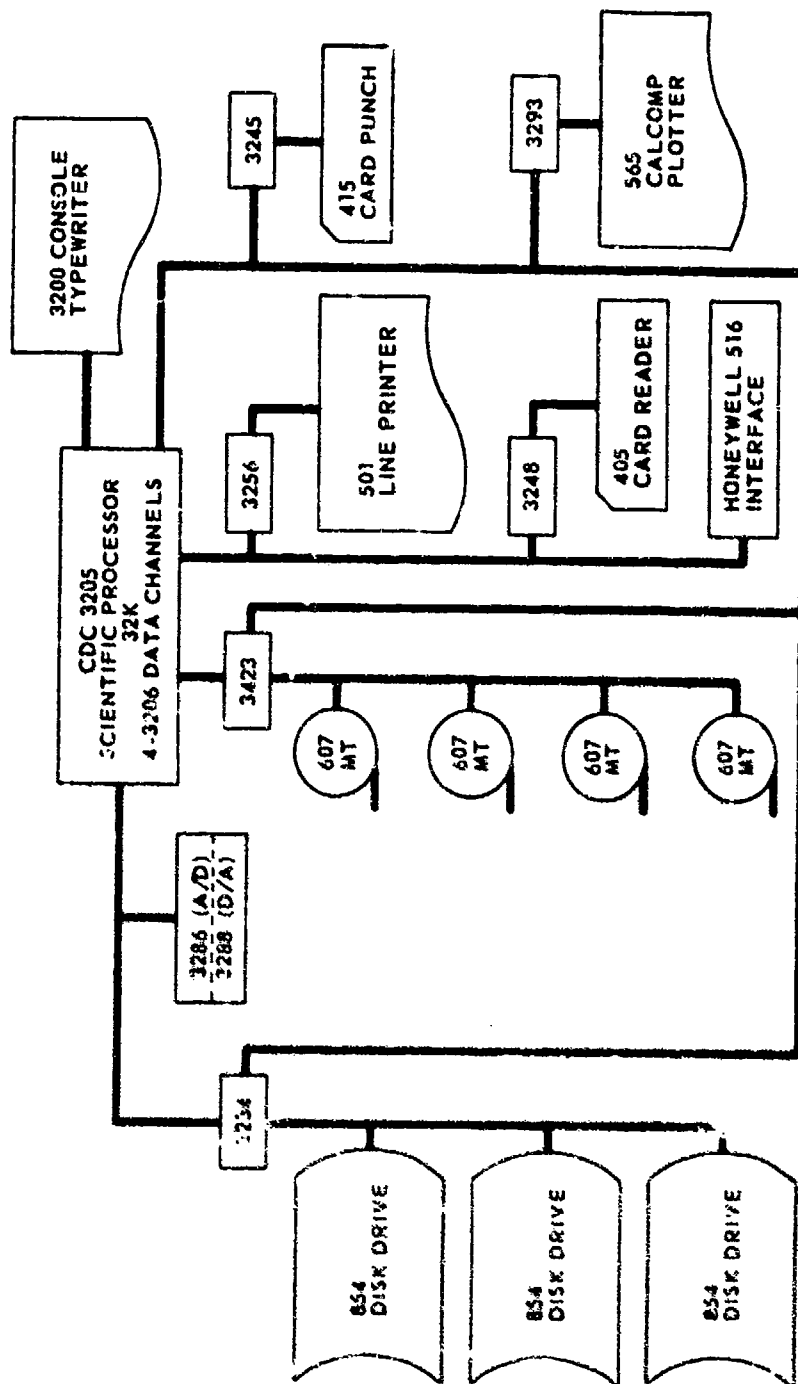


FIGURE 1
APPLIED RESEARCH LABORATORIES
CDC 3200 COMPUTER CONFIGURATION

ARL - UT
AS - 73 - 362
GEE - DR
S - 9 - 73

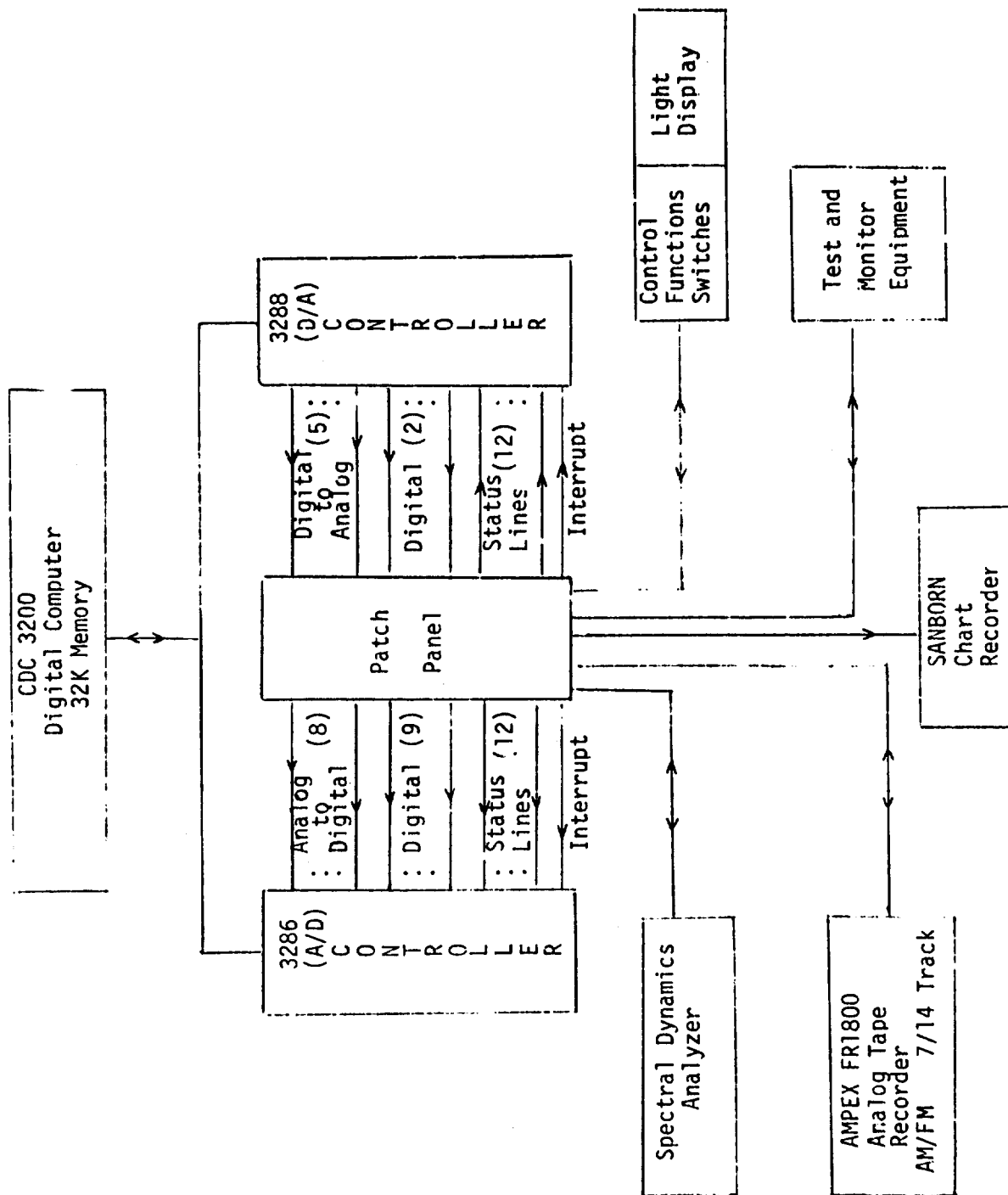


FIGURE 2
ARL DATA REDUCTION FACILITY

A Spectral Dynamics analyzer (500 line) was then used to examine the spectral characteristics of these data segments to identify ambient noise, cw sources, shots, and vibroseis source.

These data segments were passed through a 10 to 300 Hz (real time) filter to prevent aliasing and to eliminate extraneous low frequency playback system noise outside the frequency band of interest. The data were digitized at a 600 Hz (real time) rate in 8192 sample blocks and stored on digital tape. The 600 Hz sync signal for the A/D converter was obtained from the 12th harmonic of the 50 Hz carrier on the time code channel, thus eliminating wow and flutter induced by the recording/playback processes.

Additional data were processed via the Spectral Dynamics analyzer. The spectral lines computed by the analyzer were output to the digital computer and stored on digital tape.

The location in time, relative to the start of the data tape, of the data segments analyzed are approximate since no tape log was available. The estimated times were taken from the reel turn count of the playback recorder, which is not a linear system.

C. Ambient Noise

Figures 3, 4, and 5 are relative power spectra of three consecutive segments of ambient noise data with no amplifier gain changes observed visually. These data segments occurred toward the end of the first recording day. The data were digitized using the phase locked 600 Hz signal, spectra were computed with an FFT using a Hanning window, and the spectra were averaged to produce stable spectral estimates. Each spectrum covers a data block of 13.7 sec (8192 samples). The frequency resolution is 0.07 Hz. Each graph represents an average of 50 consecutive spectra or a real time interval of 11.4 min. The general spectra

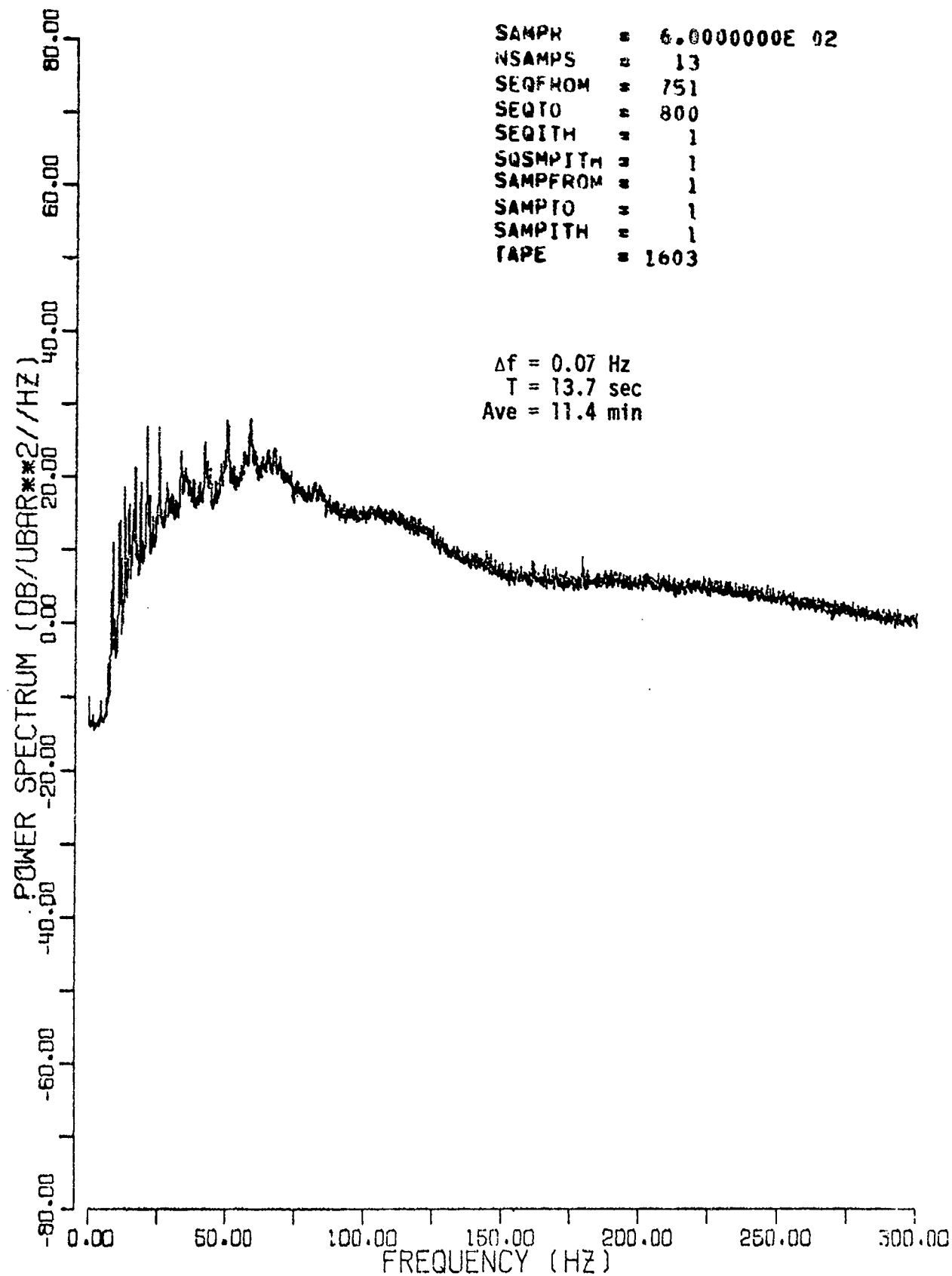


FIGURE 3
AMBIENT NOISE SPECTRA

ARL-UT
AS-74-1044
GEE
10-14-74

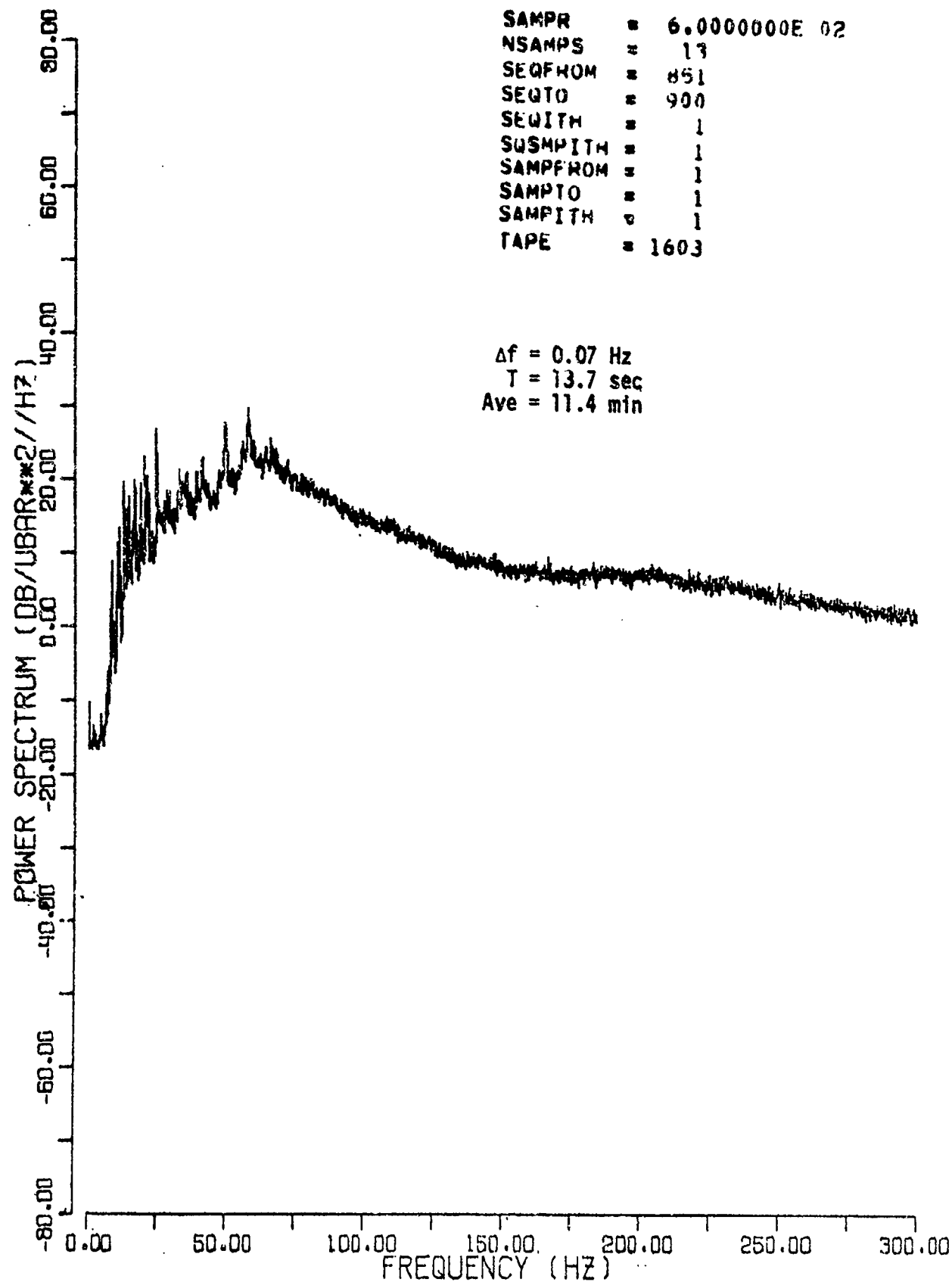


FIGURE 4
AMBIENT NOISE SPECTRA

ARL-UT
 AS-74-1045
 GEE
 10-14-74

OUTPUT FROM AVGPWRSP -

SAMPH = 6.0000000E 02
 NSAMPS = 13
 SEQFROM = 951
 SEQTO = 1000
 SEQITH = 1
 SQSMPITH = 1
 SAMPFROM = 1
 SAMPTO = 1
 SAMPITH = 1
 TAPE = 1003

$\Delta f = 0.07$ Hz
 T = 13.7 sec
 Ave = 11.4 min

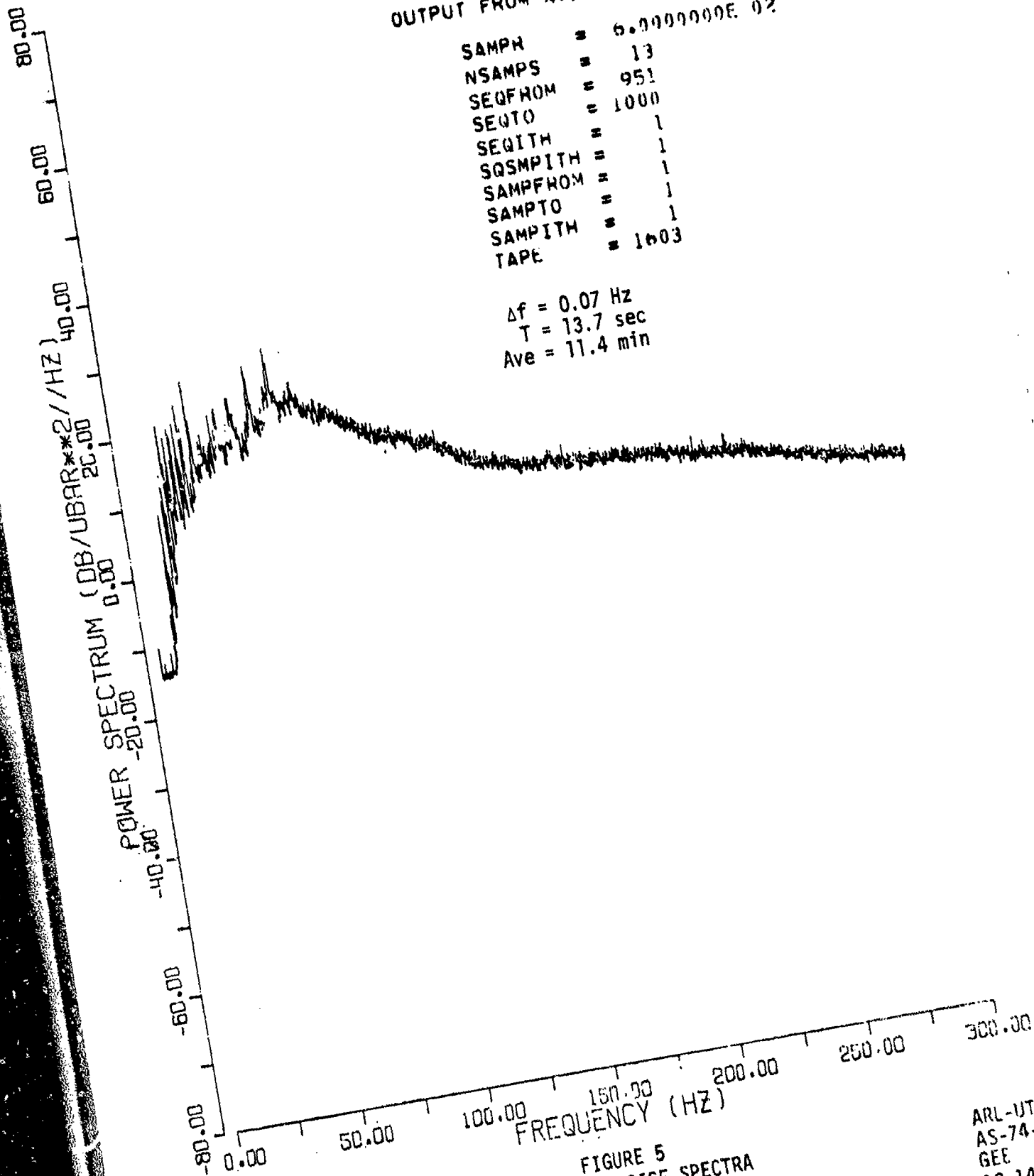


FIGURE 5
 AMBIENT NOISE SPECTRA

ARL-UT
 AS-74-1046
 GEE
 10-14-74

shape remains consistent throughout the analysis sequence. The spectral lines between 25 and 75 Hz indicate the presence of a ship in the area. Figure 3, the beginning of the analysis sequence, shows a spectral increase of approximately 4 dB in the frequency range of 100 to 125 Hz.

Figure 6 is a time varying power spectra of a different data segment of ambient noise occurring near the end of the first recording day. The relative power spectra were computed by the Spectral Dynamics analyzer with a resolution of 0.75 Hz. The display shows the frequency markers from the analyzer for reference, the frequency spectra computed for the calibration signal recorded on the ACODAC tape, and the spectra of the ambient noise. Each time trace represents an average of four power spectra computed with a 2 sec data block. The lack of low frequency lines indicates no shipping present.

D. Calibration

Figure 7 is a spectral analysis of one of the calibration signals occurring every 6 h on the ACODAC recording system. This data segment occurred approximately 1 1/3 days into the recording. The data were digitized at a 600 Hz rate in 8192 samples/sequence for 18 sequences or in data blocks of 13.7 sec. The frequency resolution is 0.07 Hz. The total length of the data sequences is 4.2 min. A spectrum is computed for each sequence, and the sequences (18) are averaged to achieve stable estimates. The calibration signal appeared to be performing its proper function.

E. Vibroscis

Figure 8 is a display of the time varying relative linear power spectra of a sequence of vibroseis data occurring approximately 9 days from start of recording. The relative power spectra were computed with a Spectral Dynamics real time analyzer that produces 500 spectral lines with 0.75 Hz resolution. Each spectrum is computed for a 2 sec data

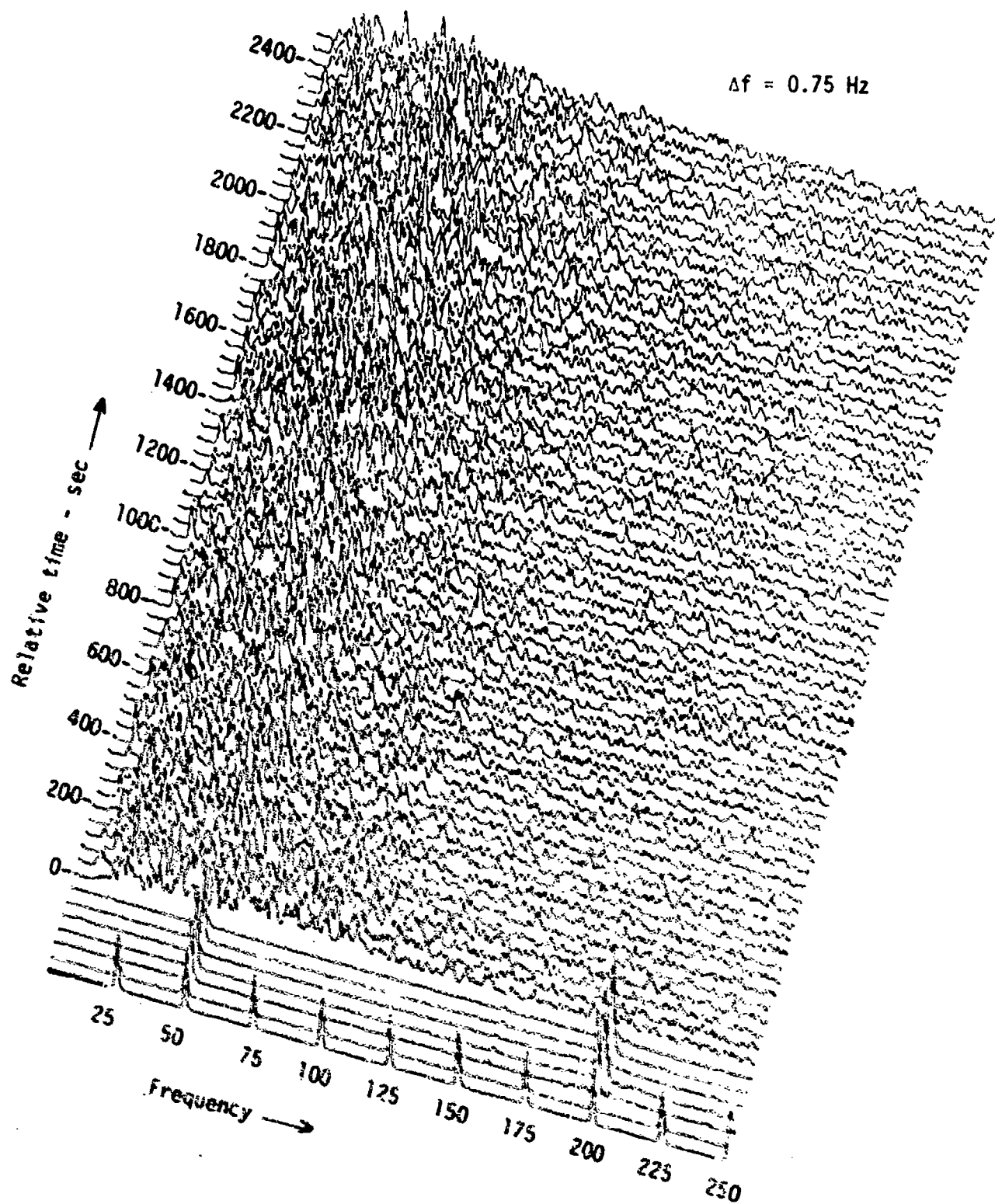


FIGURE 6
AMBIENT NOISE
TIME VARYING SPECTRA

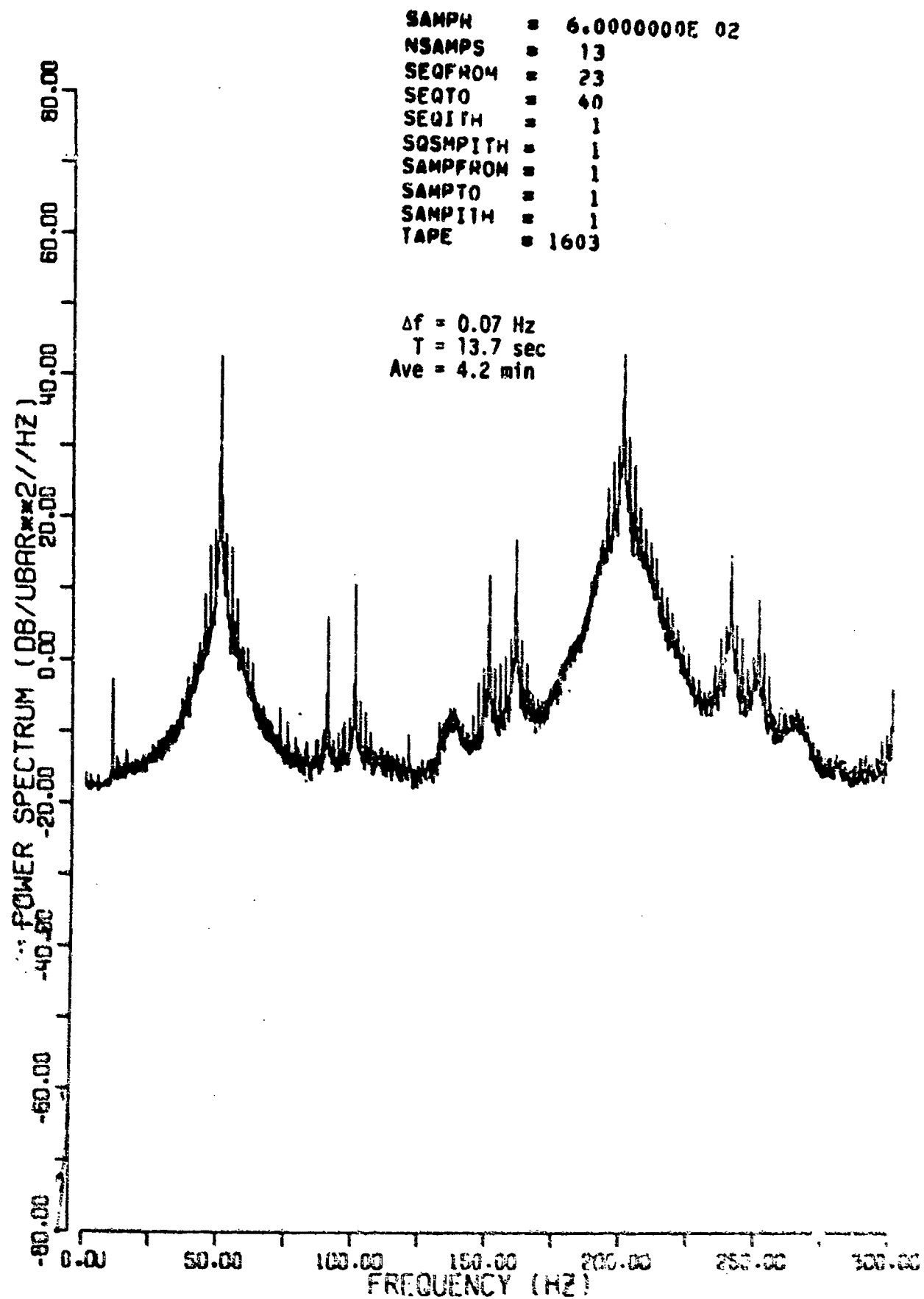


FIGURE 7
ACODAC CALIBRATION SIGNAL SPECTRA

ARL-UT
AS-74-1048
GEE
10-14-74

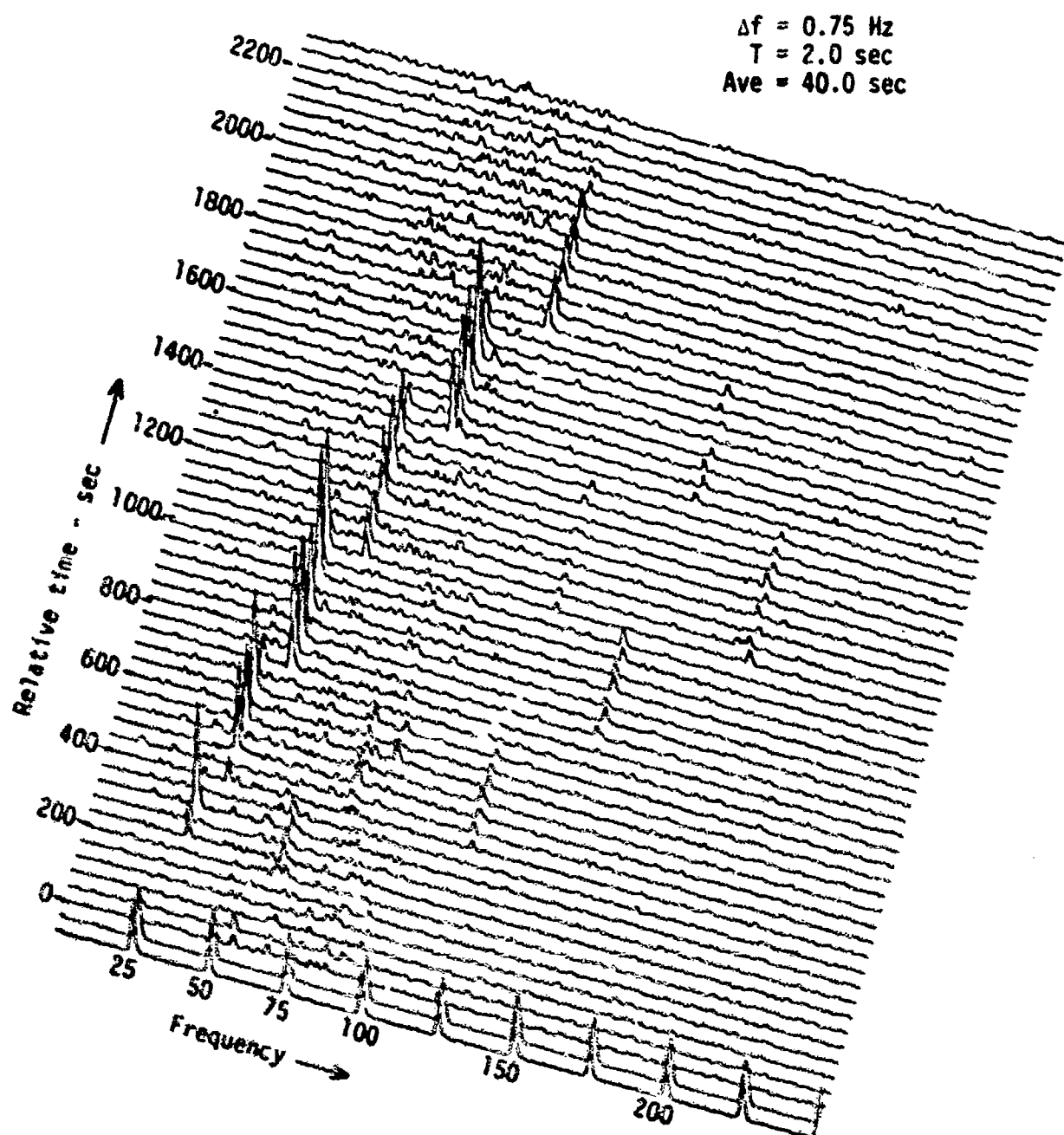


FIGURE A
 VIBROSEIS SOURCE
 TIME VARYING SPECTRA

block. The analyzer is set to average four consecutive spectra, representing the analysis of 8 sec of data, and output to the digital computer. These spectra were again averaged to represent power spectra for 40 sec data blocks. The display is linear power versus frequency versus relative time. Frequency markers from the analyzer are displayed for reference. Figure 9 is a similar display, but with log power.

F. cw Sources

A data segment, containing an apparent cw source of 90 Hz, was analyzed. The data segment occurred 2 1/2 days into the recording period. Two different types of analysis were performed: high resolution spectral analysis and adaptive spectral estimation to determine the spectral content of the data segment.

1. Spectral Analysis

High resolution power spectra of a cw source in the ambient noise background is shown in Fig. 10. The spectra are computed with an FFT algorithm and averaged in blocks of 50 (11.4 min). The frequency resolution is 0.07 Hz.

Spectral lines between 10 and 75 Hz indicate the presence of shipping. The line at 90.7 Hz is assumed to be the cw source. The side lobe structure of the spectral line indicates an amplitude modulation.

Three consecutive sets of data were analyzed in the same manner to observe if the lines were present over a longer time interval. Figures 11, 12, and 13 show how the lines vary over a 33 min data block.

Time varying power spectra of the ambient noise plus cw signal are shown in Fig. 14. The spectra are computed via an FFT using a

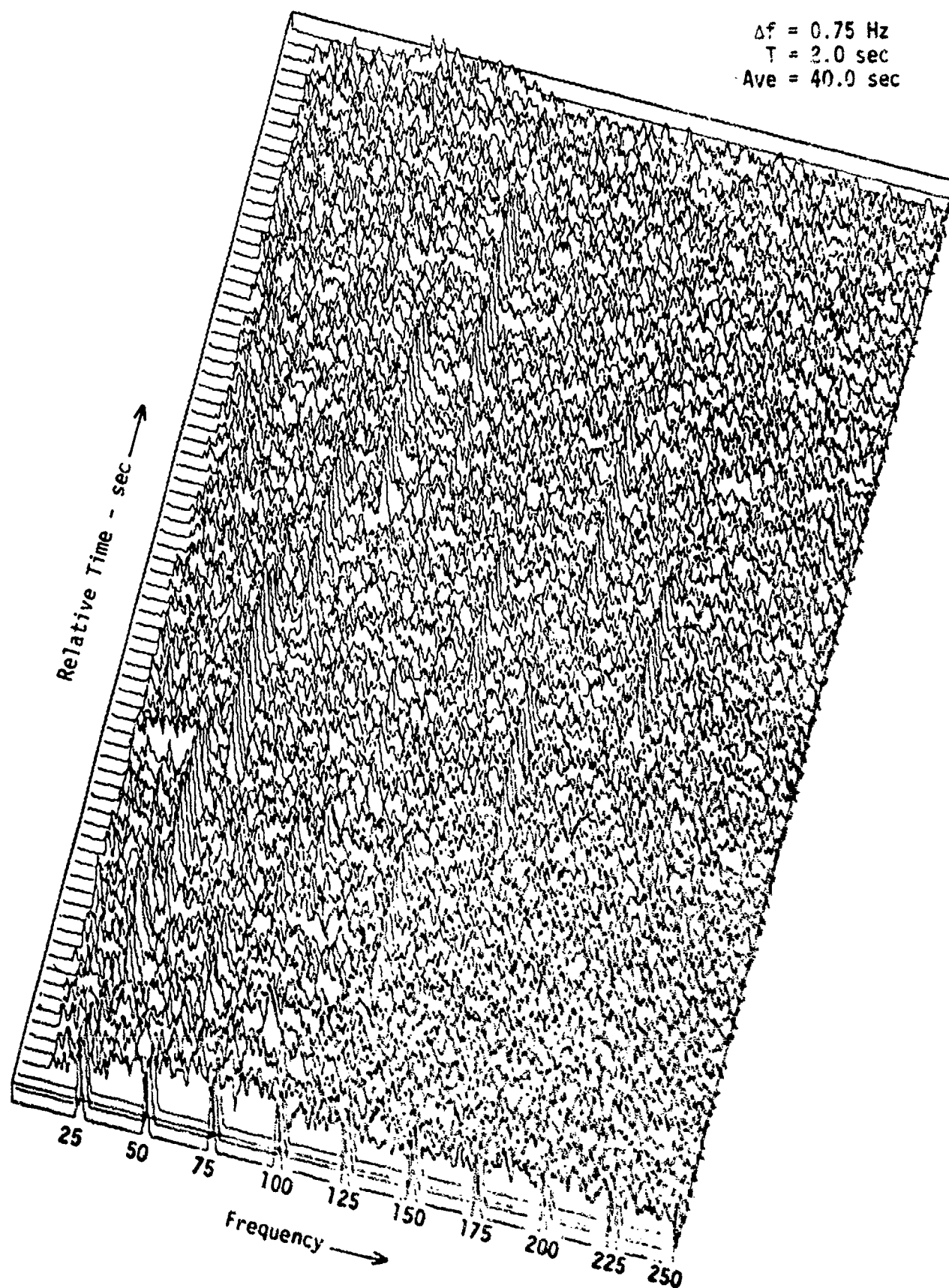


FIGURE 9
 VIBROSEIS SOURCE
 TIME VARYING SPECTRA

ARL-UT
 AS-74-1050
 GEE
 10-14-74

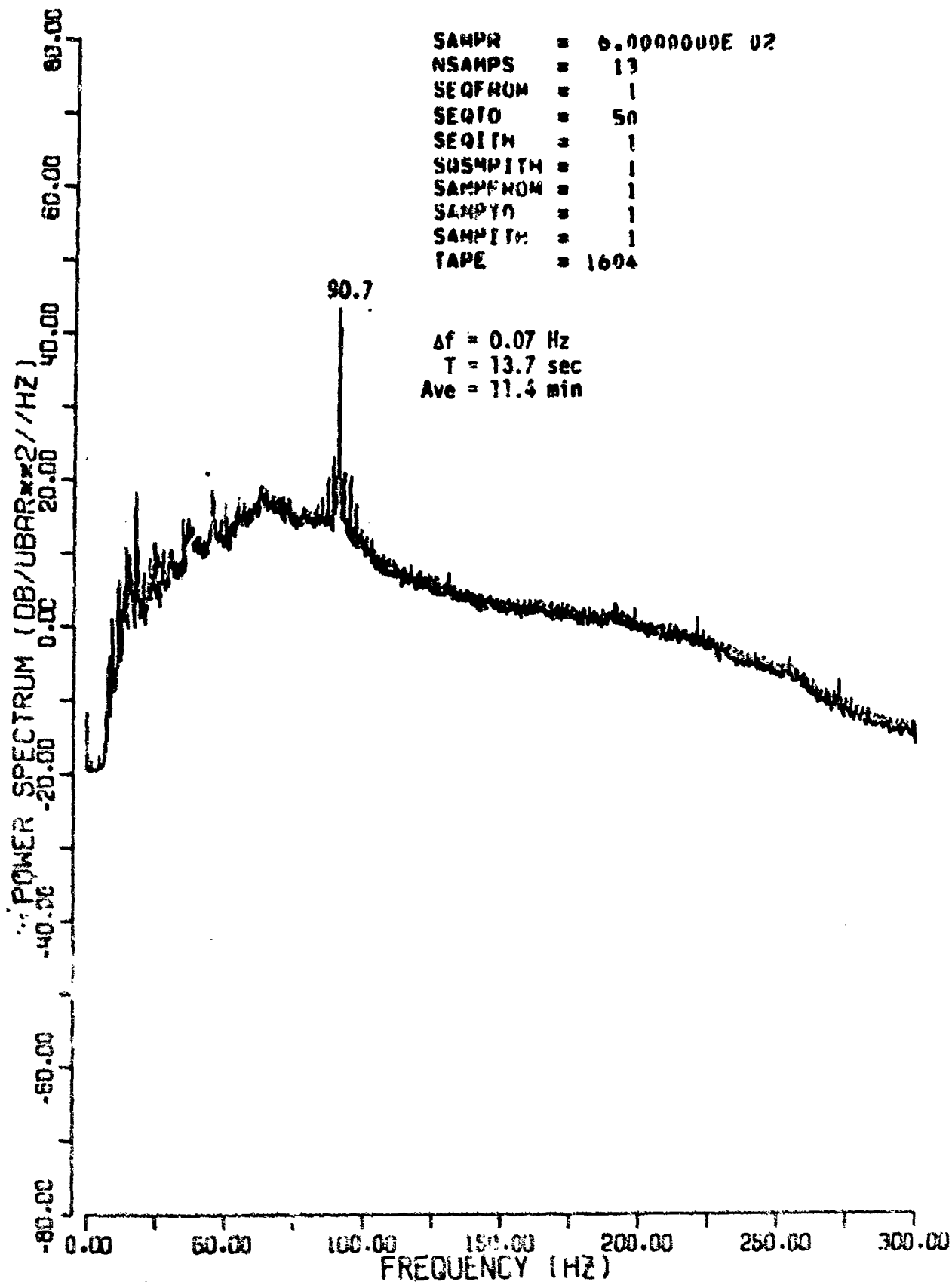


FIGURE 10
 CW SOURCE SPECTRA

ARL-UT
 AS-74-1051
 GEE
 10-14-74

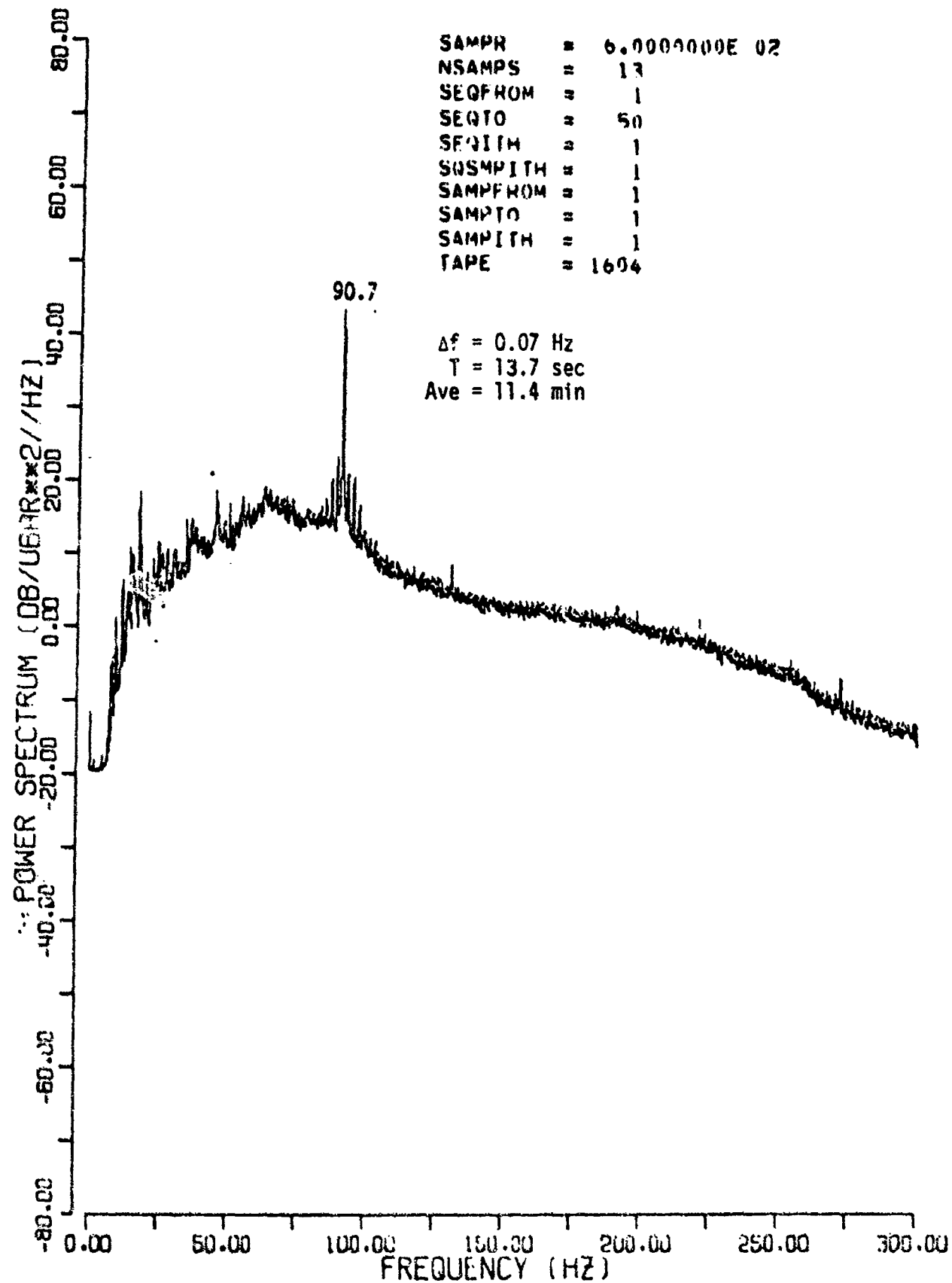


FIGURE 11
CW SOURCE SPECTRA

ARL-UT
 AS-74-1052
 GEE
 10-14-74

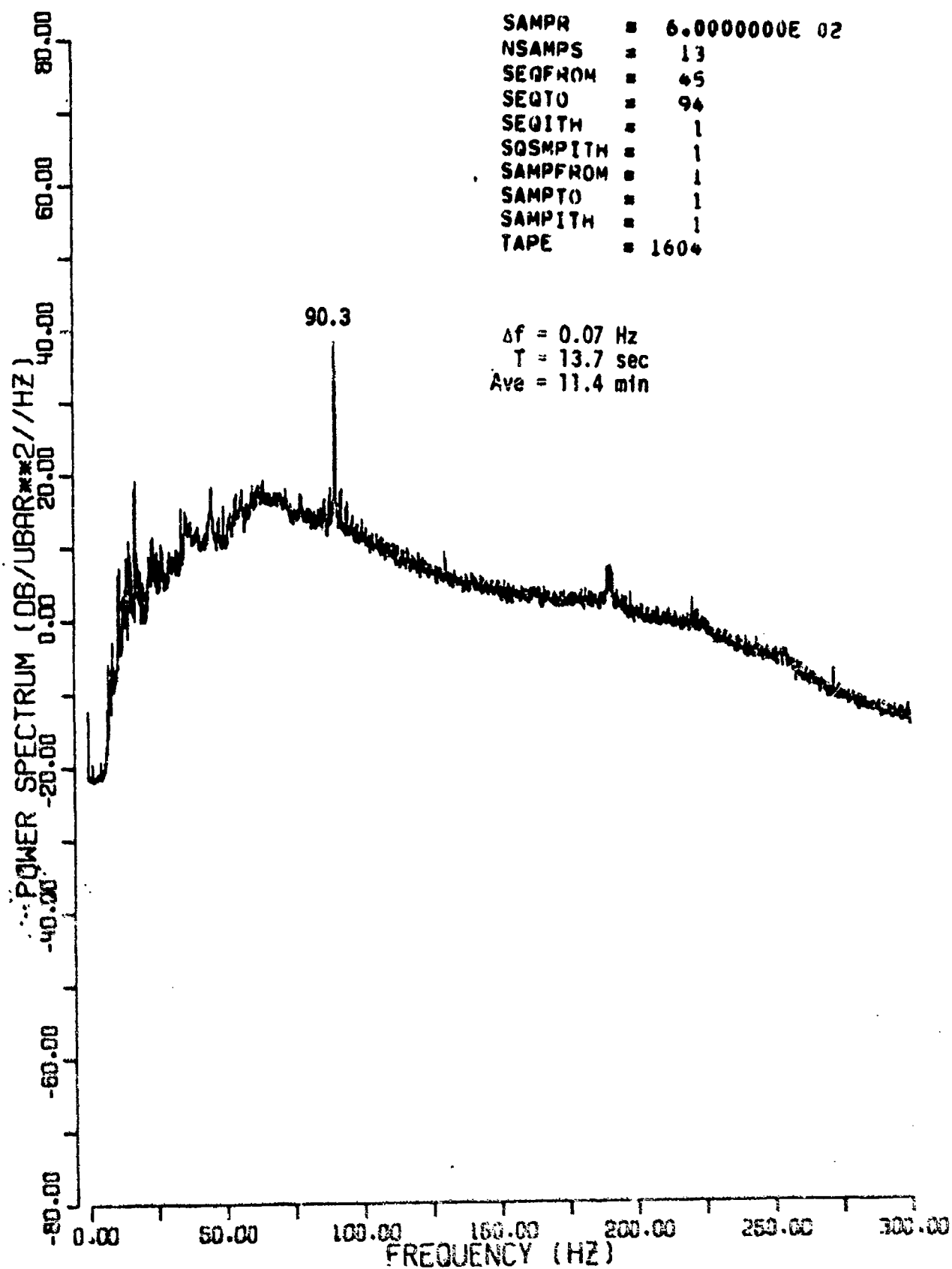


FIGURE 12
CM SOURCE SPECTRA

ARL-UT
 AS-74-1053
 GEE
 10-14-74

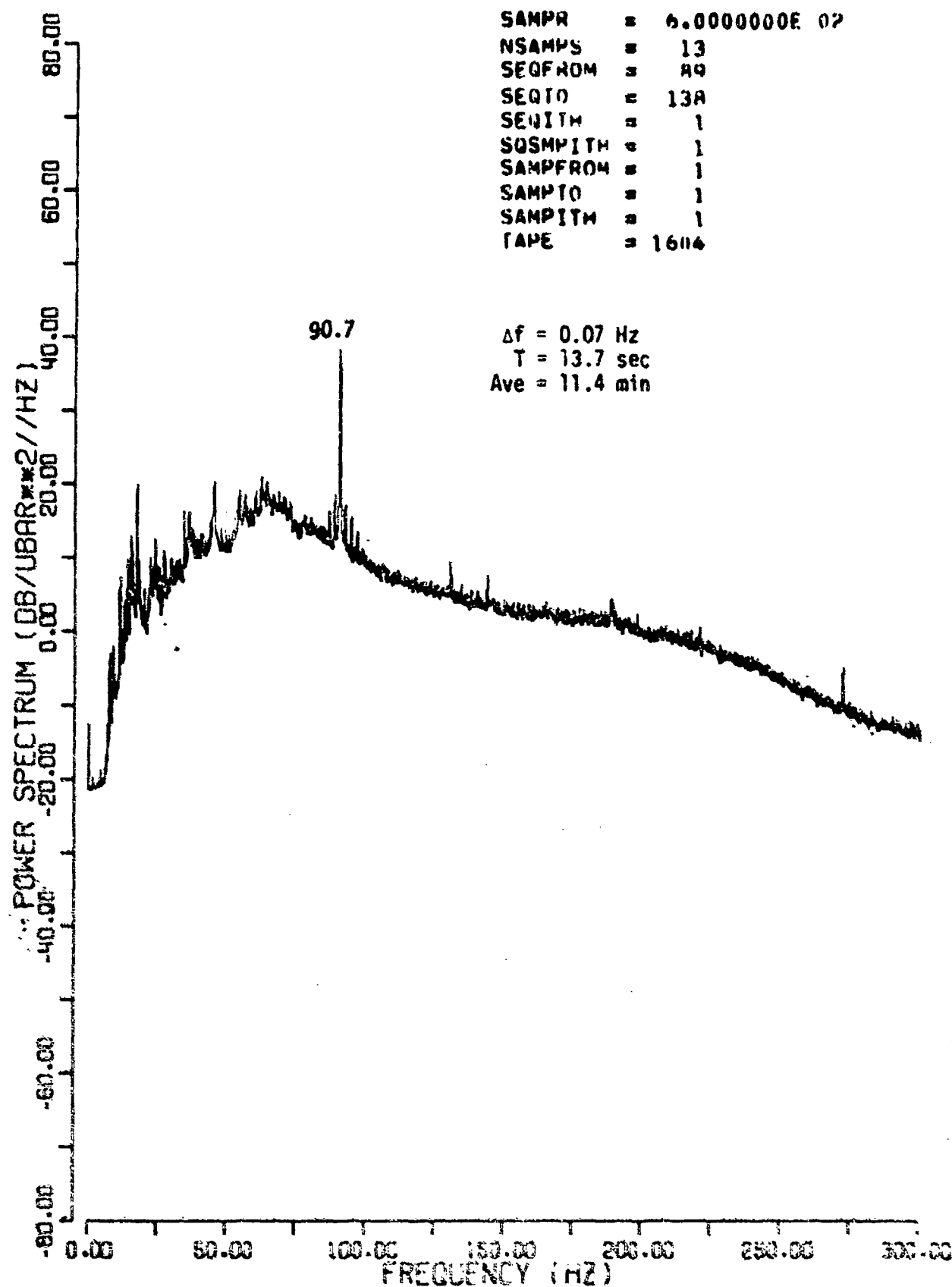


FIGURE 13
CW SOURCE SPECTRA

ARL-UT
AS-74-1054
GEE
10-14-74

$\Delta f = 8.4 \text{ Hz}$
 $T = 3.4 \text{ sec}$

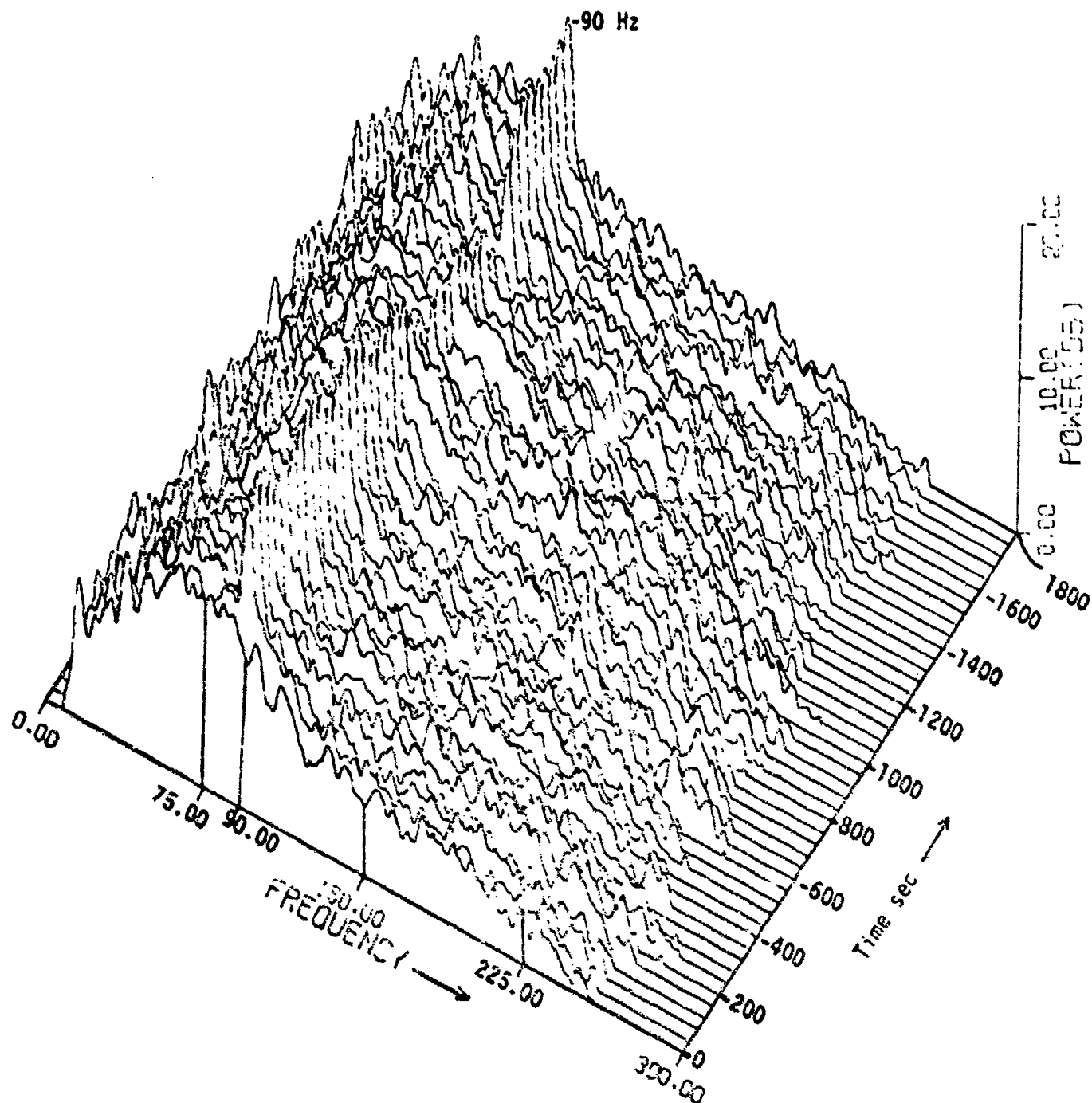


FIGURE 14
CW SOURCE
TIME VARYING SPECTRA

ARL-UT
AS-74-1055
GEE
10-14-74

Gaussian window with 30 equivalent degrees of freedom. No ensemble averaging is used. The basic frequency resolution is 0.29 Hz. Each line is an FFT on the first 2048 points from every 3rd sequence on digital tape 1604. The cw tone at 90.7 Hz is evident and it is changing in amplitude with time.

2. Adaptive Spectra Estimation

Figure 10 shows definite spectral lines. In an effort to check on the stability of these lines, a modification of the maximum entropy method (MEM) of computing spectra was used on the first 41 records of digital tape 1604. The basic program forms an autocovariance matrix, inverts it, and solves for the roots of a polynomial, which indicate resonance frequencies in the data. The primary advantage of the method is that it allows the use of a small amount of data to obtain a high resolution spectrum or the resonance frequencies in the case of this modified version. The amplitude of spectral lines is ignored by the program, but they may be found later.

Figure 15 shows the results of a time versus frequency display. The program is commanded to search for 14 roots; and up to 14 asterisks, which represent the frequencies found at that time, are displayed on each line. The 90 Hz line is strong and consistent; the other lines appear to fade in and out. The method is dependent upon signal-to-noise ratio (S/N), and as the signal fades the lines will appear to shift frequency. The conclusion is that the lines are present on the average, and they fade in and out in magnitude.

G. Validation of Data

A useful measure of the changing statistics of noise data is to test for homogeneity. That is, if two data sets have the same probability density, then they are homogeneous. In this case, a long digital

Digital Tape
Sequence No.

2 3 4 5 6 7 8 9 10 11 12 13 14 15 16 17 18 19 20 21 22 23 24 25 26 27 28 29 30 31 32 33 34 35 36 37 38 39 40 41

Time →

20

0 Hz

ARL-UT
AS-74-1051
GEE
10-14-74

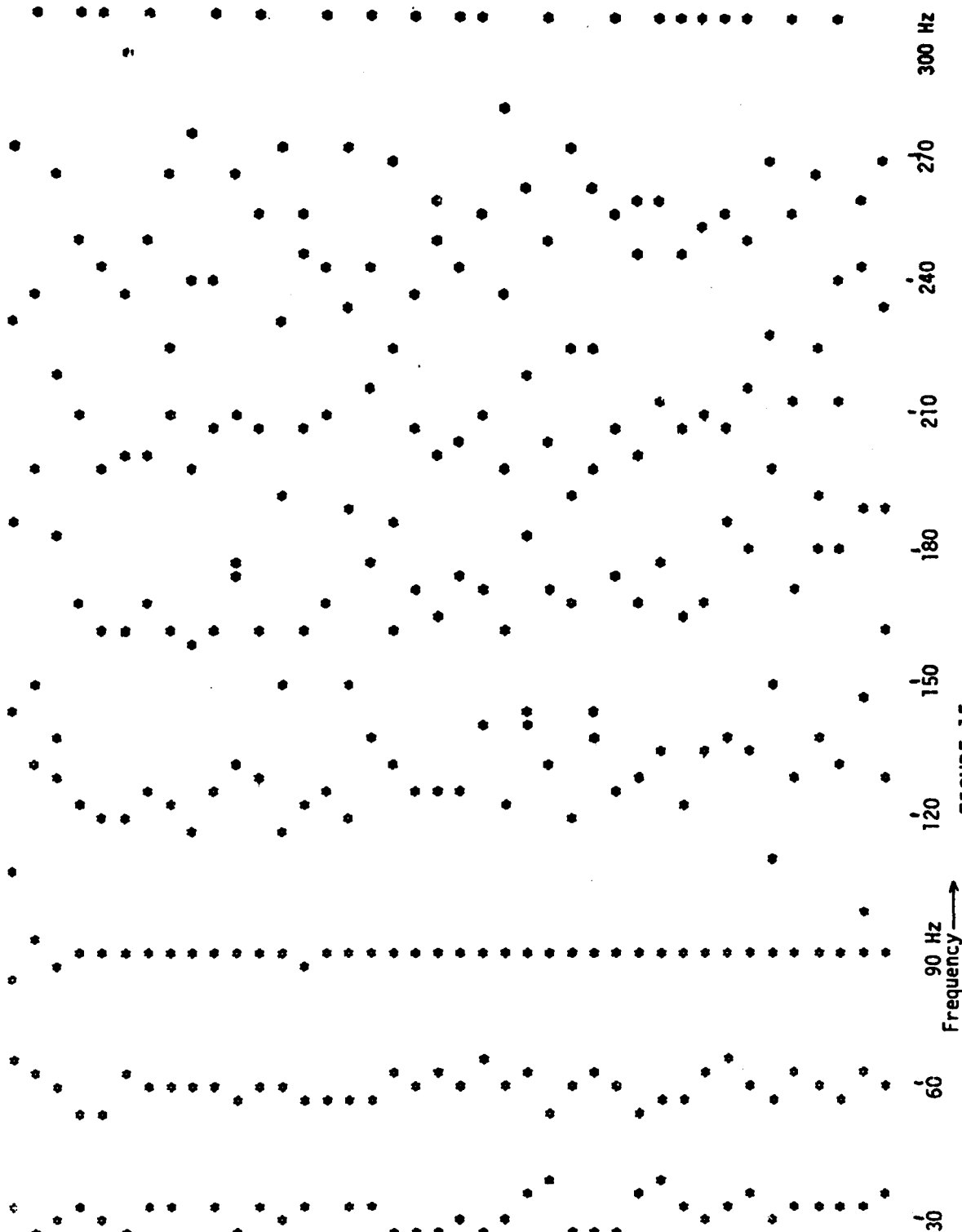


FIGURE 15

CW SOURCE
ADAPTIVE SPECTRAL ESTIMATION

tape subdivided into records of 8192 samples each was examined. This data segment occurred 2 1/2 days into the tape and contains ambient noise plus a cw signal. The 10th record was chosen as a reference and was compared to each of the other 138 records. One hundred samples were obtained from each record by picking every 10th sample from the first 1000 samples. The Kolmogorov-Smirnov (K-S) statistic was computed for each comparison and the result is shown in Fig. 16. The conclusion is that after a 2 h span of time the statistics change sufficiently for the K-S test to consistently reject the hypothesis that the data are homogeneous. After 4 h the data are again homogeneous with respect to the 10th record. This test should be repeated using different records as references for a complete analysis.

This brief analysis shows that for this environmental situation it would not be appropriate to average for more than a 2 h span of time to obtain a statistically reliable estimate of power spectra.

H. Digitization and Analysis of Shot Data

To obtain a suitable data base that would facilitate a preliminary investigation of the shot signals, a total of 36 waveforms from explosive sources were digitized. These data were approximately 3 1/2 days into the tape and were generated with a "2-shot" explosion sequence. Each received signal, from hydrophone 3, was gated in time by choosing an appropriate time delay following the first shot in each pair. The sample rate was the phase locked 600 Hz. Figure 17 shows computer plots of the first five echoes of the 36-echo sequence. The location of the shot signals are evident although only every 30th sample is plotted here. The reason for choosing a 40 sec window to select the data was to overcome instability of the triggering method. More detailed plots of the data are shown in Fig. 18. Here every 5th sample has been plotted.

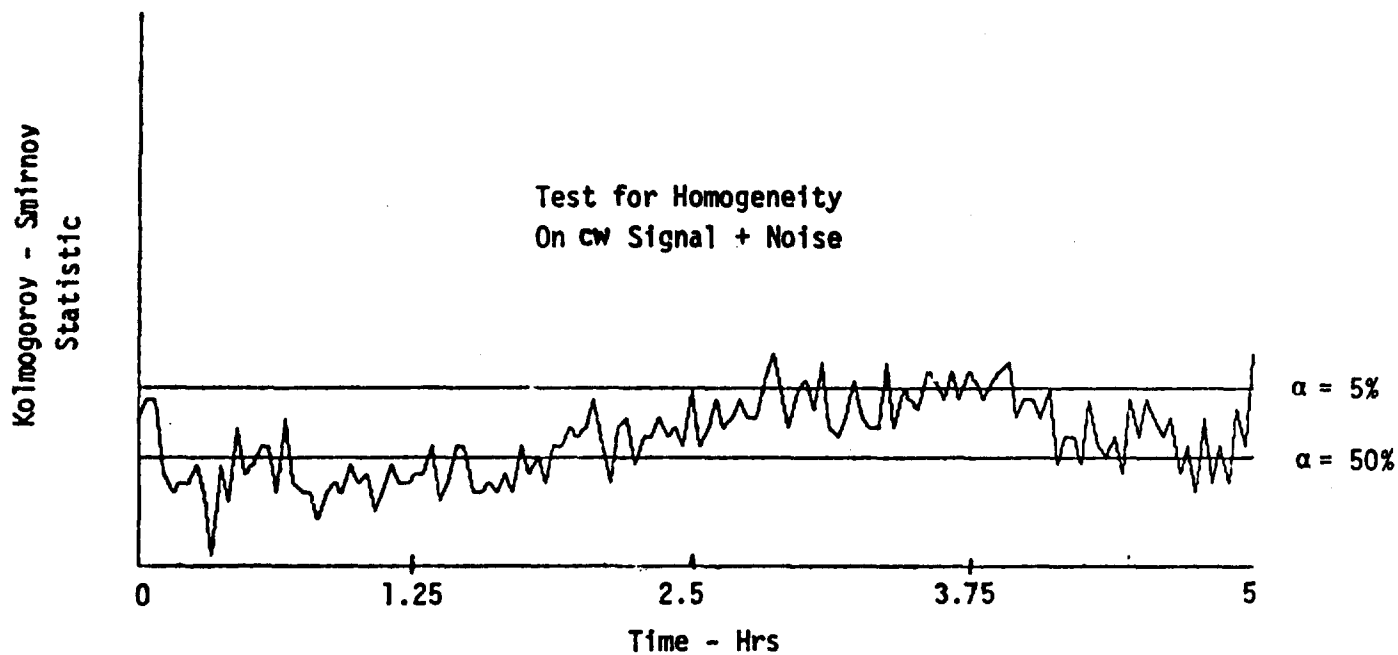


FIGURE 16
TEST FOR HOMOGENEITY
AMBIENT NOISE + CW SOURCE

ARL-UT
AS-74-1057
GEE
10-14-74

A general structure of the shot data is shown in Fig. 19 where three consecutive signals from the beginning of the data set (of 36 shots) and two consecutive signals from the end of the data set are plotted. The first three signals are similar in structure as are the last two signals. However, a structural difference, with respect to the number and arrival times of multipath signals, does exist between the set of the three earlier shots and the set of two later shots. This is to be expected since the geometry of the shot experiment changed over the duration of the measurements, and accordingly, the multipath structure would also change. Within a few consecutive shots, however, the multipath structure appears to be relatively stable.

Figure 20 provides a comparison for the waveforms of the primary arrivals of two (No. 1 and 5) shot signals. The two waveforms are very similar in shape, particularly with respect to the location and amplitudes of some of the larger peaks. Some differences between these two waveforms can be discerned, and these could be attributed to either differences in the generation of the shots or changes in the propagation environment.

To obtain a preliminary estimate of the required sample rate on the shot data, a signal was plotted with various sample rates. It was concluded that at least 600 Hz is necessary and very likely sufficient for the preservation of the information in the signal waveforms. Figure 21 illustrates the effect of reducing the sample rate on a typical signal. Misleading results will be obtained with a 300 Hz sample rate since much of the waveform structure is lost when the sample rate is changed from 600 Hz to 300 Hz.

Using Fig. 22 one can compare the shot-to-shot consistency of the second arrivals. The consistency here does not appear to be as high as that of the primary arrival (see Fig. 20). Also, the second arrivals are more spread in time, which indicates that this particular multipath component introduces a time smear into the acoustic propagation.

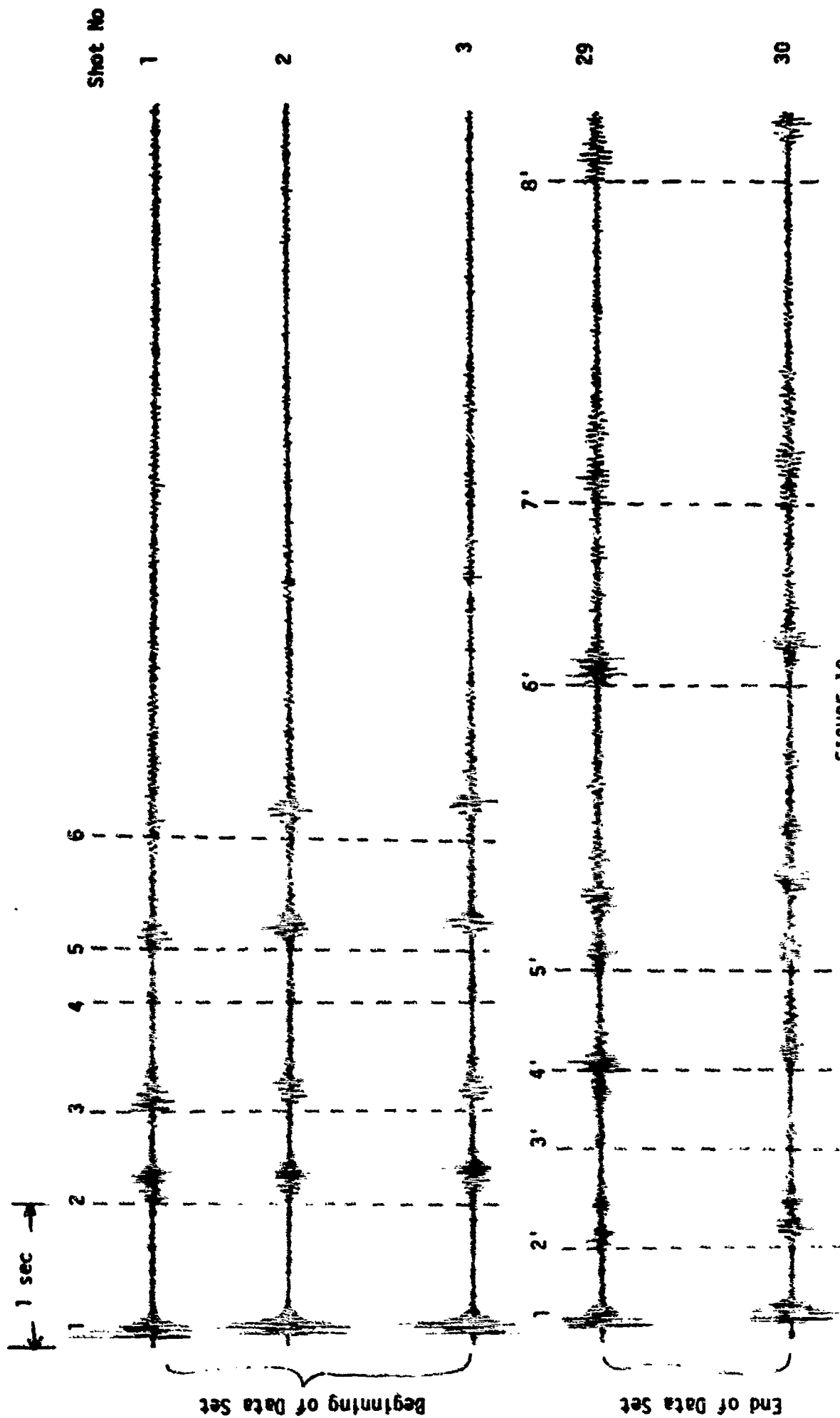


FIGURE 19
COMPARISON OF STRUCTURES OF RECEIVED SHOT SIGNALS
FROM BEGINNING AND END OF DATA SETS

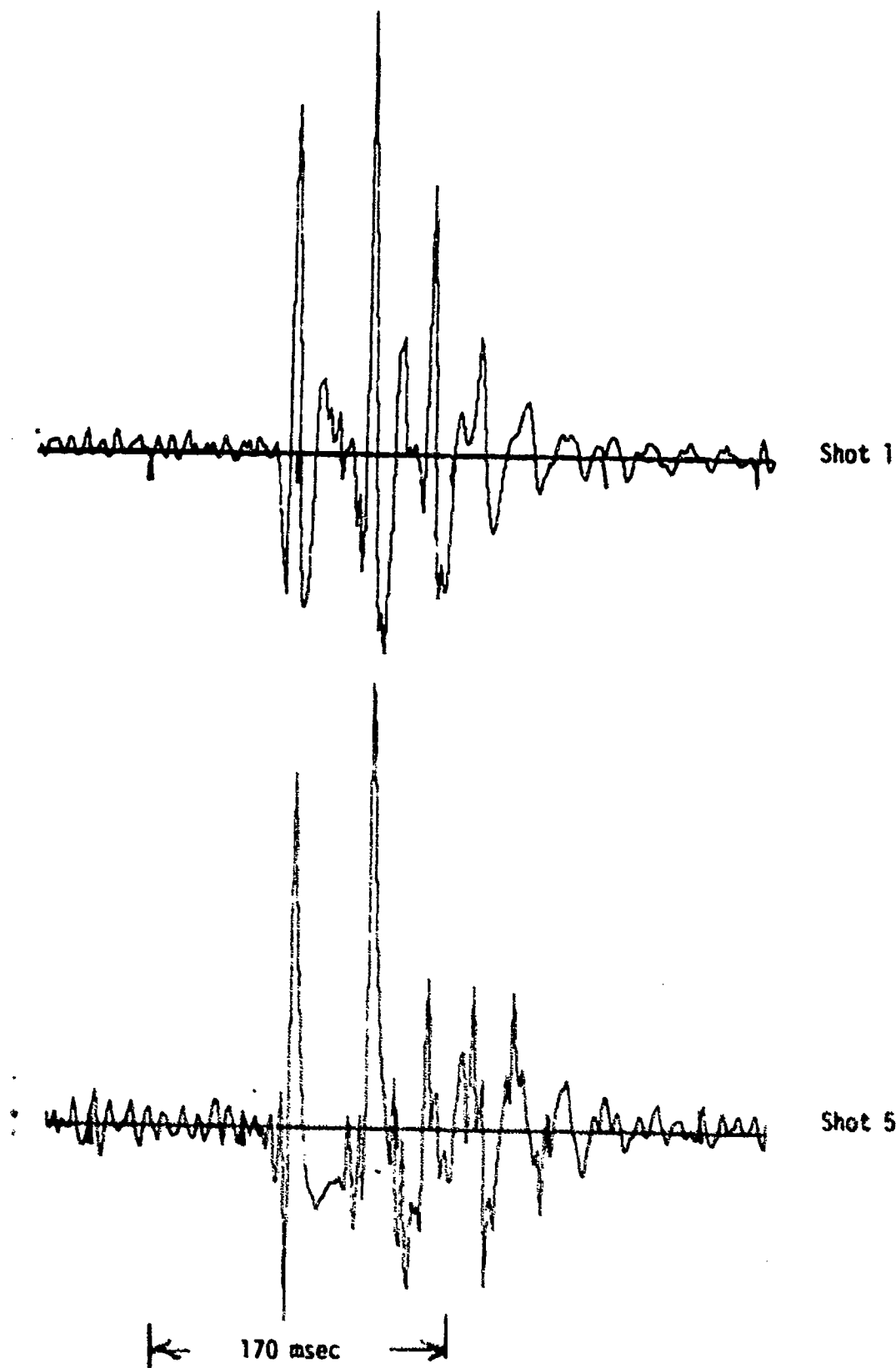


FIGURE 20
DETAILED COMPARISON OF TWO PRIMARY
ARRIVALS FROM SHOT SOURCES

ARL-UT
AS-74-1061
GEE
10-14-74

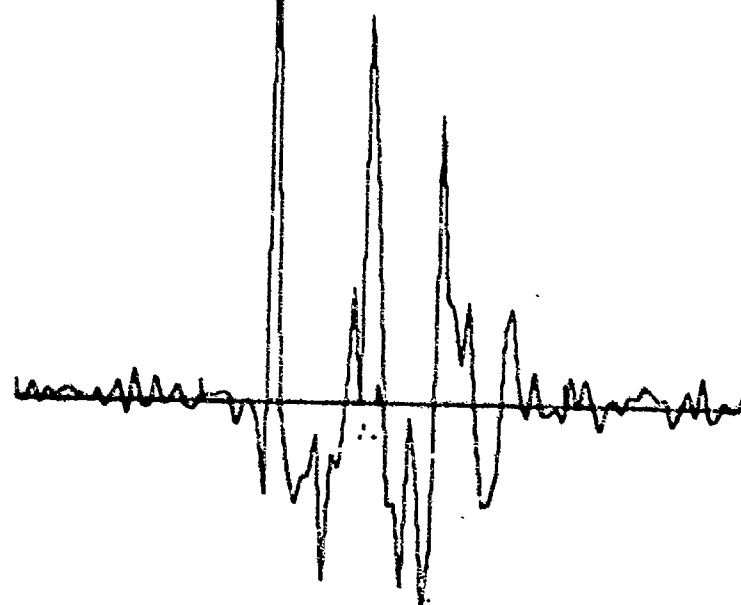
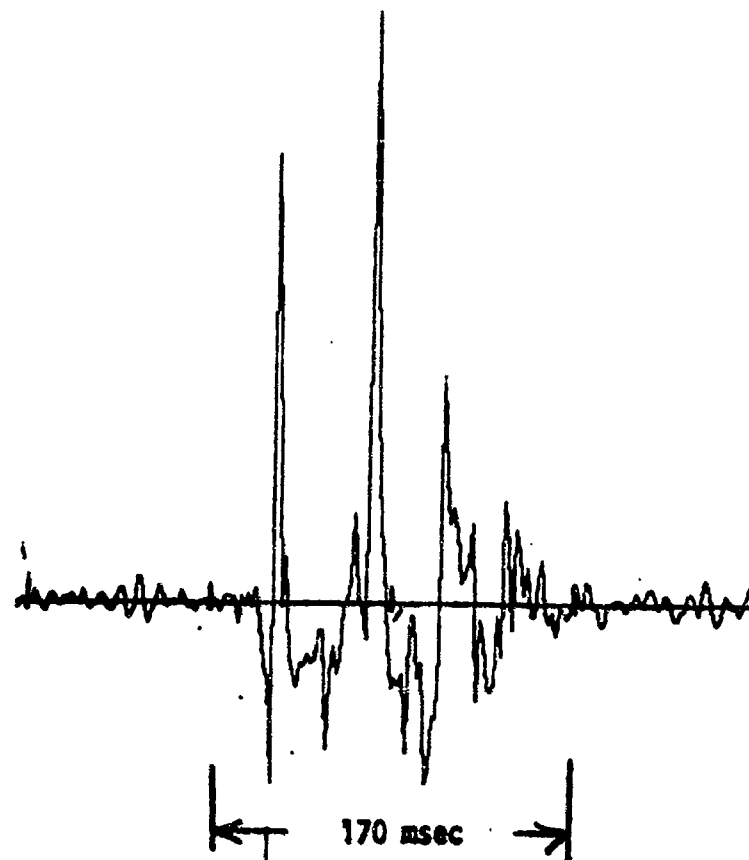


FIGURE 21
EFFECT OF REDUCTION IN SAMPLE RATE ON
PRESERVATION OF WAVEFORM STRUCTURE

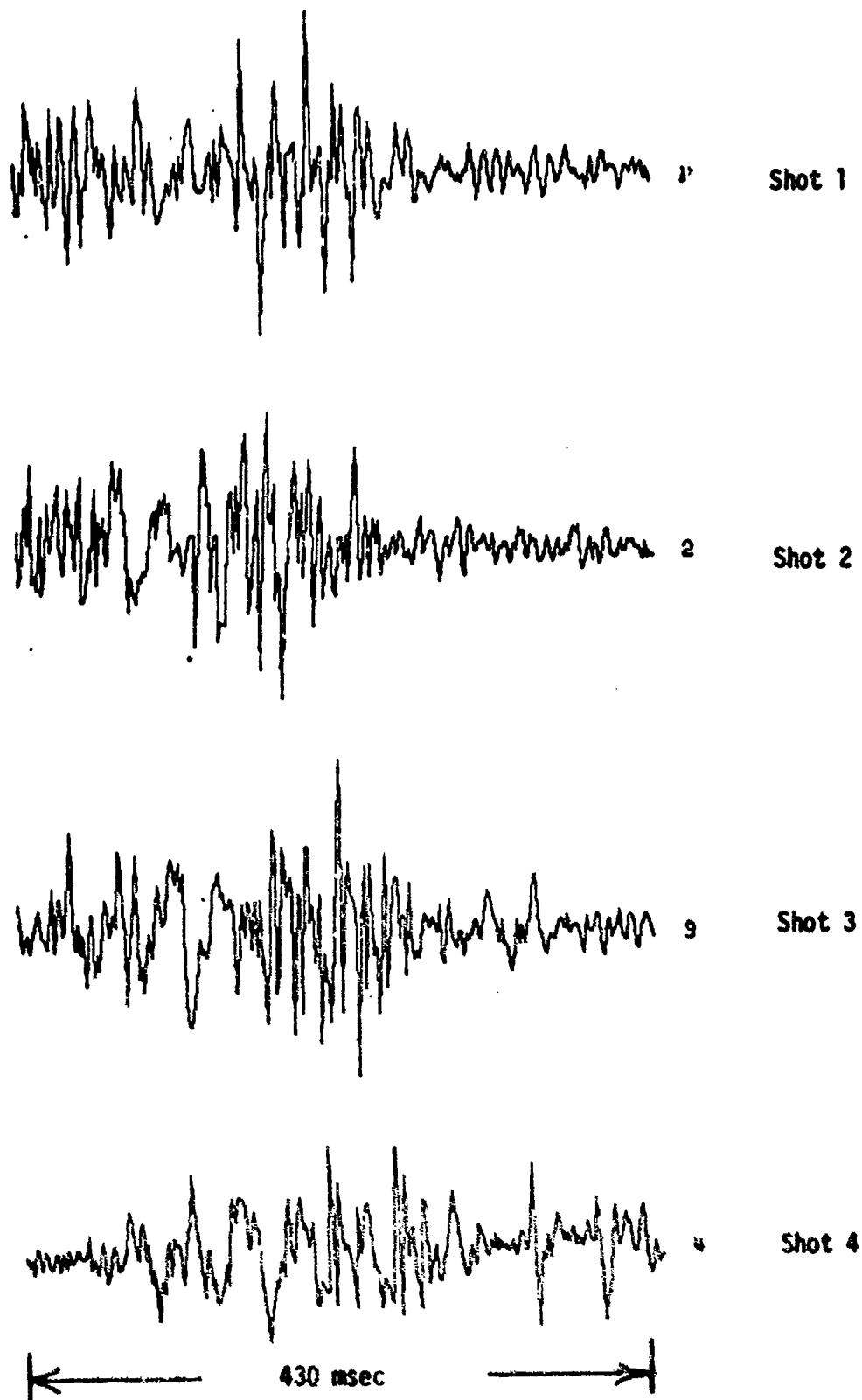


FIGURE 22
COMPARISON OF THE WAVEFORM STRUCTURES OF
THE SECOND ARRIVALS OF THE FIRST FOUR SHOTS

ARL-UT
AS-74-1063
GEE
10-14-74

I. Intensity Spectrum of Shot Data

A very limited attempt was made to estimate the intensity spectrum of the received shot data. A sample spectrum (2.34 Hz resolution) of the first arrival of the fourth shot is shown in Fig. 23. Generally, the spectrum decays from its maximum near zero frequency to a minimum at 300 Hz, the extent of the receiver filters. This estimate has many fluctuations present, some of which are undoubtedly due to statistical inaccuracies in the estimate. Time permitting, the estimate would be improved by several techniques such as averaging several spectra or using appropriate smoothing functions.

Before proceeding with the computation of the spectra, however, the shot data should be more accurately described with respect to its deterministic or random structure. If the shot data were entirely deterministic and repeated consistently over the duration of the experiment, then all of the spectral information could, in principle, be obtained from one sample function. However, the shot data do appear to have random components and particularly so in the 2nd, 3rd, 4th, etc., arrivals. When this is the case then appropriate ensemble techniques must be employed to obtain a statistically reasonable estimate of the intensity spectra of the data. This technique should be used carefully, however, since the "time" spectrum of the shot data may change during the course of an experiment due to a change in the experimental geometry and propagation conditions. In this case, an ensemble spectra could be misleading since it would be derived from data that were essentially inhomogeneous. This problem can only be solved after a preliminary investigation of the statistical properties of the received shot data.

J. Estimation of Signal-to-Noise Ratio

One of the more important quantities is the S/N of any given set of shot data. In this analysis the S/N of a typical signal was estimated

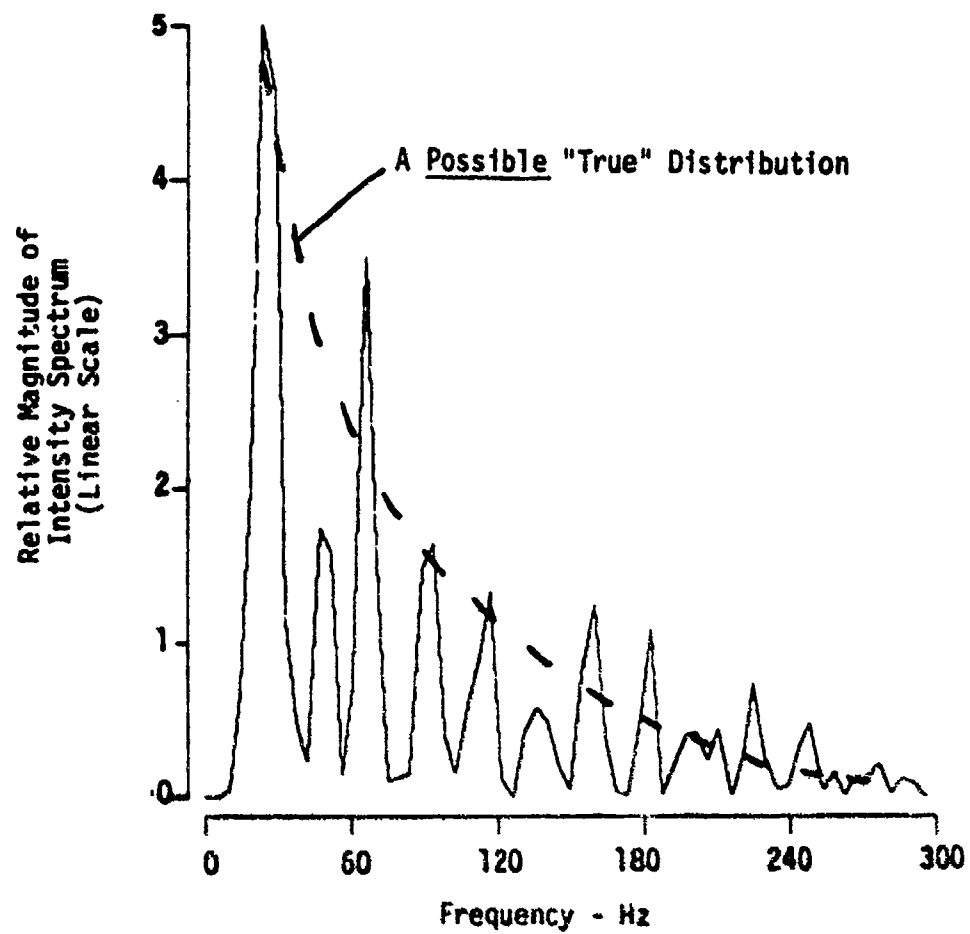
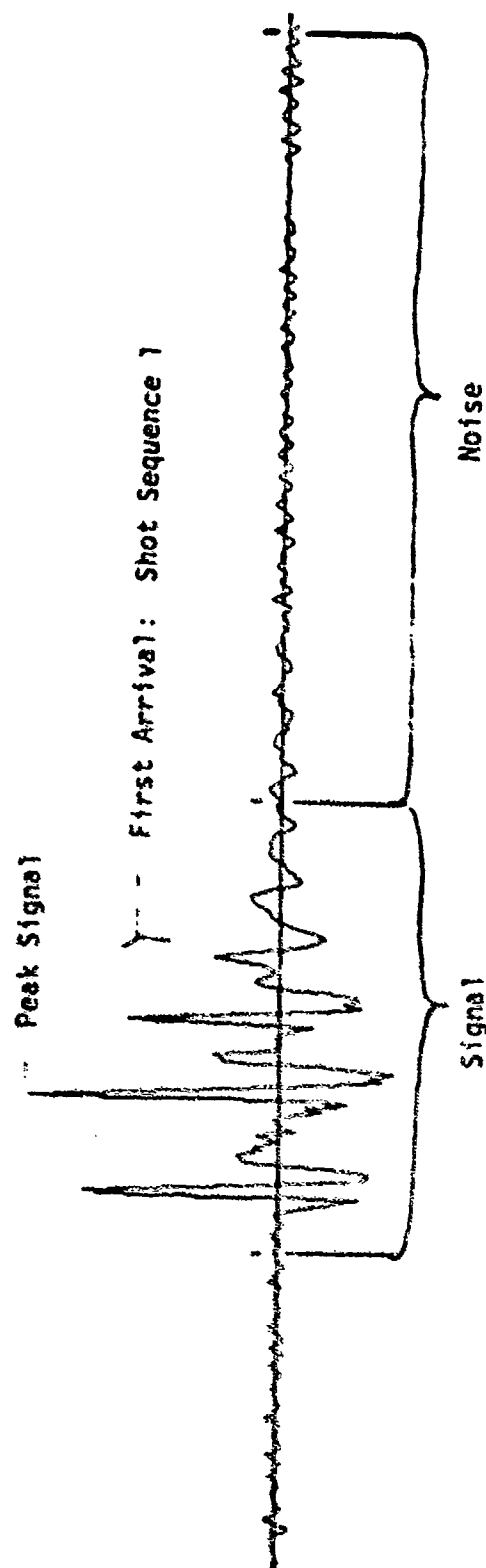


FIGURE 23
INTENSITY SPECTRUM OF THE FIRST ARRIVAL OF
THE FOURTH SHOT SEQUENCE

ARL-UT
AS-74-1064
GEE
10-14-74

according to two definitions of S/N and several averaging times used in the estimation of the noise background. The problem is illustrated in Fig. 24. In this case the signal is relatively easy to locate, a situation that likely will not always occur. The epoch of the signal is noted as well as a particular window used for the estimate of the noise power or intensity. The two S/N's estimated are computed using the peak of the signal and the average energy of the signal (see Fig. 25). The stability of the estimate should improve as the averaging time of the noise estimate improves. This is illustrated very clearly in Fig. 25 where it can be seen that the S/N estimate approaches a stable value when an averaging time of 0.5 sec or greater is used. To determine useful S/N values, analysis of the effect of averaging time should be performed to obtain higher confidence in the results as well as a savings in processing time.



$$\text{ENERGY } S/N = 10 \log \frac{S}{N}$$

S = SIGNAL ENERGY/DURATION OF SIGNAL

N = AVERAGE INTENSITY OF NOISE

$$\text{PEAK } S/N = 10 \log \frac{P^2}{N}$$

P = MAXIMUM AMPLITUDE OF SIGNAL

FIGURE 24
ESTIMATION OF SHOT SIGNAL-TO-NOISE RATIO, S/N

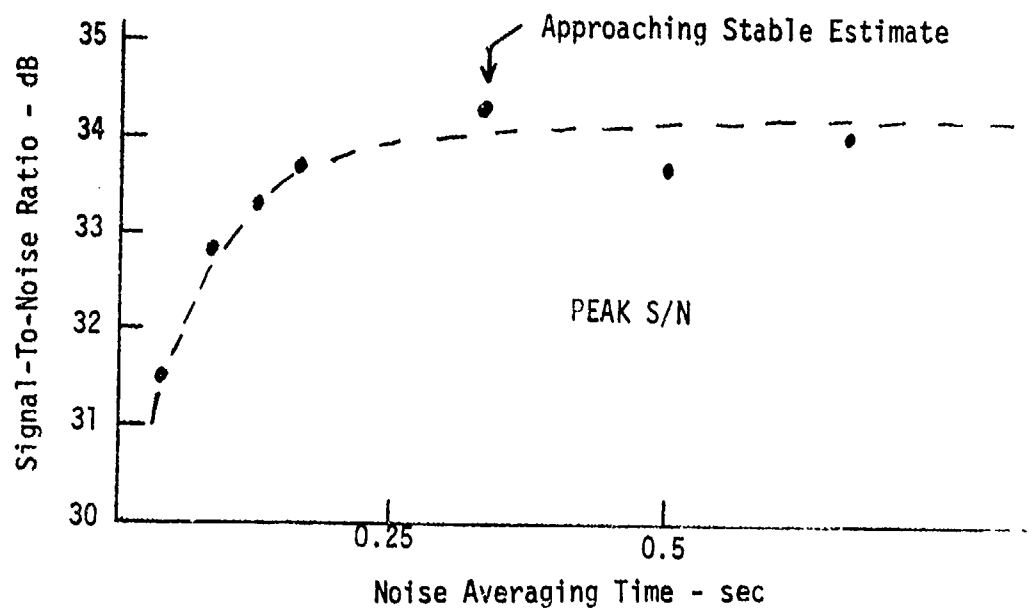
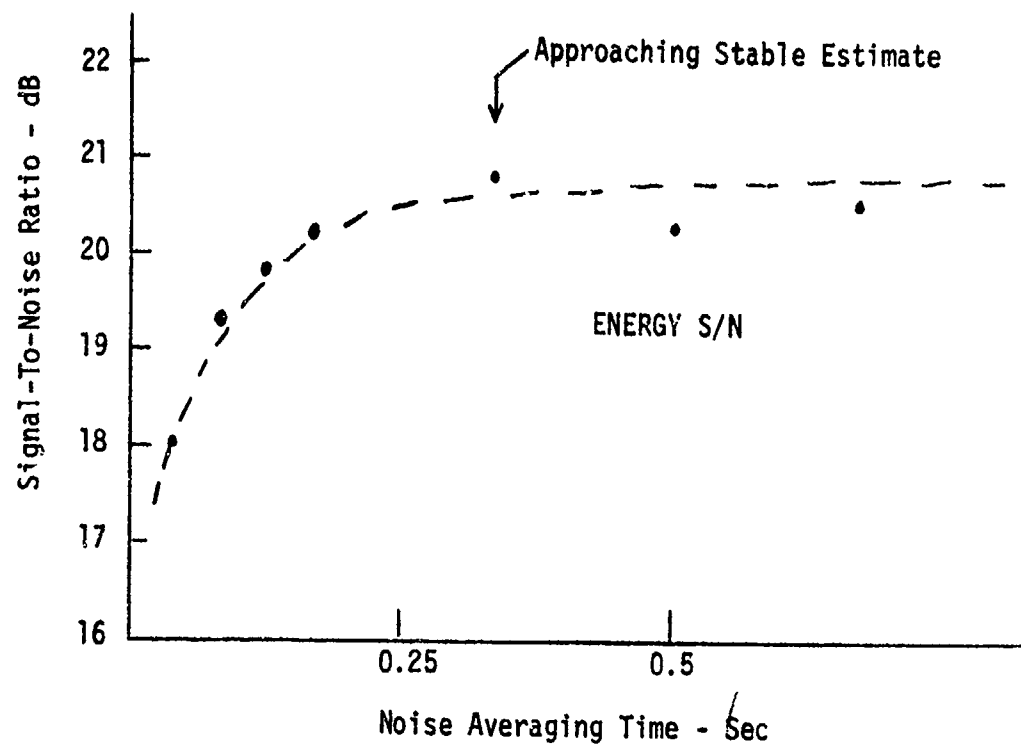


FIGURE 25
SIGNAL TO NOISE RATIO ESTIMATES AS
FUNCTIONS OF AVERAGING TIME OF NOISE

II. ANALYSIS OF THE BLAKE TEST ACODAC DATA (ARL-TM-73-12)

A. Blake Test Analysis

1. Introduction

The Blake Test was conducted at sea in a deep water environment for the purpose of evaluating the ACODAC system self-noise effects on system performance. Data tapes from the Woods Hole Oceanographic Institute (WHOI) and the University of Miami (UM) ACODAC systems were duplicated and furnished to ARL for analysis in support of the Test Director (UM). The UM array parted early into the test leaving only hydrophone channel 6 recording data.

2. Data Reduction Procedures

Data reduction was accomplished using the hardware/software systems currently in operation at ARL. These systems are described in Section I (ARL-TM-73-11). The variances on these basic procedures are outlined in this report with the description of each type of analysis performed.

3. Analysis Constraints

The data analysis was somewhat constrained by the nature of the test, which included a tight time schedule for the completion of the analysis. The data tapes were received at ARL on 20 June 1973 and the results were presented at a meeting with the Test Director at WHOI on 25 June 1973.

Other constraints that slowed the analysis were the lack of a time code reader and test event log. The ACODAC tapes were edited and consistent events were located on each tape. For reference in coordinating this analysis with other analyses, the time code was digitized by quadrature sampling and decoded with the digital computer. The ACODAC amplifier gains were read with the same procedure.

4. Data Tape Quality

The duplicate ACODAC analog tapes were examined for "quality" prior to the analysis. The signal levels on the Blake Test tapes were compared to the Church Gabbro tape previously analyzed (Section I). Table I gives the signal level on the tape, using identical playback electronics, for the Church Gabbro, Blake WHOI, and Blake UM tapes. The peak calibration signals for the Blake Test tapes were 10 to 20 dB below comparable signal levels on the Church Gabbro tape. The ARL playback system noise, using blank tape in the recorder, is also given in Table I.

TABLE I
SIGNAL LEVEL CHECK FOR
THE ACODAC TAPES
Signal Levels (dB re 1 Vrms)

<u>Hydrophone Channel</u>	<u>Playback* system noise</u>	<u>Church Gabbro</u>	<u>WHOI (Blake)</u>	<u>UM Blake</u>
1	-49	-11	-21	-
2	-45	-9	-21	-
3	-49	-11	-33	-
4	-47	-10	-27	-
5	-47	-15	-43	-
6	-47	-9	-29	-43

*Playback system noise was determined by using blank tape.

B. ACODAC Calibration Analysis

1. Purpose

The analysis time period for the Blake Test data did not permit an extensive study of the stability of the ACODAC system calibration. To establish a "quality check" on the data for each hydrophone to be analyzed, the calibration signal recorded immediately prior to the ambient noise data was examined. This calibration occurred between the 50 and 100 mile shot sequences.

2. Data Reduction Procedures

The time compressed (40:1) analog data was bandpass filtered (10 to 300 Hz) and digitized. The A/D converter was synced to the 12th harmonic (600 Hz) of the 50 Hz carrier of the time code to reduce tape recorder inaccuracies. The spectra were computed with a FFT algorithm to a resolution of 0.073 Hz. The data block for the FFT is 13.65 sec. A Hanning window was applied to each spectrum for smoothing. The spectra shown in Figs. 1 through 7 represent an ensemble average of 2.3 min. The spectra have been corrected for the playback amplifier gain but not for the ACODAC amplifier gain. Table II is an explanation of the labels for the spectra.

3. Spectral Analysis

Table III is a summary of the peak and noise spectral levels of the calibration signal for the WHOI and UM arrays. For the WHOI array, hydrophone channels 1, 2, and 4 show a consistent peak signal-to-noise ratio (S/N) of at least 50 dB at 50 Hz. Hydrophone channels 3, 5, and 6 of the WHOI array indicate a lower dynamic range. For all hydrophone channels the 200 Hz calibration signal is approximately 10 dB lower than the 50 Hz calibration signal. All of the channels contain harmonics of the calibration signals of significant levels.

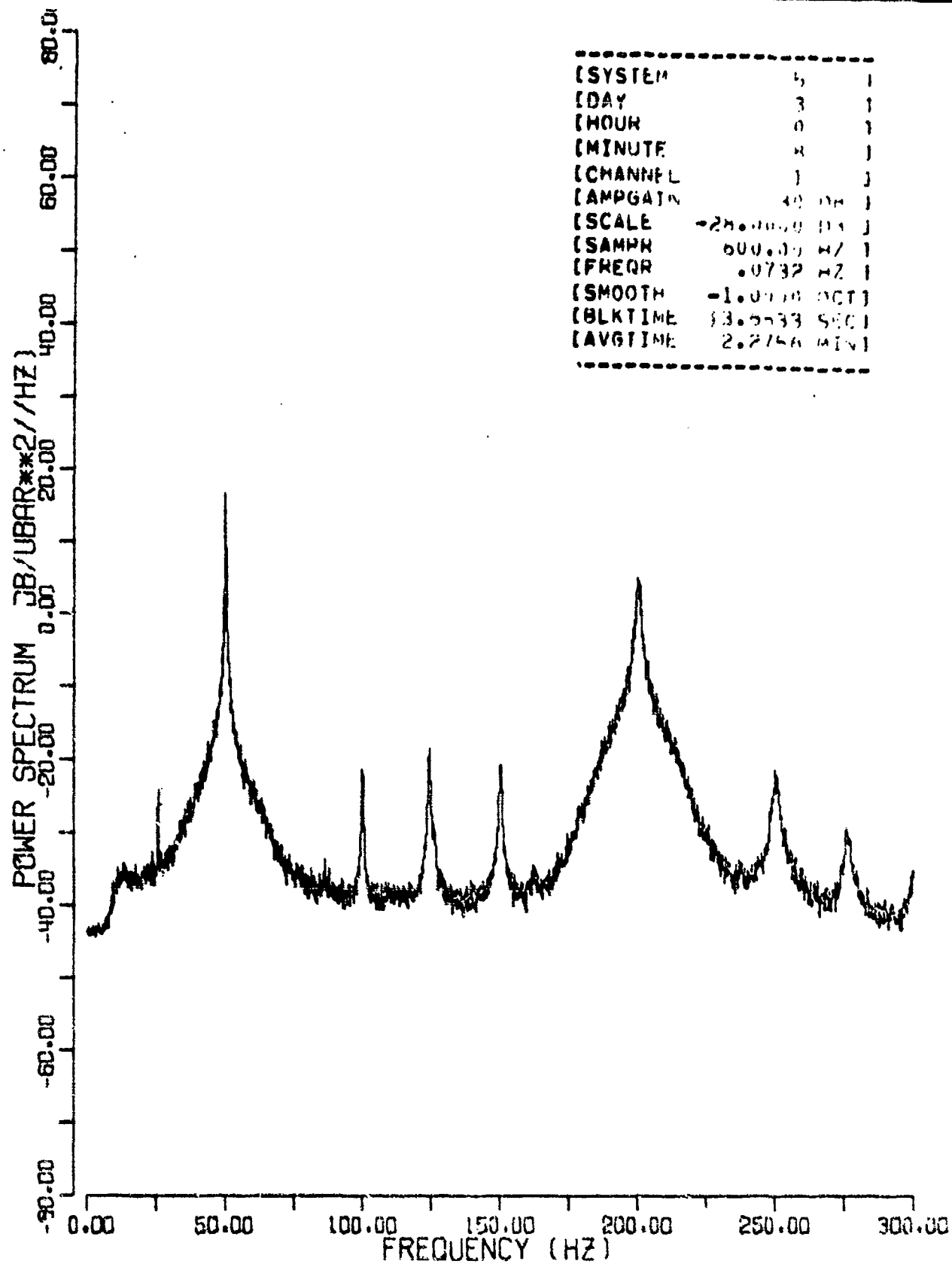


FIGURE 1
CALIBRATION SPECTRA FOR
WHCI ARRAY - HYDROPHONE 1

ARL-UT
AS-74-1067
GEE
10-14-74

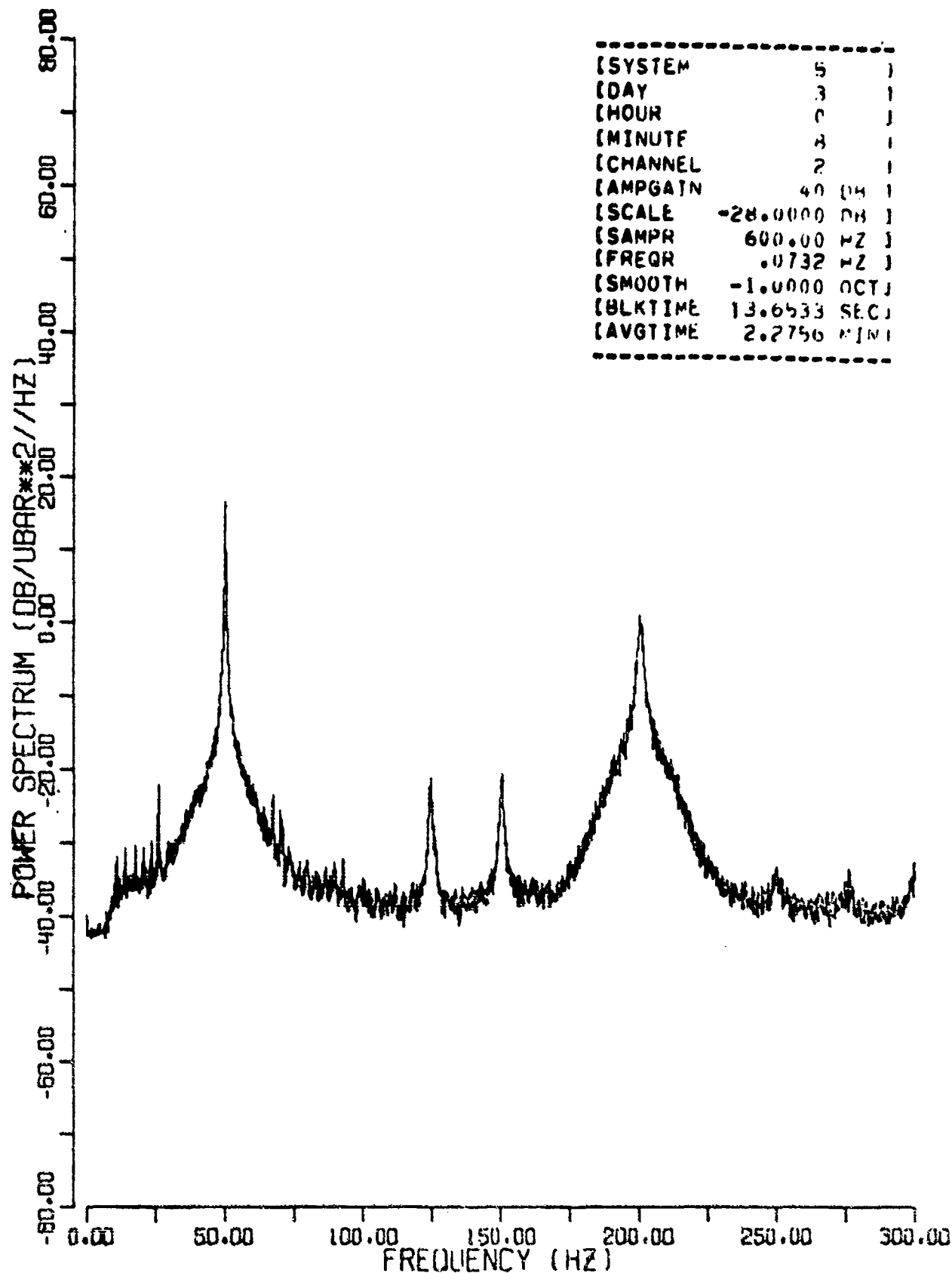
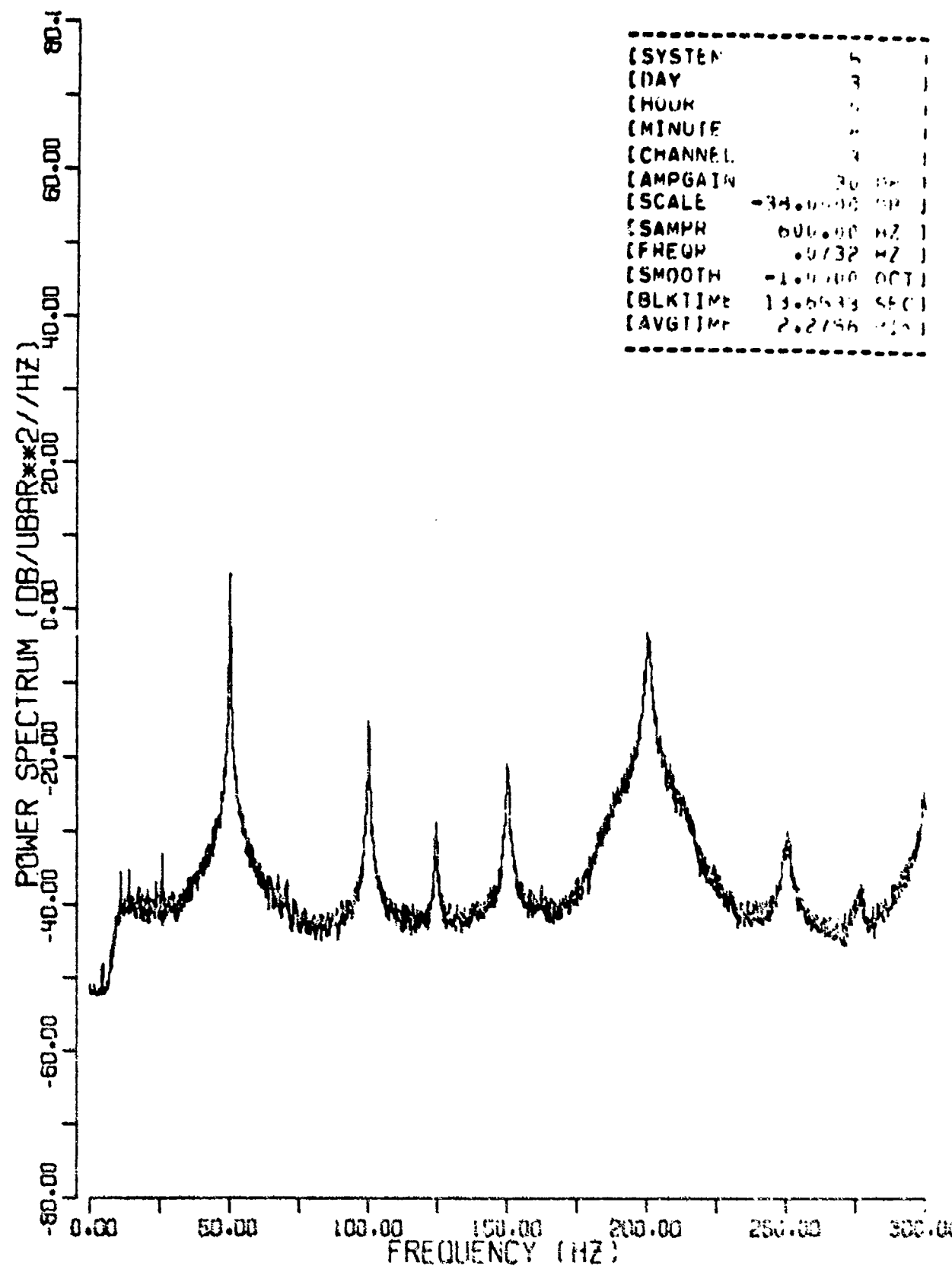


FIGURE 2
CALIBRATION SPECTRA FOR
WHOI ARRAY - HYDROPHONE 2

39<

ARL-UT
AS-74-1068
GEE
10-14-74



```

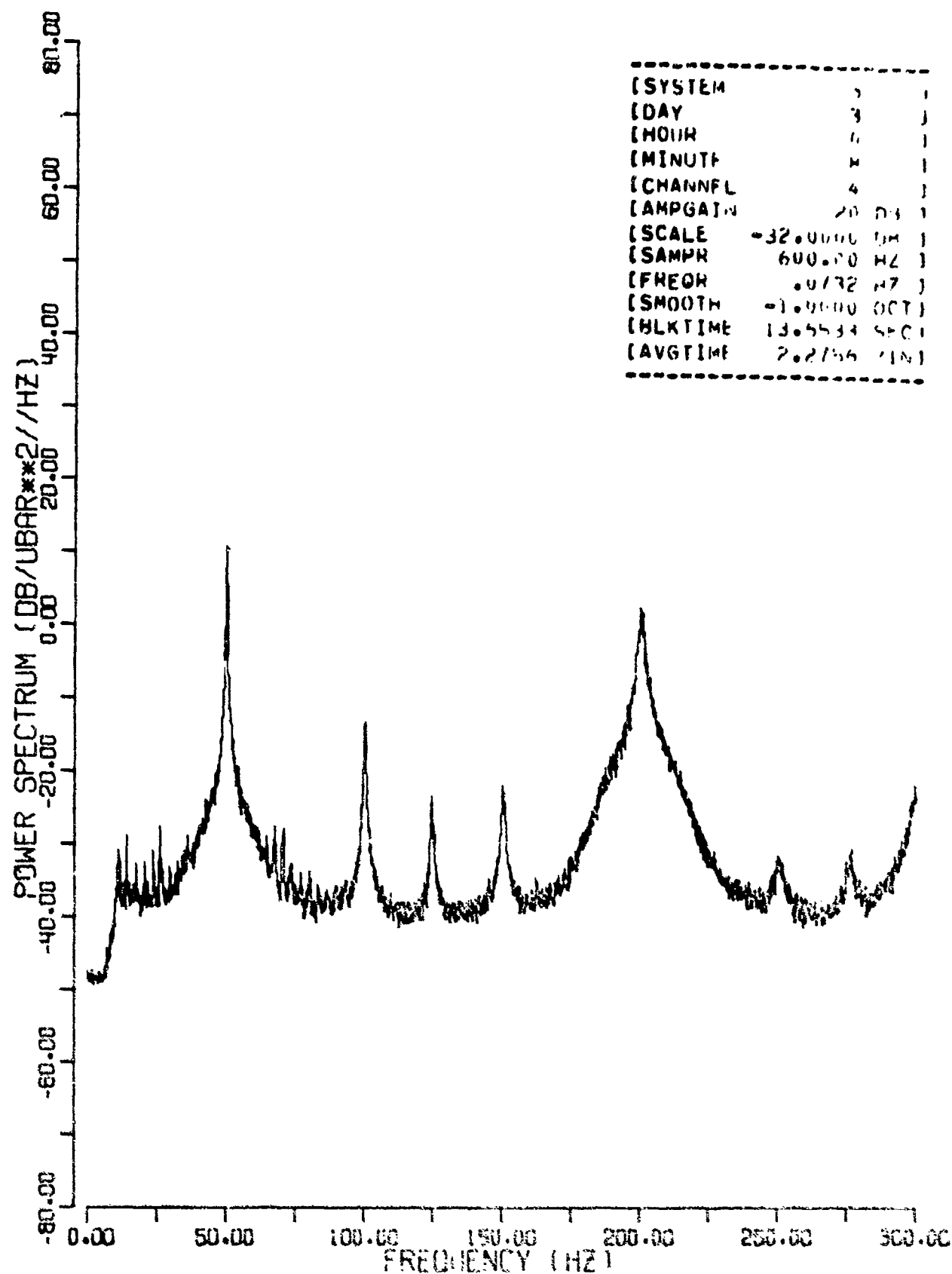
[SYSTEM      5 ]
[DAY         3 ]
[ HOUR       0 ]
[MINUTE      0 ]
[CHANNEL     0 ]
[AMPGAIN     20 ]
[SCALE      -34.0000 DB ]
[SAMPFR      600.00 HZ ]
[FREQW       0.0732 HZ ]
[SMOOTH      -1.0000 OCT ]
[BLKTIME     13.6533 SEC ]
[AVGTIME     2.2756 SEC ]

```

FIGURE 3
CALIBRATION SPECTRA FOR
WHOI ARRAY - HYDROPHONE 3

ARL-UT
AS-74-1069
GEE
10-14-74

40<



```

-----
[SYSTEM      3      ]
[DAY         3      ]
[MOHR        6      ]
[MINUTE      4      ]
[CHANNEL     4      ]
[AMPGAIN     20 DB  ]
[SCALE      -32.0000 DB ]
[SAMPR       600.00 HZ ]
[FREQH       0.0732 HZ ]
[SMOOTH      -1.0000 OCT]
[HLKTIME     13.5534 SEC]
[AVGTIME     2.2756 MIN]
-----

```

FIGURE 4
CALIBRATION SPECTRA FOR
WHOI ARRAY - HYDROPHONE 4

ARL-UT
AS-74-1070
GEE
10-14-74

41<

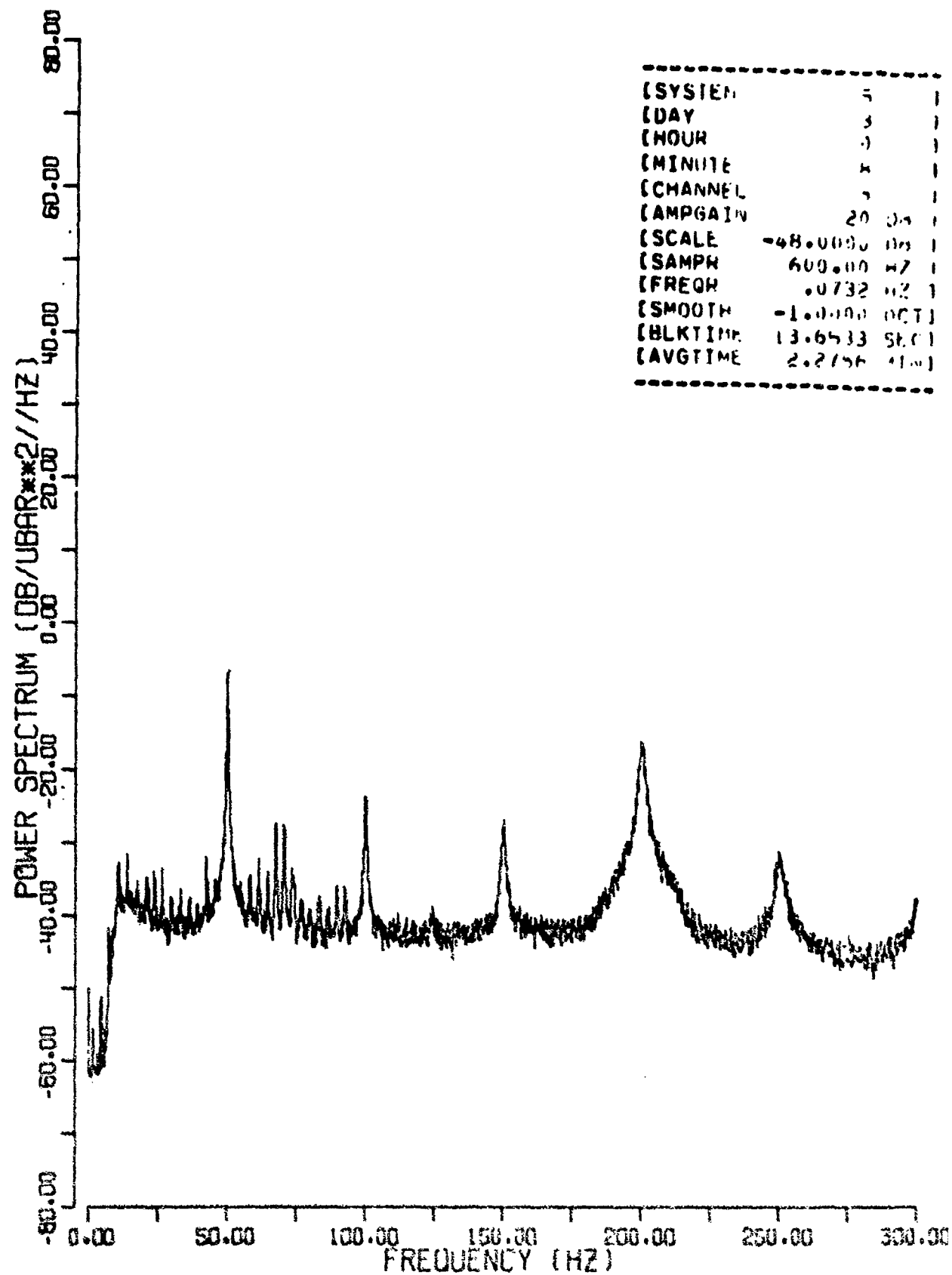


FIGURE 5
CALIBRATION SPECTRA FOR
WHOI ARRAY - HYDROPHONE 5

ARL-UT
AS-74-1071
GEE
10-14-74

42<

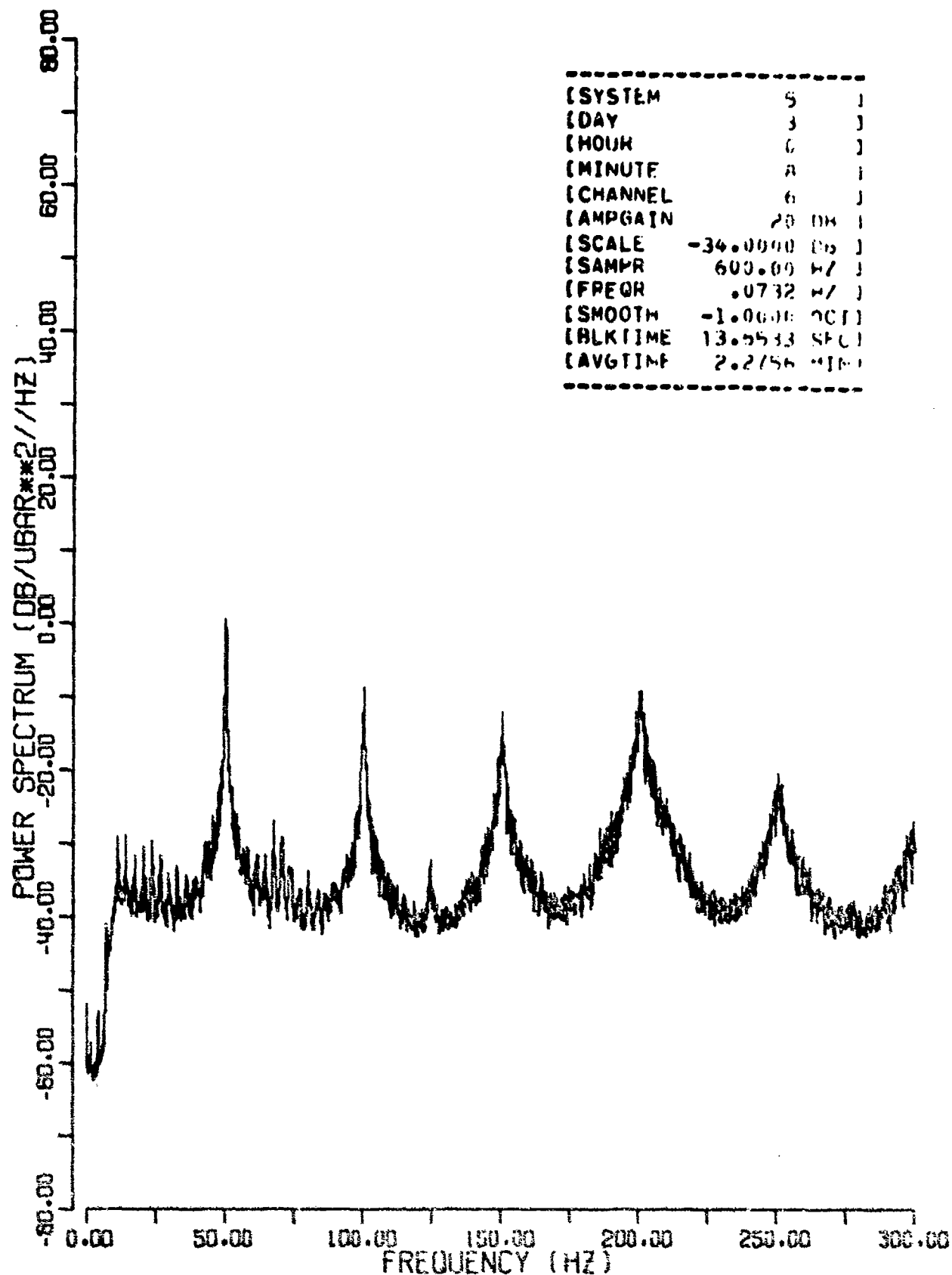
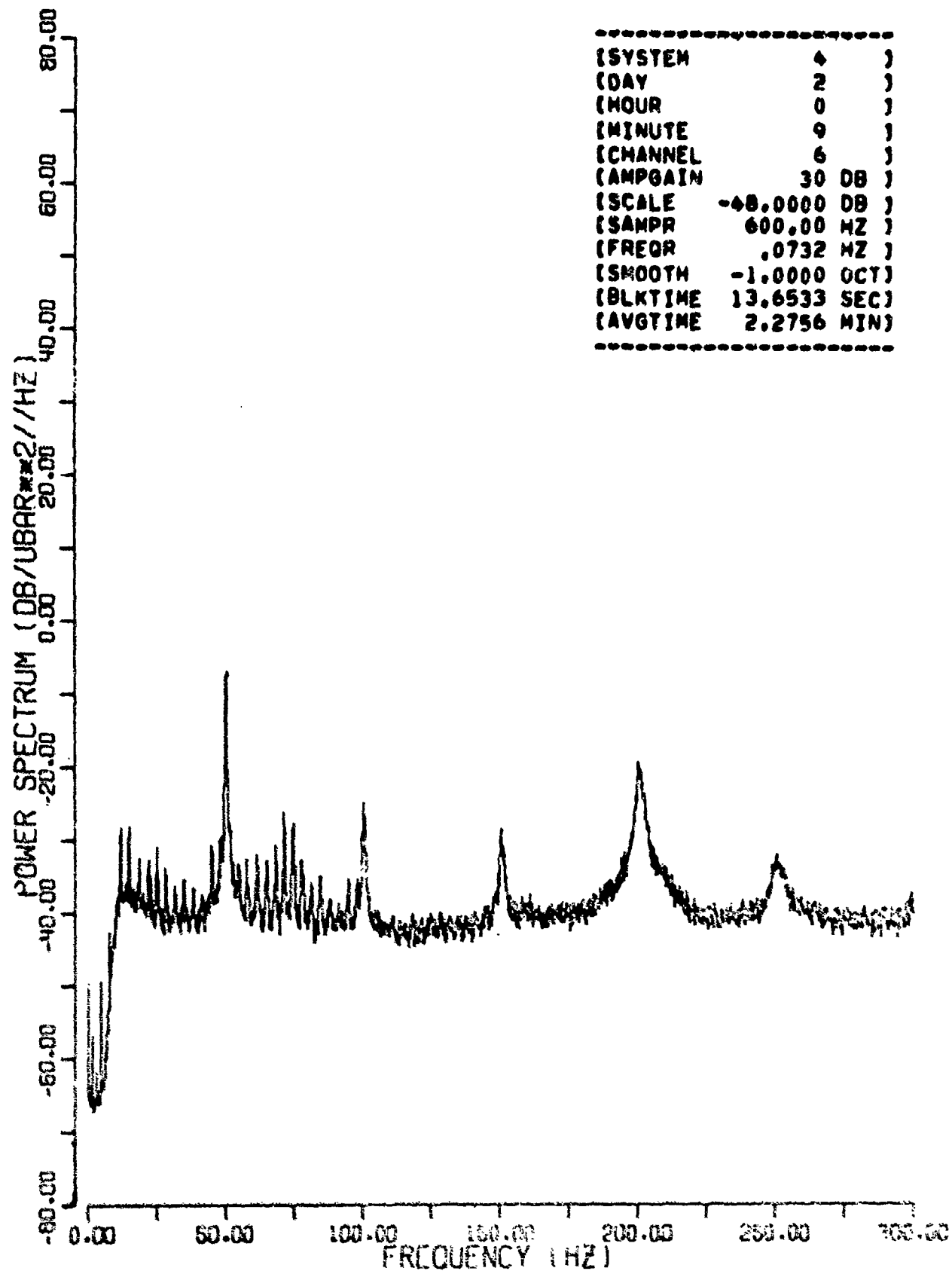


FIGURE 6
CALIBRATION SPECTRA FOR
WHOI ARRAY - HYDROPHONE 6

ARL-UT
AS-74-1072
GEE
10-14-74

43<



```

-----
(SYSTEM      4      )
(DAY        2      )
(HOUR       0      )
(MINUTE     9      )
(CHANNEL    6      )
(AMP GAIN   30 DB  )
(SCALE     -48.0000 DB )
(SAMP R    600.00 HZ )
(FREQ R     .0732 HZ )
(SMOOTH    -1.0000 OCT)
(BLK TIME   13.6533 SEC)
(AVG TIME   2.2756 MIN)
-----

```

FIGURE 7
CALIBRATION SPECTRA FOR
UM ARRAY - HYDROPHONE 6

ARL-UT
AS-74-1973
GEE
10-14-74

44<

TABLE II
CALIBRATION SPECTRA LABELS

<u>LABEL</u>	<u>EXPLANATION</u>
SYSTEM	5 WHOI Array 4 UM Array
DAY } HOUR } MIN }	Time Code
CHANNEL	Hydrophone number (top hydrophone = 1)
AMPGAIN	ACODAC Amplifier Gain as Decoded
SCALE	Playback Amplifier Gain
SAMPN	Sampling rate, Hz
FREQR	Frequency resolution, Hz
SMOOTH	Smoothing window -1 = Hanning window .3333 = 1/3 octave filter
BLKTIME	Data block length, sec
AVGTIME	Ensemble averaging time, min.

TABLE III
CALIBRATION SPECTRAL LEVELS IN DECIBELS
WHOI Array

<u>Hydrophone Number</u>	<u>Noise (10-300)</u>	<u>50</u>	<u>100</u>	<u>125</u>	<u>150</u>	<u>200</u>	<u>250</u>
1	-38	+17	-21	-18	-21	+5	-22
2	-38	+17	-36	-18	-18	+1	-34
3	-42	+5	-15	-28	-21	-2	-30
4	-39	+11	-13	-23	-22	+3	-32
5	-42	-7	-24	-39	-27	-16	-31
6	-39	+1	-9	-32	-12	-9	-20

UM Array

6	-40	-7	-25	-42	-20	-20	-32
---	-----	----	-----	-----	-----	-----	-----

Hydrophone channel 6 of the UM array showed a peak S/N of 33 dB at 50 Hz. The 200 Hz cal signal is 13 dB below the level of the 50 Hz cal signal.

The broadening of the cal spectral lines at 50 and 200 Hz may have been caused by feed over of the calibration signal into the time code track thereby causing the A/D sync signal to vary.

C. Ambient Noise Analysis

1. Data Analyzed

The data chosen for the ambient noise analysis were recorded between the 50 and 100 mile shot sequence. The decoded time code read day 3, hour 0, minutes 8 to 46 for the WHOI array and day 2, hour 0, minutes 9 to 46 for the UM array.

2. Data Reduction Procedures

The analog data on the ACODAC tapes were time compressed (40:1) in playback, bandpass filtered (10 to 300 Hz), amplified, and digitized. The A/D converter word is 11 bits plus sign and was synced to the 12th harmonic (600 Hz) of the 50 Hz carrier of the time code to minimize record/reproduce errors. The spectra were computed with a FFT algorithm with a resolution of 0.073 Hz. Each data block analyzed was 13.65 sec. A Hanning window was used for smoothing. The spectra were ensemble averaged for 11.4 min. Each spectra is corrected for the playback amplifier gain but not for the ACODAC system gain. Table IV is an explanation of the labels for the spectra.

TABLE IV
CALIBRATION SPECTRA LABELS

<u>LABEL</u>	<u>EXPLANATION</u>
SYSTEM	5 WHOI Array 4 UM Array
DAY } HOUR } MIN }	Time Code
CHANNEL	Hydrophone number (top hydrophone = 1)
AMPGAIN	ACODAC Amplifier Gain as Decoded
SCALE	Playback Amplifier Gain
SAMPR	Sampling rate, Hz
FREQR	Frequency resolution, Hz
SMOOTH	Smoothing window -1 = Hanning window .3333 = 1/3 octave filter
BLKTIME	Data block length, sec
AVGTIME	Ensemble averaging time, min.

3. Spectra

Figures 8 through 15 give the ambient noise spectra for 11.4 min of data as a function of depth. The spectral lines at frequencies less than 50 Hz are assumed to be due to ship traffic. Table V gives the relative spectral levels for the peak near 50 Hz and the system noise, both record and playback, at 300 Hz. These spectral levels and the differences between the 50 and 300 Hz levels indicate the errors resulting from the improper operation of the different hydrophone channels of the ACODAC systems and the analog tape duplication.

D. Strumming Analysis

1. Purpose

The Blake Test was conducted to evaluate the self-noise or strumming effects on the performance degradation of different hydrophone array configurations. The WHOI array is the taut array type, and the UM array is the compliant array type. The UM array parted very early in the test; therefore the only data presented is for the WHOI or taut array configuration. Spectra of ambient noise data for the frequency range of 0 to 6.25 Hz were used to illustrate the effects of strumming. The data segment was recorded beginning at time code day 3, hour 0, minute 8.

2. Data Reduction Procedures

The analog ACODAC tape was time compressed (320:1) in playback, bandpass filtered (1 Hz to 100 Hz), and amplified. This analog signal was input to a Spectral Dynamics SD301C Real Time Analyzer (RTA), which output 500 spectral lines with a frequency resolution of 0.19 Hz into the CDC 3200 digital computer. The ensemble averager of the RTA was used to average the spectra for 64 sec. The reduction procedure consisted of first digitizing the frequency markers from the RTA for reference, and then digitizing the spectra of a data segment for each hydrophone channel.

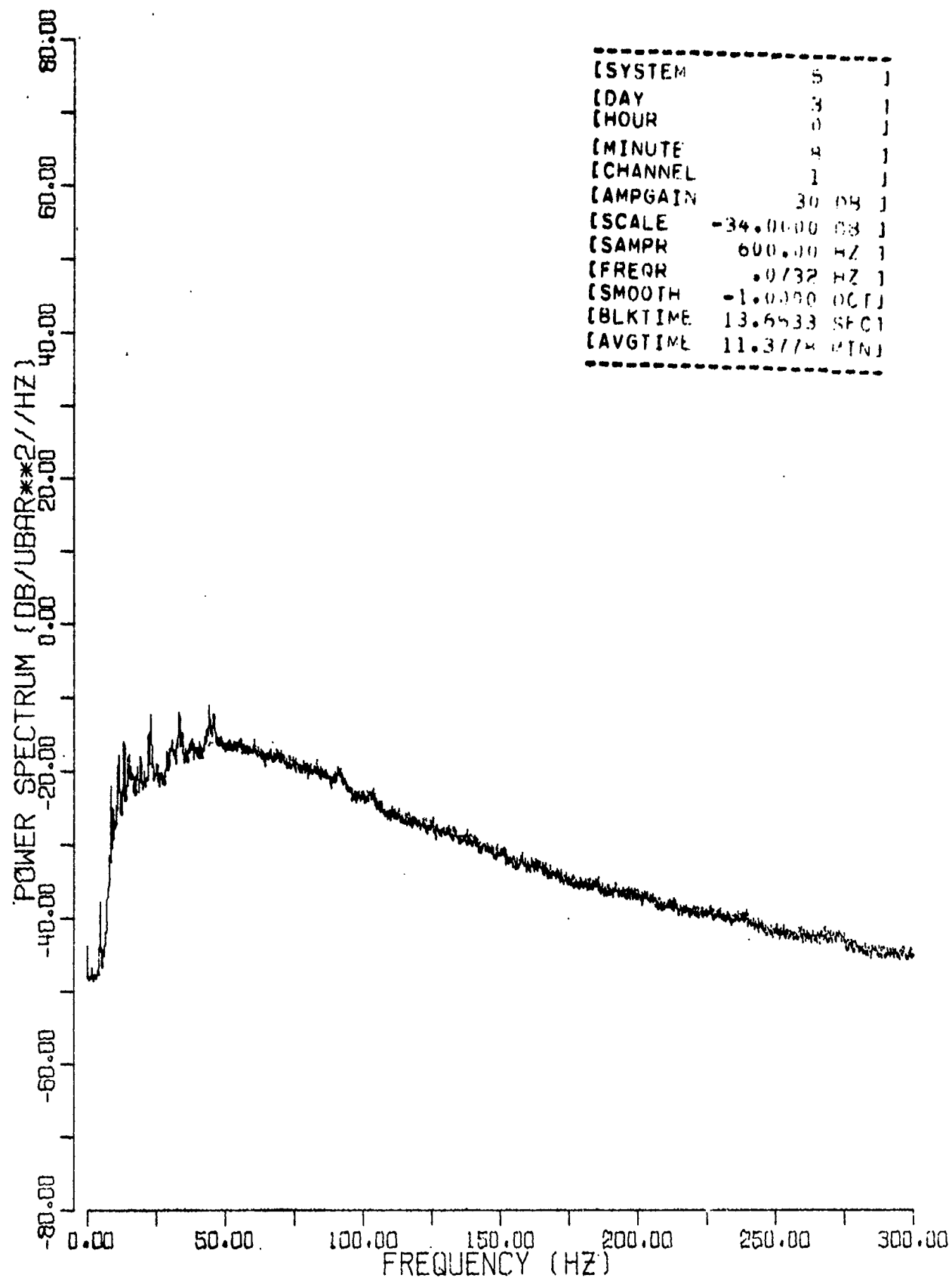


FIGURE 8
AMBIENT NOISE SPECTRA FOR
WHOI ARRAY-HYDROPHONE 1

50<

ARL-UT
AS-74-107
GEE
10-14-74

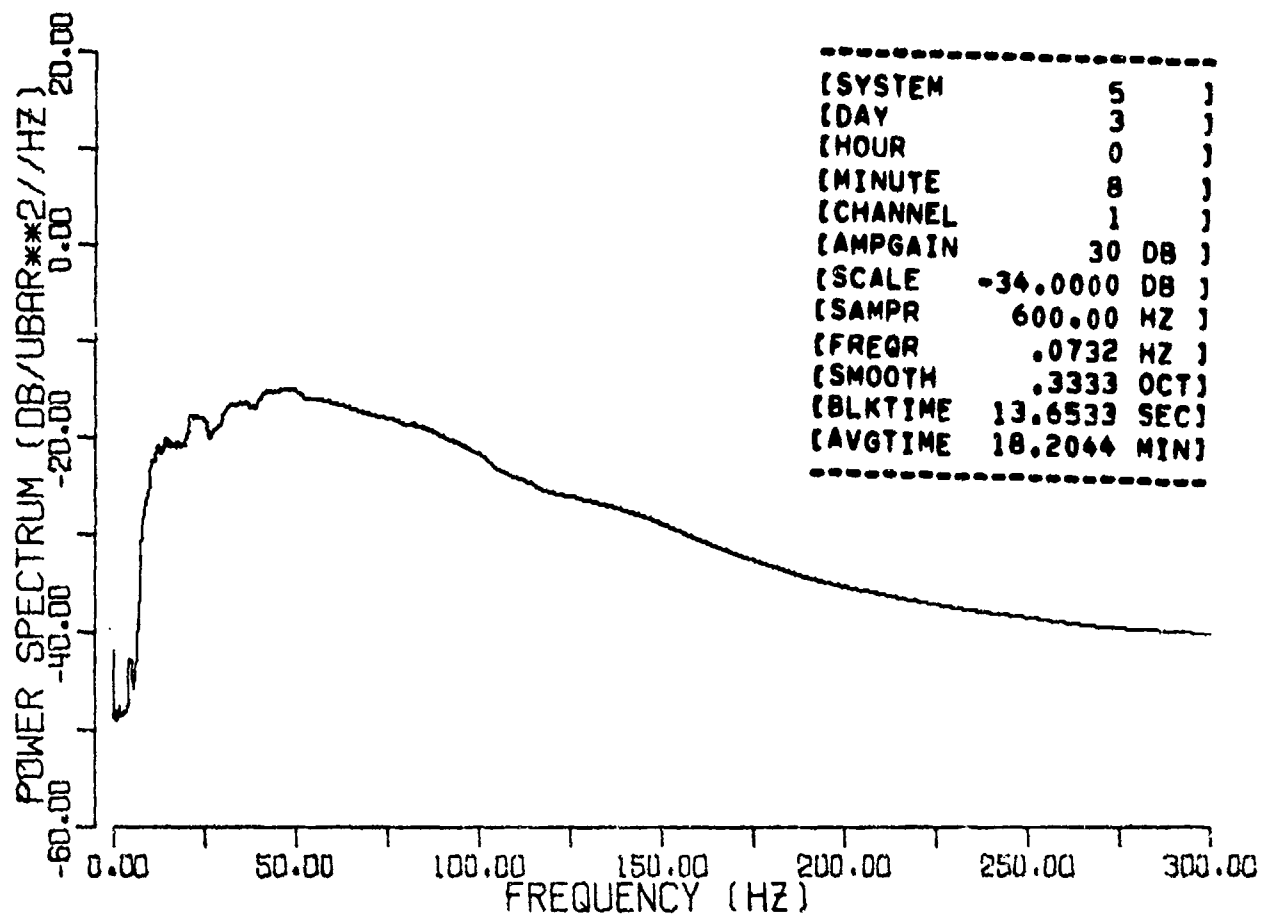


FIGURE 9

1/3 OCTAVE SPECTRA OF AMBIENT NOISE
FOR WHOI ARRAY-HYDROPHONE 1

ARL-UT
AS-74-1075
GEE
10-14-74

51<

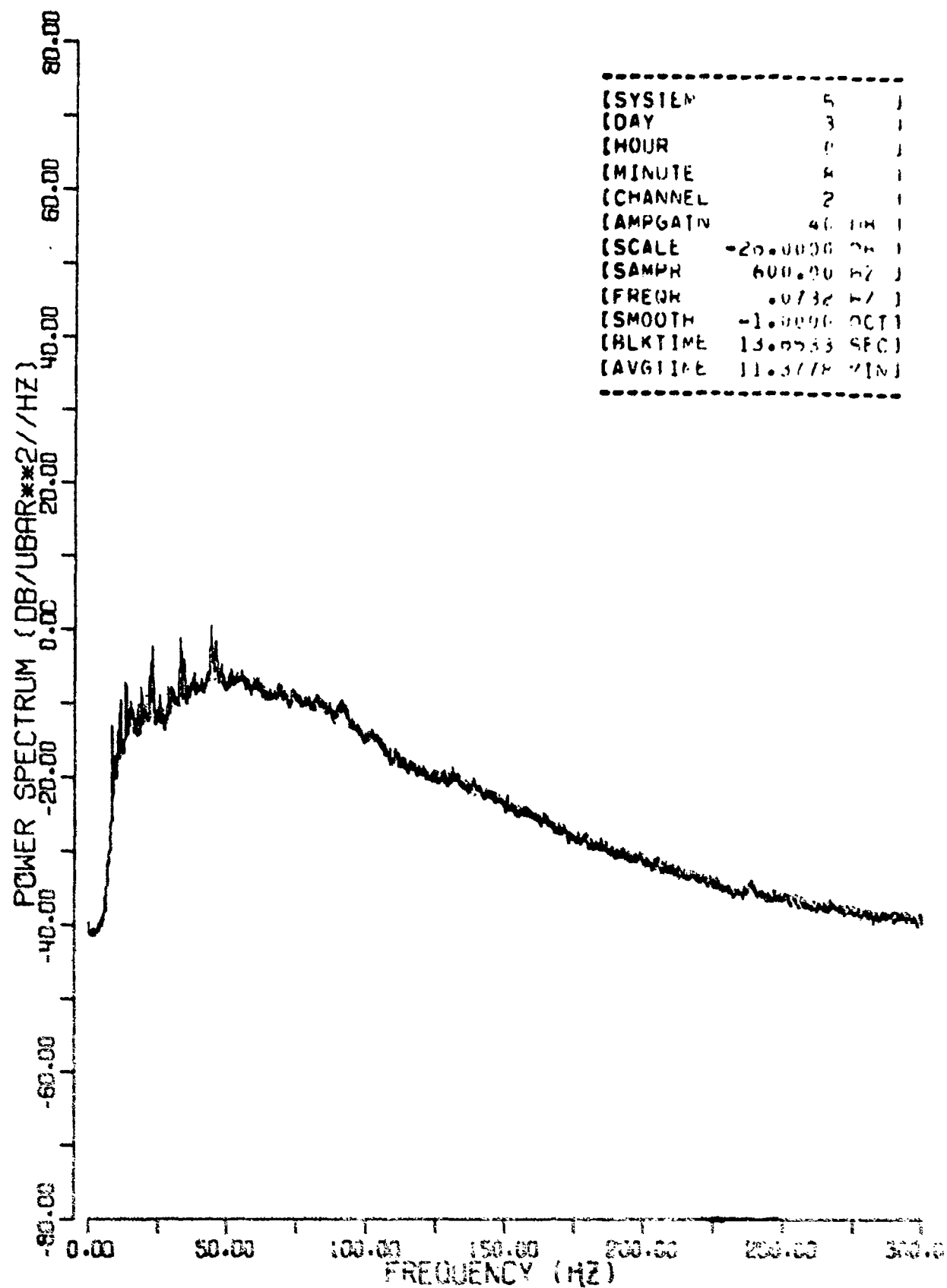
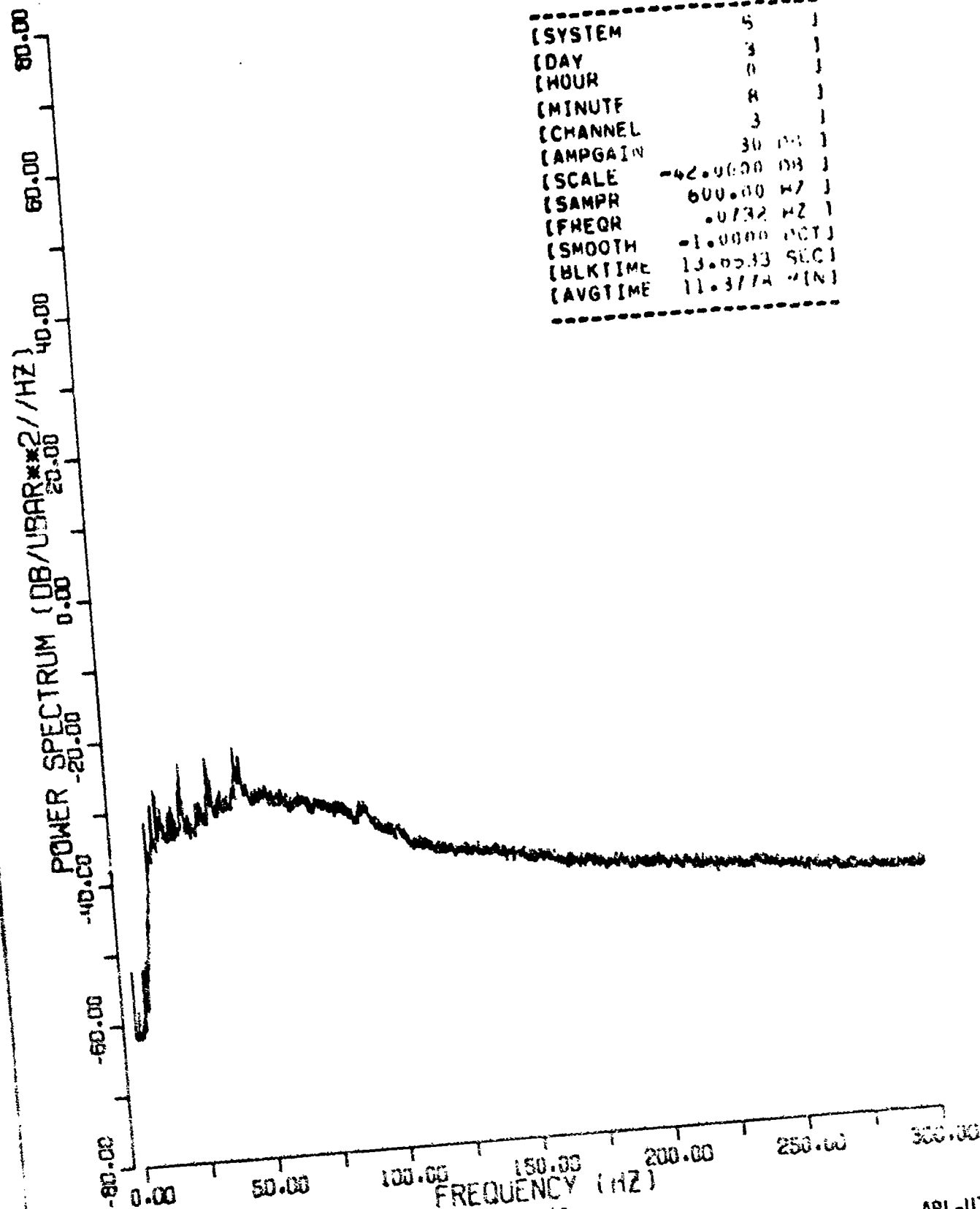


FIGURE 10
AMBIENT NOISE SPECTRA FOR
WHOI ARRAY-HYDROPHONE 2

52<

ARL-UT
AS-74-107
GEE
10-14-74



```

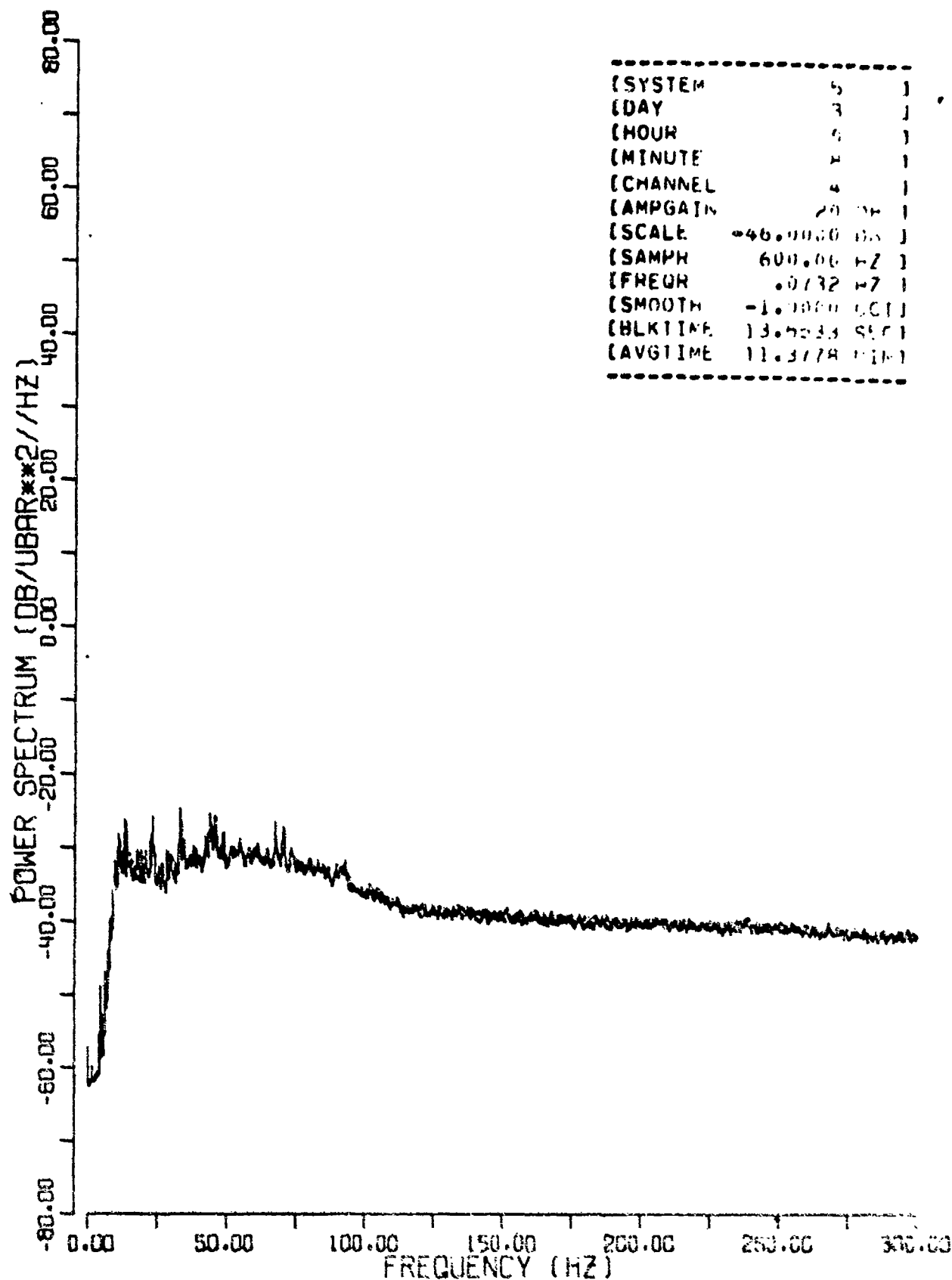
-----
[SYSTEM          5      ]
[DAY             3      ]
[HOURL           0      ]
[MINUTE          8      ]
[CHANNEL         3      ]
[AMP GAIN        30 DB ]
[SCALE          -42.00 DB ]
[SAMP RATE       600.00 HZ ]
[FREQ RES        0.732 HZ ]
[SMOOTH          -1.0000 OCT ]
[BLK TIME       13.0000 SEC ]
[AVG TIME       11.3774 MIN ]
-----

```

FIGURE 11
 AMBIENT NOISE SPECTRA FOR
 W-31 ARRAY-HYDROPHONE 3

53<

ARL-UT
 AS-74-1077
 GEE
 10-14-74



```

-----
[SYSTEM      5      ]
[DAY         3      ]
[HOURL       6      ]
[MINUTE      4      ]
[CHANNEL     4      ]
[AMPGAIN     20.00  ]
[SCALE      -46.0000 DB ]
[SAMPR       600.00 HZ ]
[FREQUR      0.0732 HZ ]
[SMOOTH      -1.0000 OCT]
[BLKTIME     13.0033 SEC]
[AVGTIME     11.3778 MIN]
-----

```

FIGURE 12
 AMBIENT NOISE SPECTRA FOR
 WHOI ARRAY-HYDROPHONE 4

54<

ARL-UT
 AS-74-1078
 GEE
 10-14-74

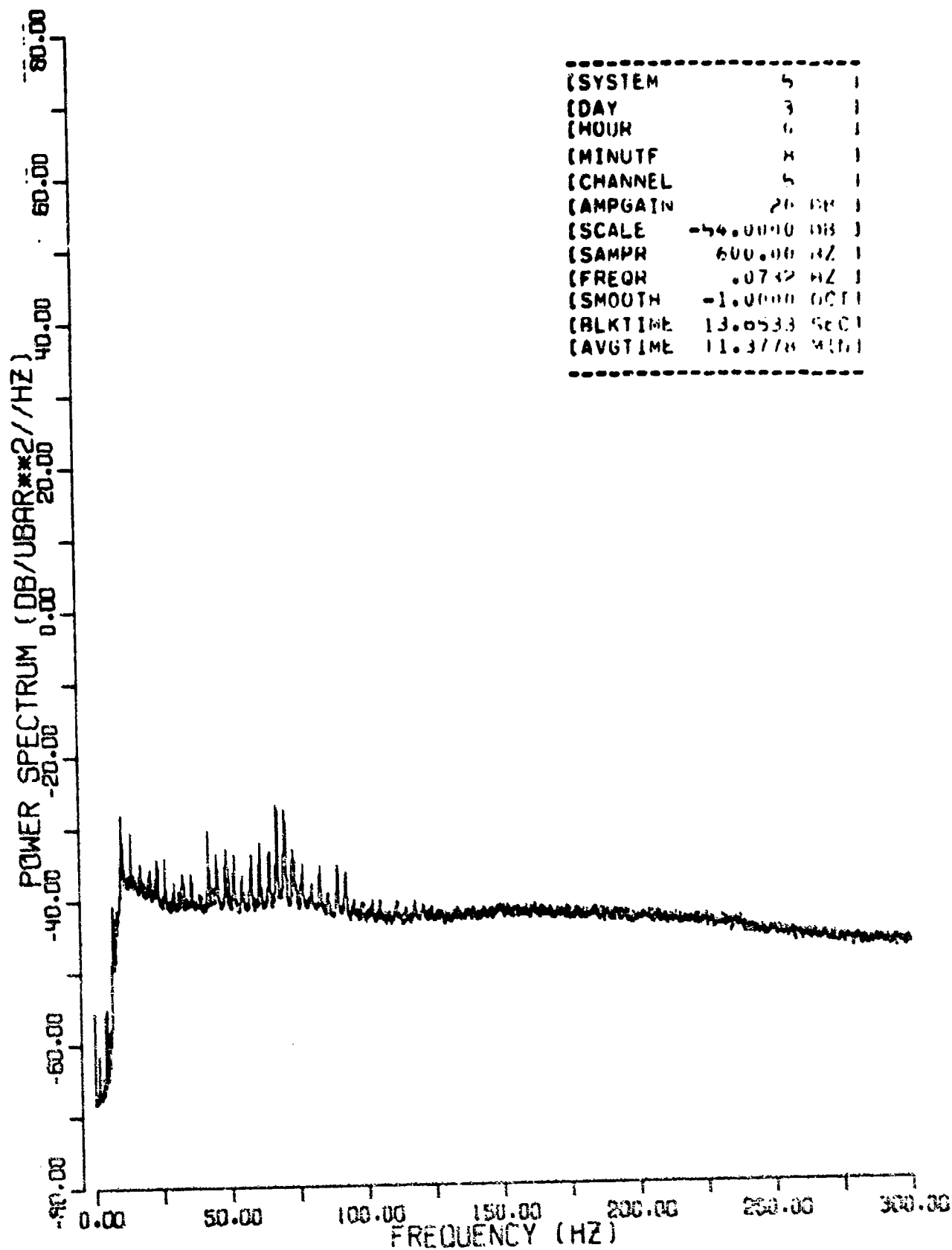


FIGURE 13
 AMBIENT NOISE SPECTRA FOR
 WHOI ARRAY-HYDROPHONE 5

ARL-UT
 AS-74-1079
 GEE
 10-14-74

55<

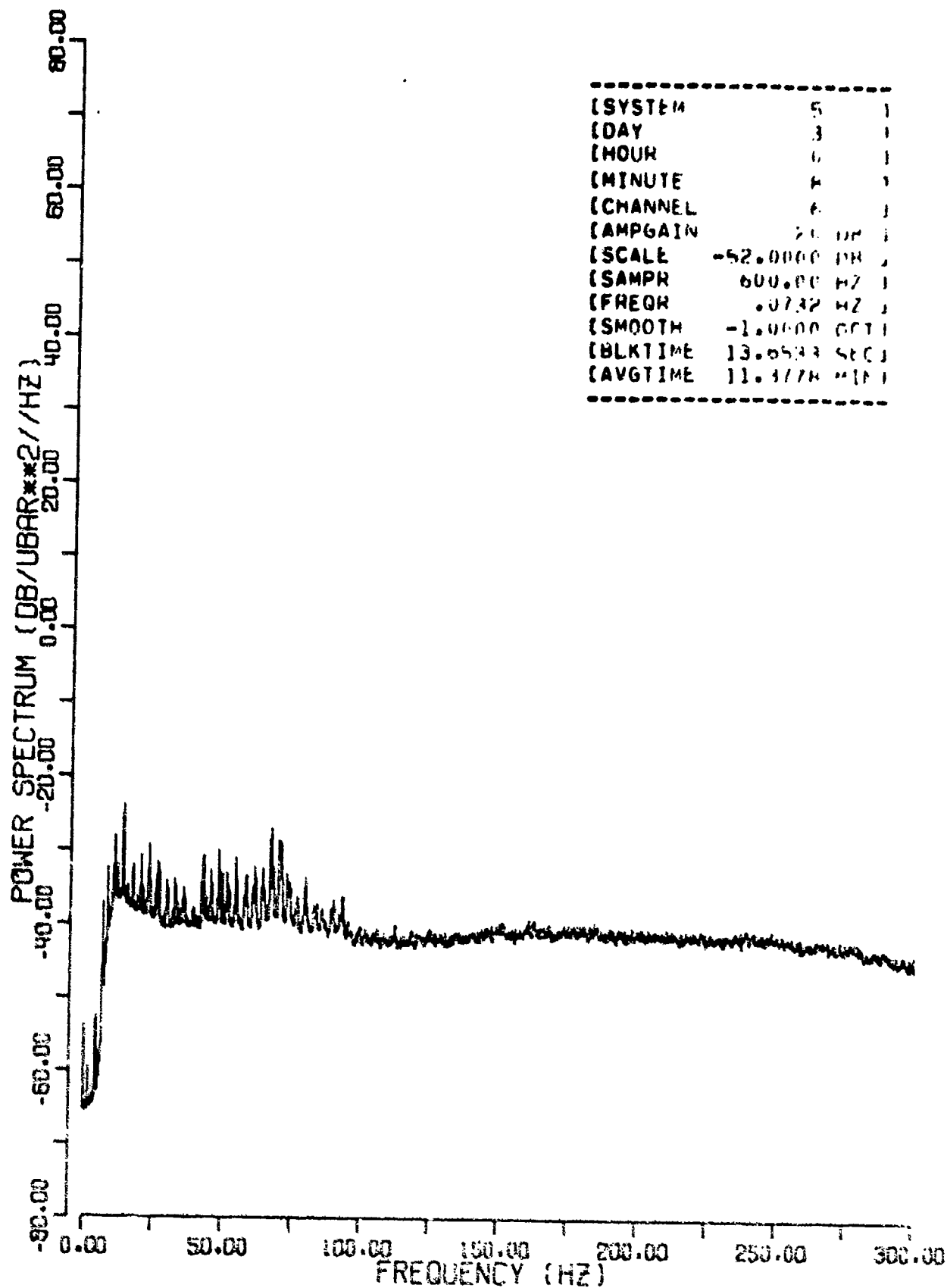


FIGURE 14
 AMBIENT NOISE SPECTRA FOR
 WHOI ARRAY-HYDROPHONE 6

56<

ARL-UT
 AS-74-1080
 GEE
 10-14-74

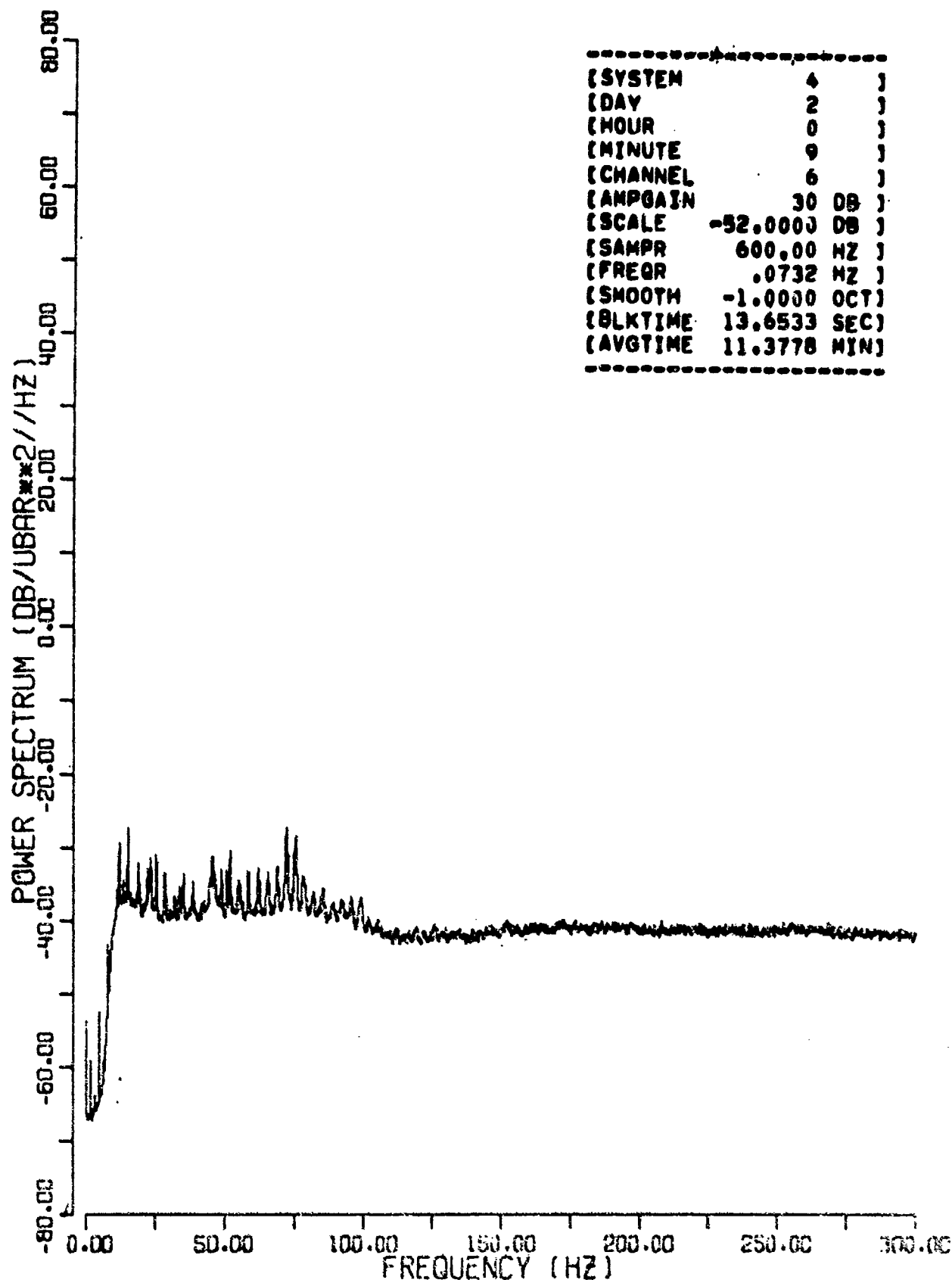


FIGURE 15
AMBIENT NOISE SPECTRA FOR
UM ARRAY-HYDROPHONE 6

ARL-UT
AS-74-1081
GEE
10-14-74

57<

TABLE V
 AMBIENT NOISE
 RELATIVE SPECTRAL LEVELS IN DECIBELS
 WHOI Array

Hydrophone Number	Relative Spectral Levels		Difference Between Levels
	50 Hz	300 Hz (system noise)	
1	-16	-45	29
2	-7	-39	32
3	-29	-46	17
4	-31	-41	10
5	-40	-47	7
6	-40	-45	5

UM Array

6	-39	-42	3
---	-----	-----	---

The spectra are relative in magnitude on a channel-to-channel basis since the ACODAC system gain corrections have not been applied. Playback system noise spectra levels are shown for hydrophone channels 5 and 6.

3. Results

Figures 16 through 21 are time varying spectra of the ambient noise field. These spectra illustrate the large levels below 6 to 25 Hz due to the strumming or self-noise of the array. The effects of the large amplitude low frequency signals in depressing the gains of the ACODAC amplifiers and reducing the dynamic range of the system are illustrated in the spectra. The effects of the strumming vary from hydrophone channel to hydrophone channel. The decoded ACODAC amplifier gains are 30, 40, 30, 20, 20, and 20 dB on hydrophone channels 1 through 6, respectively.

E. Shot Data Analysis

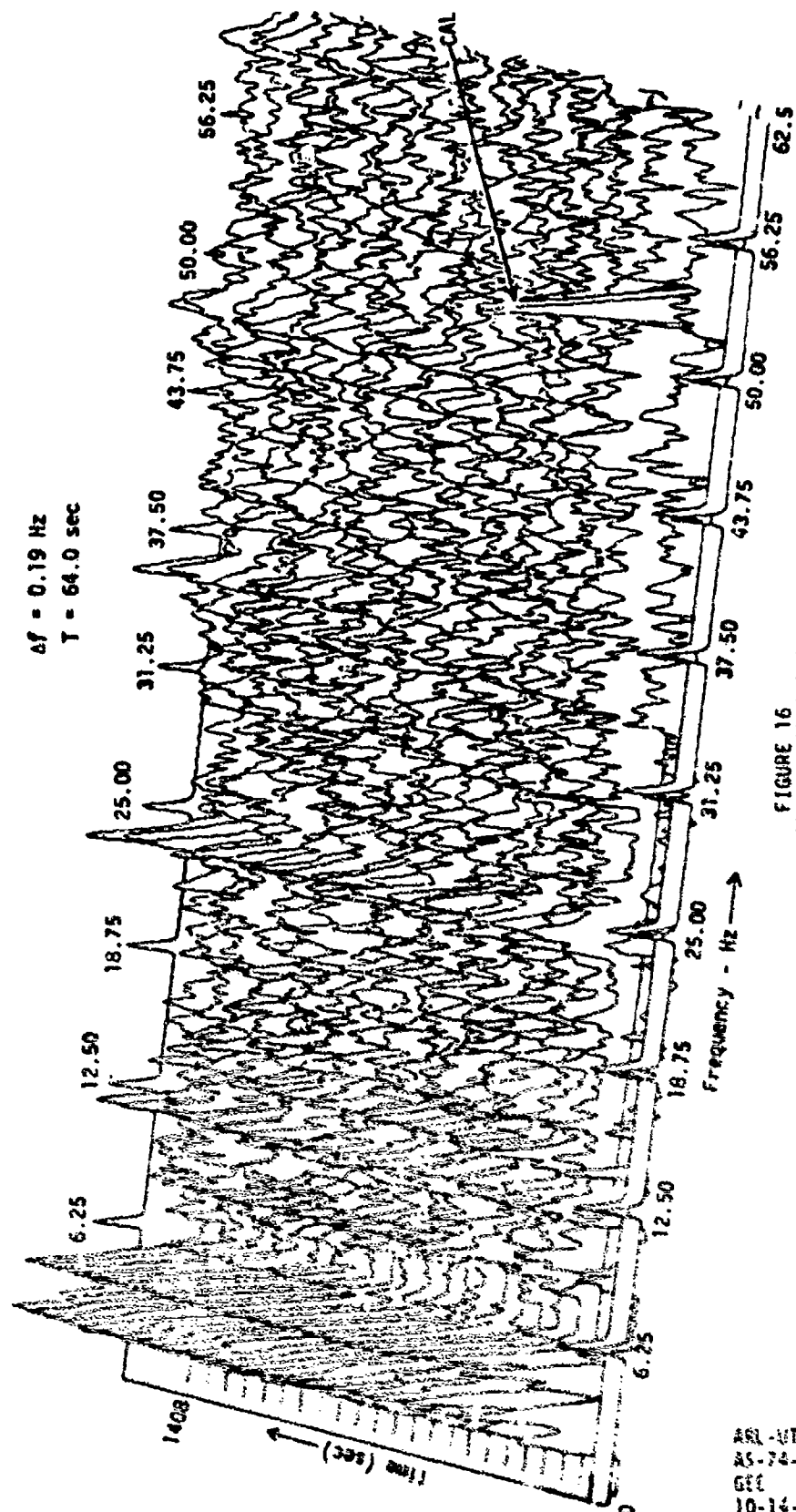
1. Introduction

Shots were dropped as sources at ranges of 10, 20, 50, and 100 miles from the two ACODACS. For each range, at least two shots each were used at depths of 300 and 800 ft. The actual shot pattern as determined from the ACODAC tapes is shown in Table VI.

TABLE VI - SHOT PATTERN

Range from Arrays, miles	Number of Shots at each Depth	
	300 ft	800 ft
10	4	2
20	3	3
50	2	2
100	3	3

59<



$\Delta f = 0.19 \text{ Hz}$
 $T = 64.0 \text{ sec}$

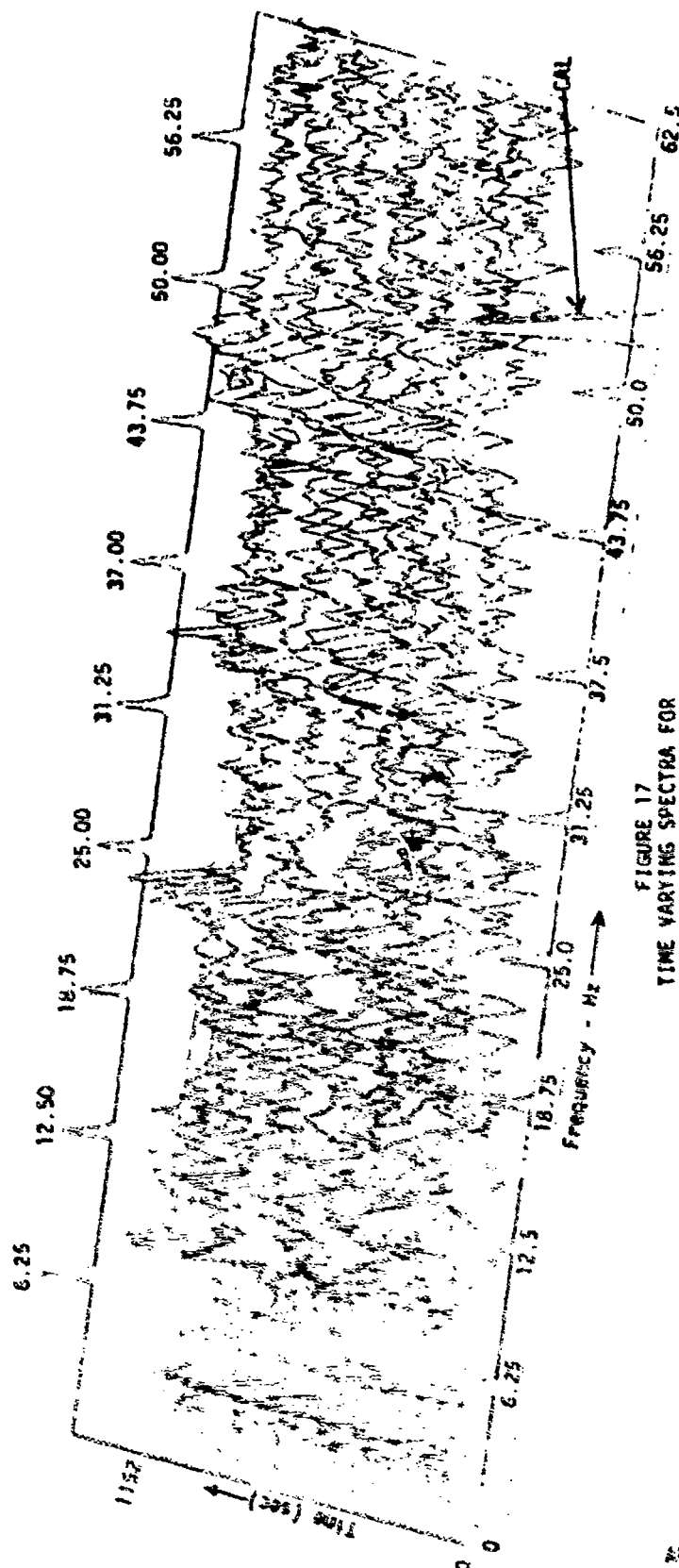


FIGURE 17
 TIME VARYING SPECTRA FOR
 MICROPHONE 2

ARL-UT
 AS-74-1083
 GII
 10-14-74

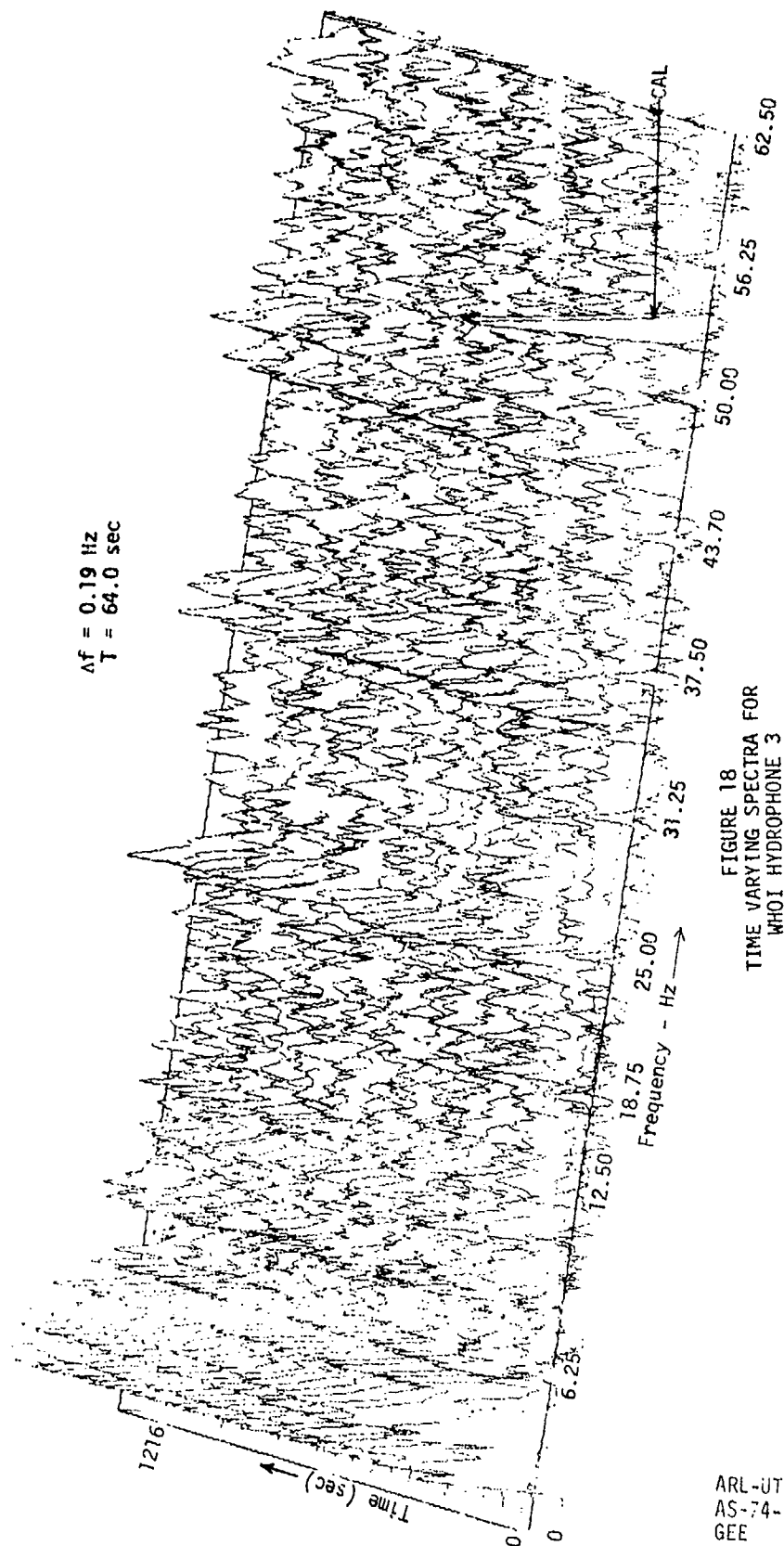


FIGURE 18
 TIME VARYING SPECTRA FOR
 WHOI HYDROPHONE 3

ARL-UT
 AS-74-1084
 GEE
 10-14-74

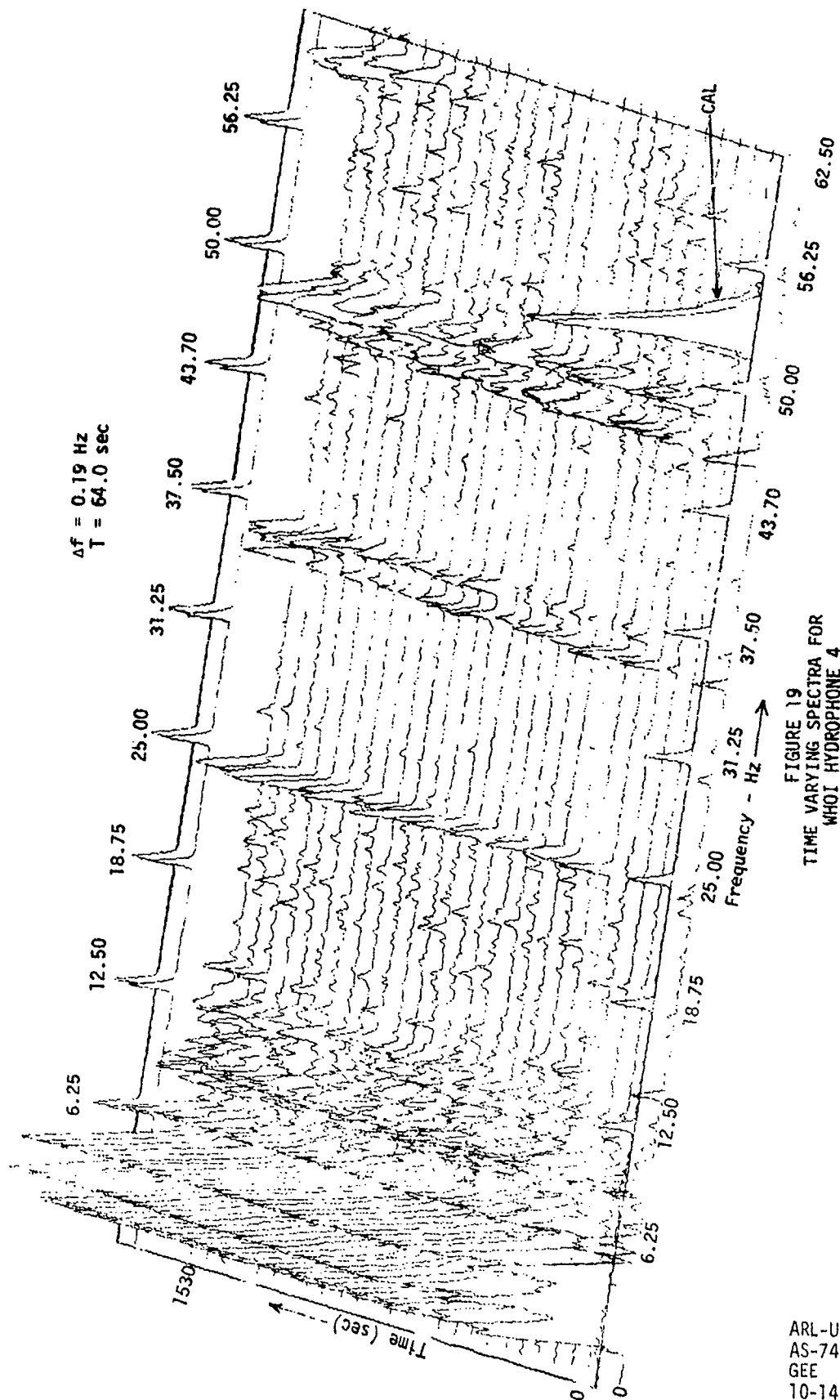


FIGURE 19
 TIME VARYING SPECTRA FOR
 WHOI HYDROPHONE 4

ARL-UT
 AS-74-1085
 GEE
 10-14-74

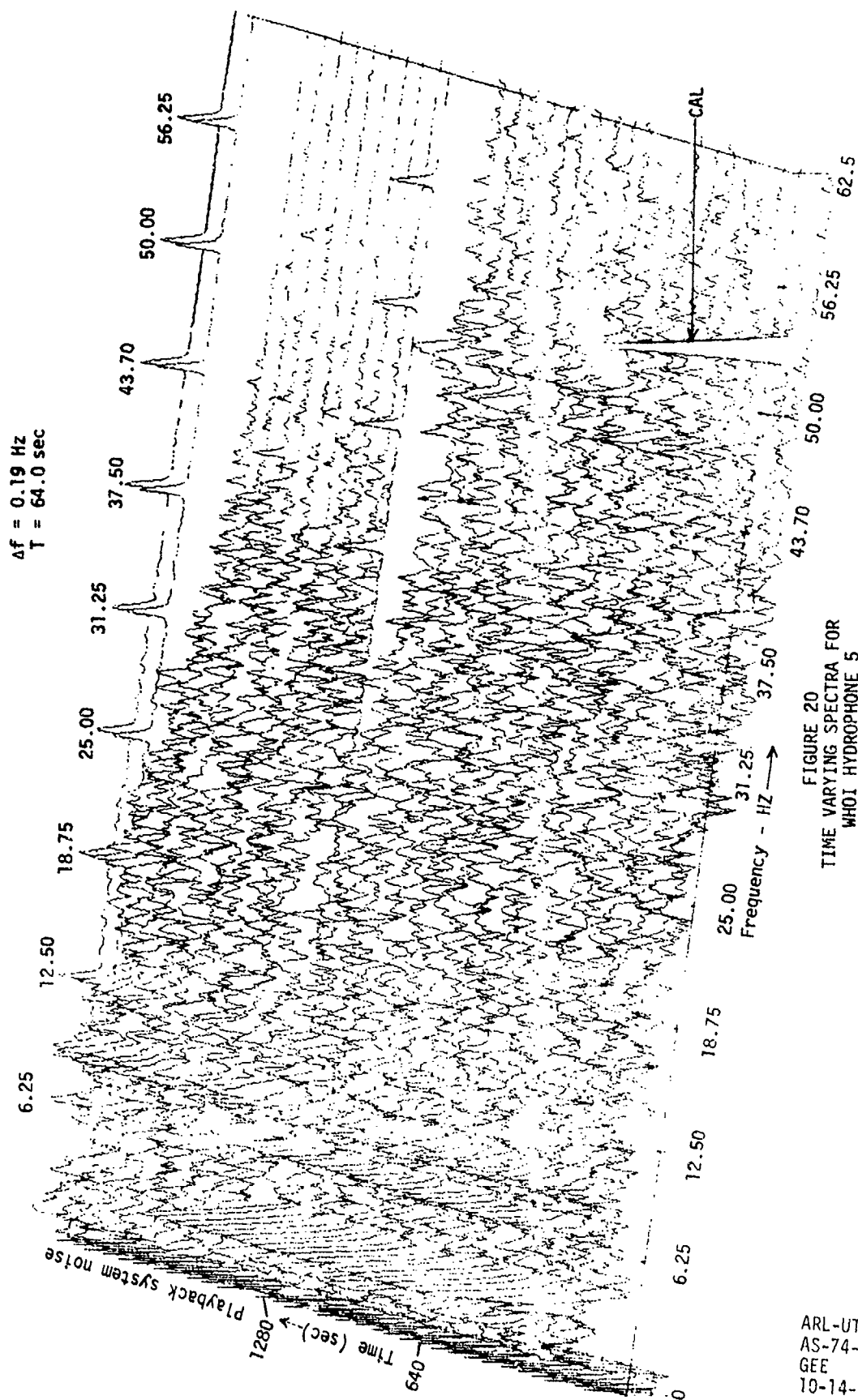


FIGURE 20
 TIME VARYING SPECTRA FOR
 WHOI HYDROPHONE 5

ARL-UT
 AS-74-1086
 GEE
 10-14-74

$\Delta f = 0.19 \text{ Hz}$
 $T = 64.0 \text{ sec}$

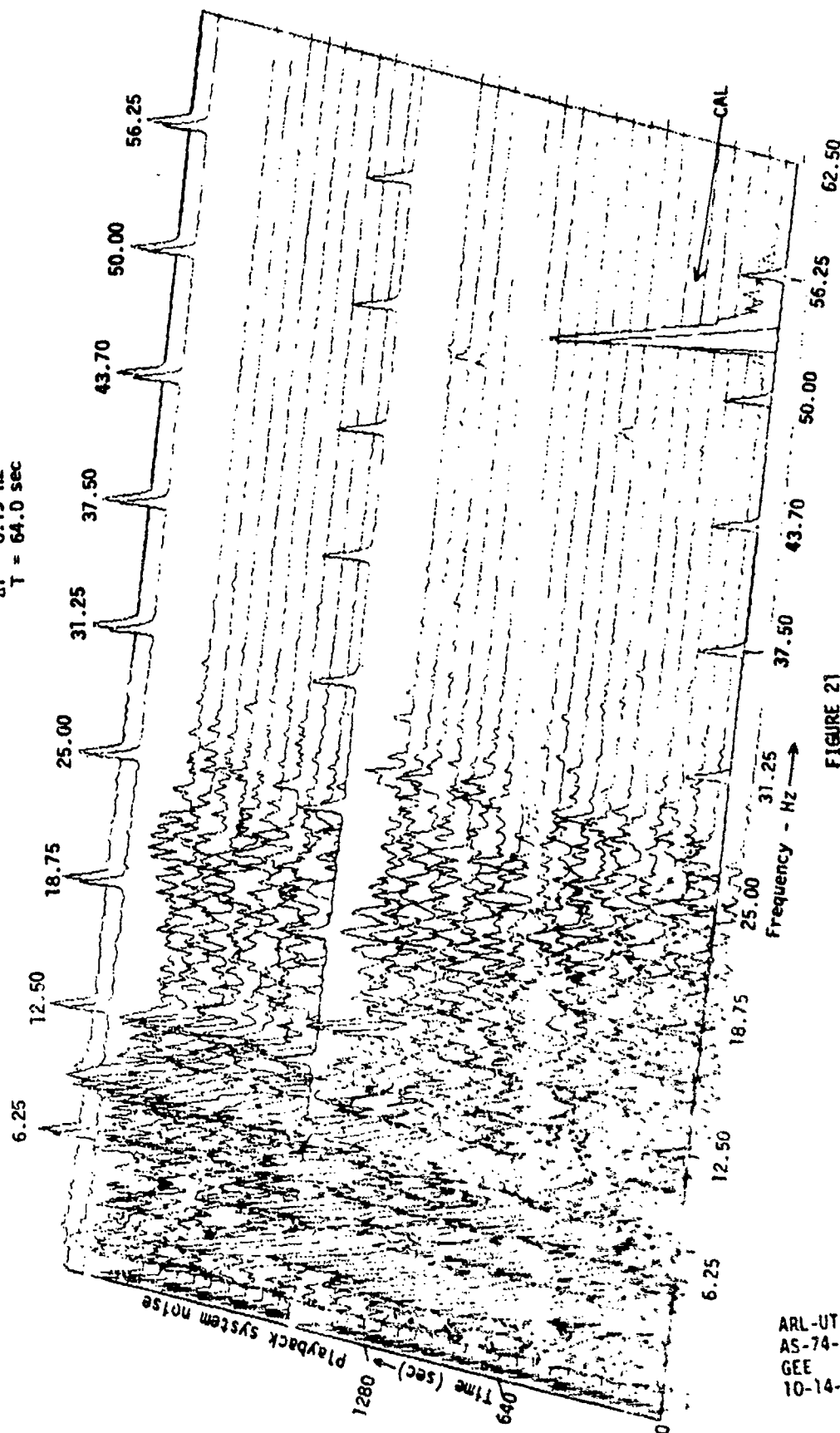


FIGURE 21
 TIME VARYING SPECTRA FOR
 WHOI HYDROPHONE 6

ARL-UT
 AS-74-1087
 GEE
 10-14-74

For digitizing, the analog ACODAC tape was passed through a 10 to 300 Hz bandpass filter. The sampling rate of 600 Hz was obtained from the 12th harmonic of the 50 Hz carrier on the time code channel. This phase locked sampling technique eliminated wow and flutter introduced by the recording and playback processes. For each shot sequence of two to four shots (at a given range), the digitizing process was started by using the first shot in the sequence as a trigger. After the trigger, 20 consecutive blocks of 8192 samples (13.65 sec at the 600 Hz sampling rate) were obtained for a total continuous digital record length of 273 sec. An example of one such sample sequence is shown in Figs. 22 and 23. These illustrate the signals from hydrophone 1 of the WHOI ACODAC for shots at 300 ft and a 10 mile range. The illustrations are from hard copies of an off-line CRT presentation of the digitized data. Four shots, including the trigger shot, are clearly shown. Recording system gain changes are obvious in the figures.

2. Multipath Structure of Signals

The second, third, and fourth shots, in Figs. 22 and 23, exhibit multipath structure with at least three large stable multipath signals following the principal arrival. In Fig. 24, an expanded presentation of the data for the second shot is shown. Also shown is the output of the same hydrophone for the 800 ft shot at the same 10 mile range. The multipath structure is similar for the two depths except that the third and fourth arrivals are earlier for the 800 ft shot. These third and fourth arrivals also appear to consist of two destructively interfering signals for the 800 ft shot.

3. Signal-to-Noise Ratio

The principal arrival for the second shot in each sequence of shots was selected for S/N analysis. The S/N was estimated according to two definitions of S/N (Fig. 25). The two S/N estimates are computed

66<

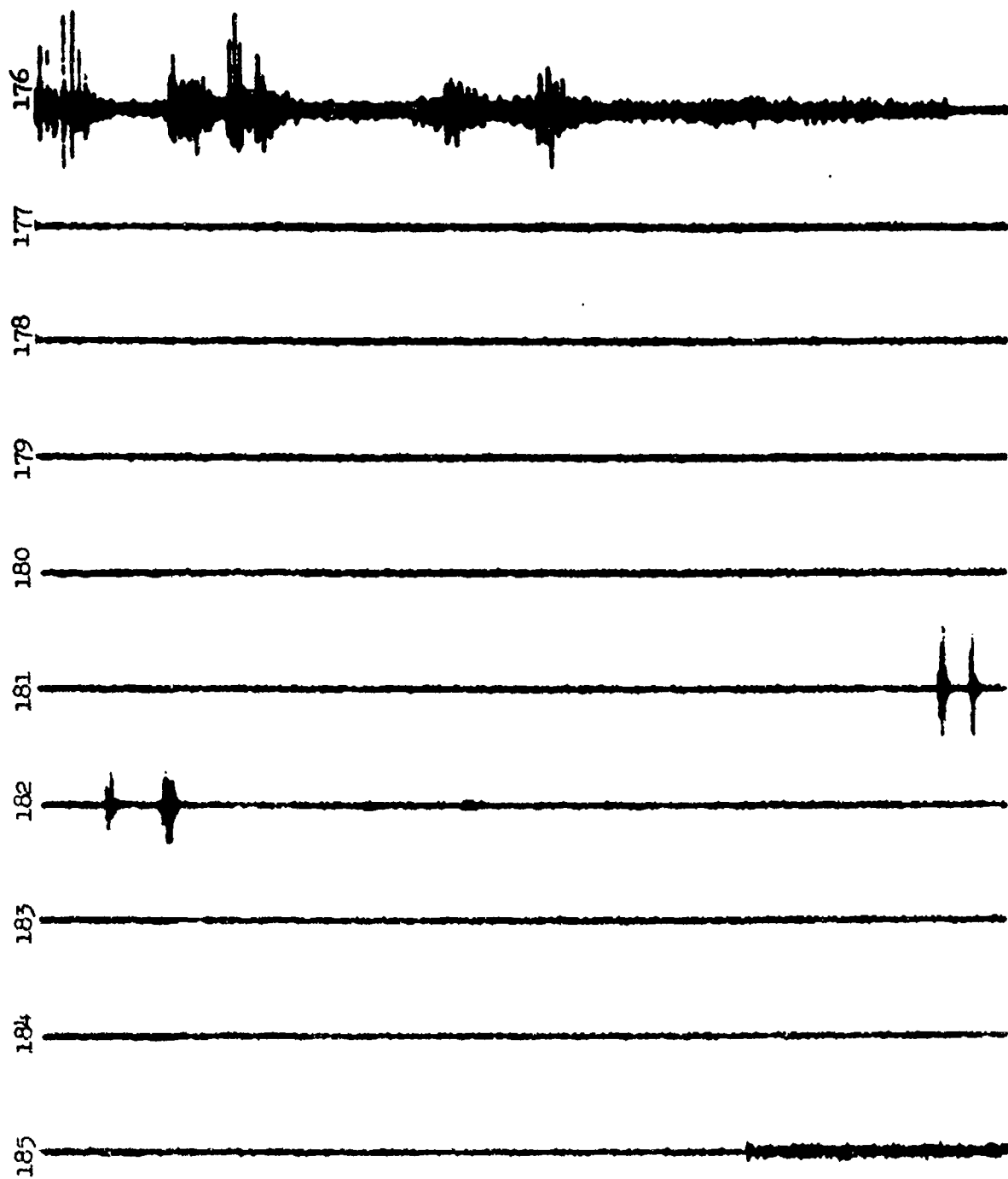


FIGURE 22
 AMPLITUDE VERSUS TIME, DIGITIZED RECORD
 4-SHOT SEQUENCE, 10 mile RANGE,
 300 ft SHOT DEPTH, WHOI HYDROPHONE 1
 FIRST HALF

67<

ARL-UT
 AS-74-1088
 GEE
 10-14-74

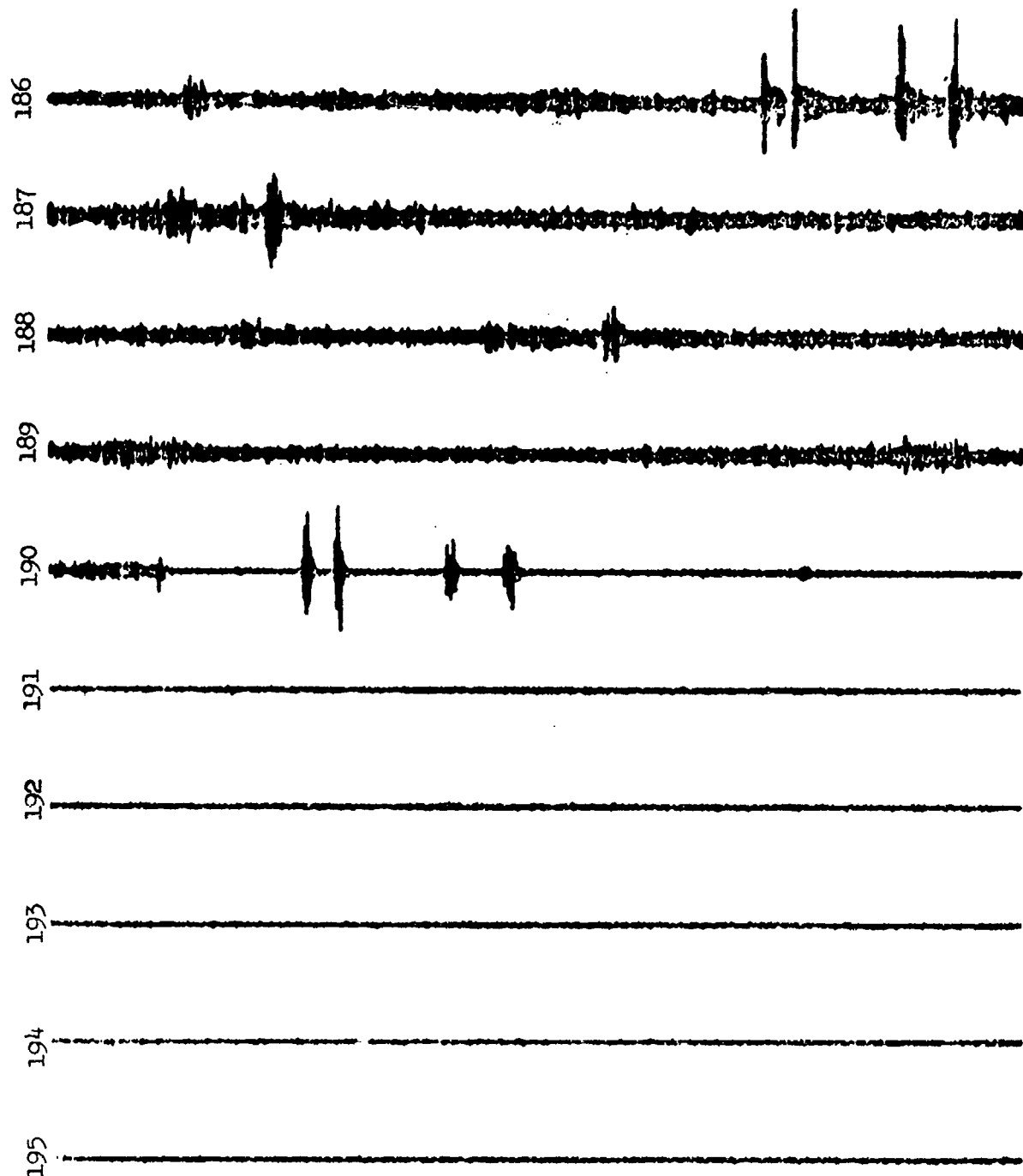


FIGURE 23
 AMPLITUDE VERSUS TIME, DIGITIZED RECORD
 4-SHOT SEQUENCE, 10 mile RANGE,
 300 ft SHOT DEPTH, WHOI HYDROPHONE 1
 FIRST HALF

68<

ARL-UT
 AS-74-
 GEE
 10-14-

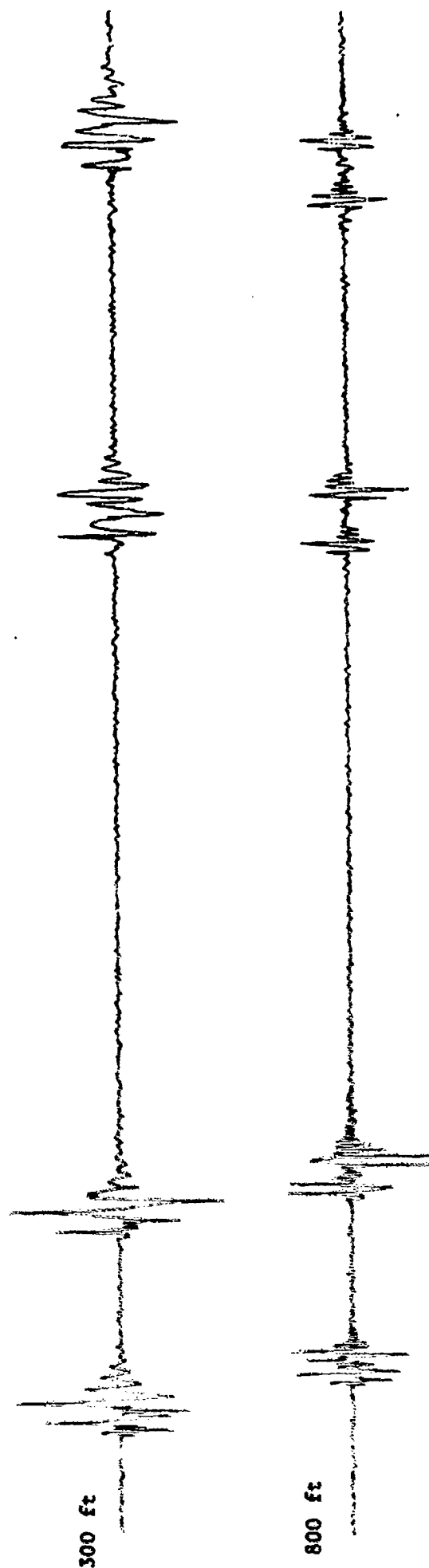
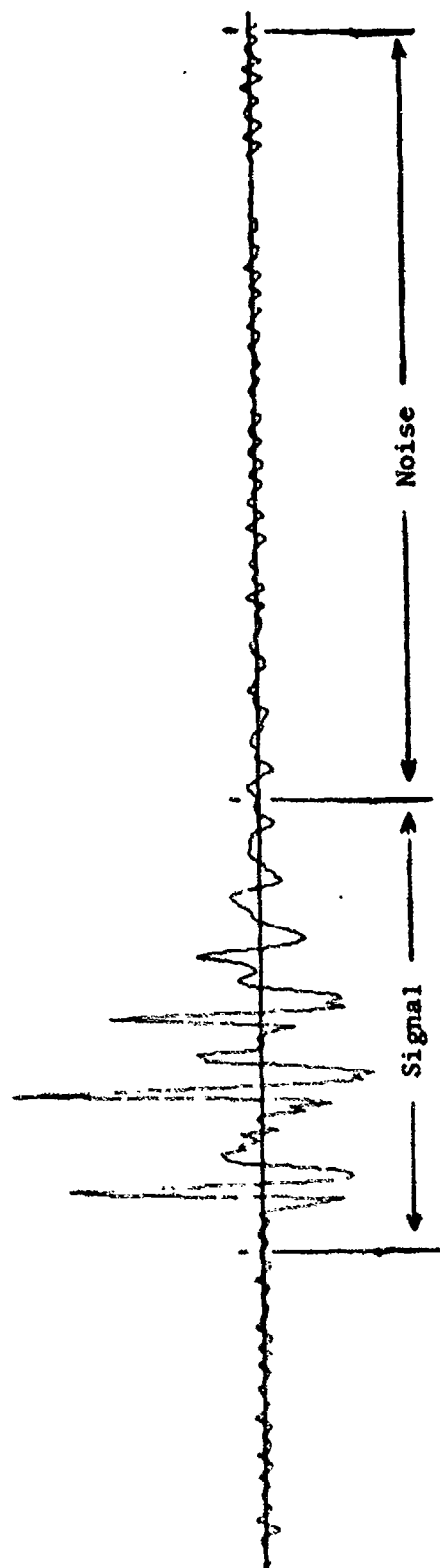


FIGURE 24
 AMPLITUDE VERSUS TIME RECORD OF TWO SHOTS
 SHOWING MULTIPATH ARRIVALS,
 10 mile RANGE, WHOI HYDROPHONE 1

63



$$\text{Energy } S/N = 10 \log S/N$$

S = Signal Energy/Duration of Signal

N = Average Intensity of Noise

$$\text{Peak } S/N = 10 \log P^2/N$$

P = Maximum Amplitude of Signal

FIGURE 25
ESTIMATION OF SHOT SIGNAL-TO-NOISE
RATIO (S/N)

70<

using the peak of the signal and the average energy of the signal. Based on the previous ARL examination of the shot S/N (Section I), an averaging time of 0.33 sec was used in estimating the average noise intensity.

In Fig. 26, the amplitude versus time plot is shown for the second shot of each sequence, received by hydrophone 1 of the WHOI ACODAC. Also shown in Fig. 26 are the S/N's for each of the illustrated shots. The temporal limits used in computing average signal energy are indicated in the illustration. This same set of information is given for the signals from the remaining hydrophones in Appendix A.

The S/N results for all hydrophones are summarized in Table VII. Some clearly discernible trends in these data are further illustrated in Figs. 27 through 34.

In Fig. 27, the peak S/N is shown versus hydrophone number (WHOI ACODAC) for the 10 mile range shots. Subsequent figures show these ratios for successively greater ranges: 20 miles (Fig. 28), 50 miles (Fig. 29), and 100 miles (Fig. 30). At the 10 and 20 mile ranges, the near surface hydrophones exhibit the best values of S/N, with S/N decreasing with increasing depth of the hydrophone. At the 50 mile range, a greatly reduced S/N is evident in the data from hydrophone 3, with values from the deep hydrophones almost equaling the two shallowest ones. At the 100 mile range, hydrophones 2, 3, and 4 possess the higher S/N values, with the ratio falling off both above and below these depths. Clearly, the most consistently high S/N values are exhibited by hydrophone 2, though hydrophone 1 shows higher S/N for some ranges and shot depths.

These conclusions are further illustrated in Fig. 31, where S/N values for hydrophones 1 and 2 are plotted versus range. The greatly

TABLE VII

SIGNAL-TO-NOISE RATIOS: SHOT DATA

Range/Depth of Charge	Hydrophone						
	W1	W2	W3	W4	W5	W6	M6
10 miles, 300 ft	27.8	28.2	28.7	24.6	20.6	11.1	21.3
	39.9	37.9	40.1	33.0	32.1	22.5	28.7
10 miles, 800 ft	23.5	21.5	20.7	17.9	20.3	12.8	14.4
	32.3	33.0	33.0	27.2	31.5	25.6	27.9
20 miles, 300 ft	25.4	20.2	27.7	23.9	22.0	14.0	7.11
	39.2	32.9	38.1	37.0	31.9	23.9	19.2
20 miles, 800 ft	28.8	22.4	25.2	23.7	16.0	14.8	19.3
	40.1	33.3	35.3	36.2	26.8	27.8	28.8
50 miles, 300 ft	19.8	19.8	8.84	15.7	11.7	10.5	5.15
	29.2	29.2	19.6	25.3	24.3	26.0	18.9
50 miles, 800 ft	27.7	21.1	5.16	19.1	21.6	15.5	3.20
	36.2	34.8	14.5	31.9	35.2	27.6	13.9
100 miles, 300 ft	12.5	24.9	24.3	24.6	No	7.05	5.29
	25.3	37.1	34.8	37.5	Signal	17.2	14.9
100 miles, 800 ft	19.9	22.4	24.4	23.9	16.8	10.8	0.45
	32.1	34.9	37.5	35.2	29.2	22.1	11.1

Energy S/N

Peak S/N









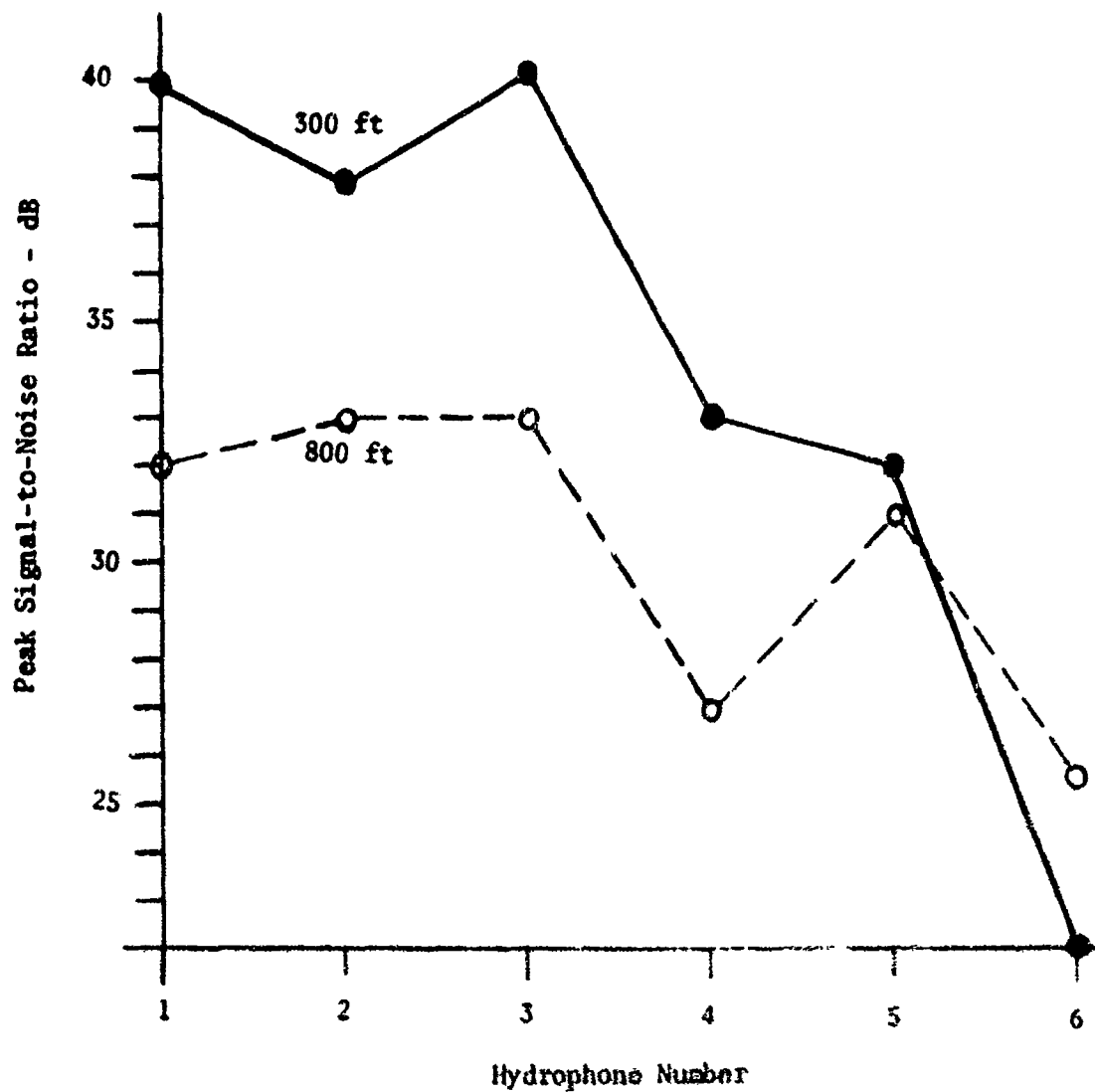
		S/N - dB	
		Energy	Peak
W1-10-300		27.8	39.9
W1-10-800		23.5	32.2
W1-20-300		25.4	39.2
W1-20-800		28.8	40.1
W1-50-300		19.8	29.2
W1-50-800		27.7	36.2
W1-100-300		12.5	25.3
W1-100-800		19.7	32.0

FIGURE 26
SHOT SIGNAL AND SIGNAL-TO-NOISE RATIO

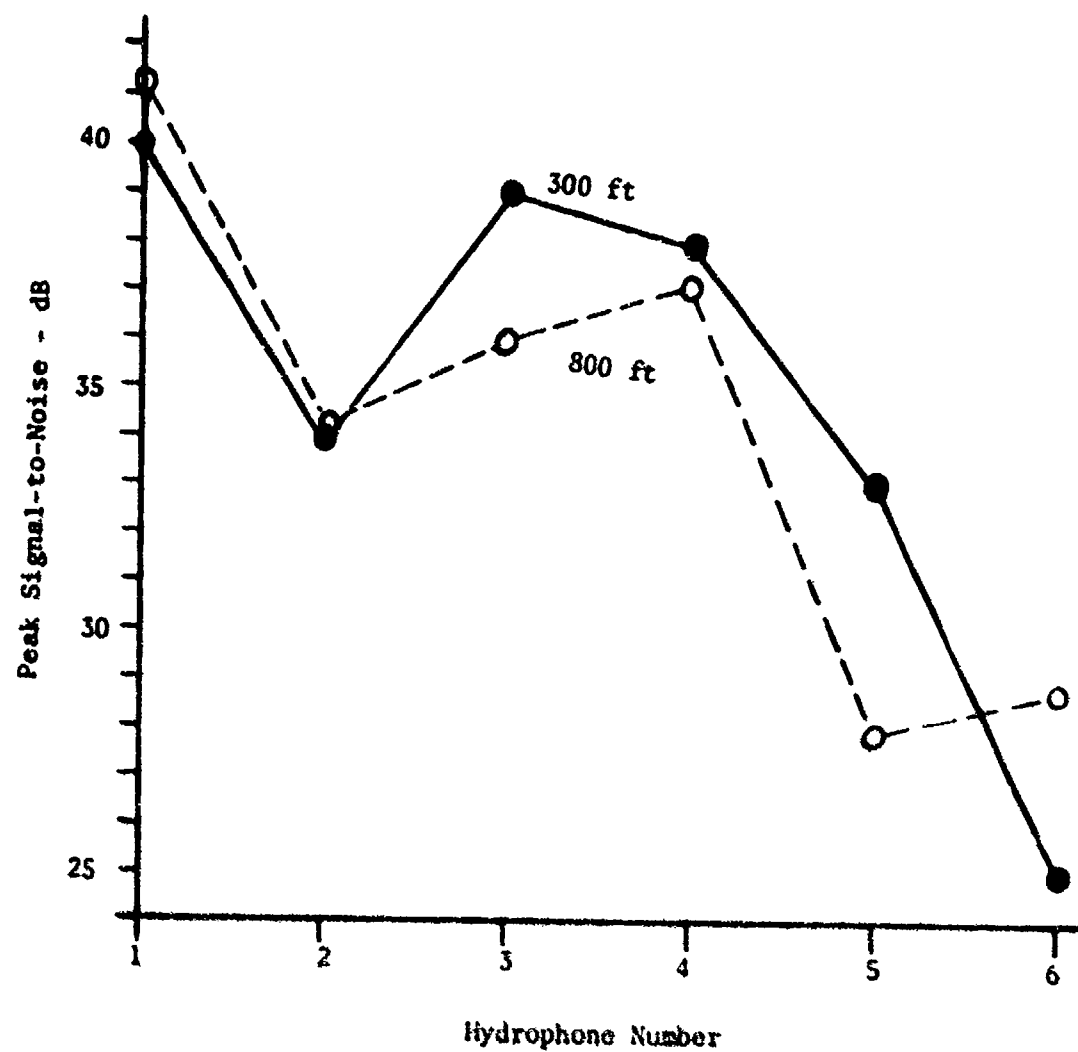
ARL-UT
AS-74-1092
GEE
10-14-74



Range of Shot = 10 miles

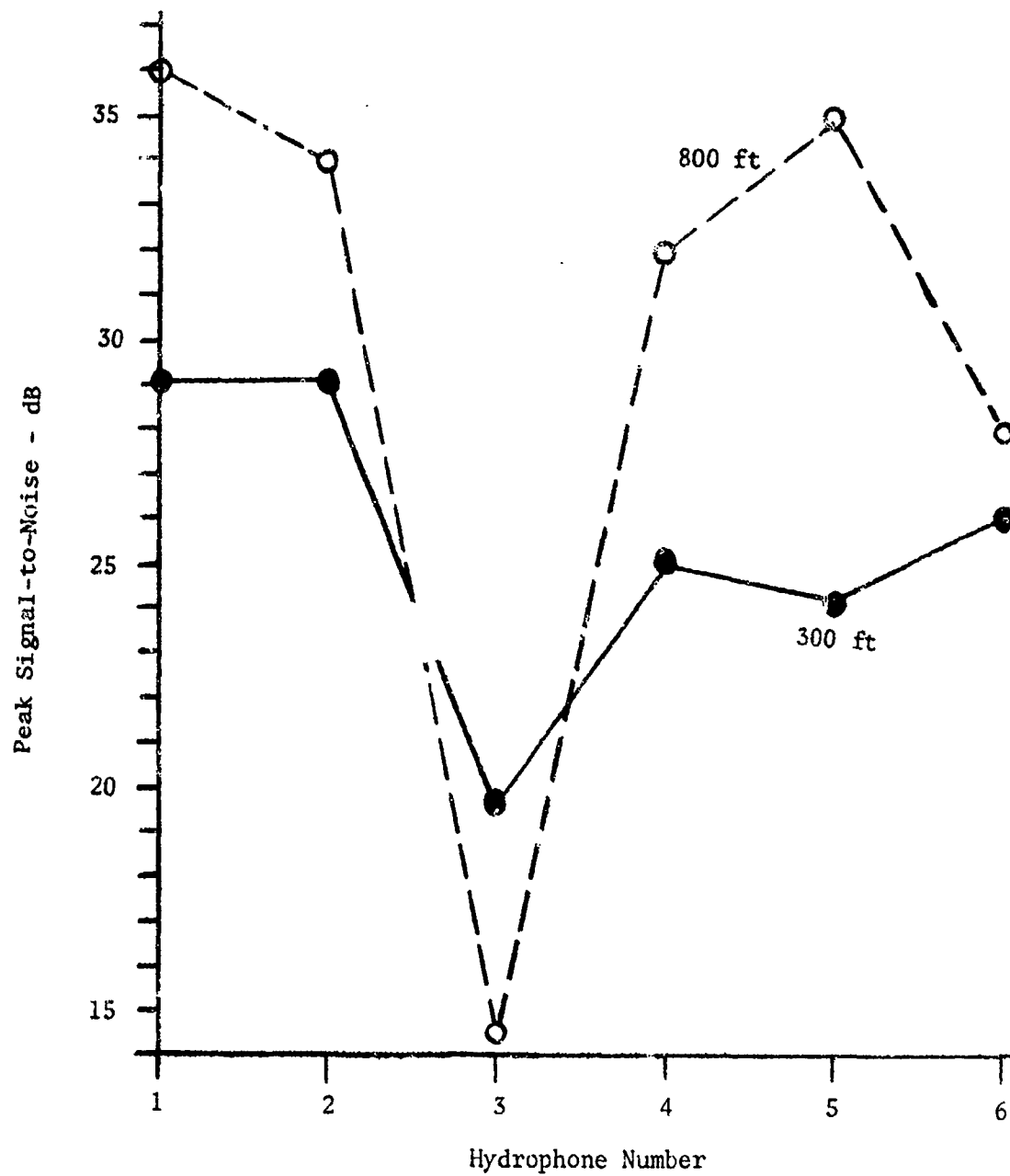
FIGURE 27
SIGNAL-TO-NOISE RATIO OF SHOT DATA AS A FUNCTION
OF WHOI HYDROPHONE NUMBER

74-



Range = 20 miles

FIGURE 28
SIGNAL-TO-NOISE RATIO OF SHOT DATA AS A FUNCTION
OF WHOI HYDROPHONE NUMBER

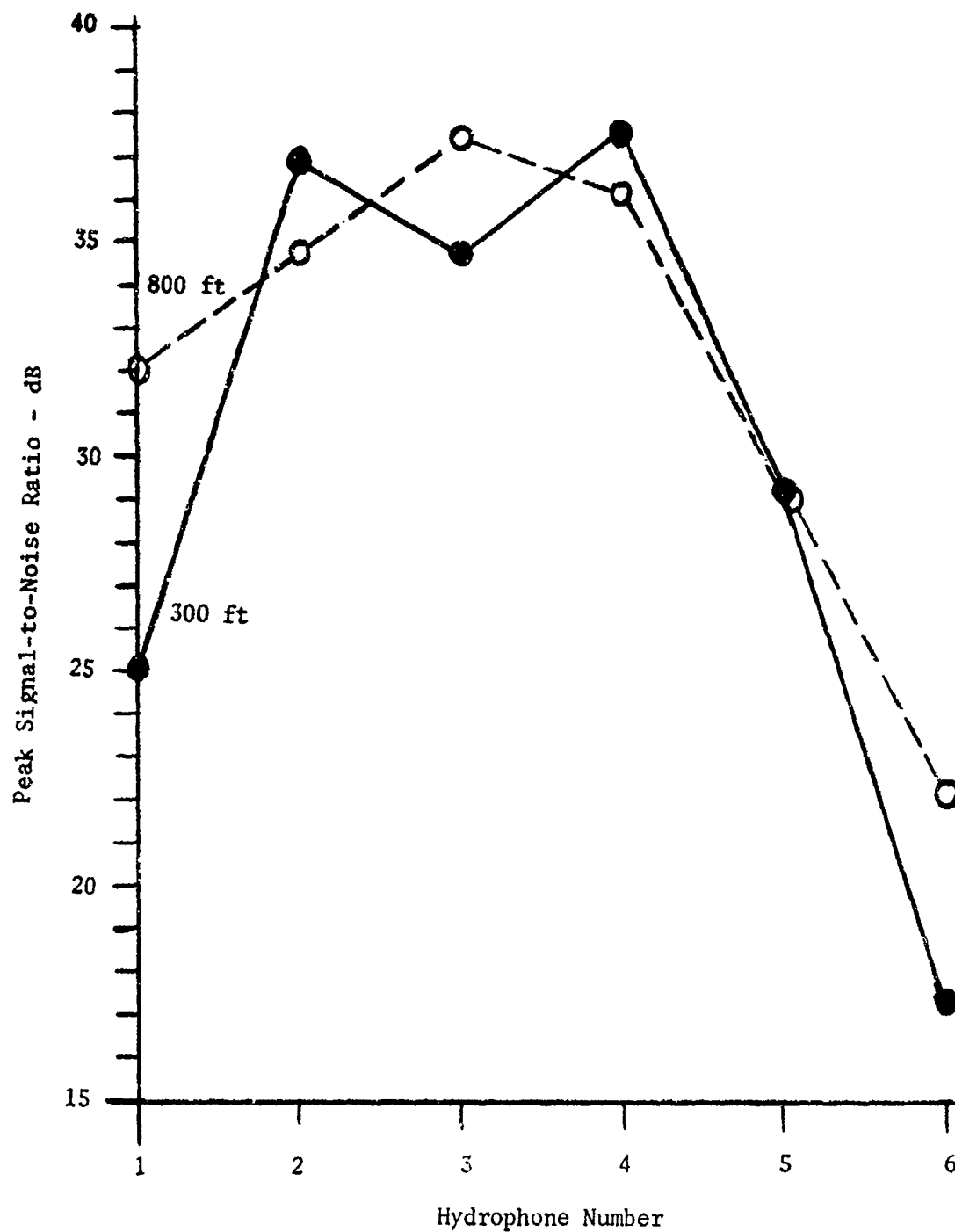


Range of Shot = 50 miles

FIGURE 29
SIGNAL-TO-NOISE RATIO OF SHOT DATA AS A FUNCTION
OF WHOI HYDROPHONE NUMBER

76<

ARL-UT
AS-74-
GEE
10-14-



Range of Shot = 100 Miles

FIGURE 30
SIGNAL-TO-NOISE RATIO OF SHOT DATA AS A FUNCTION
OF WHOI HYDROPHONE NUMBER

77<

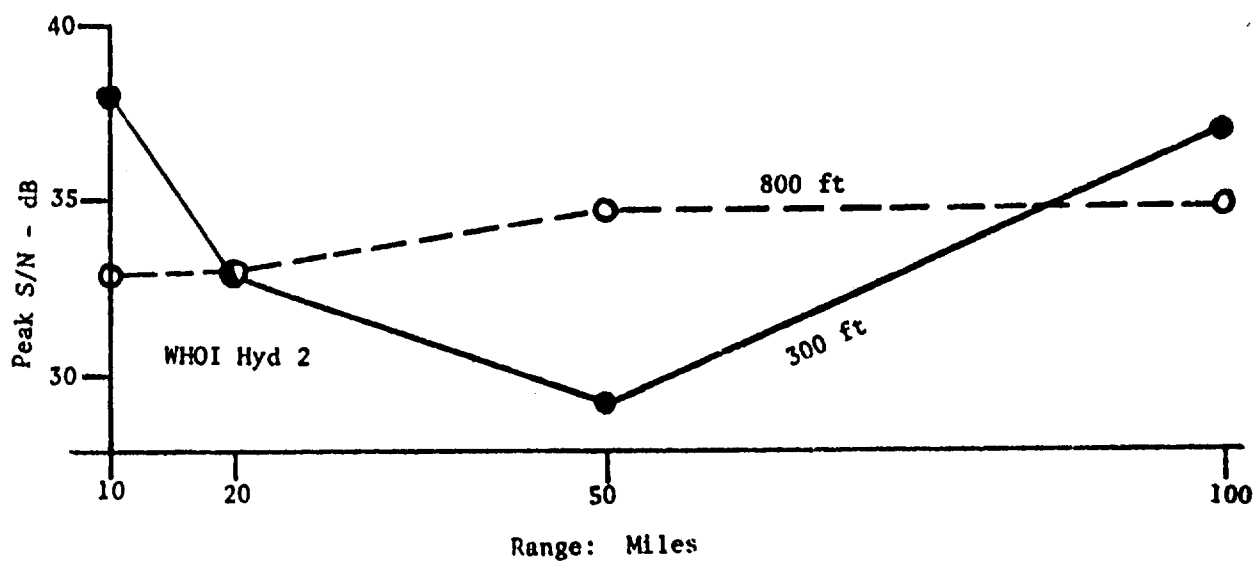
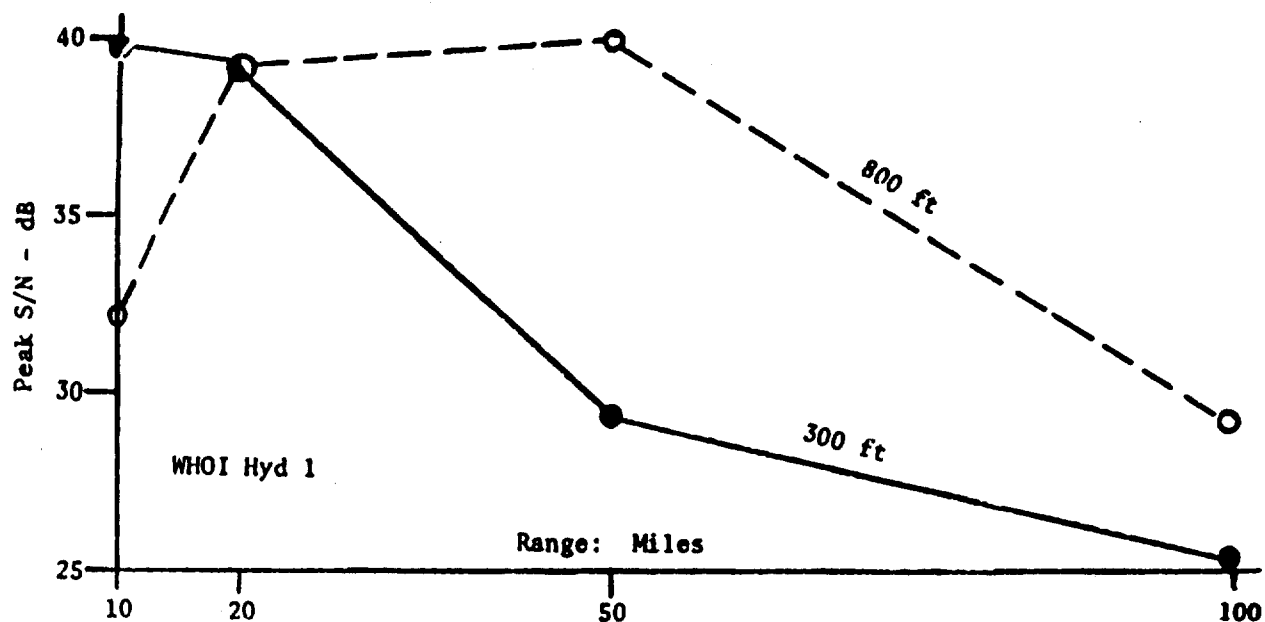


FIGURE 31
VARIATION OF S/N WITH RANGE OF SHOT

78

APL-UT
AS-74-1097
GEE
10-14-74

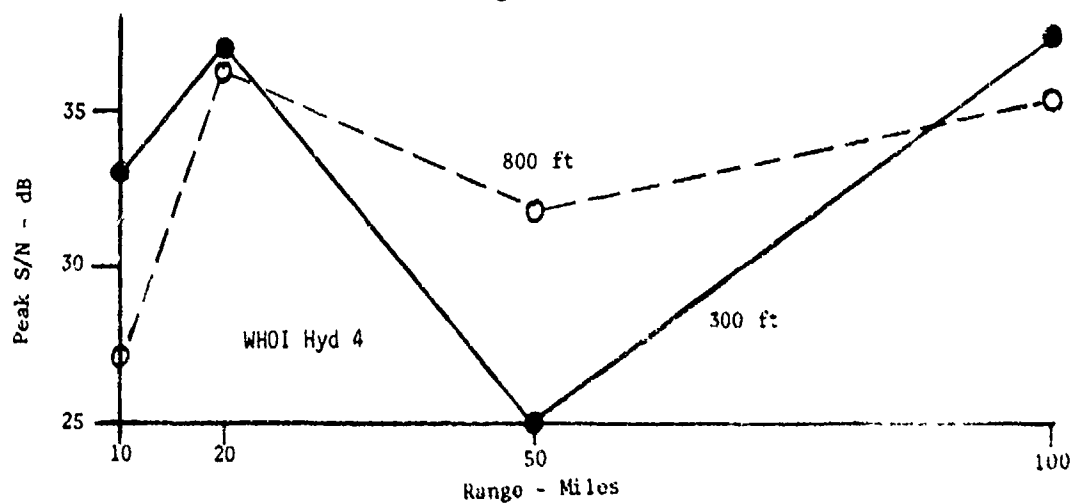
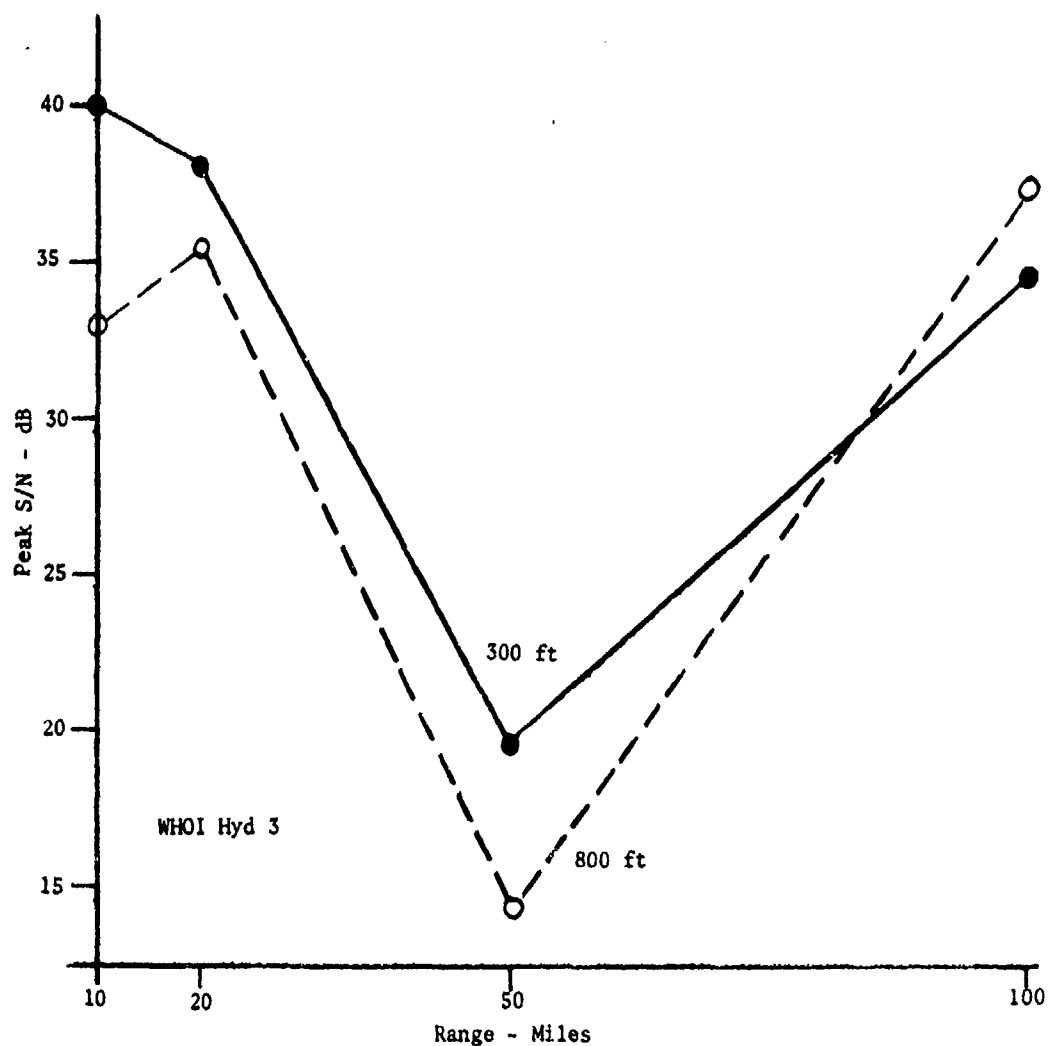


FIGURE 32
VARIATION OF S/N WITH RANGE OF SHOT

79

41

ARL-UT
AS-74-109R
GEE
10-14-74

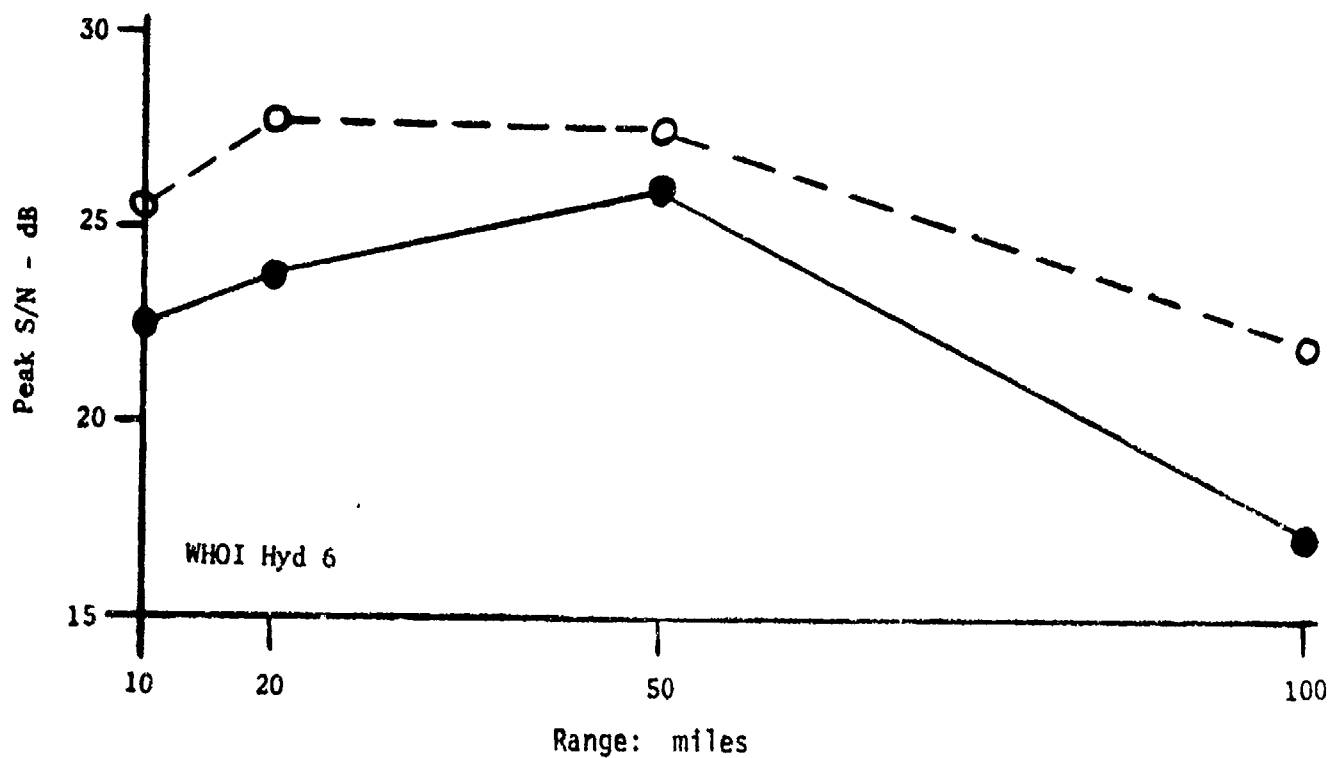
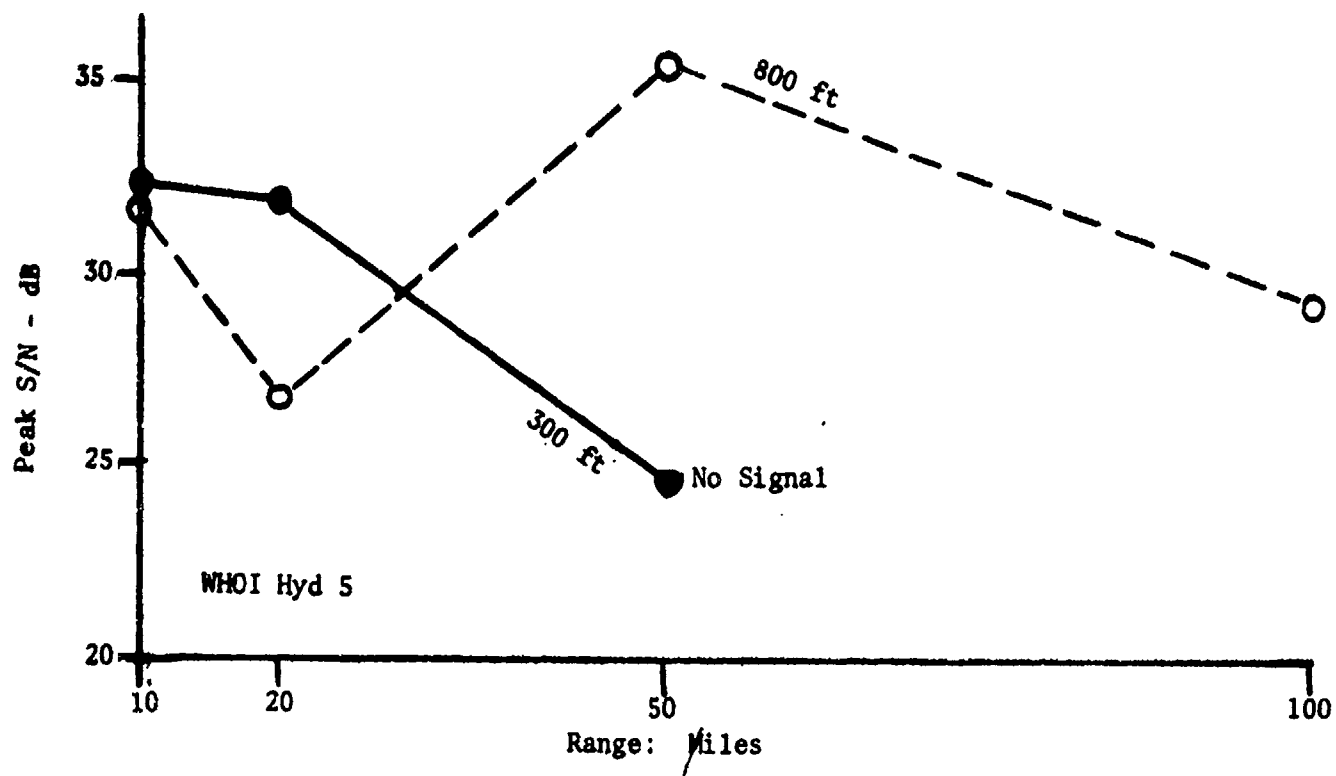


FIGURE 33
VARIATION OF S/N WITH RANGE OF SHOT

80

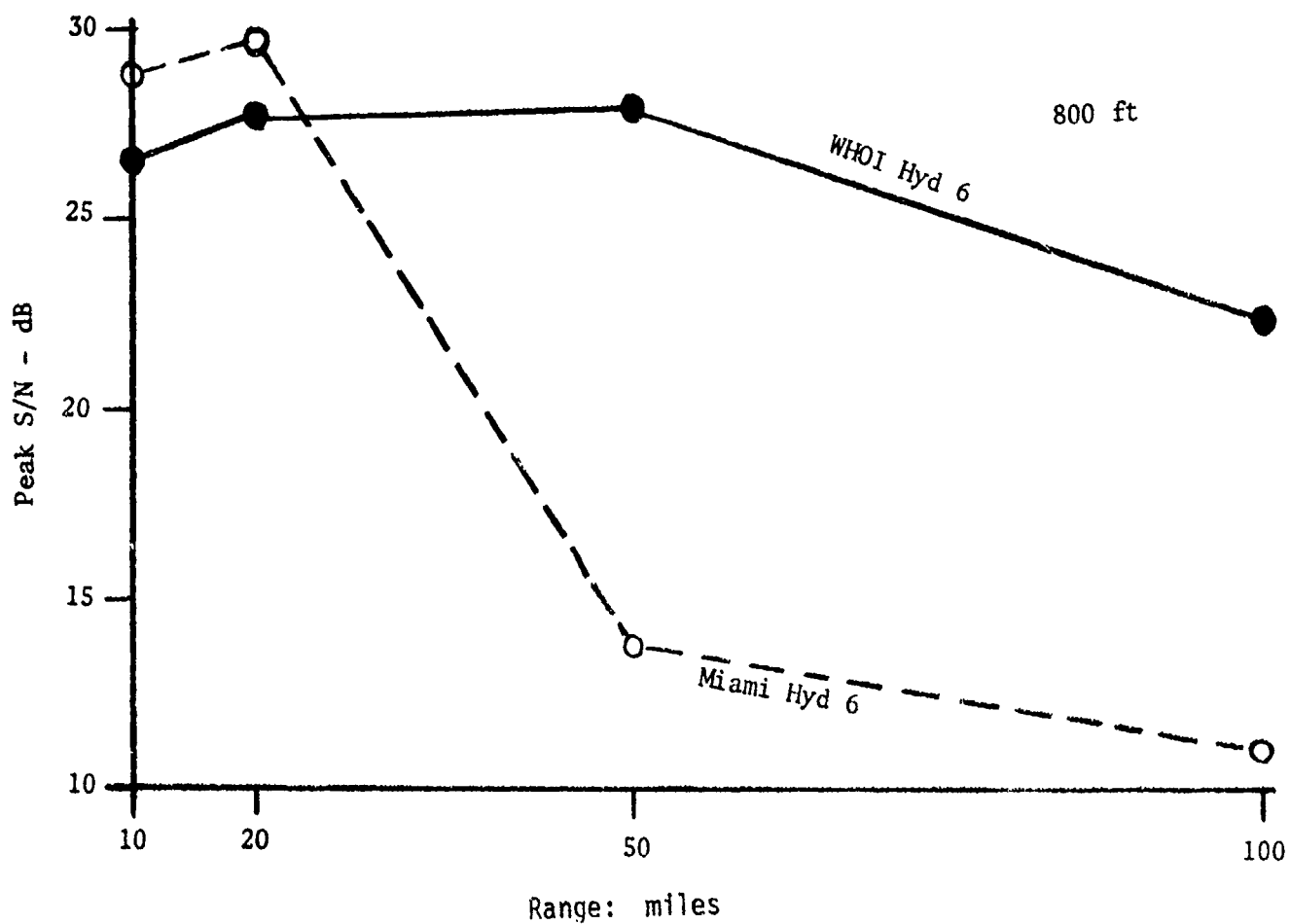
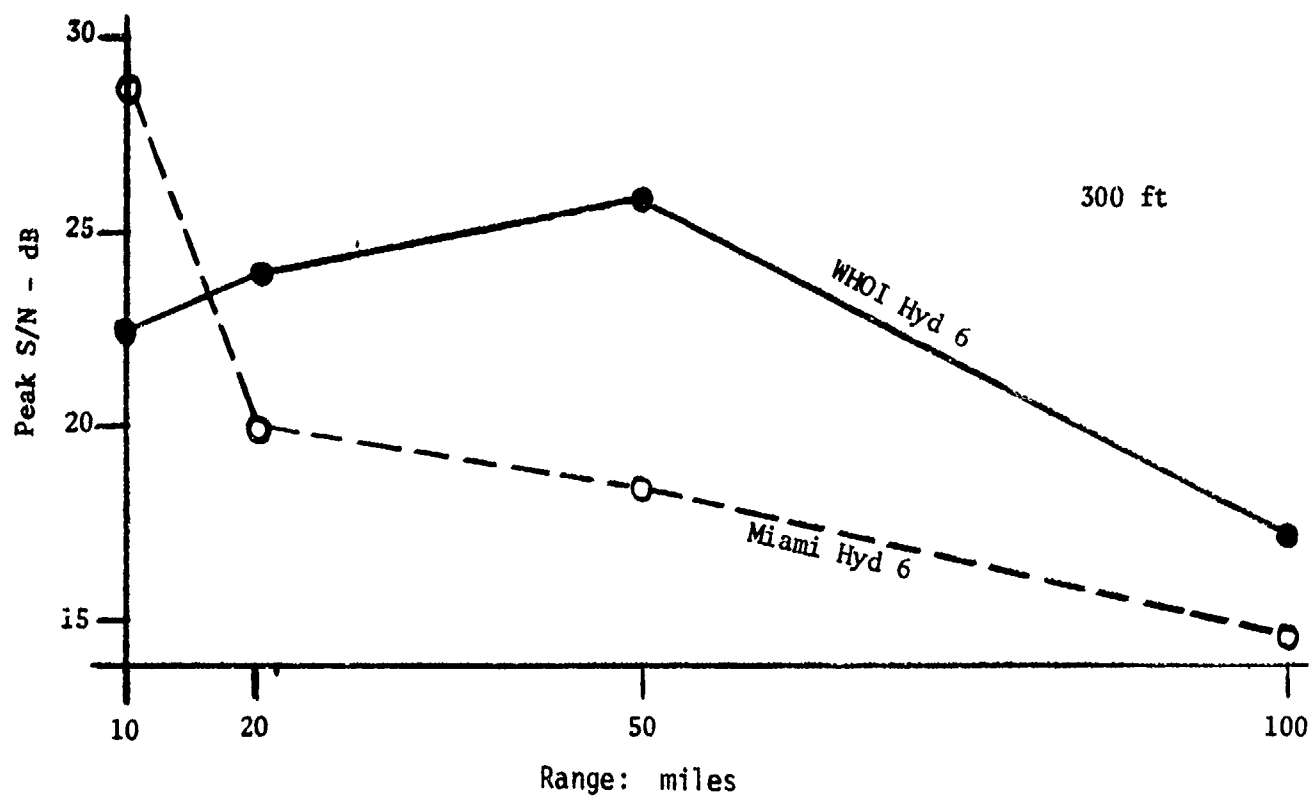


FIGURE 34
COMPARISON OF WHOI AND MIAMI HYDROPHONE
6 SHOT S/N

decreased S/N for hydrophones 3 and 4 is evident in Fig. 32, which shows S/N versus range for these two hydrophones. The same information is shown for hydrophones 5 and 6 in Fig. 33.

In Fig. 34, S/N values are compared for hydrophone 6 of both the WHOI and UM ACODACs. Although comparable S/N was exhibited by the two systems at the two shorter ranges, at the long ranges the S/N was consistently higher at the WHOI ACODAC, especially for the deeper shots.

4. Spectrum

The intensity spectrum was estimated for the same shots used in the S/N analysis (the second shot in each sequence). In Figs. 35 and 36, the spectra (2.34 Hz resolution) are shown for 300 ft and 800 ft shots received by hydrophone 1 at the 10 mile range. The same information is presented for other ranges and hydrophones in Appendix B. Though there is considerable variation in the fine structure of these spectra, they all agree in general form by having a low frequency maximum and a general decay with increasing frequency to the bandpass filter limit of 300 Hz.

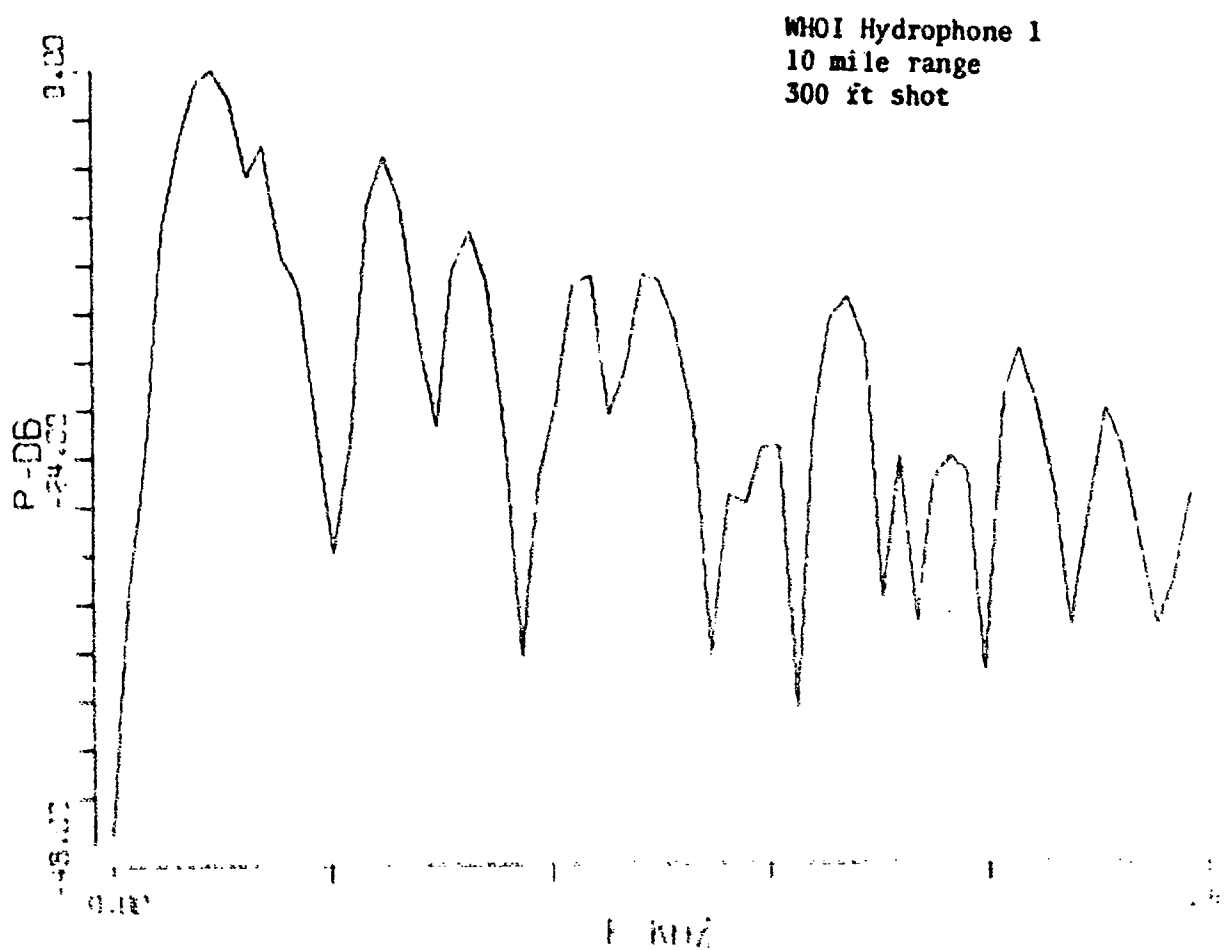


FIGURE 35
SHOT SPECTRUM

83-

ARL-UT
AS-74-1101
GEE
10-14-74

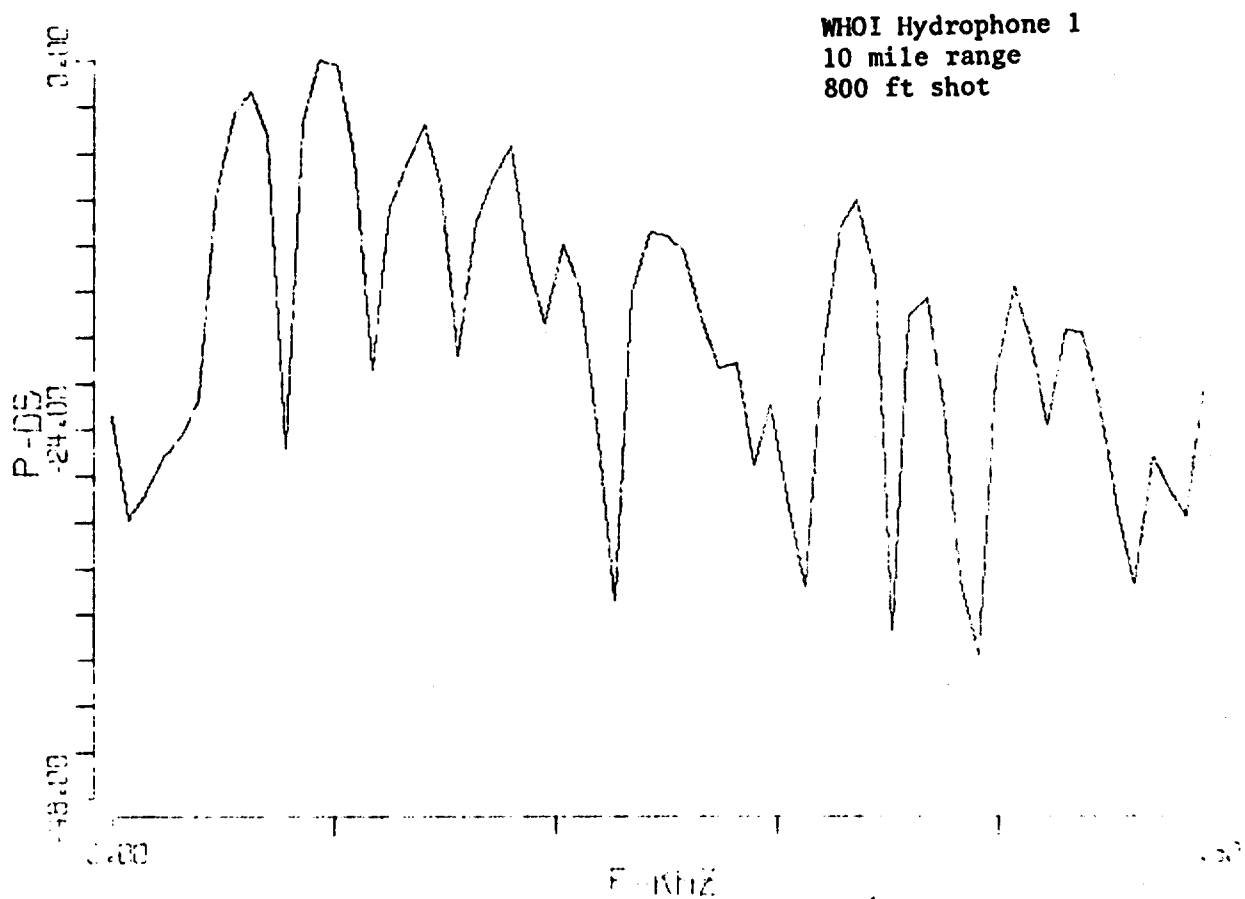


FIGURE 36
SHOT SPECTRUM

81<


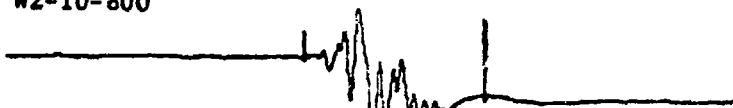

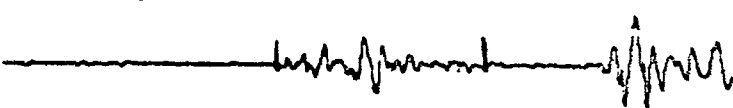
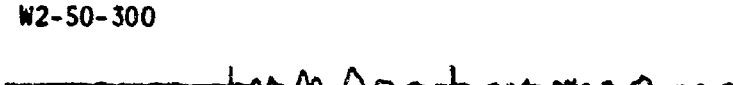



APPENDIX A



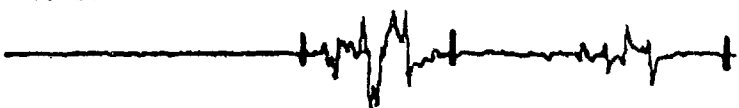
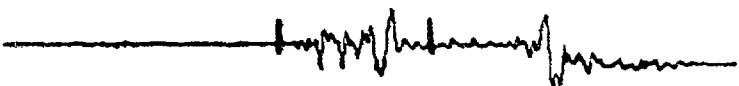
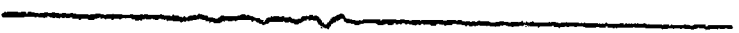
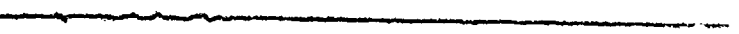


Received Signal Amplitude Versus
Time and Signal-to-Noise Ratio





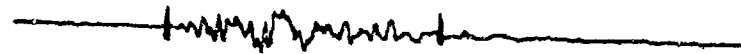



Label Example:

W2-10-300
WHOI 10 300 ft shot depth
| mile Range
Hydrophone

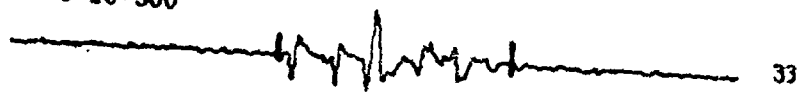
85

		S/N - dB		
		Energy	Peak	
W2-10-300		9	28.2	37.9
W2-10-800		10	21.5	33.0
W2-20-300		1	20.2	32.9
W2-20-800		12	22.4	33.3
W2-50-300		13	19.8	29.2
W2-50-800		14	21.1	34.8
W2-100-300		15	24.9	37.1
W2-100-800		16	22.4	34.9

			S/N - dB	
			Energy	Peak
W3-10-300		17	28.7	40.1
W3-10-800		18	20.7	33.0
W3-20-300		19	27.7	38.1
W3-20-800		20	25.2	35.3
W3-50-300		21	8.84	19.6
W3-50-800		22	5.16	14.5
W3-100-300		23	24.3	34.8
W3-100-800		24	24.4	37.5

		S/N - dB	
		Energy	Peak
W4-10-300		25	
		24.6	33.0
W4-10-800		26	
		17.9	27.2
W4-20-300		27	
		23.9	37.0
W4-20-800		28	
		23.7	36.2
W4-50-300		29	
		15.7	25.3
W4-50-800		30	
		19.1	31.9
W4-100-300		31	
		24.6	37.3
W4-100-800		32	
		23.9	35.2

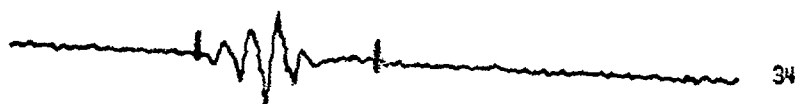
W5-10-300



S/N - dB

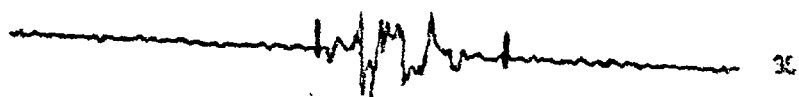
Energy
20.6 Peak
32.1

W5-10-800



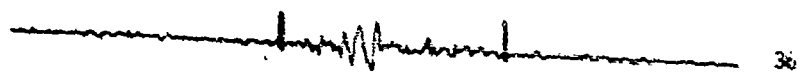
20.3 31.5

W5-20-300



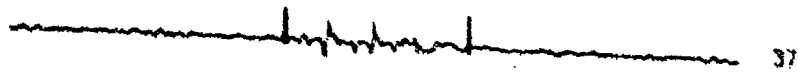
22.0 31.9

W5-20-800



16.0 26.8

W5-50-300



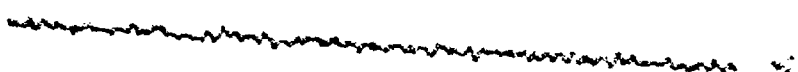
11.7 24.5

W5-50-800



21.6 35.2

W5-100-300

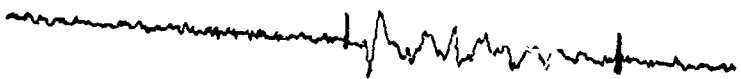



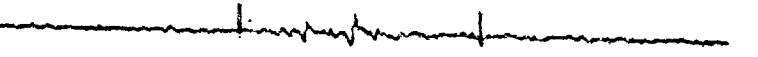
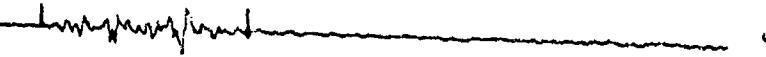




No Signal

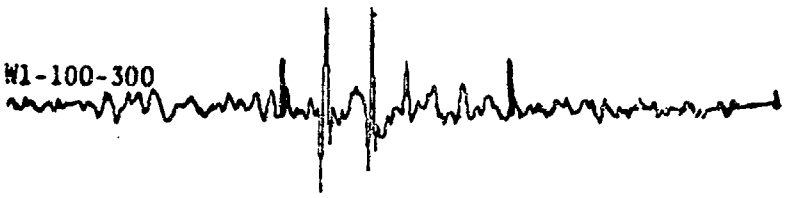
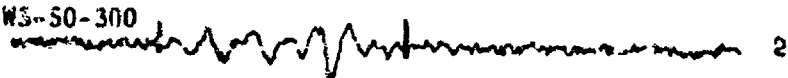
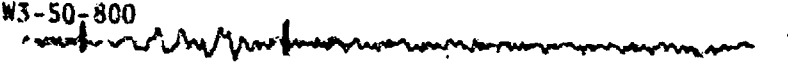
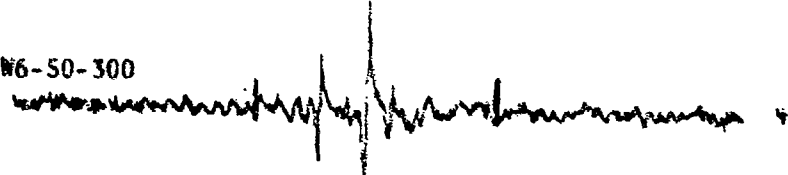
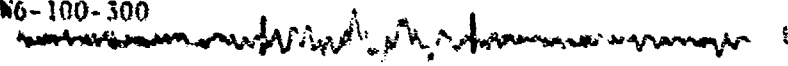
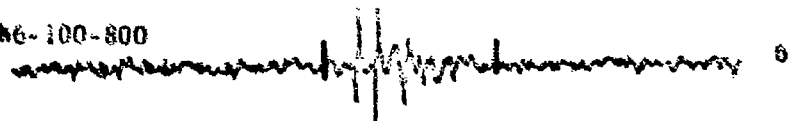
W5-100-800

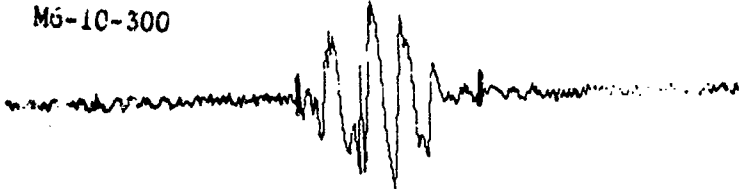


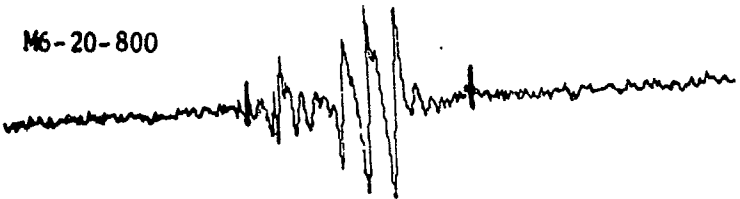
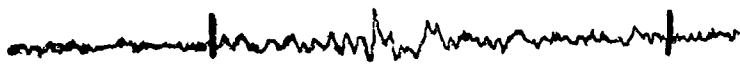


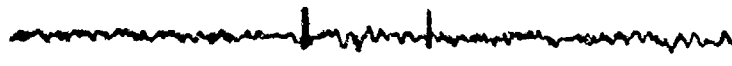


16.8 29.1

		<u>S/N - dB</u>	
		Energy	Peak
W6-10-300	 41	11.1	22.5
W6-10-800	 42	12.8	25.6
W6-20-300	 43	14.0	23.9
W6-20-800	 44	14.3	27.8
W6-50-300	 45	10.5	26.0
W6-50-800	 46	15.5	27.6
W6-100-300	 47	7.05	17.2
W6-100-800	 48	10.5	22.1

90<

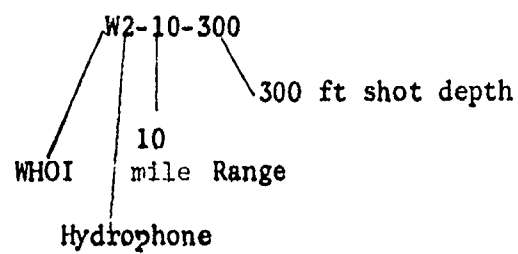
		<u>S/N - db</u>	
		Energy	Peak
W1-100-300		12.5	25.3
W3-50-300	 2	8.84	19.6
W3-50-800	 3	5.16	14.5
W6-50-300	 4	10.5	26.0
W6-100-300	 6	7.05	17.2
W6-100-800	 6	10.8	22.1

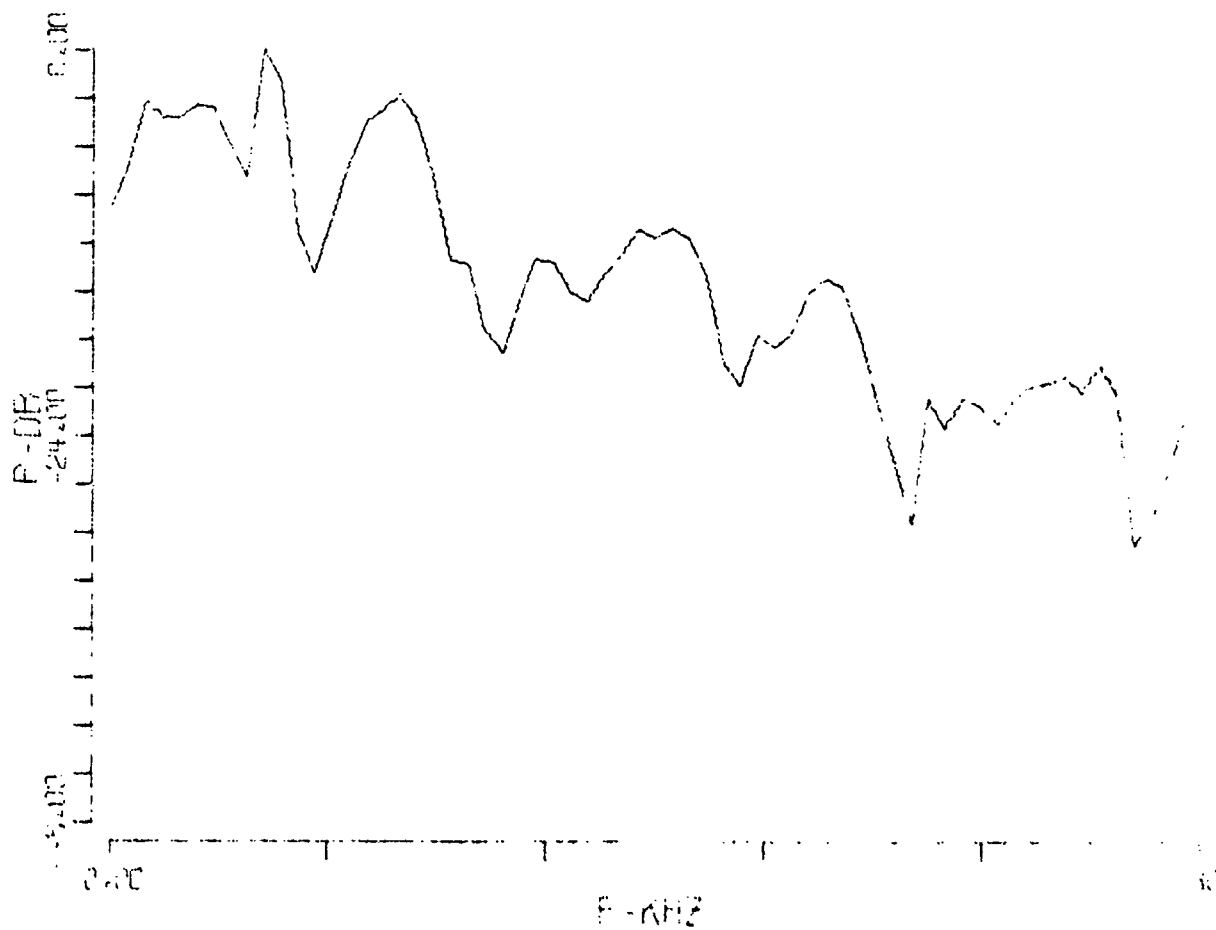
		S/N - dB	
		Energy	Peak
M6-10-300		21.3	28.7
	1		
M6-10-800		14.4	27.9
	5		
M6-20-300		7.19	19.2
	2		
M6-20-800		19.3	28.8
	6		
M6-50-300		5.15	18.9
	3		
M6-50-800		3.20	13.9
	7		
M6-100-300		5.29	14.9
	4		
M6-100-800		0.45	11.1
	8		

APPENDIX B

Shot Spectra

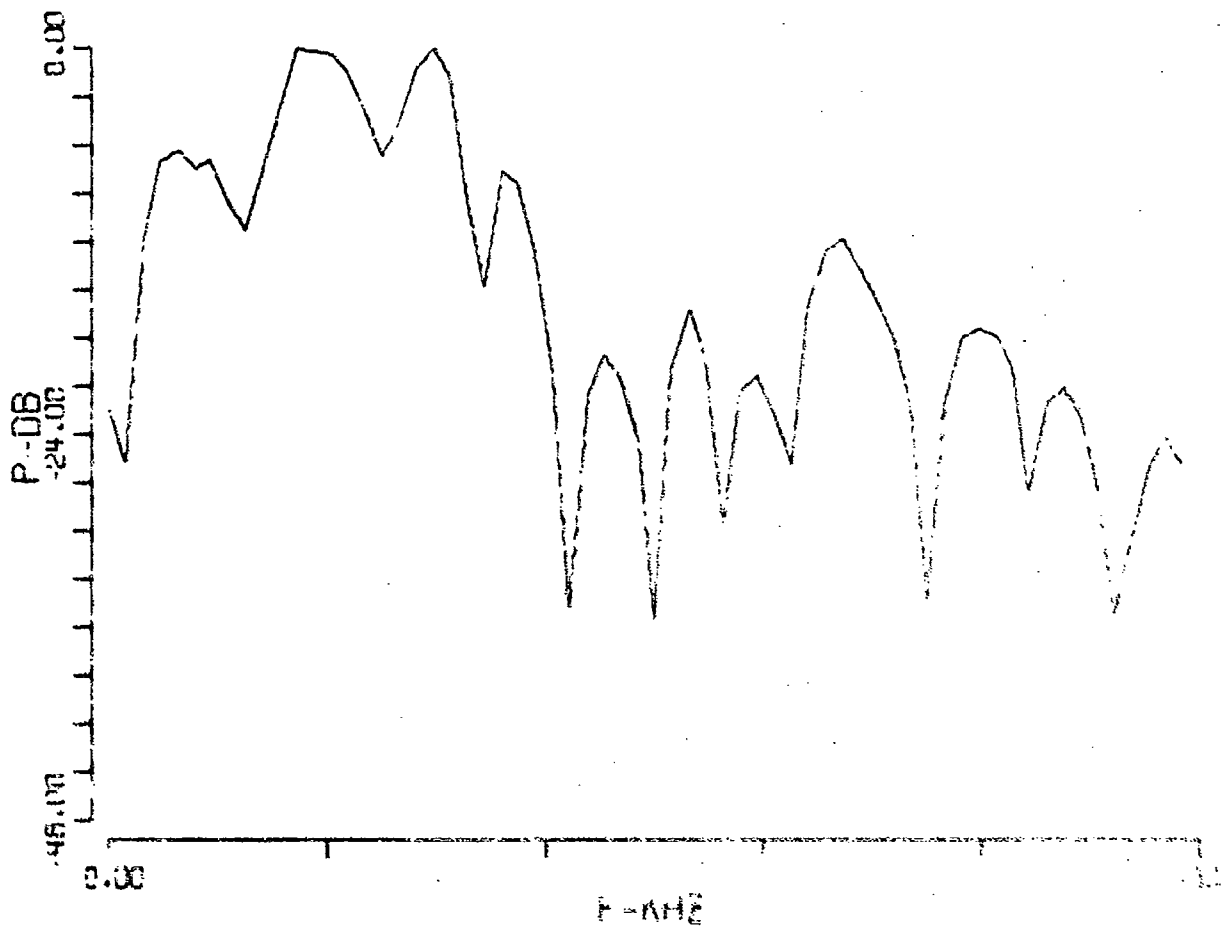
Label Example:





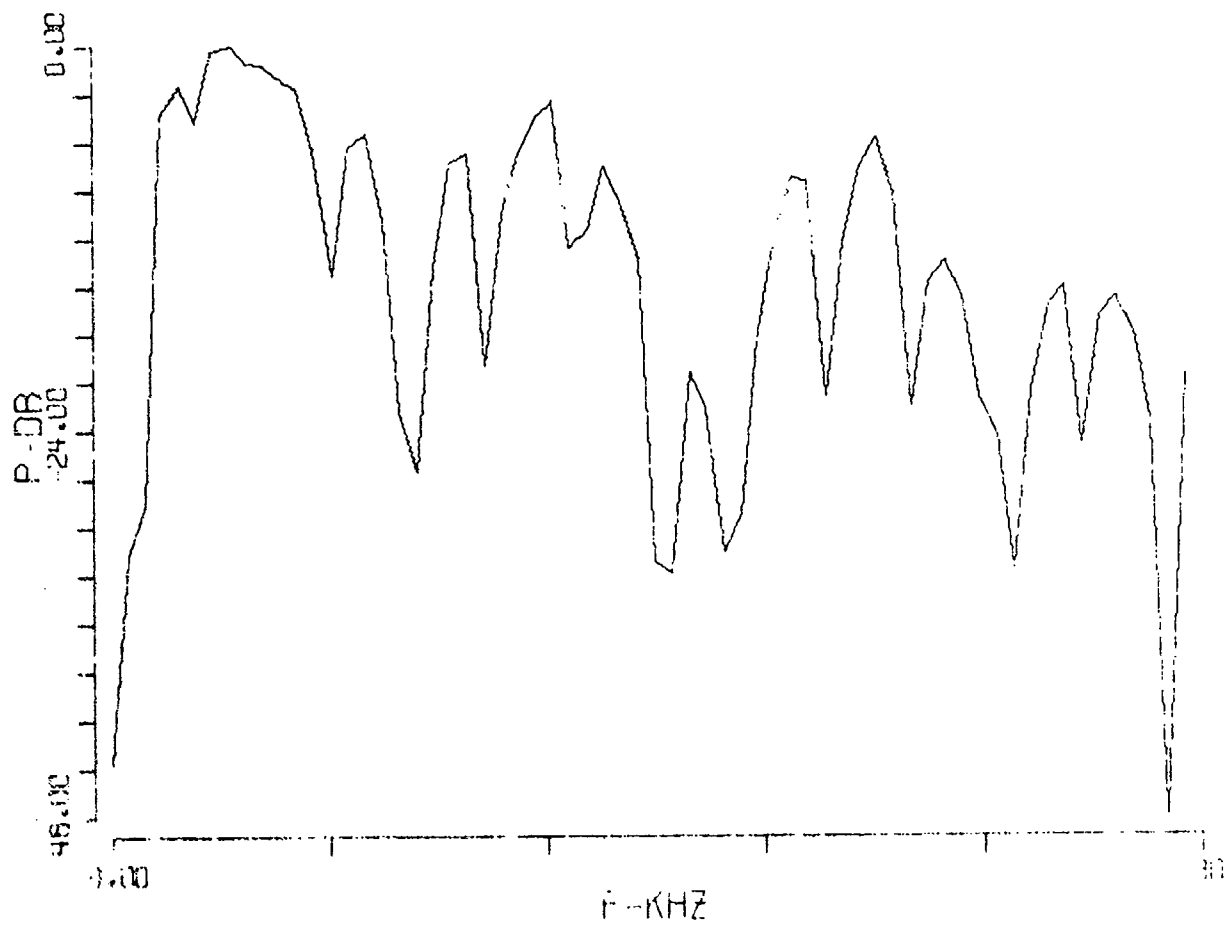
W1-20-300

94

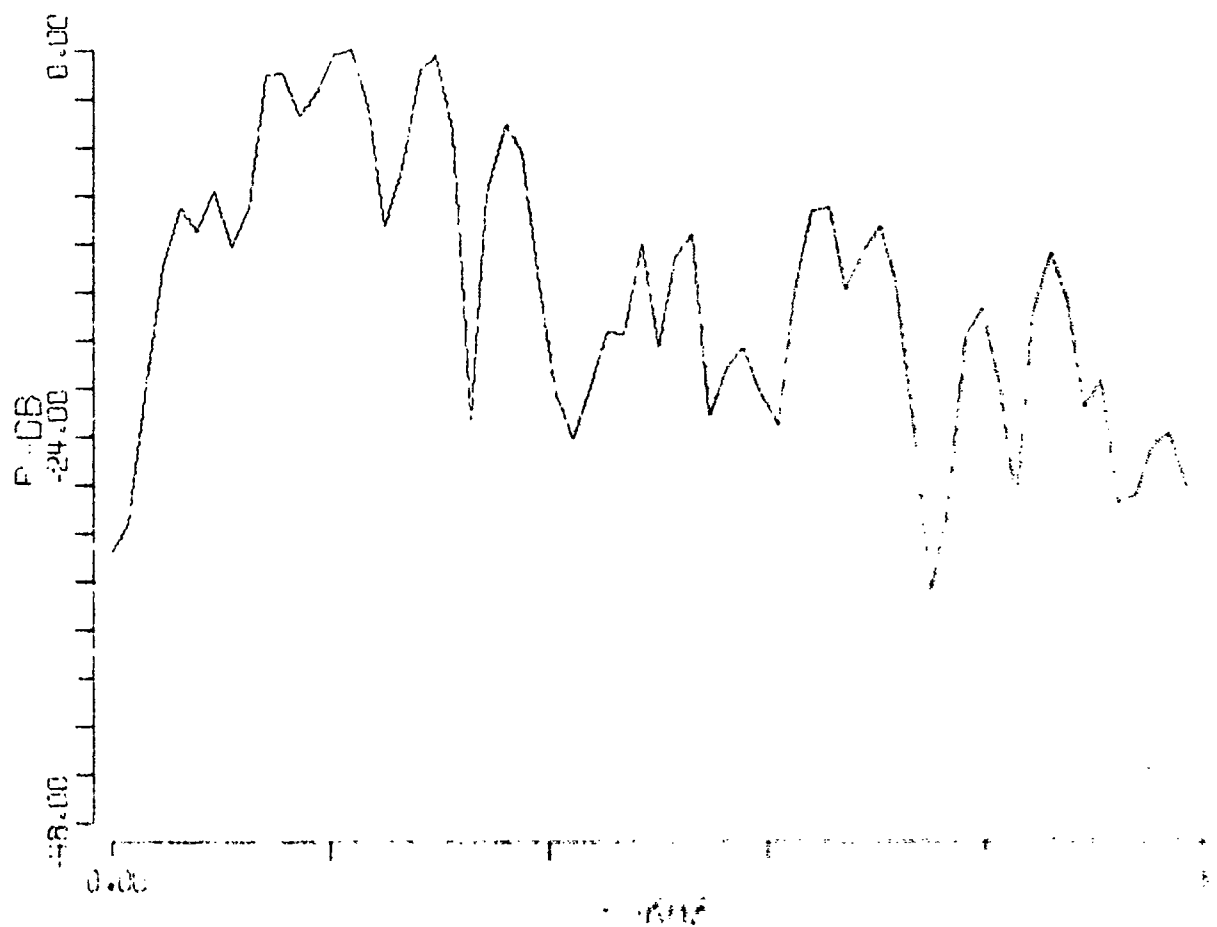


W1-20-800

95°

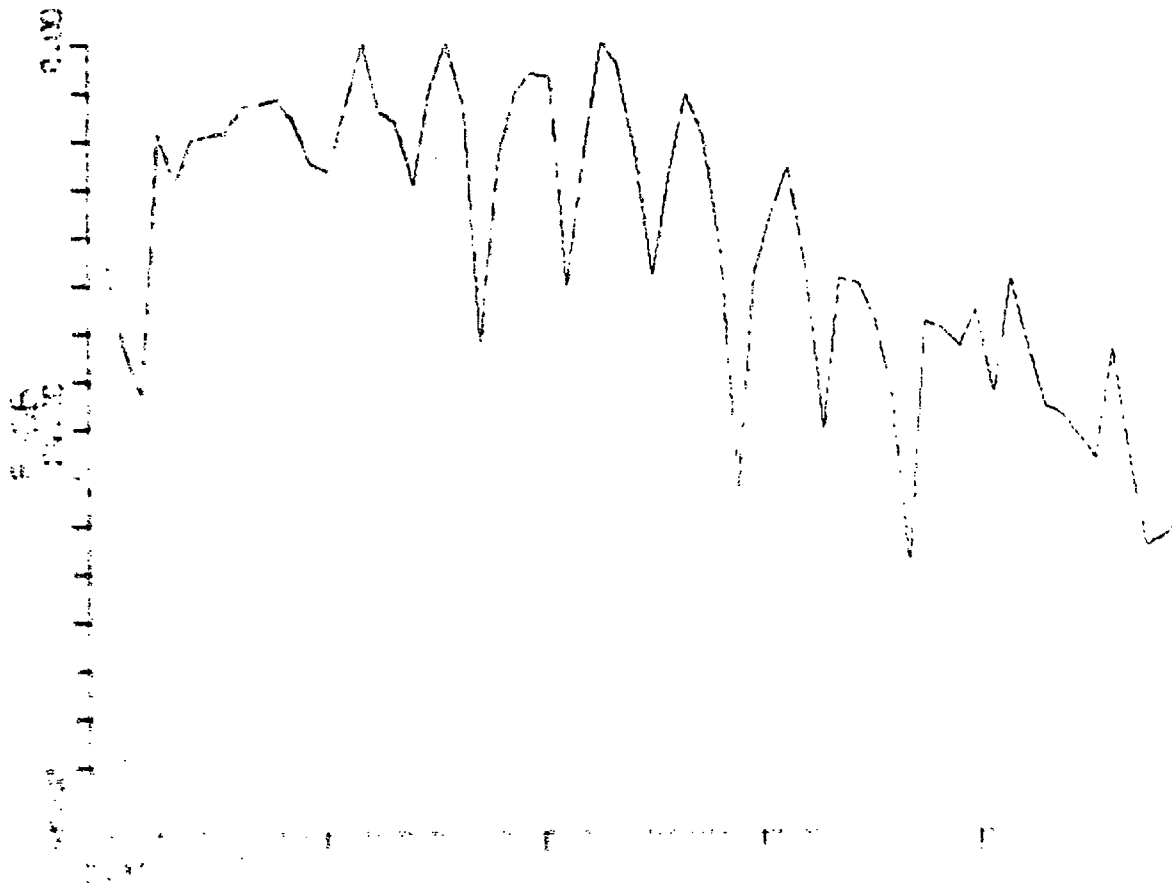


W1-50-300



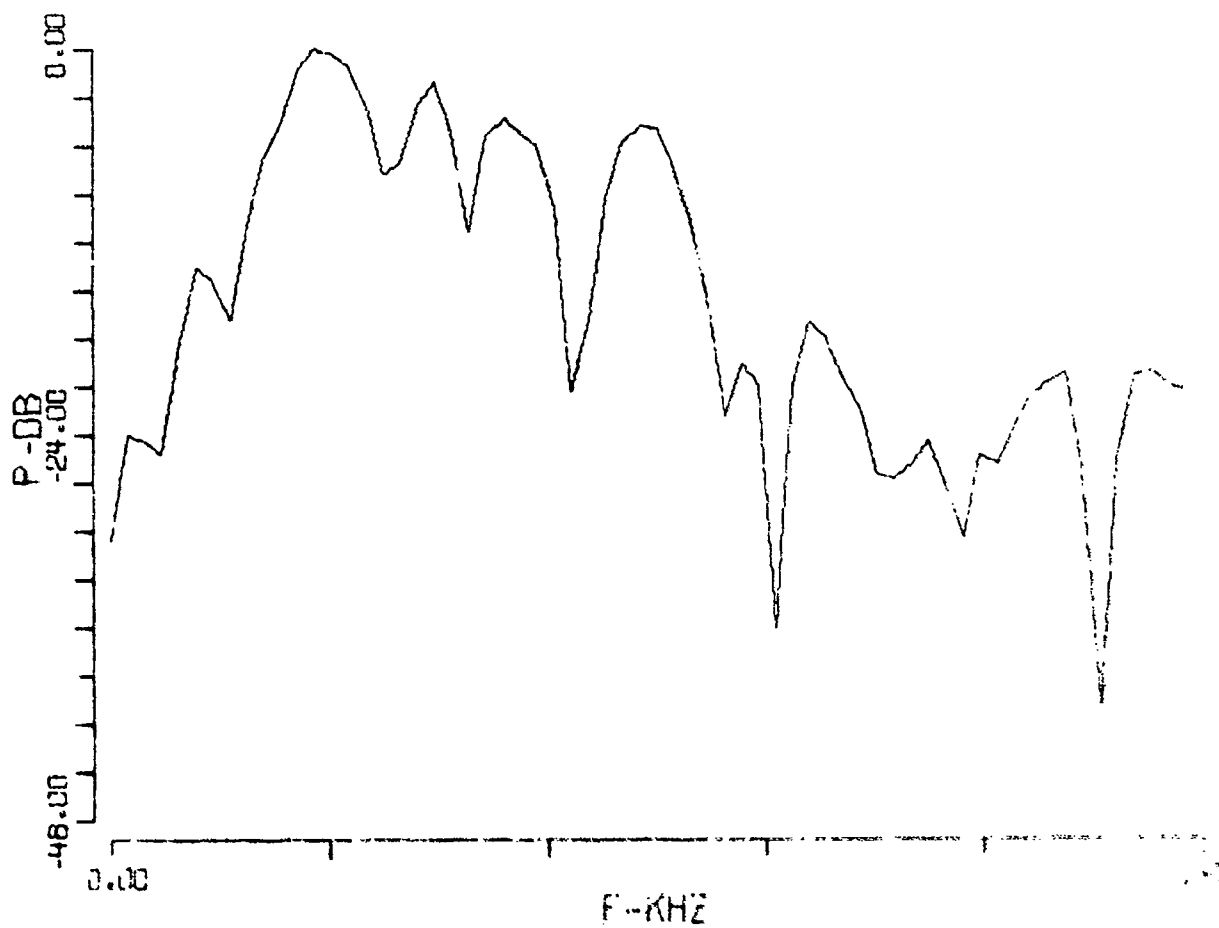
W1-50-800

37



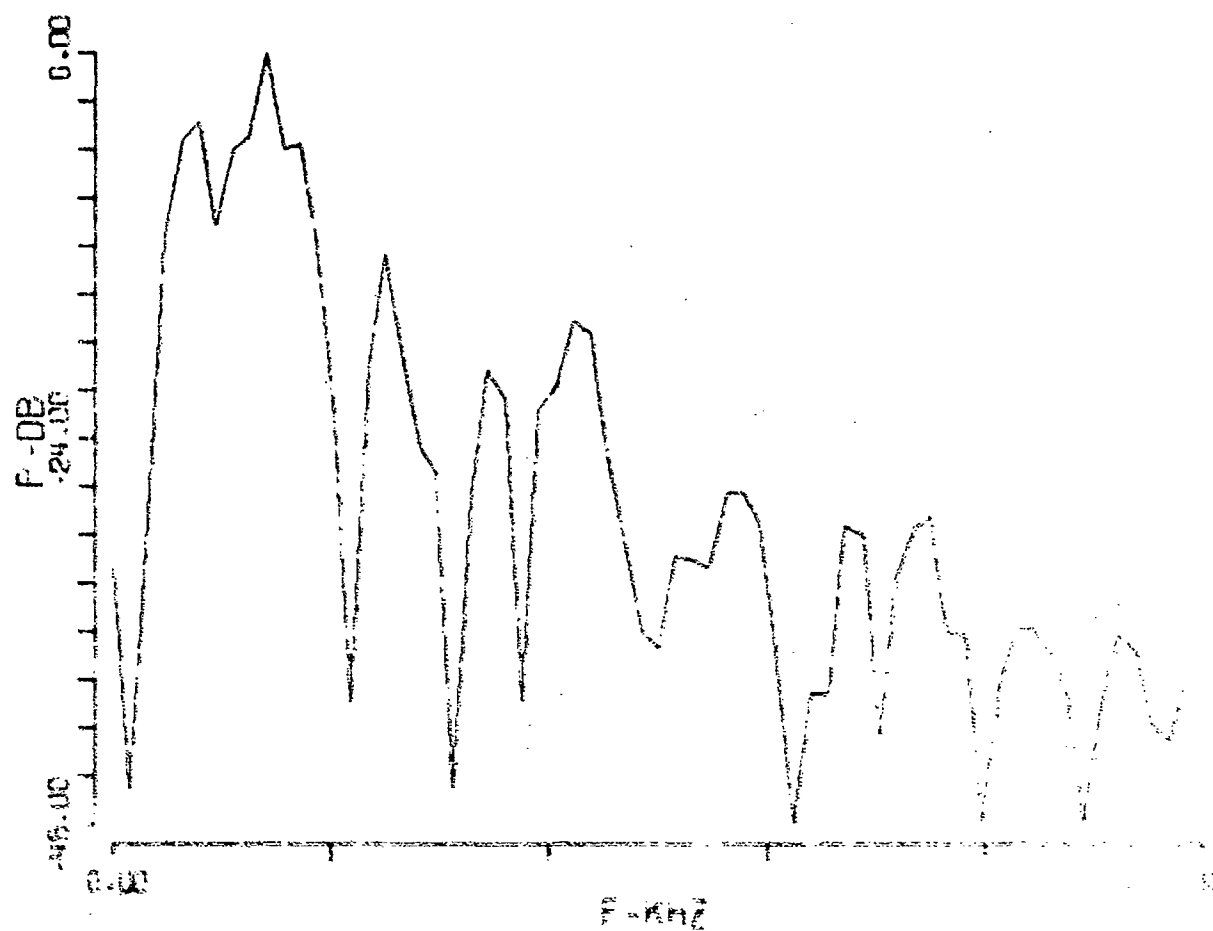
W1-100-300

98<



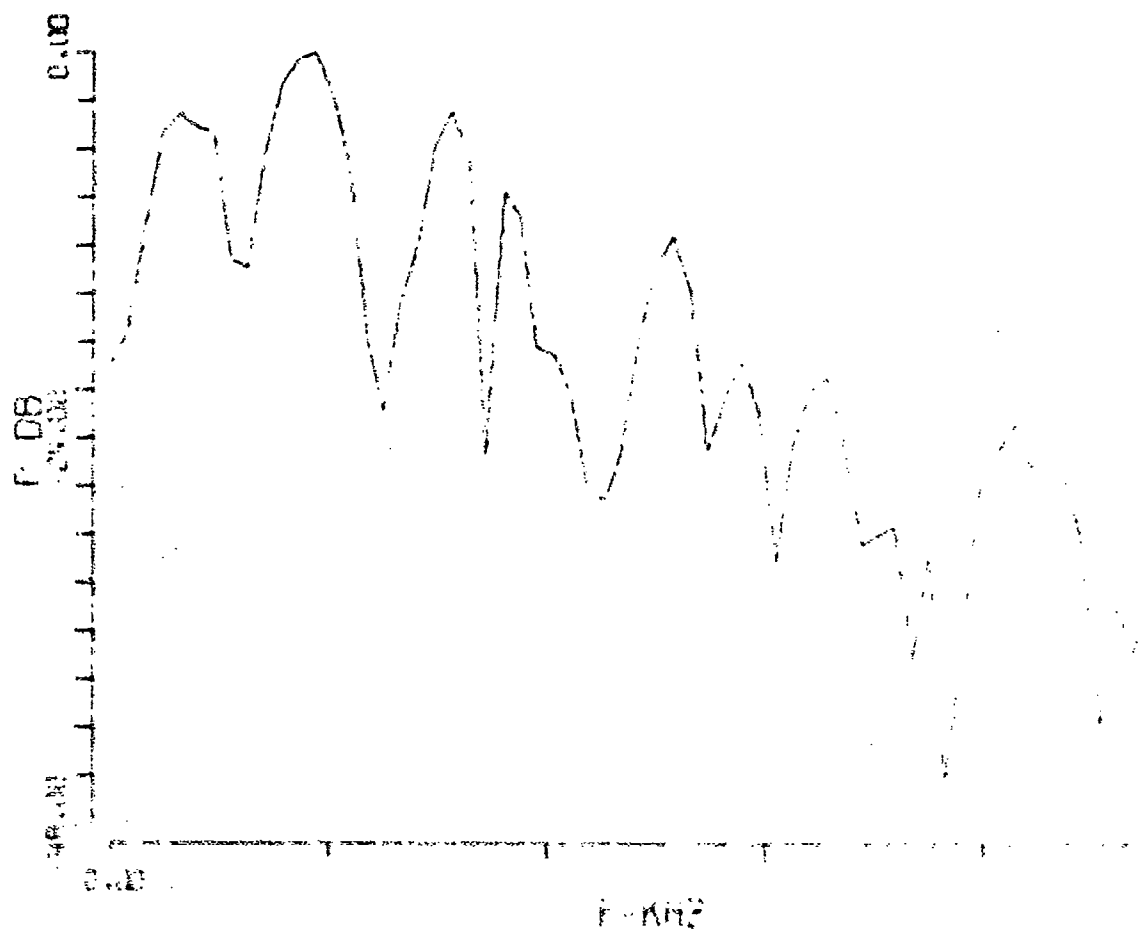
W1-100-800

SSC



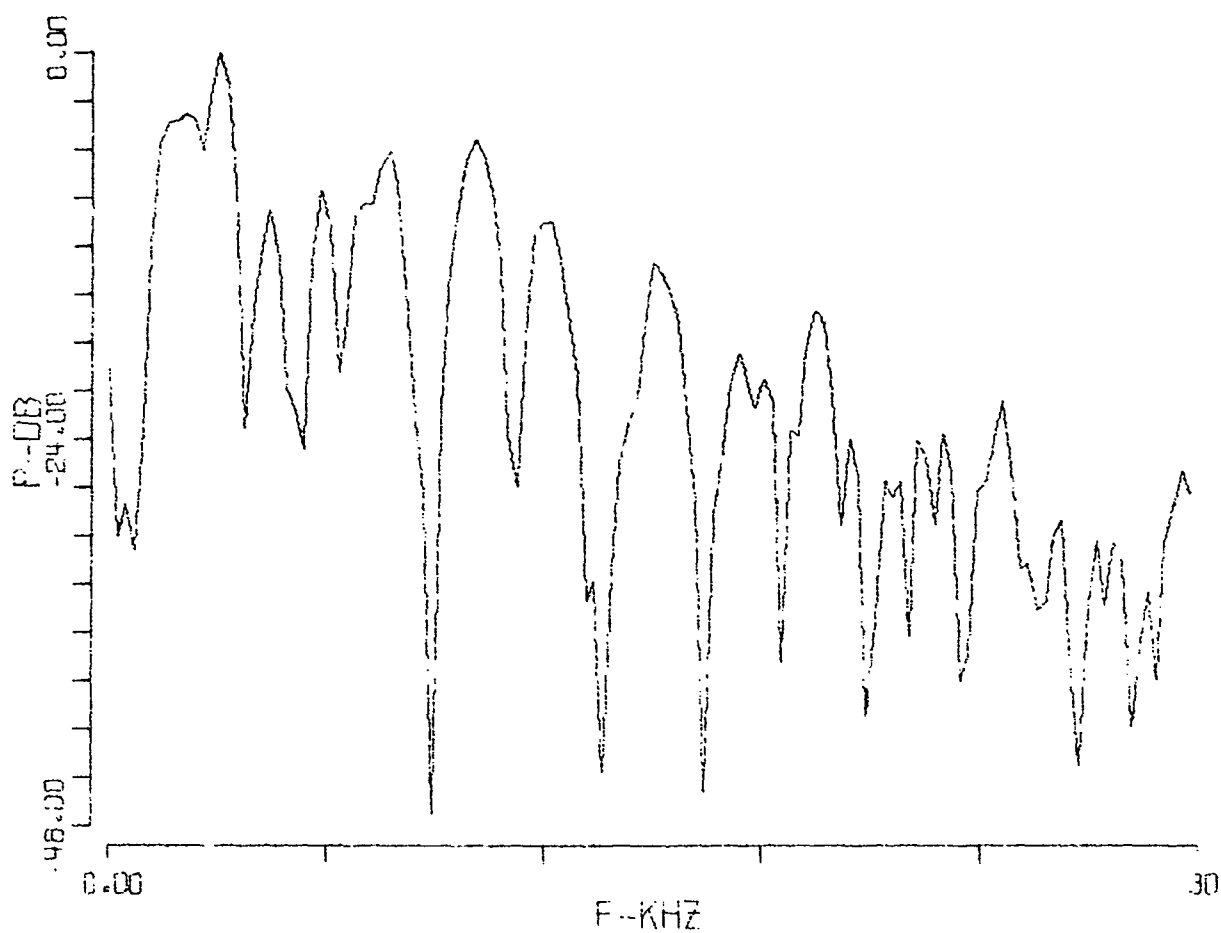
N2-10-300

100<



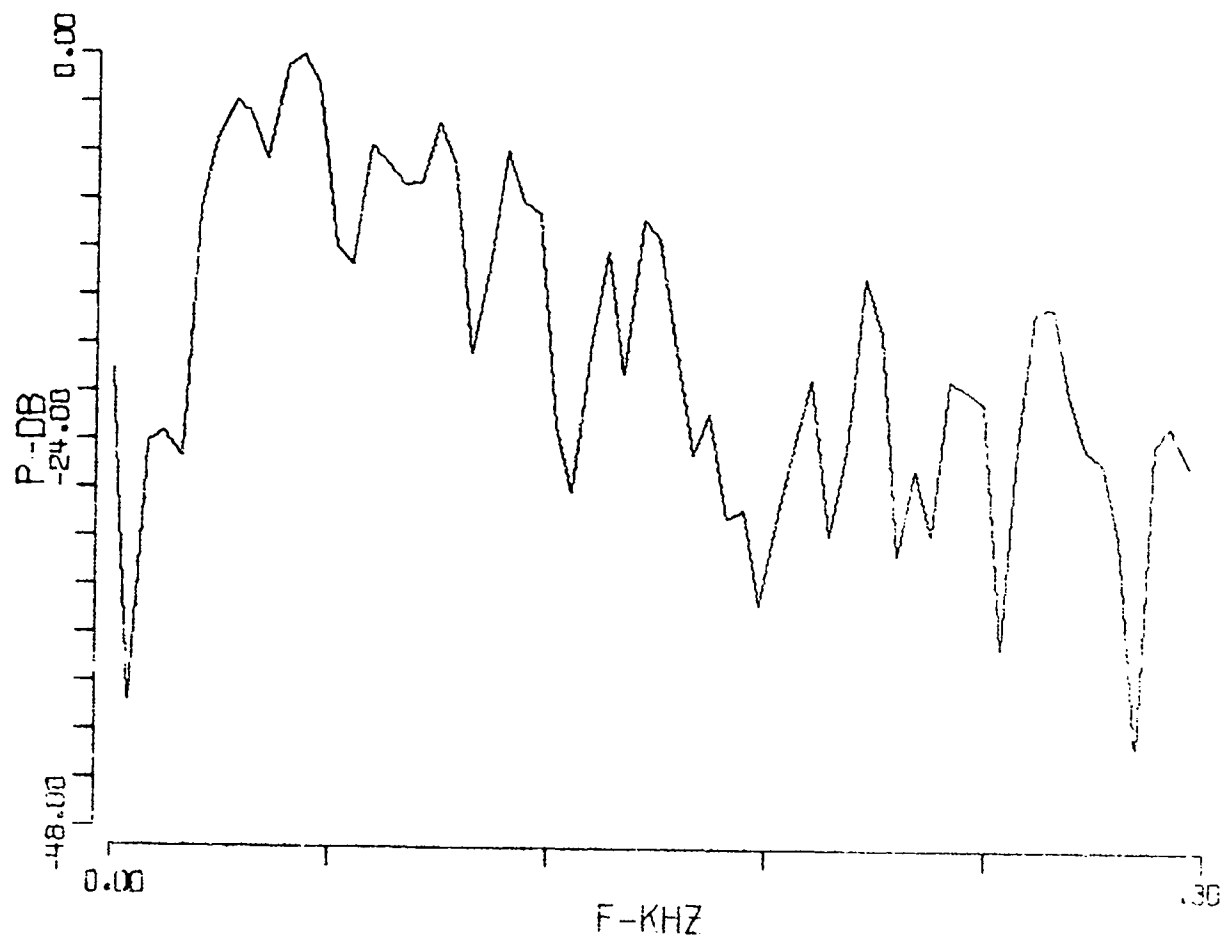
W2-10-800

161<



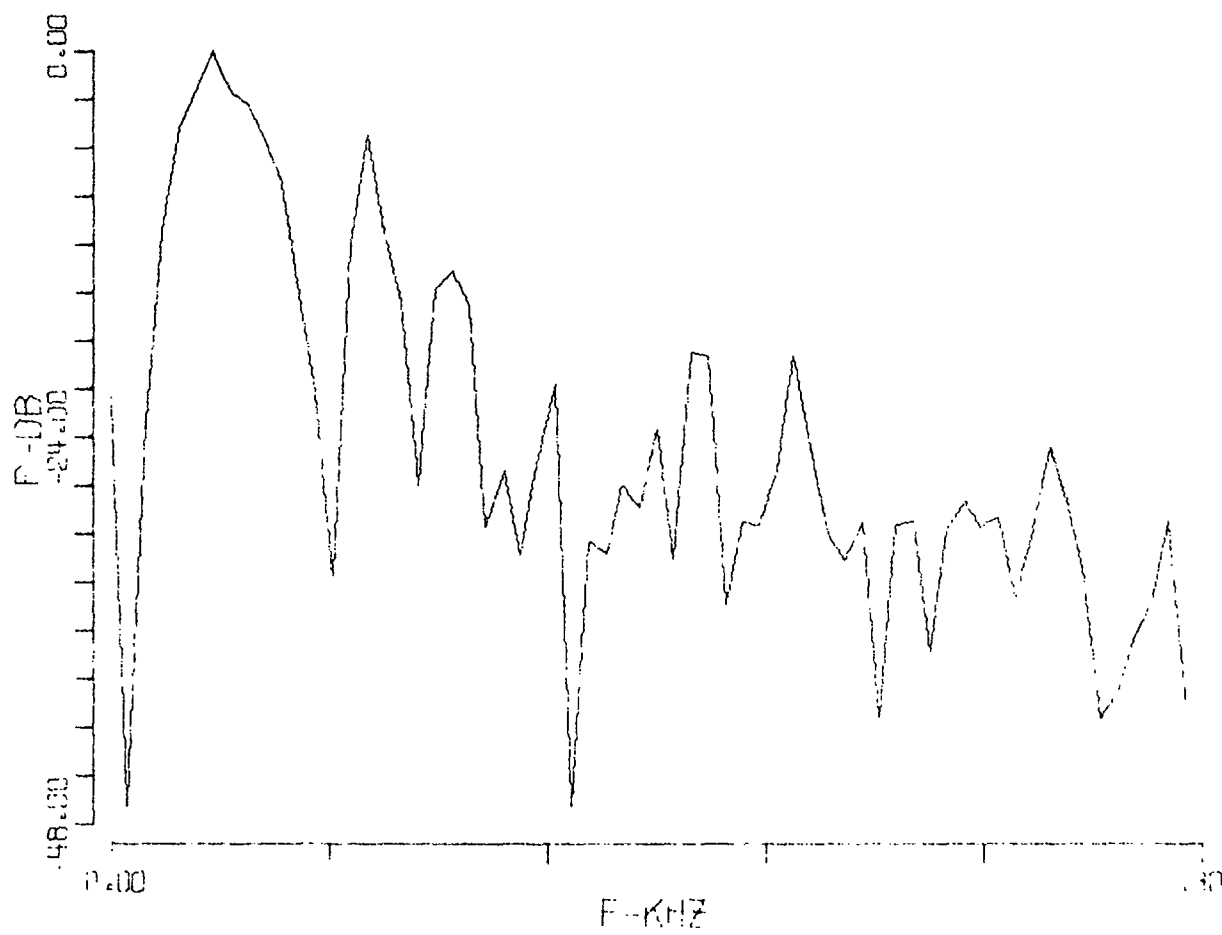
W2-20-300

102<



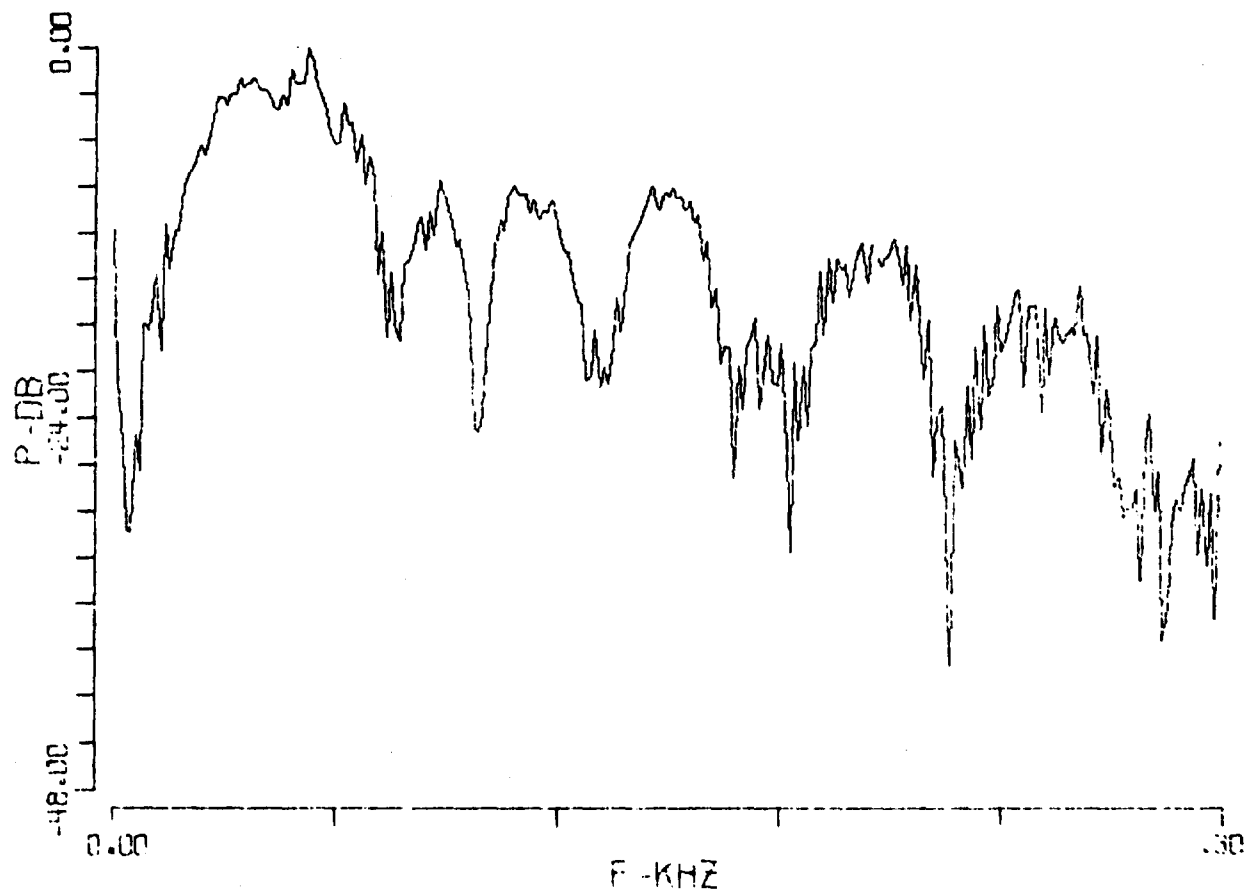
W2-20-800

103<



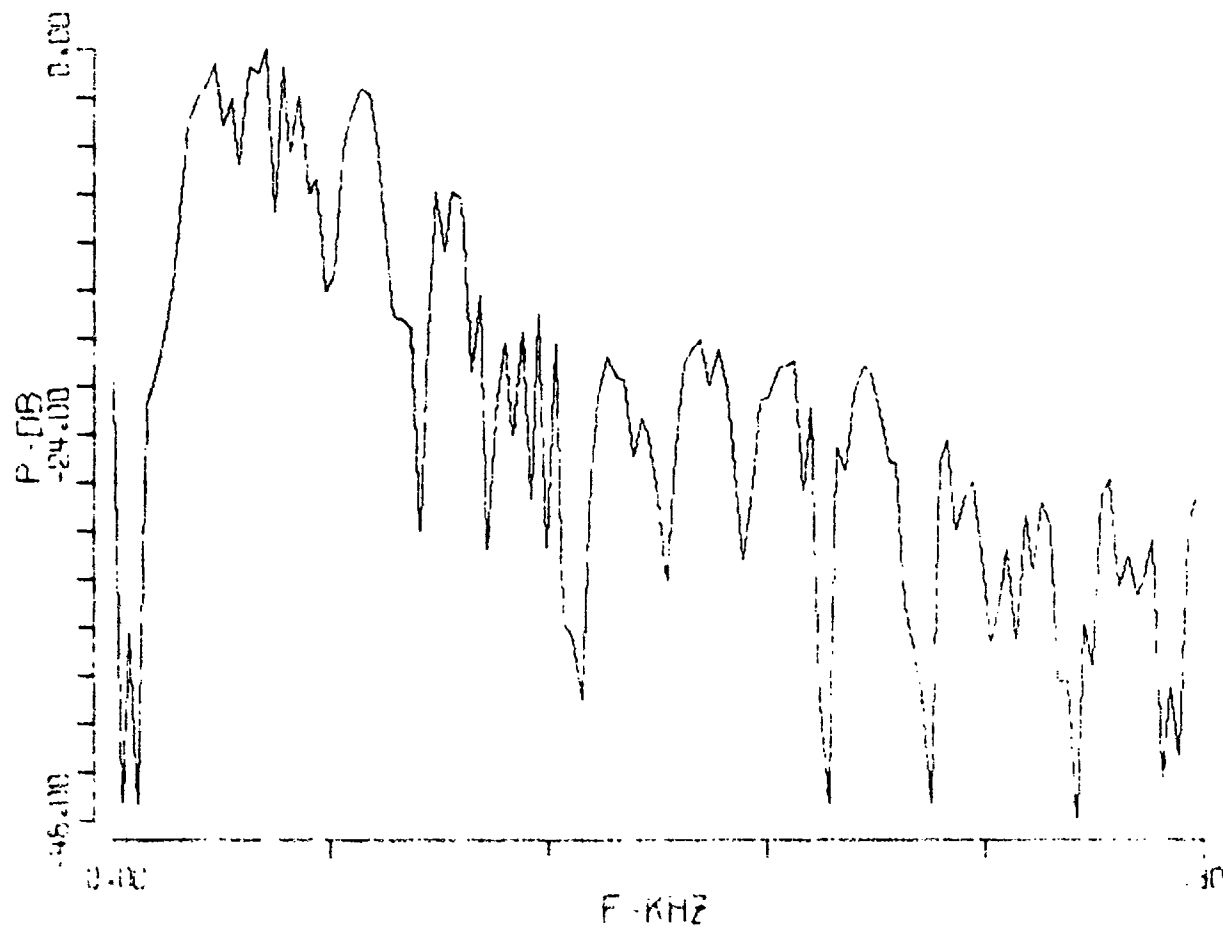
W2-50-300

104<



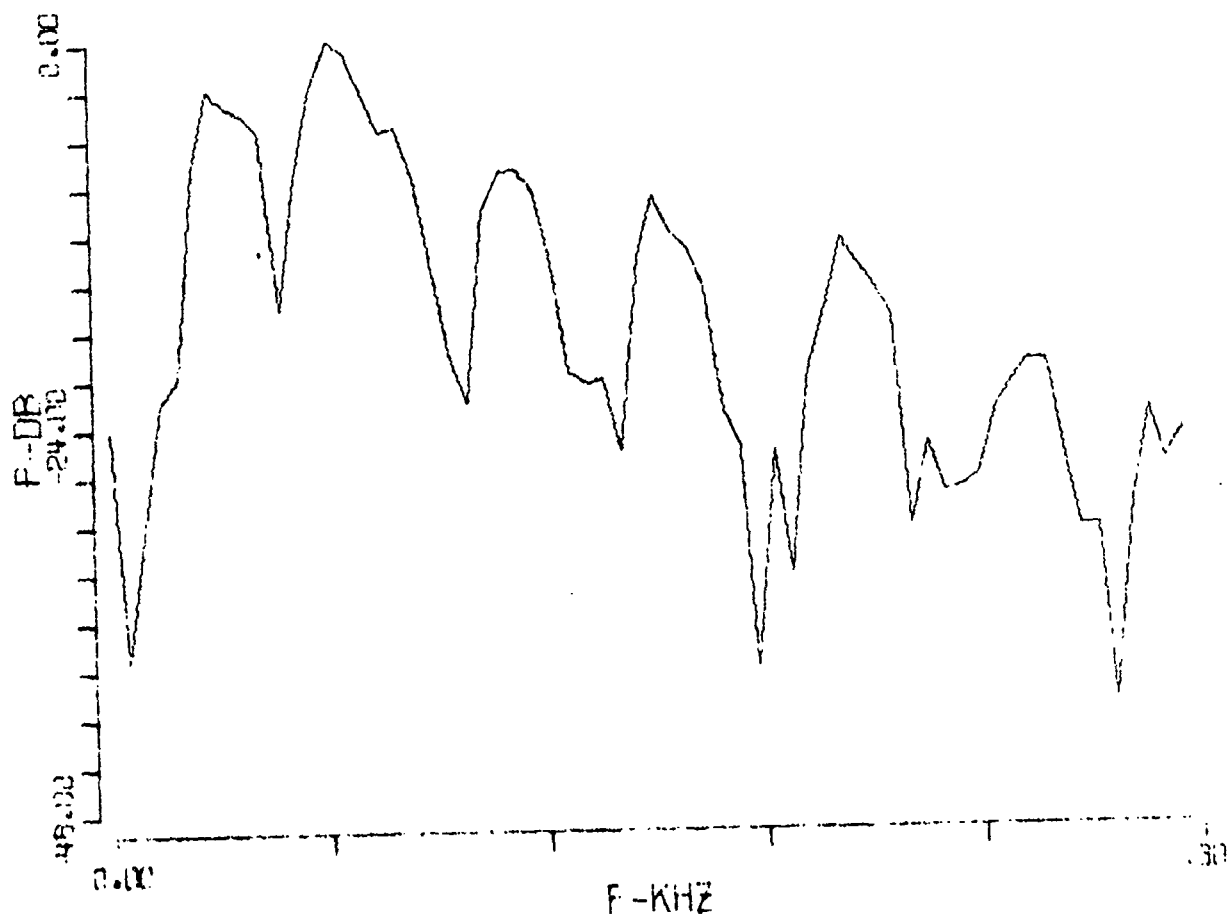
W2-50-800

105<



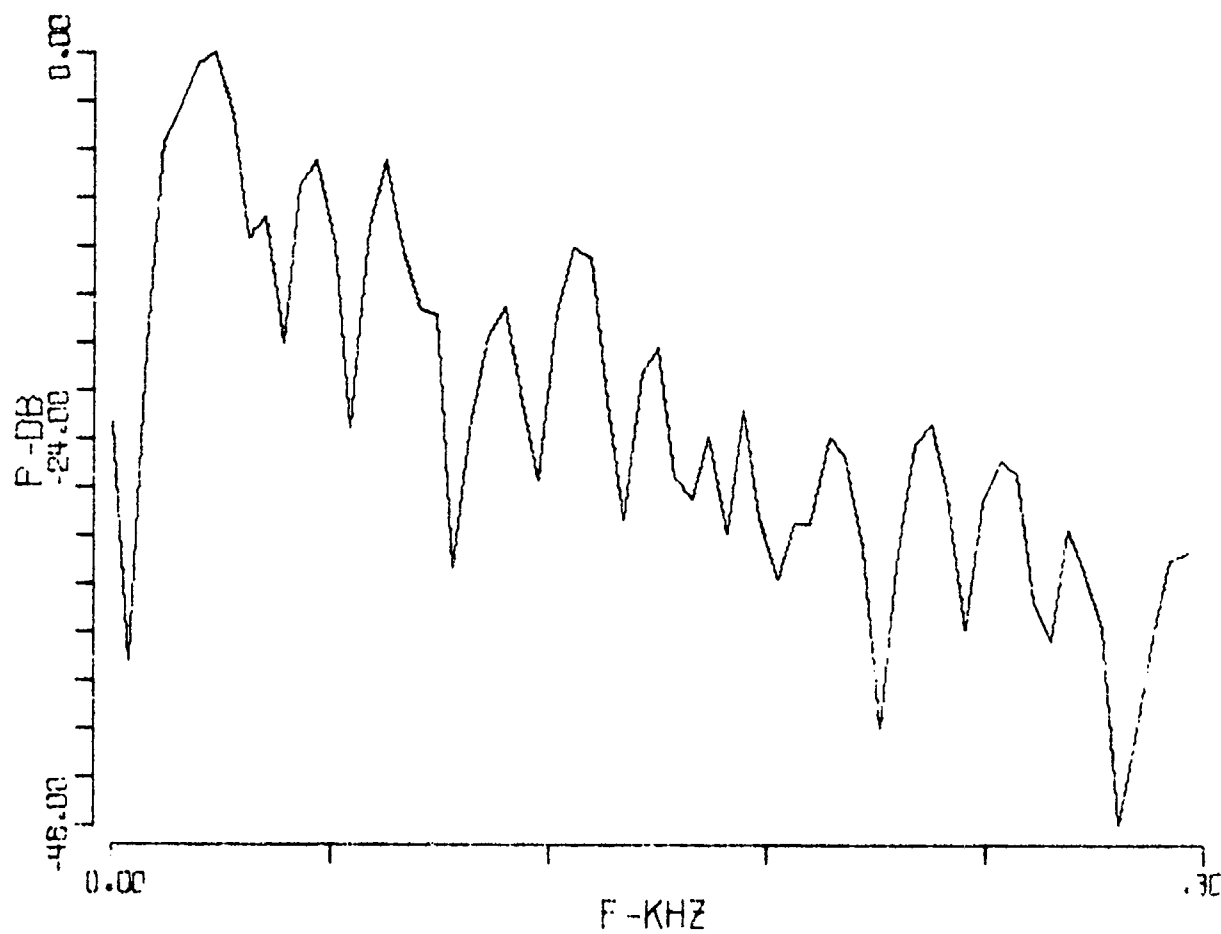
W2-100-300

11.6<



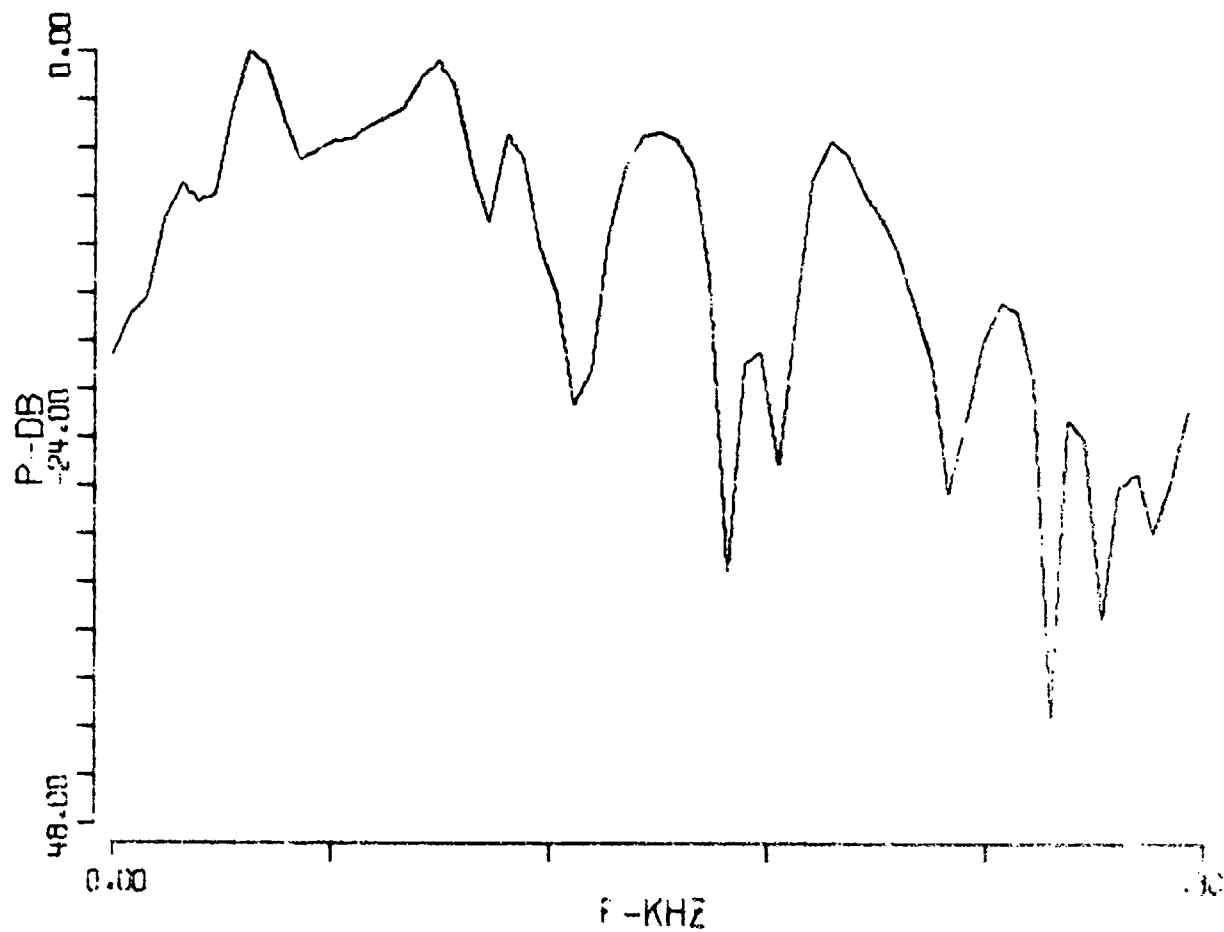
W2-100-800

10.7



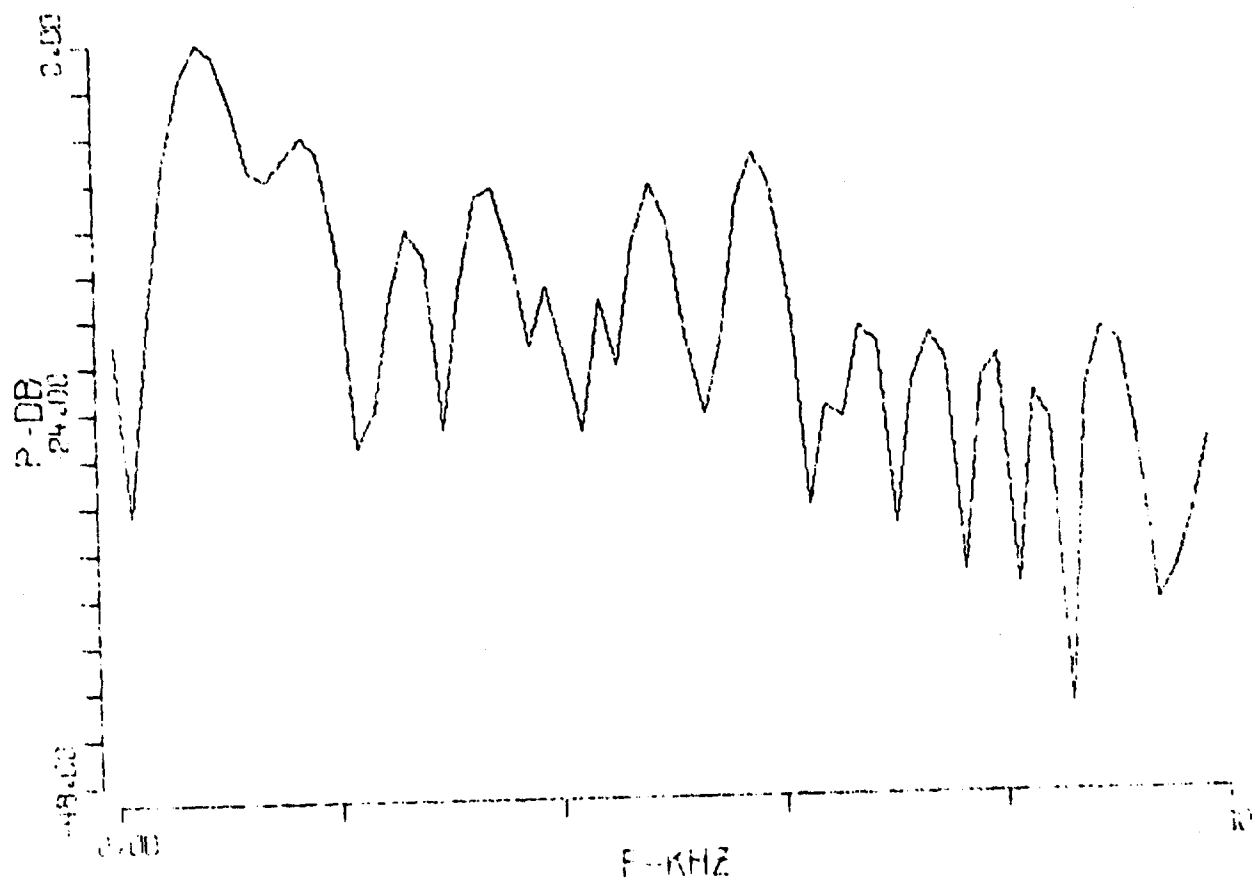
W3-10-300

108<



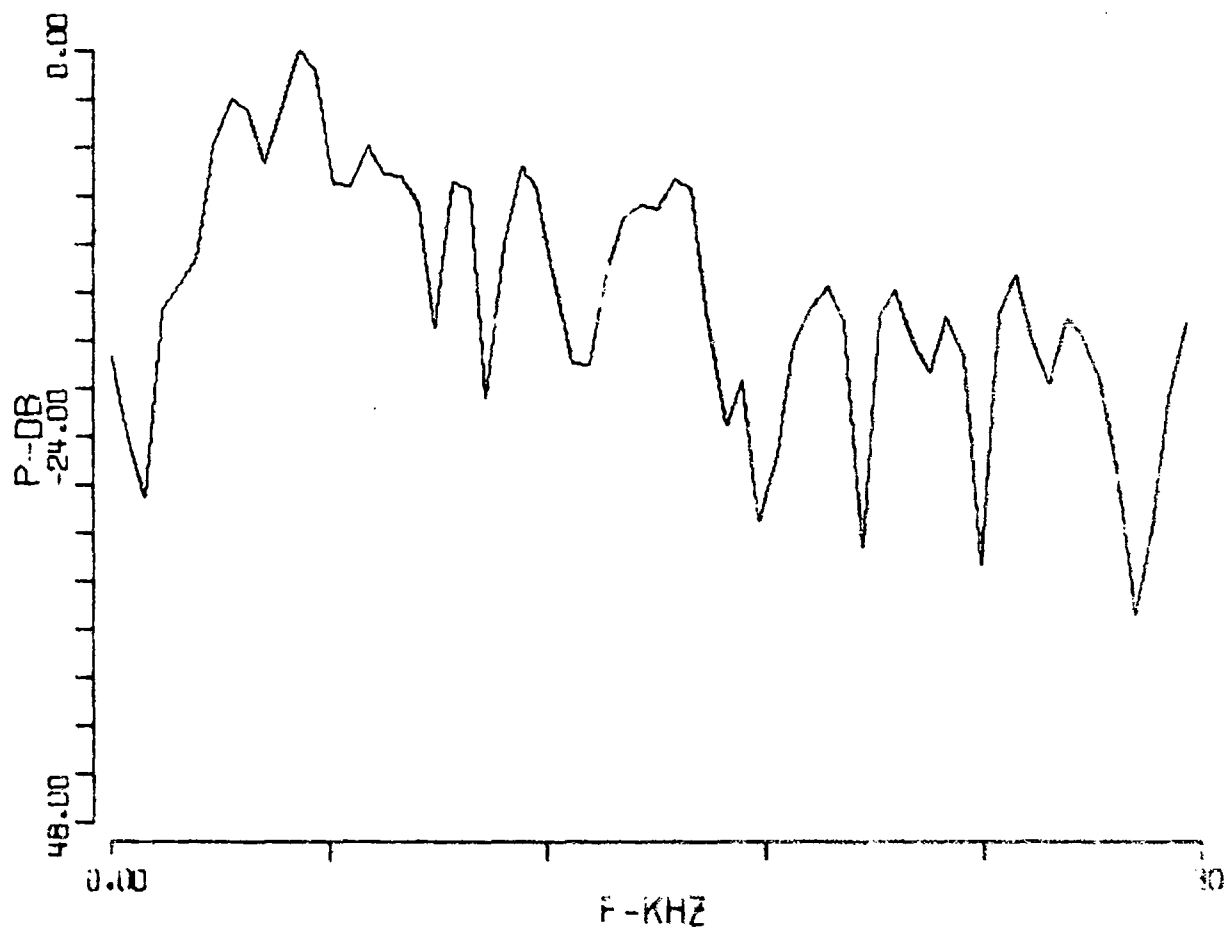
W3-10-800

: 193<



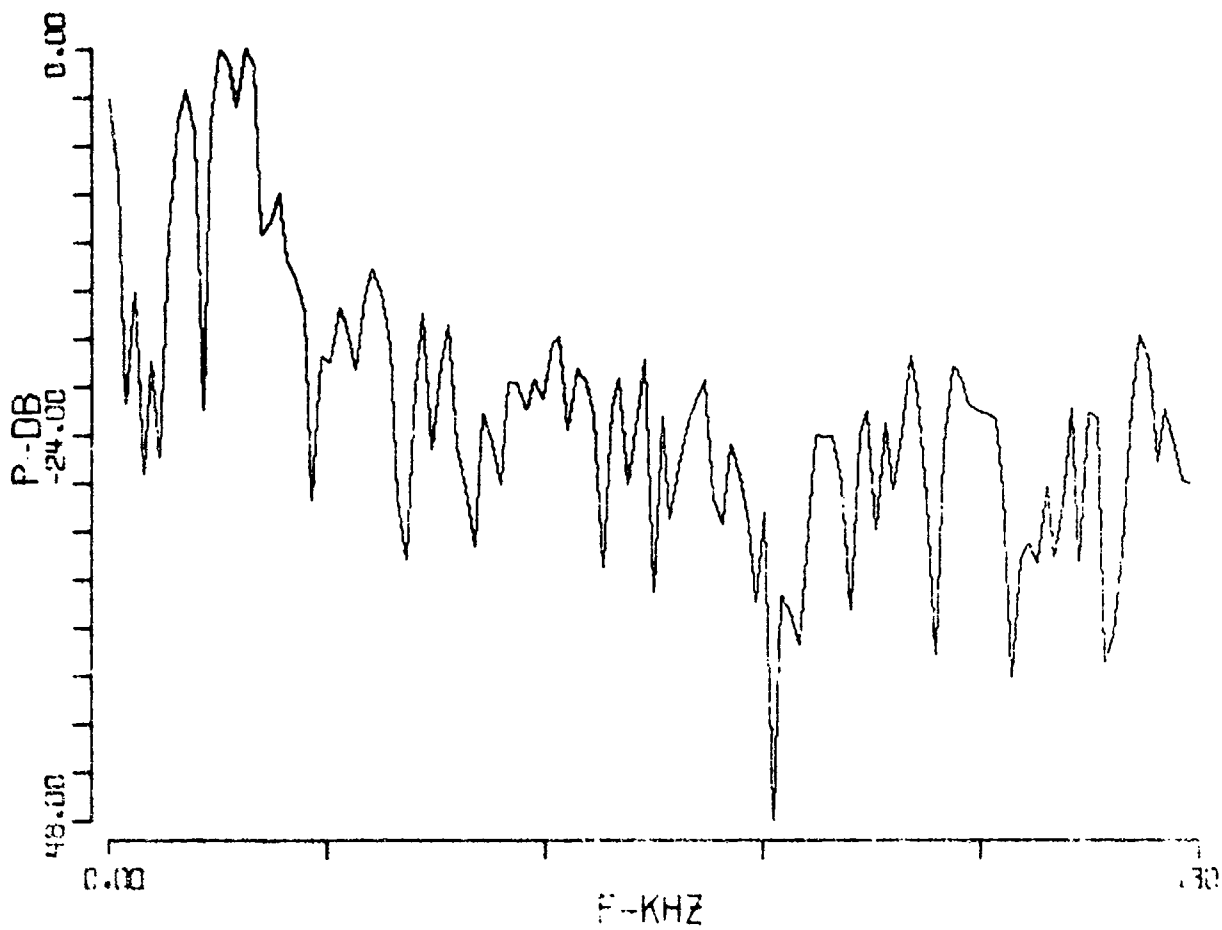
W3-20-300

110<



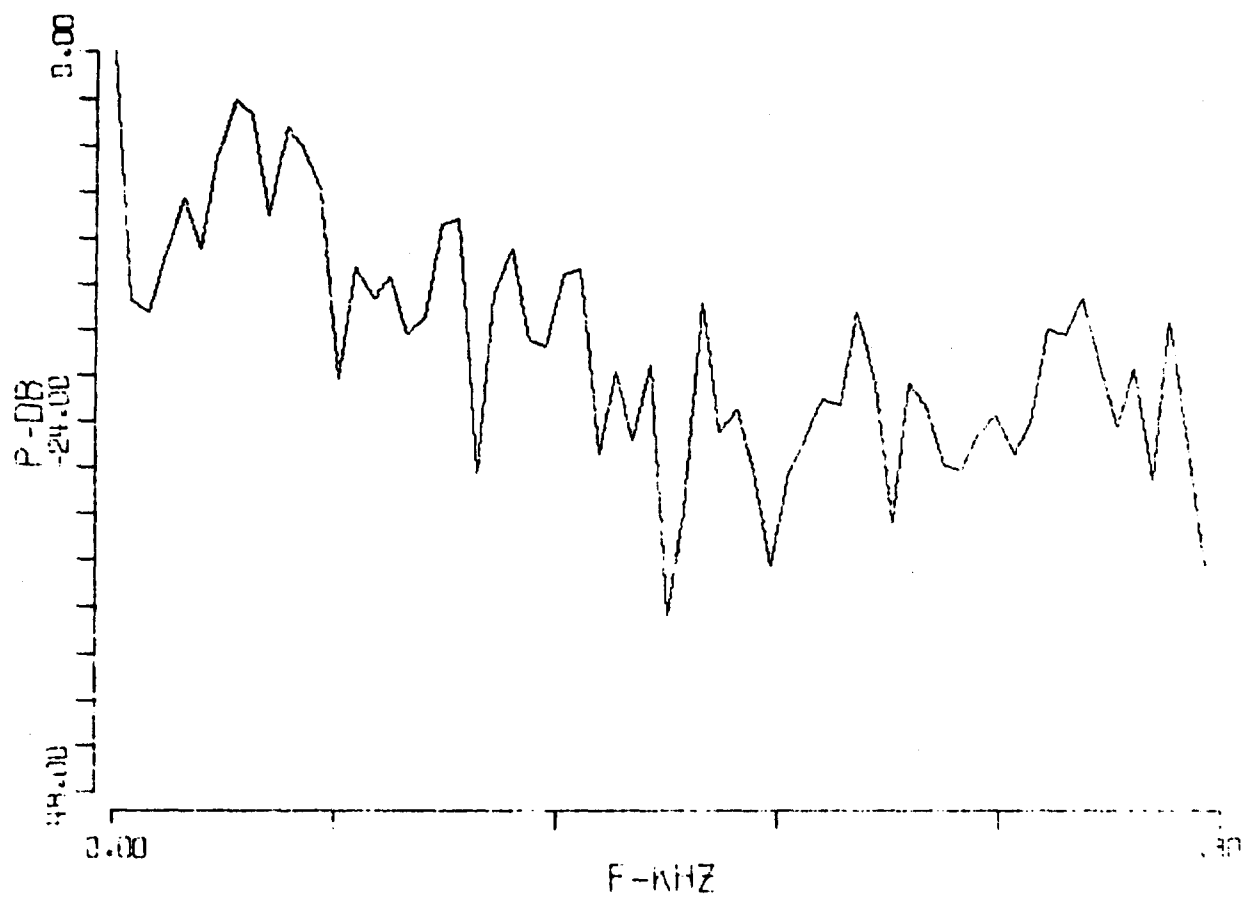
W3-20-800

111<



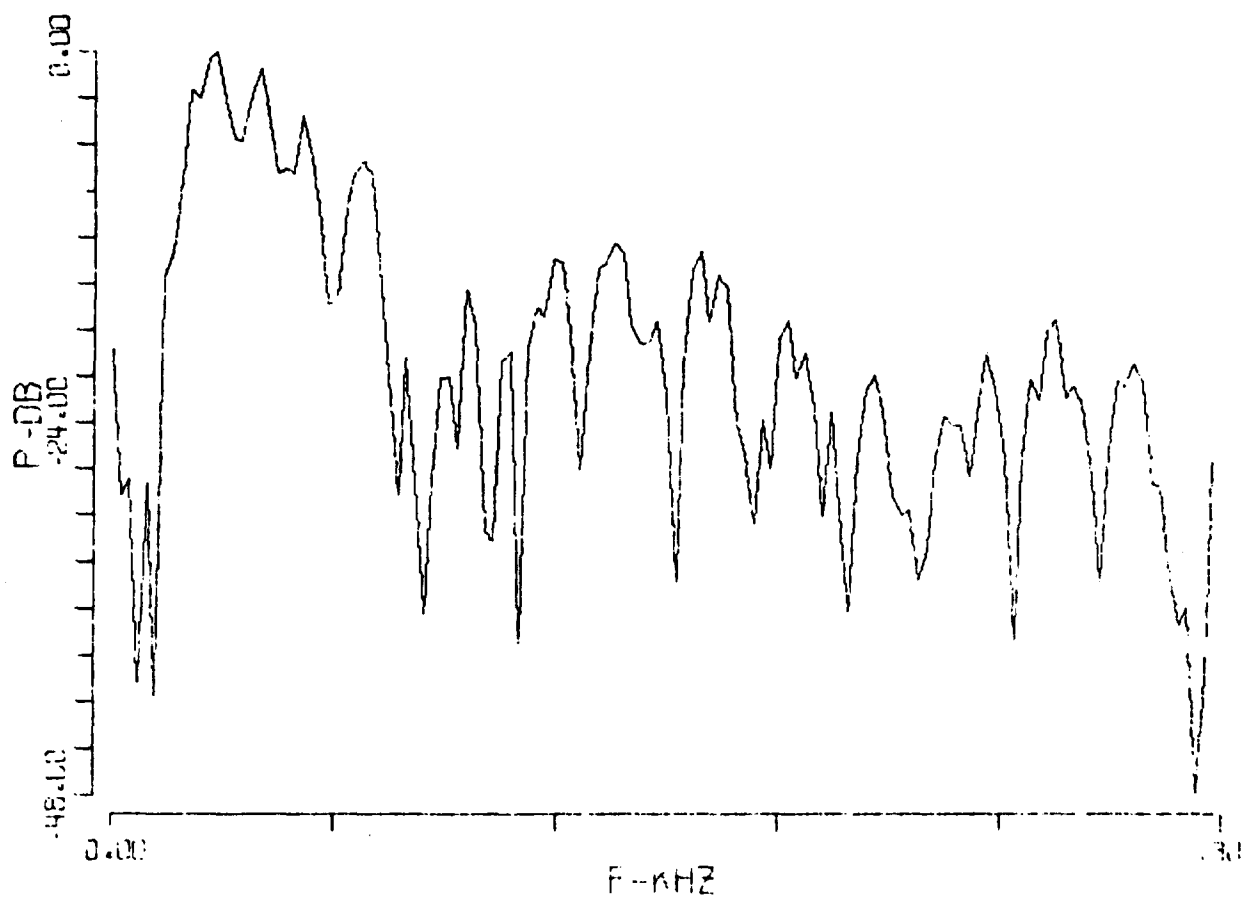
W3-50-300

112<



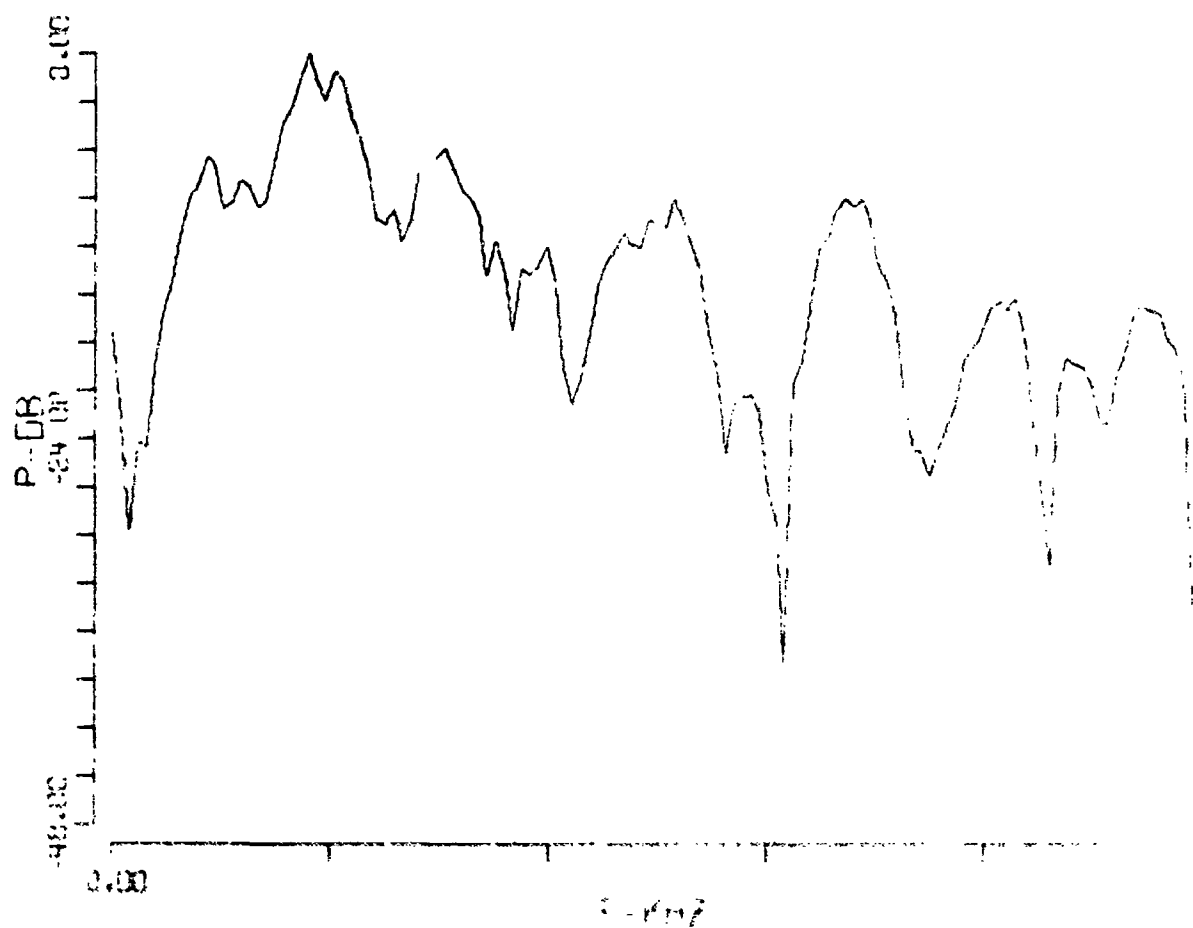
W3-50-800

113<



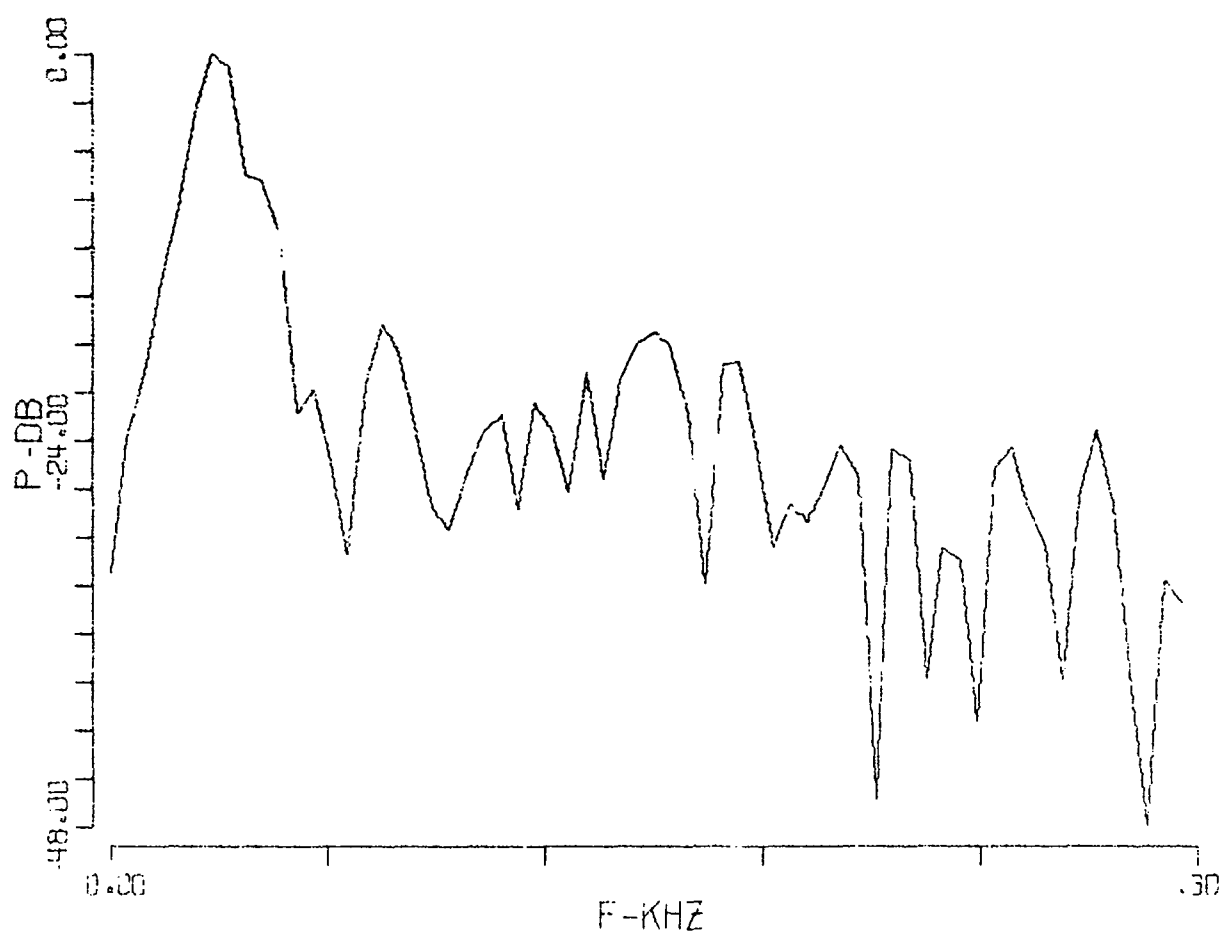
W3-100-300

114<



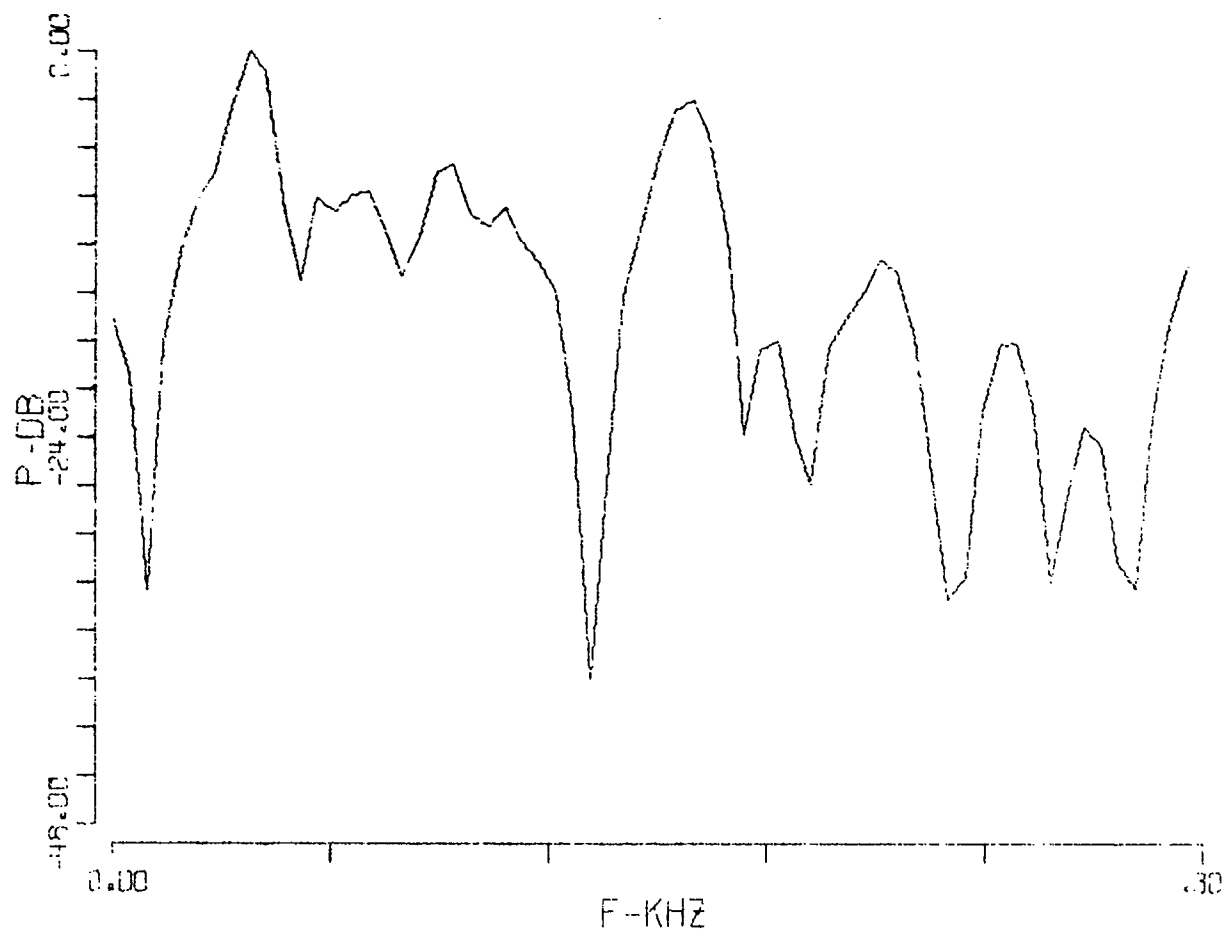
W3-100-800

115-



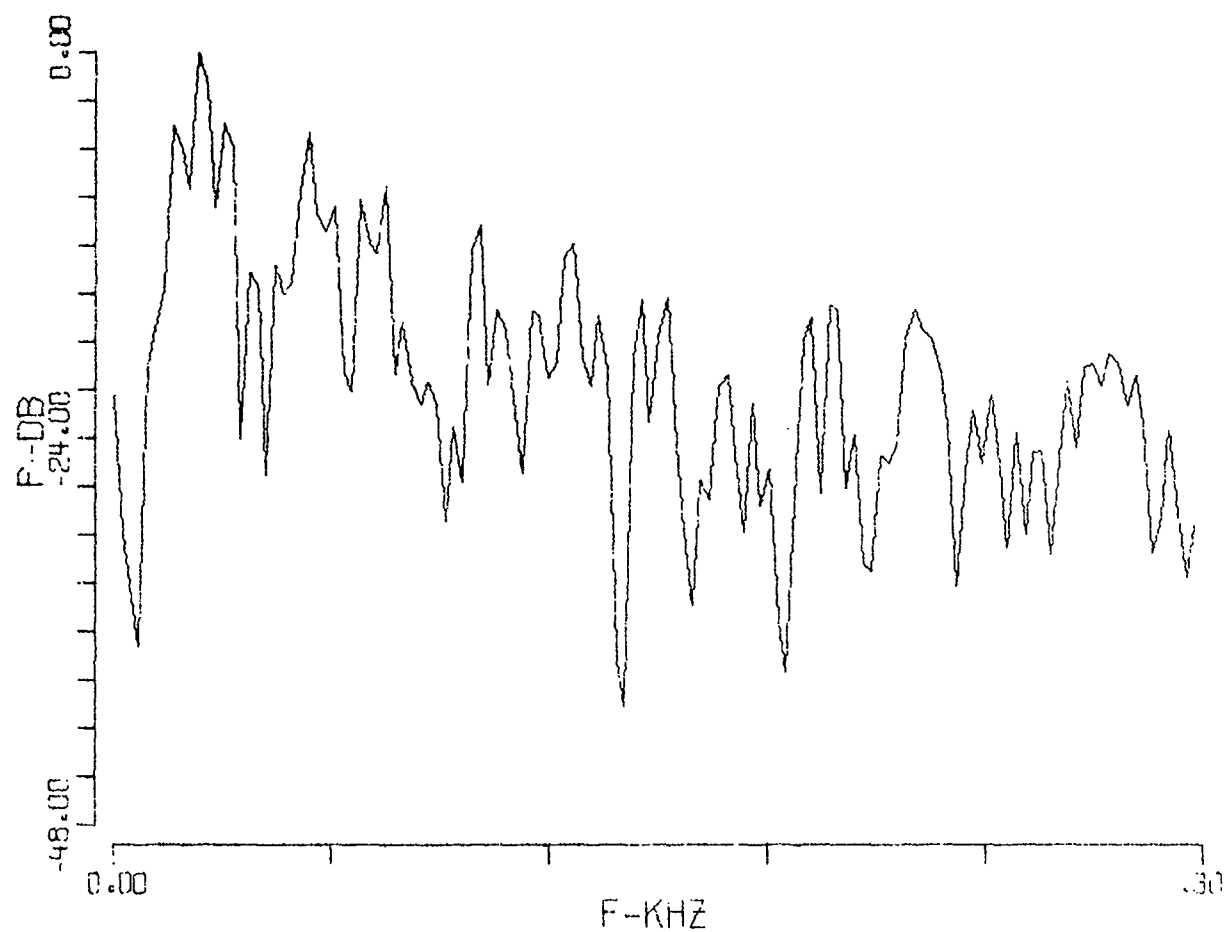
W4-10-300

116<



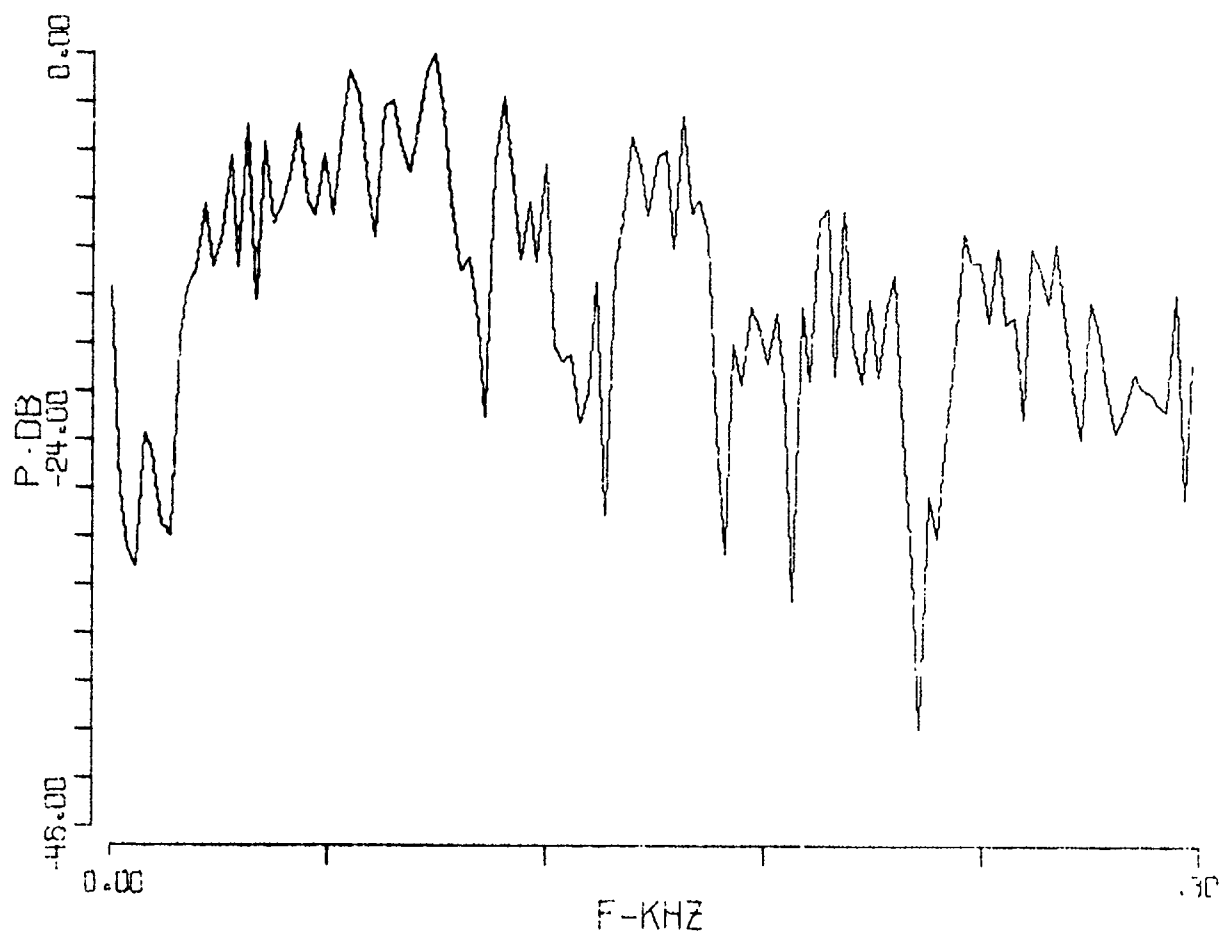
W4-10-800

117<



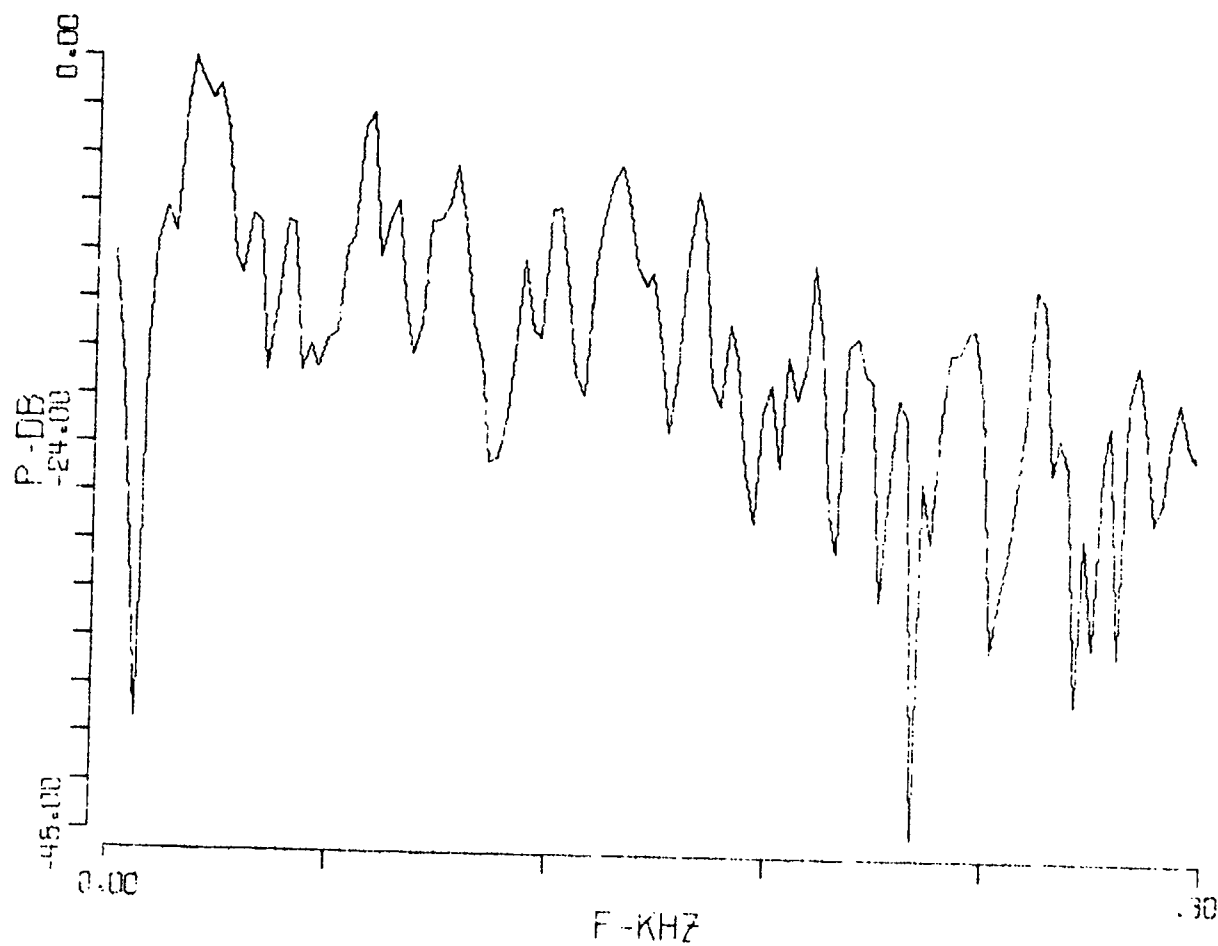
W4-20-300

118<



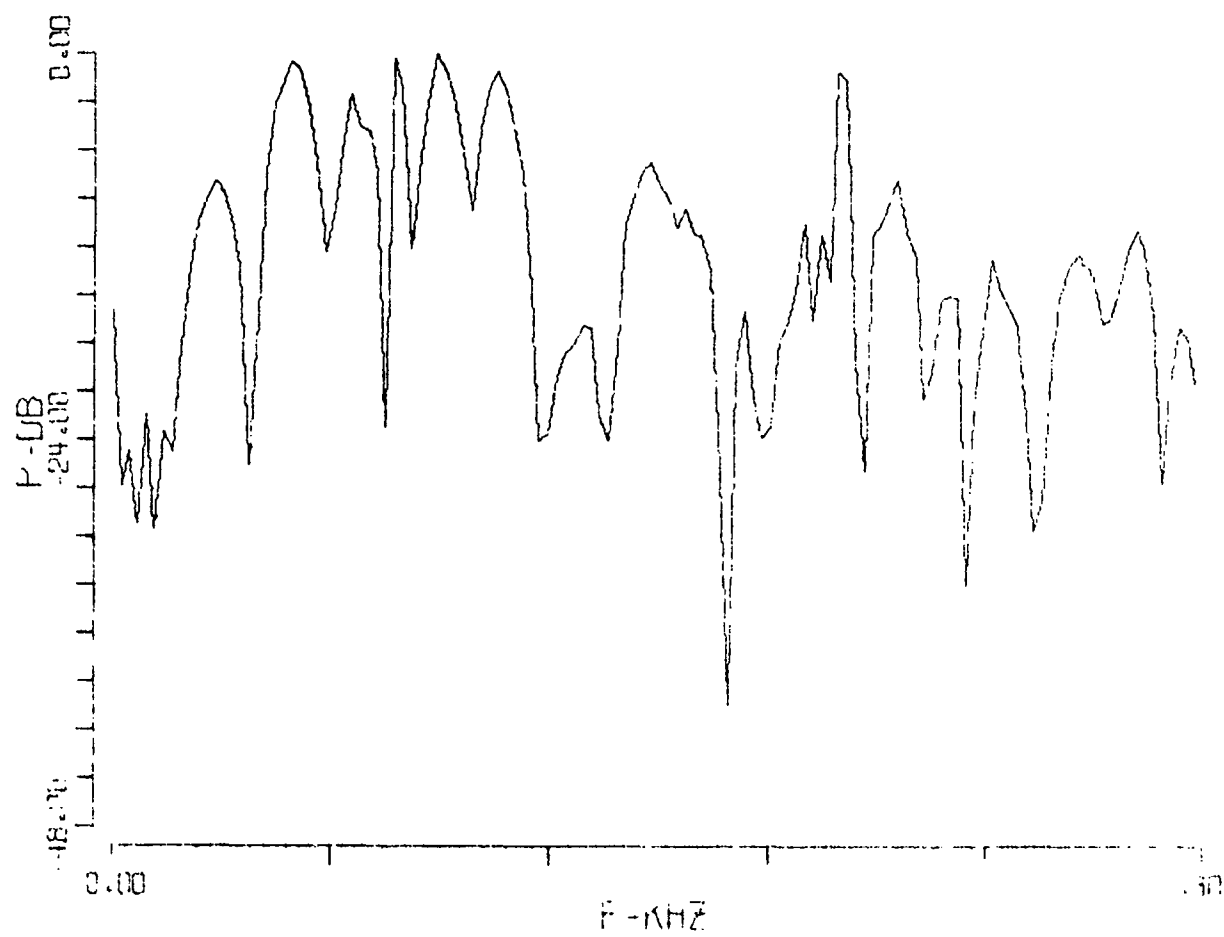
W4-20-800

119<



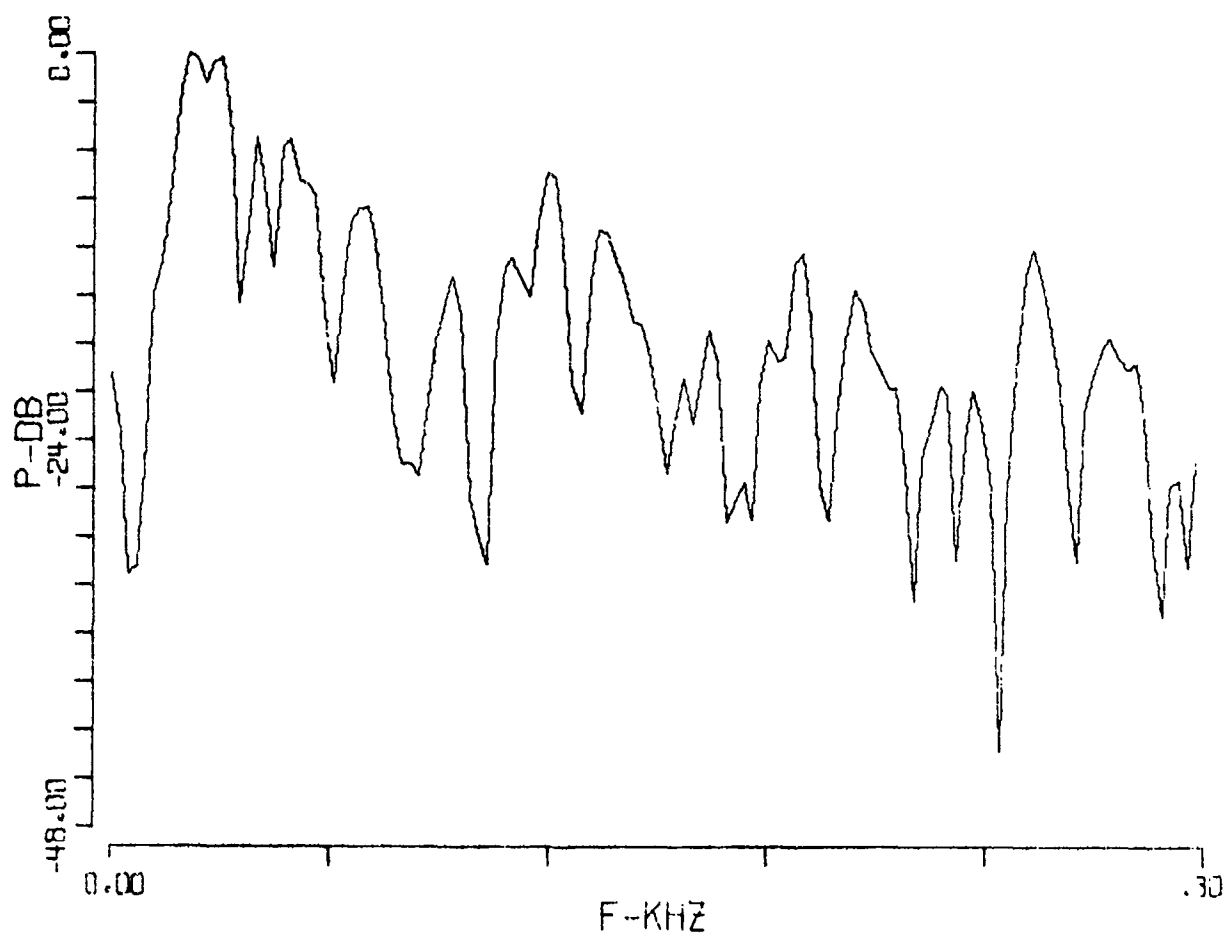
W4-50-300

120<



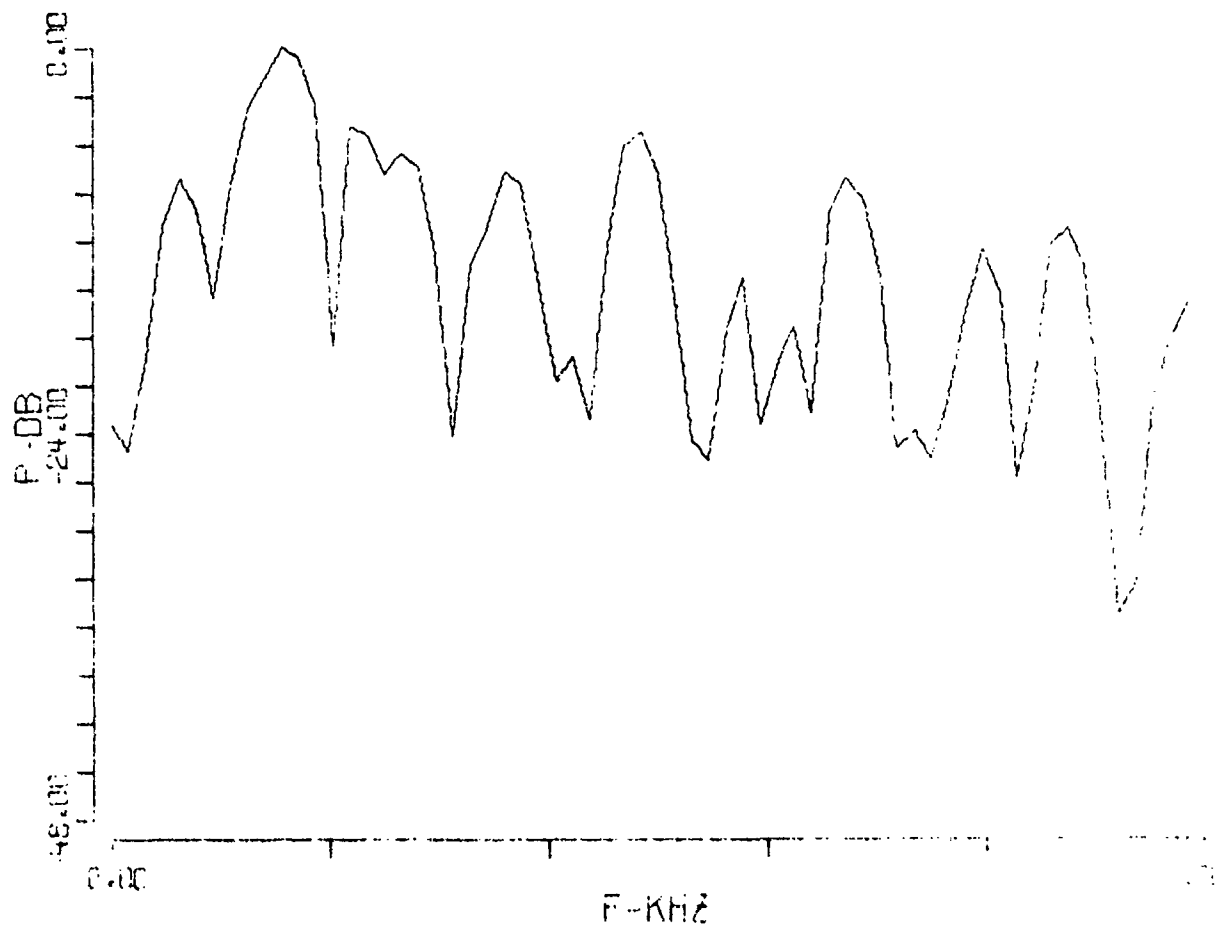
W4-50-800

121<



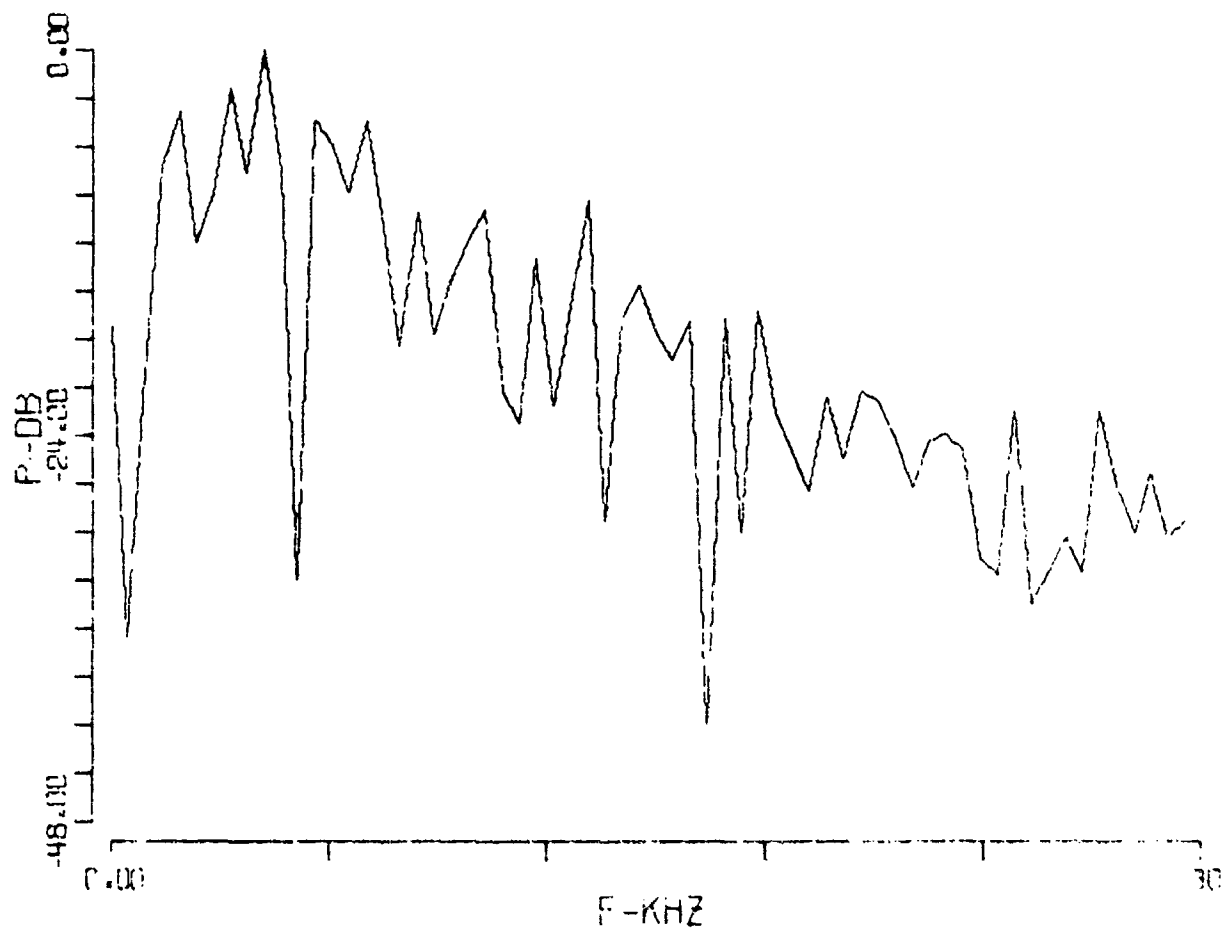
W4-100-300

122<



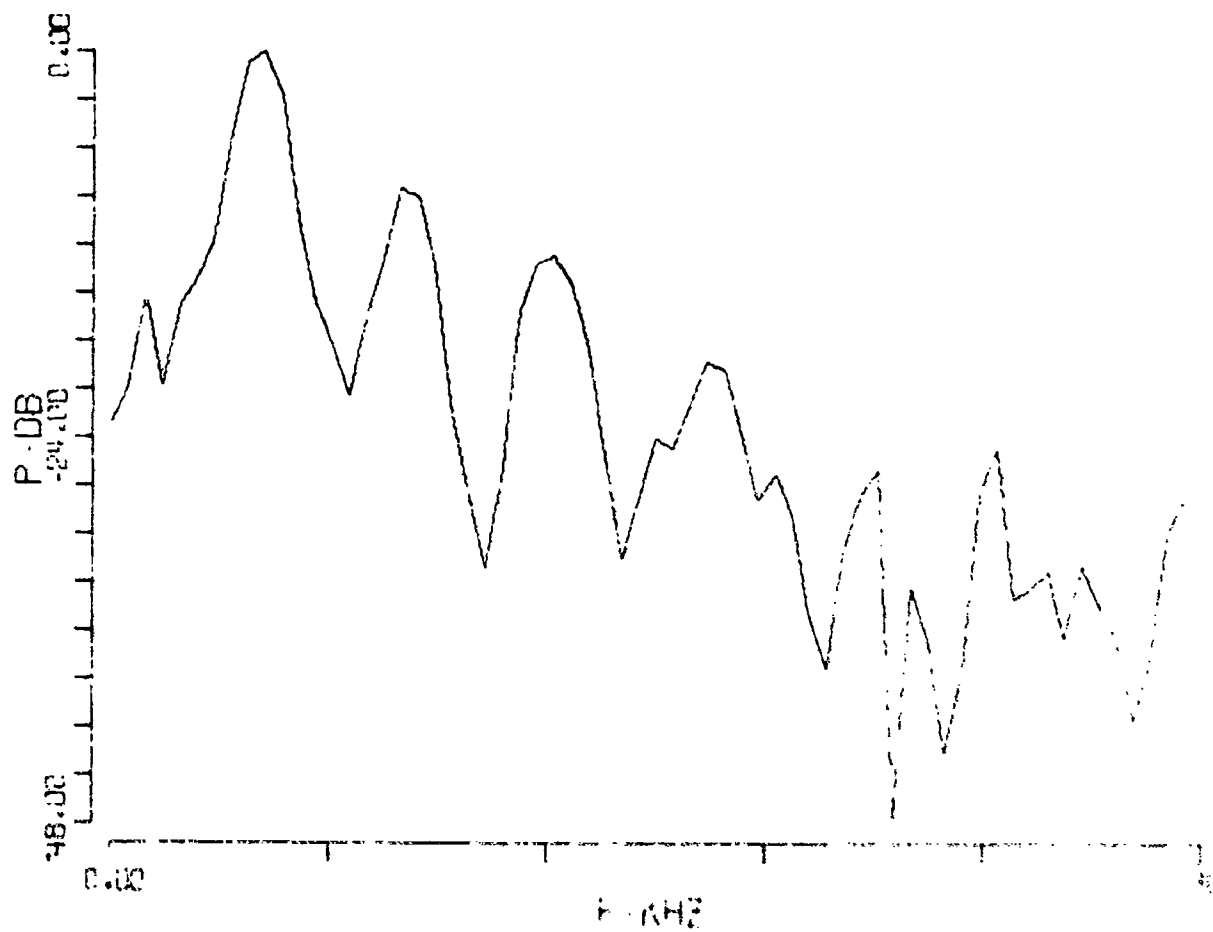
W4-100-800

123<



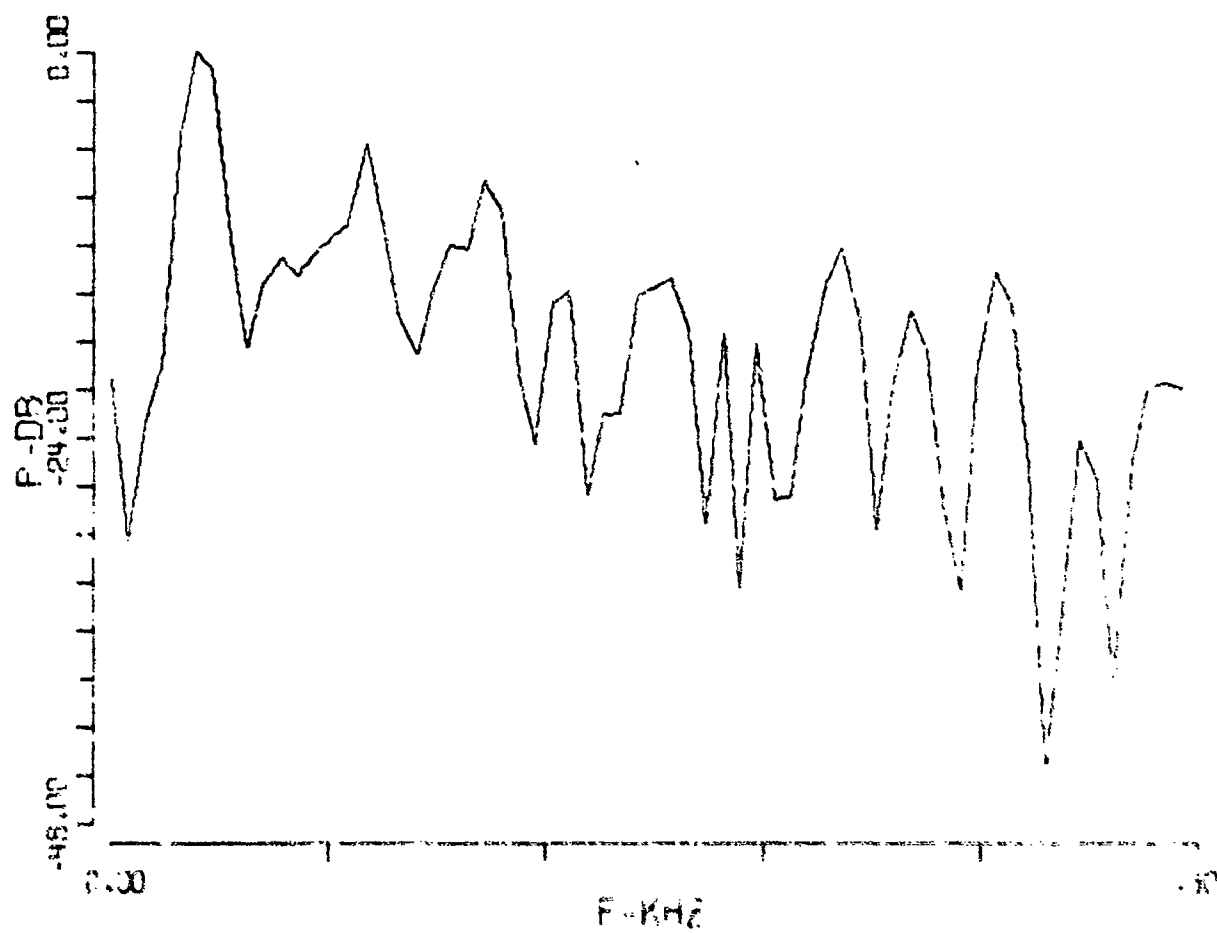
WS-10-300

124<



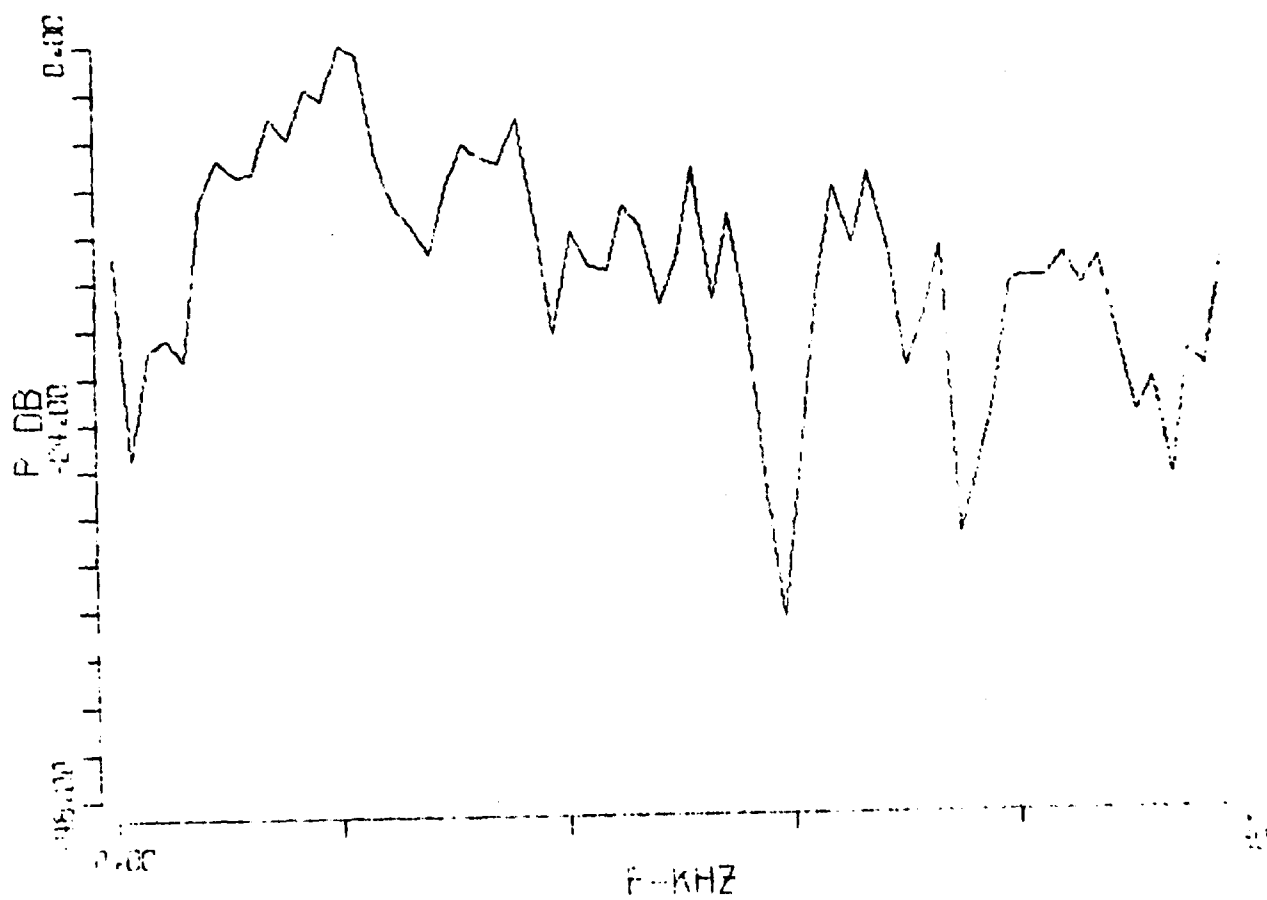
NS-10-800

125<



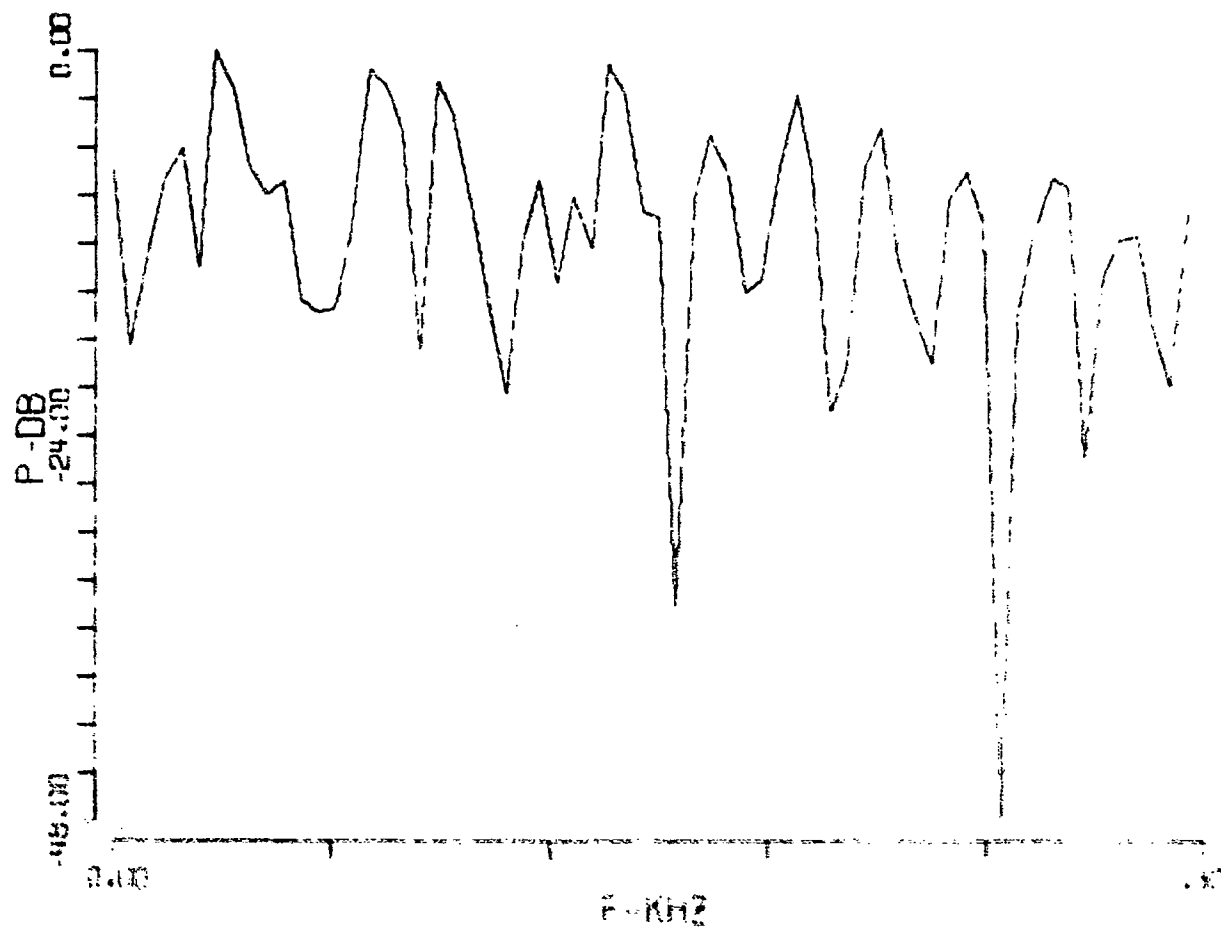
NS-20-300

126<



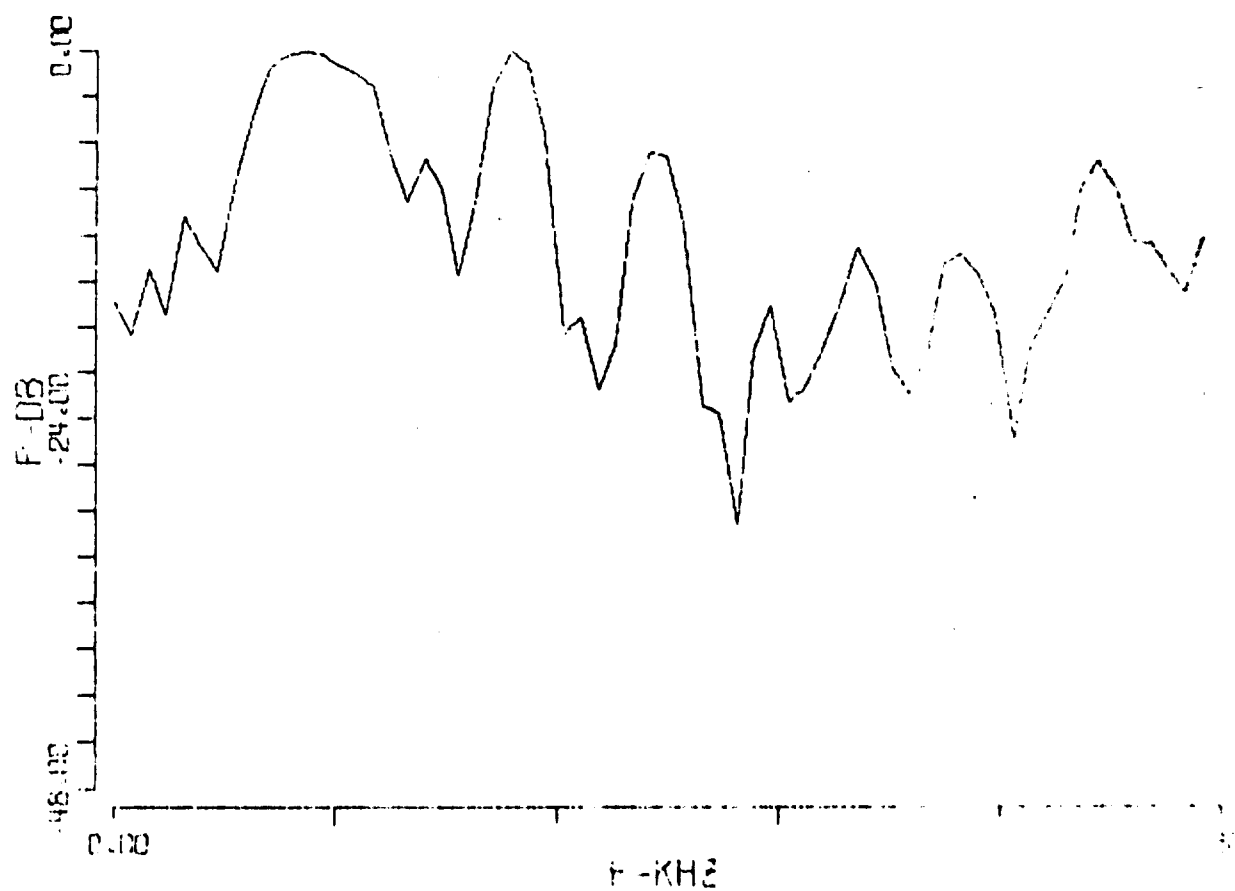
W5-20-800

127<



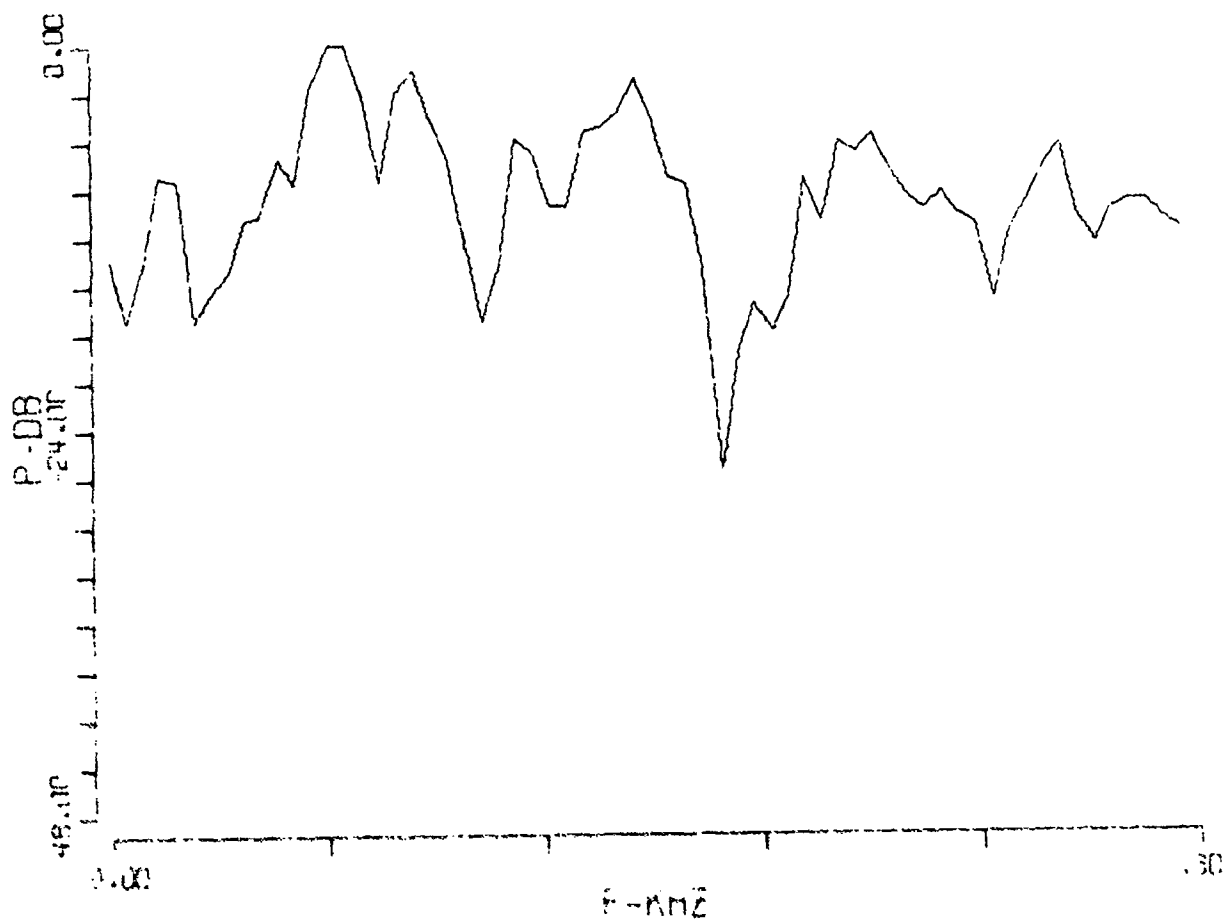
NS-50-300

128<



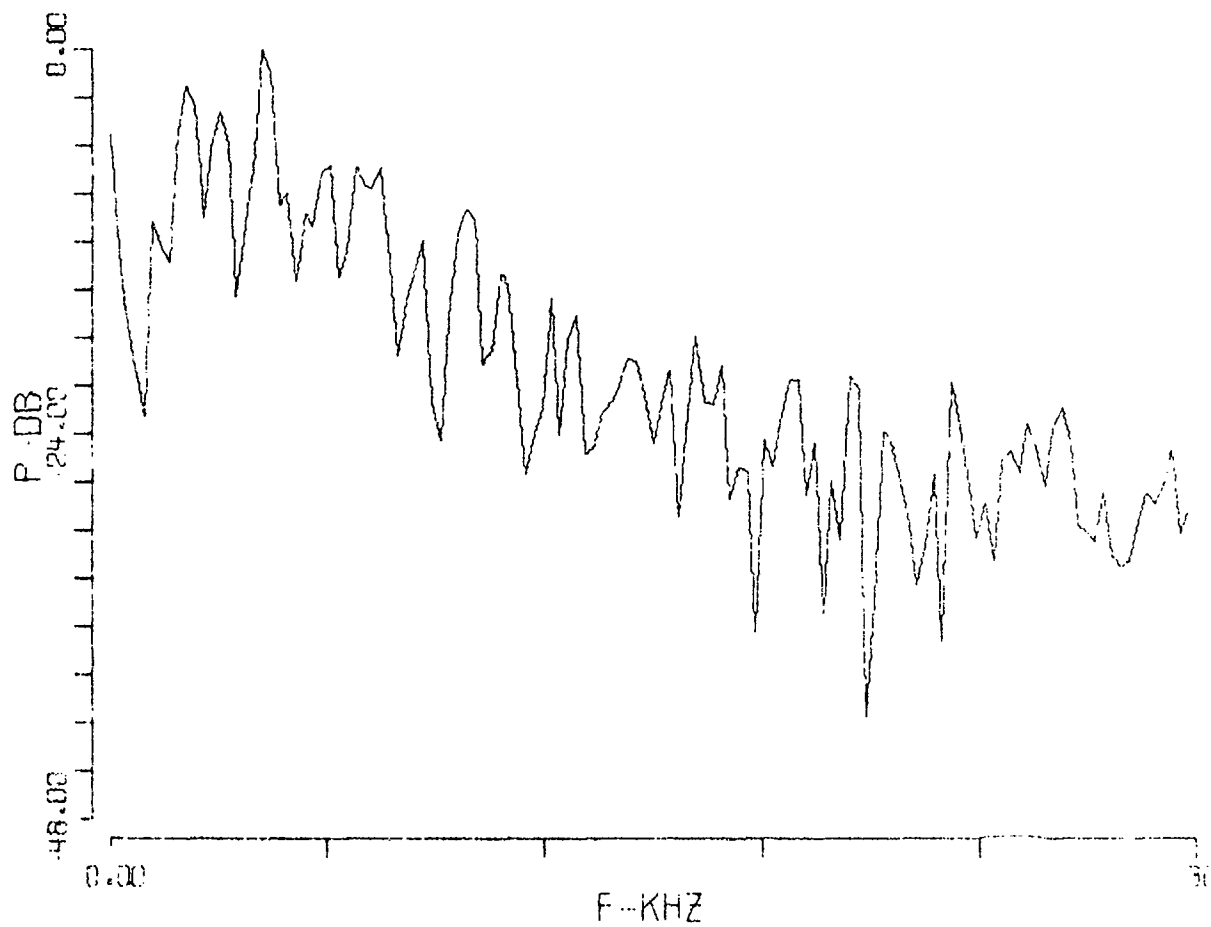
W5-50-800

129<



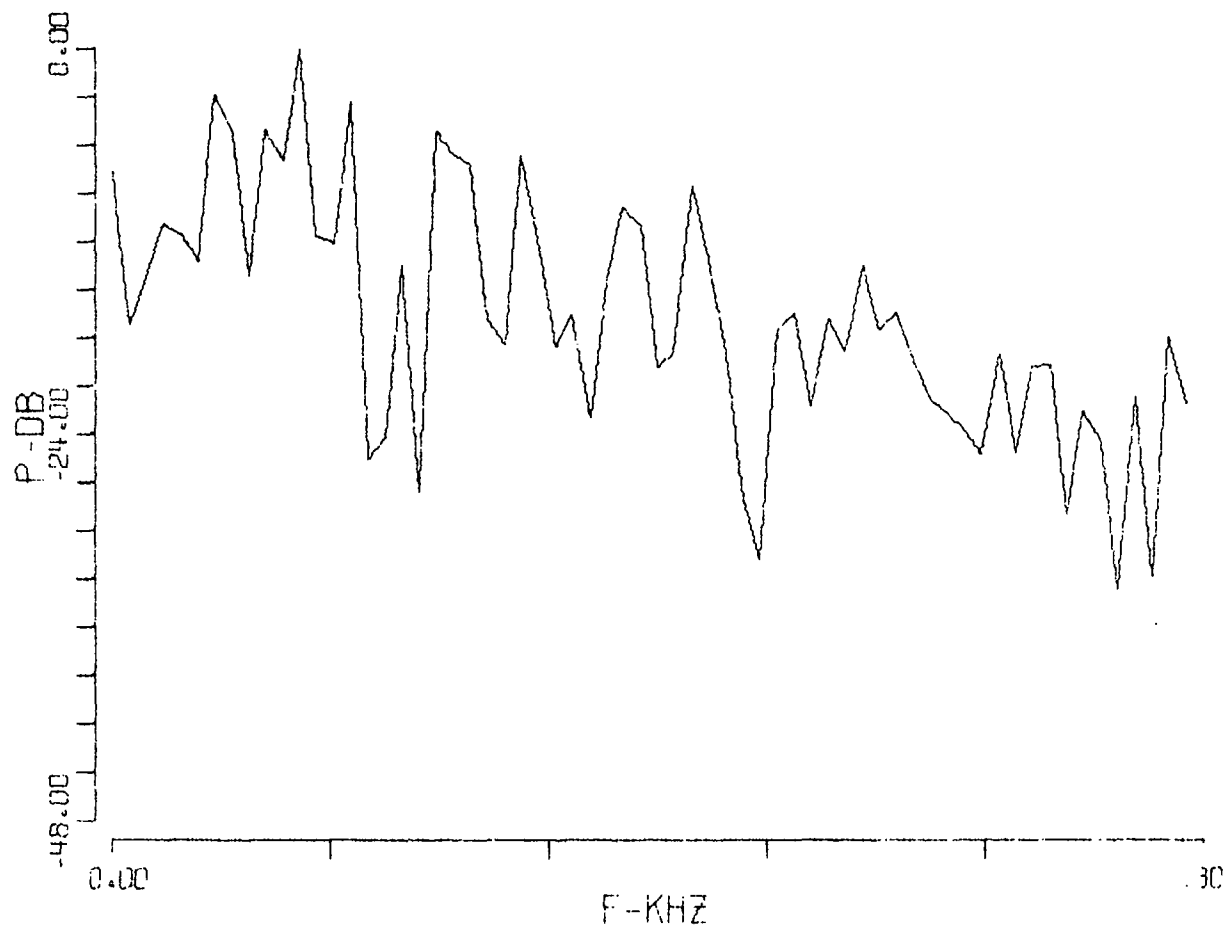
NS-100-800

130-



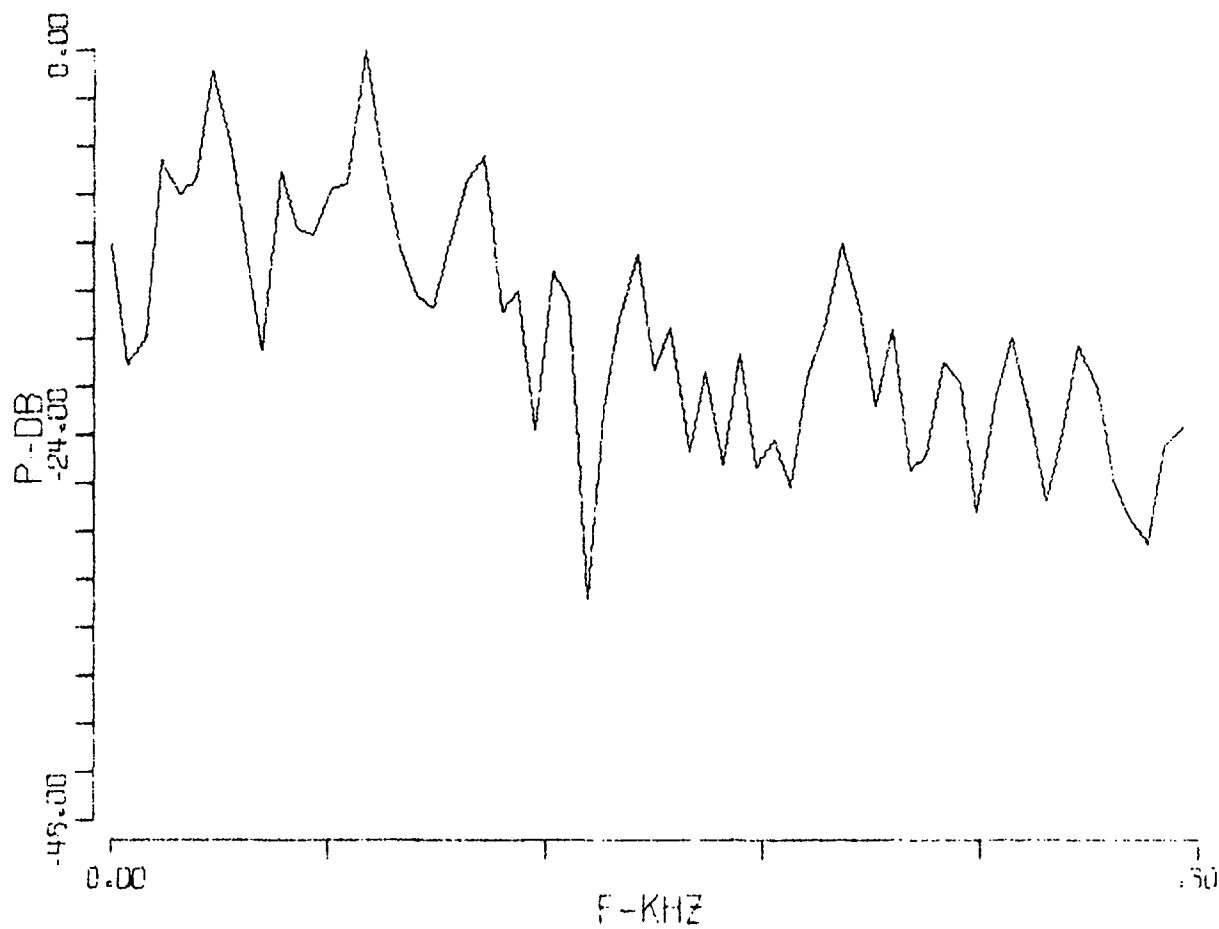
W6-10-300

131<



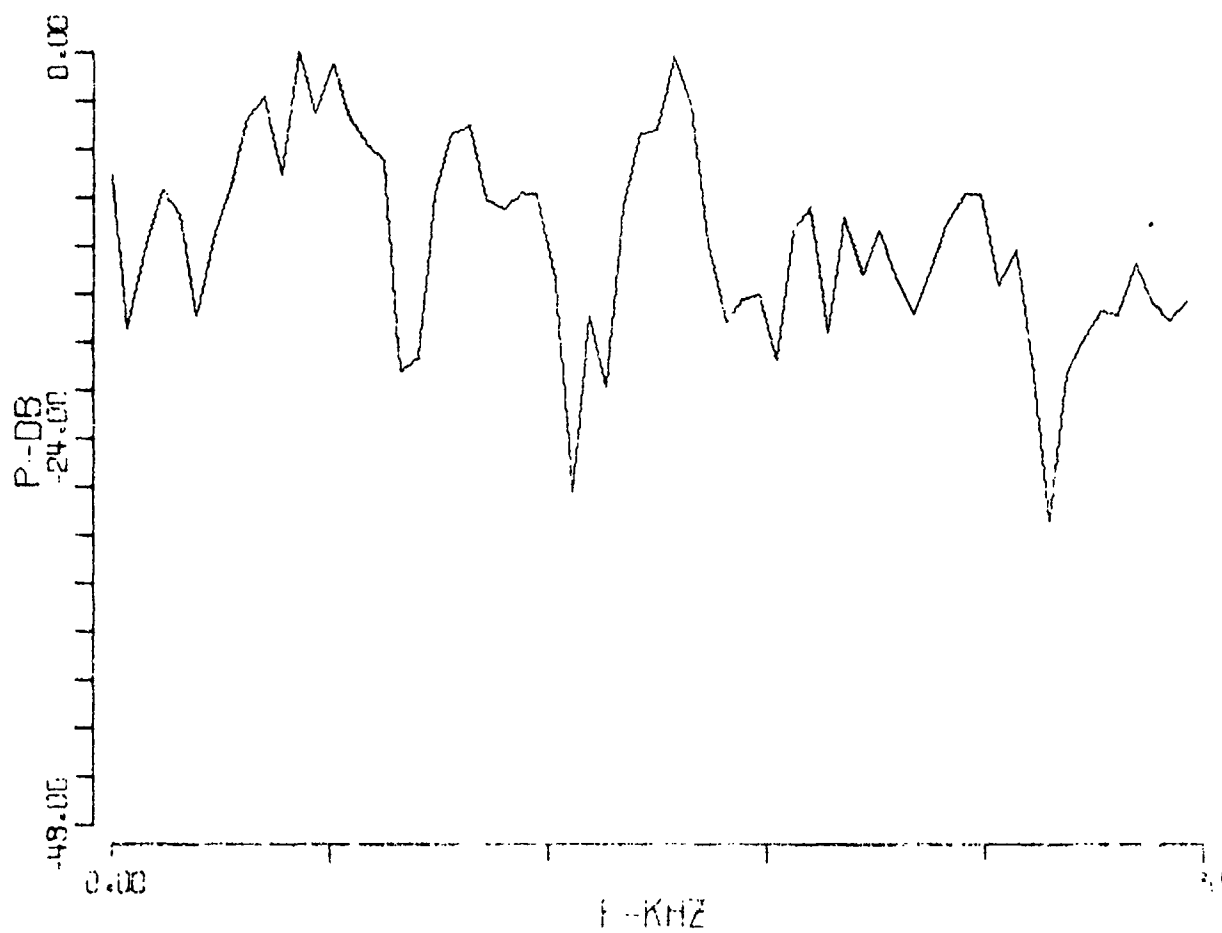
W6-10-800

132<



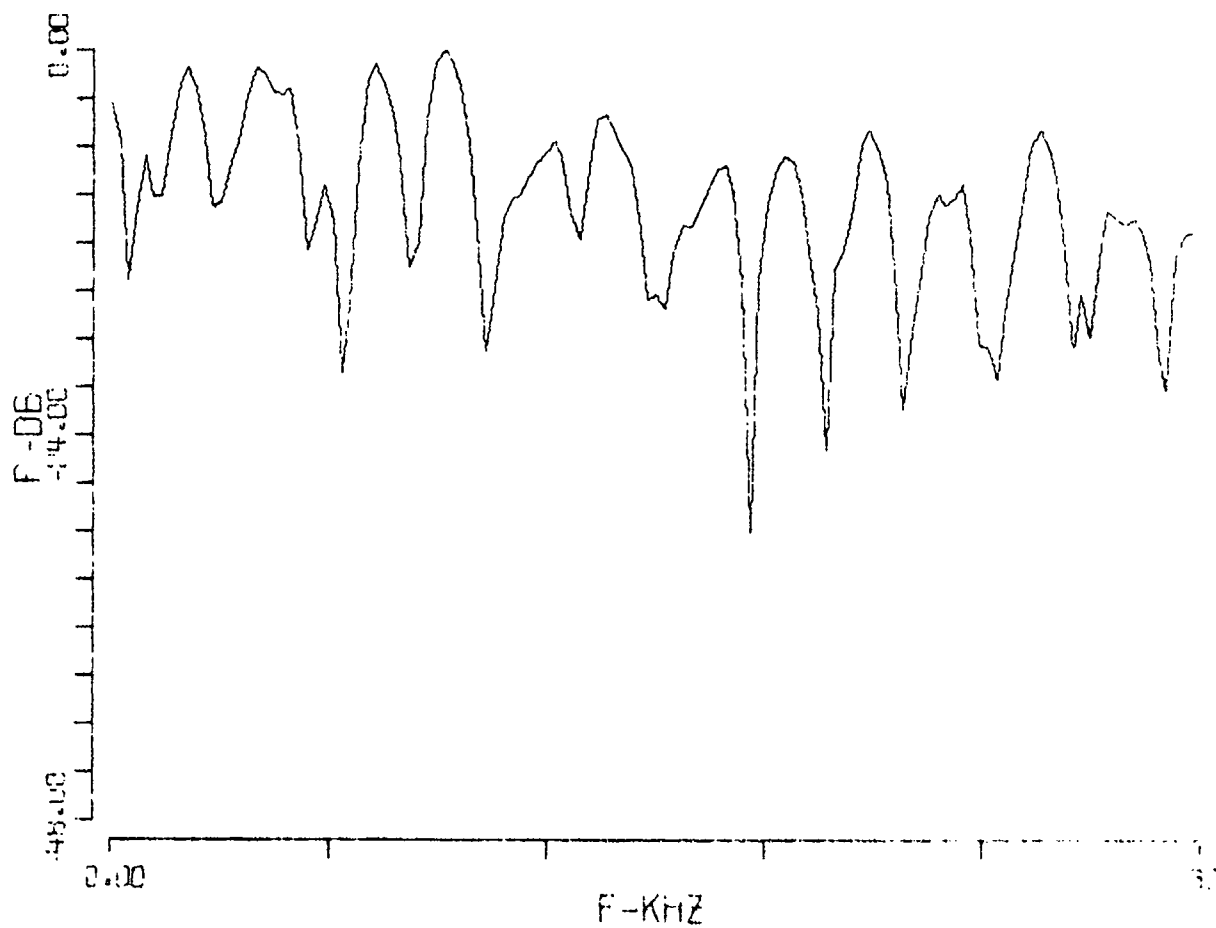
W6-20-300

133<



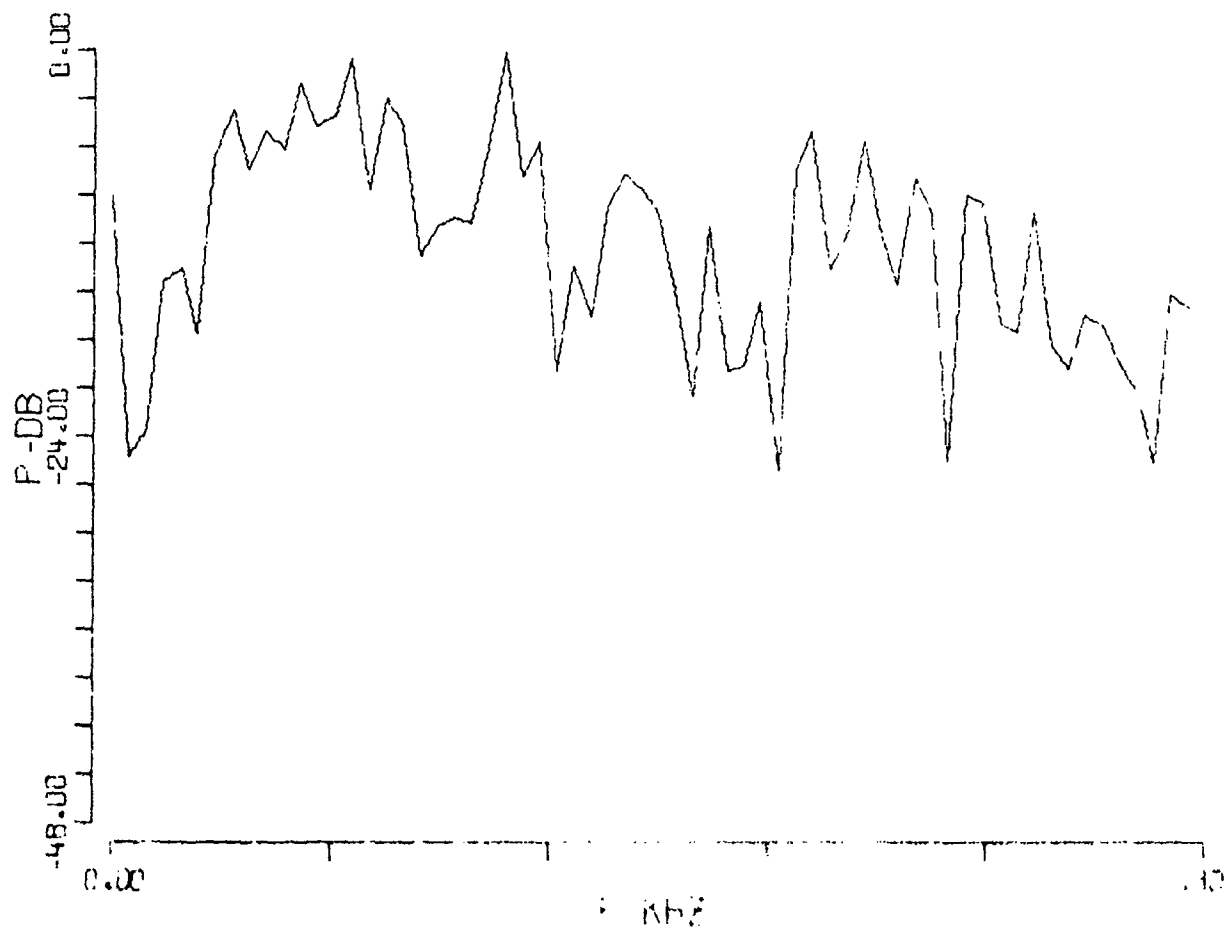
W6-20-800

134-



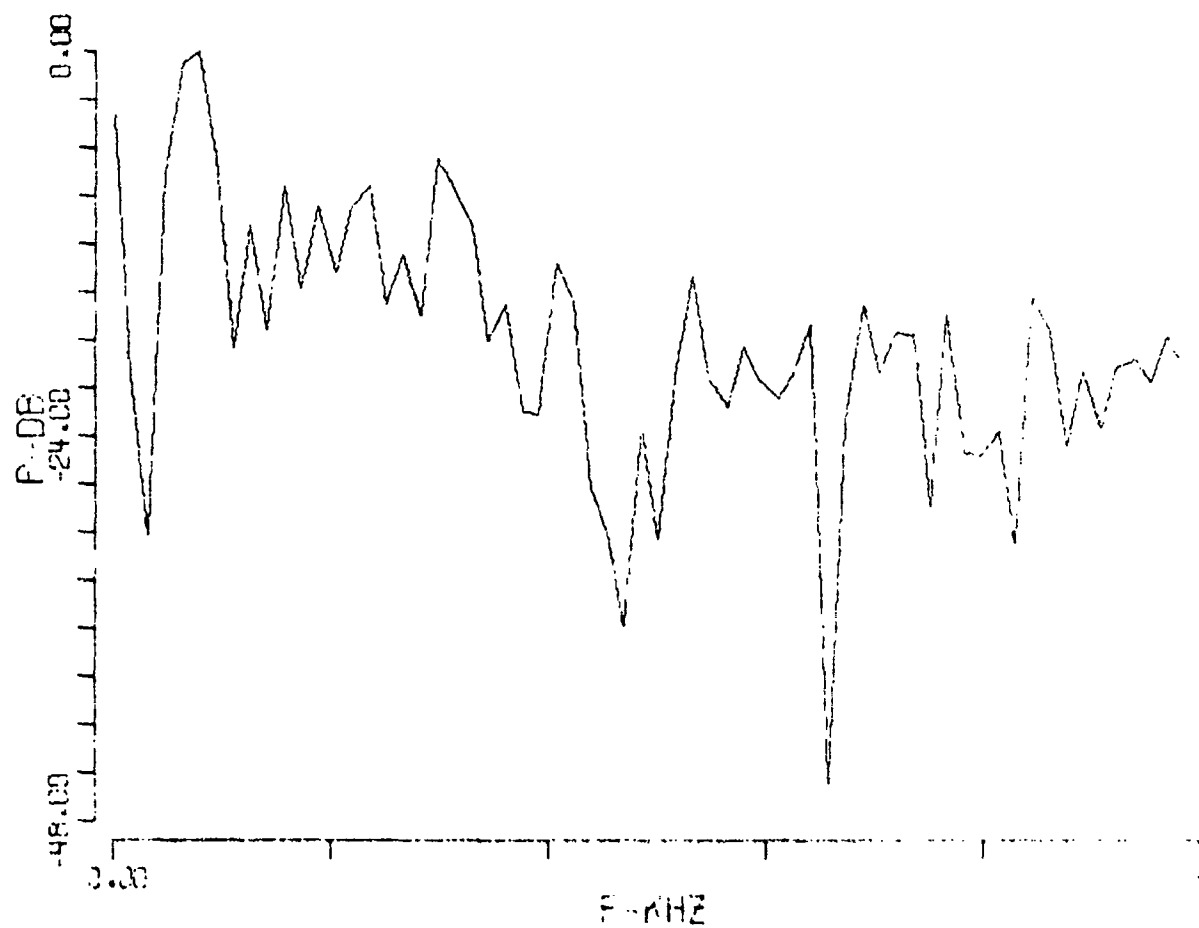
W6-50-300

135<



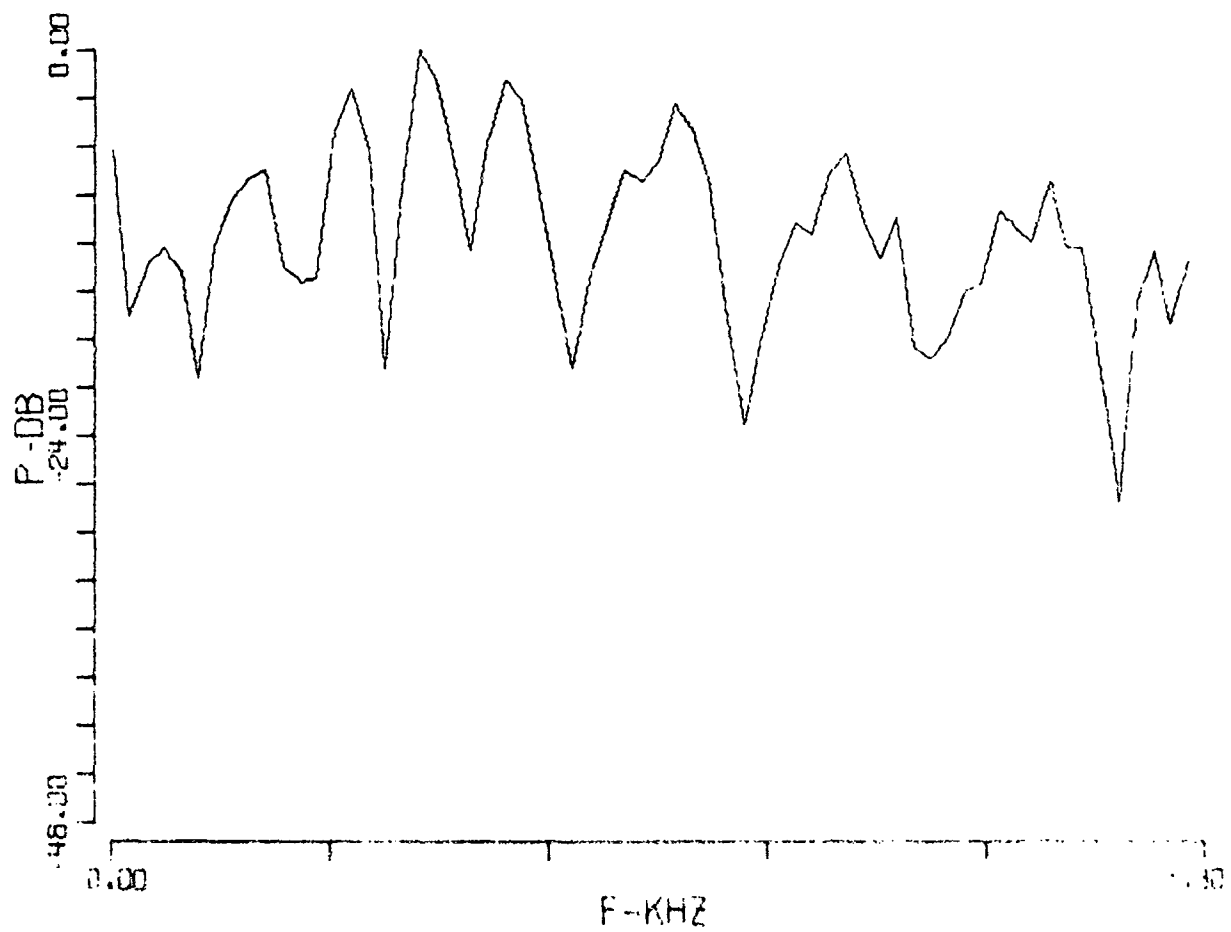
W6-50-800

136



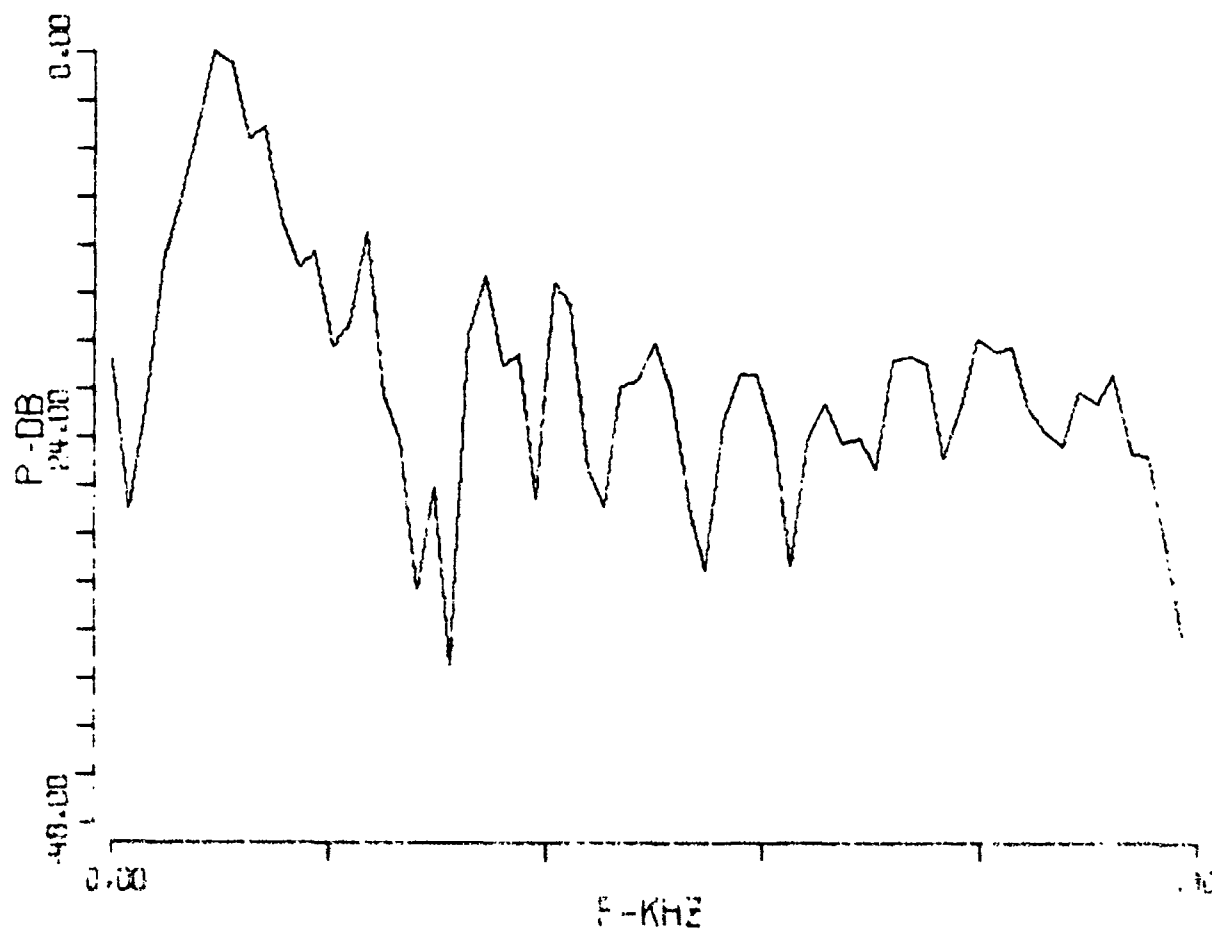
W6-100-300

137<



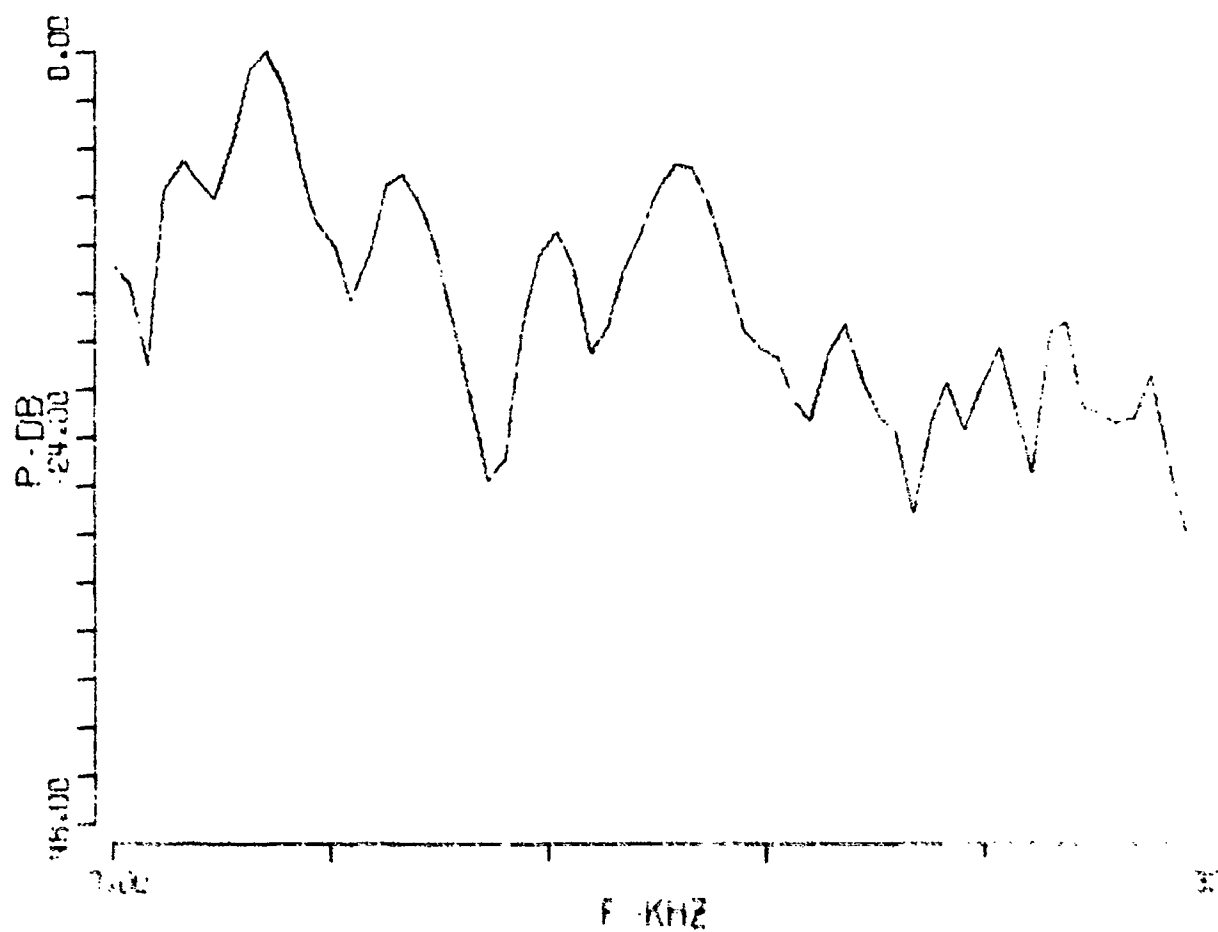
W6-100-800

138<



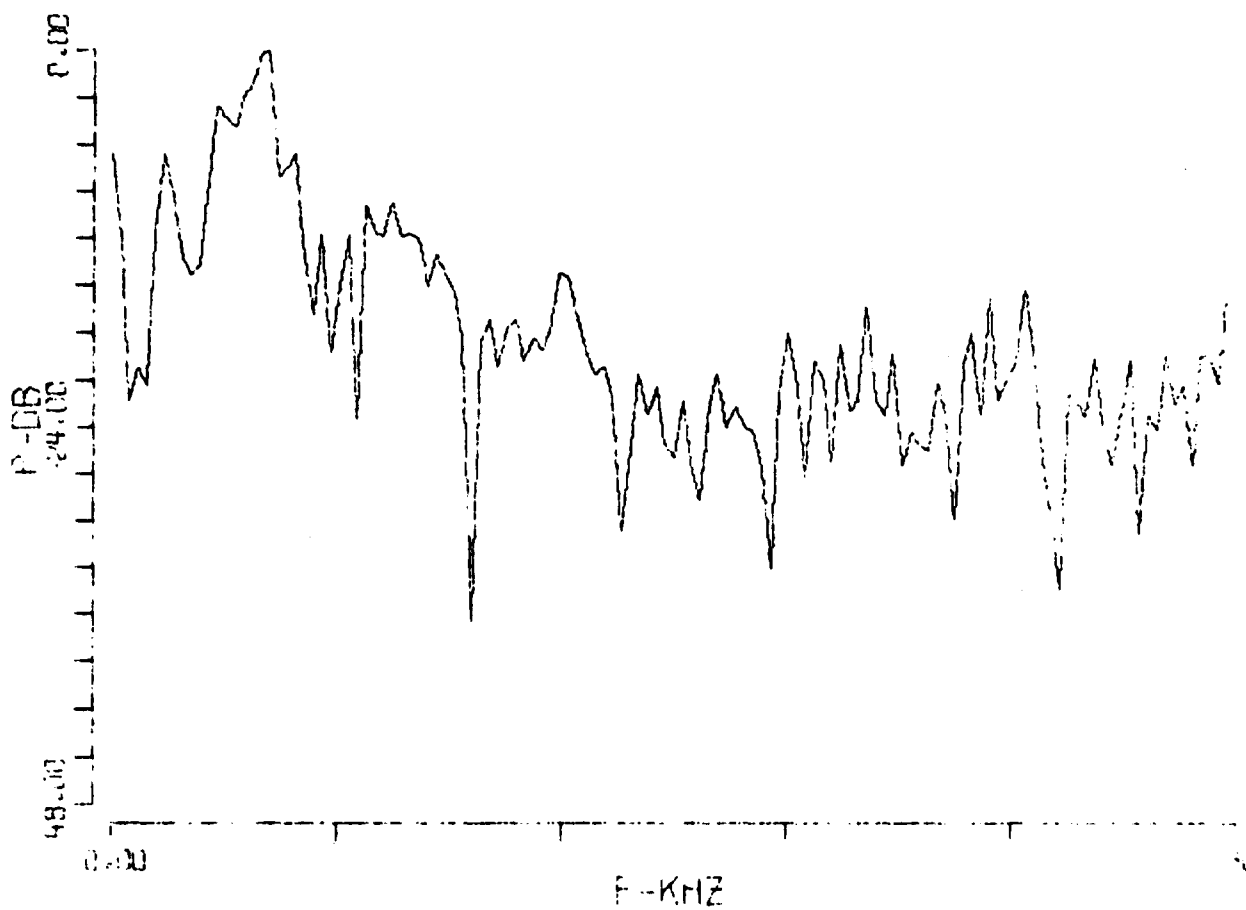
M6-10-300

133<



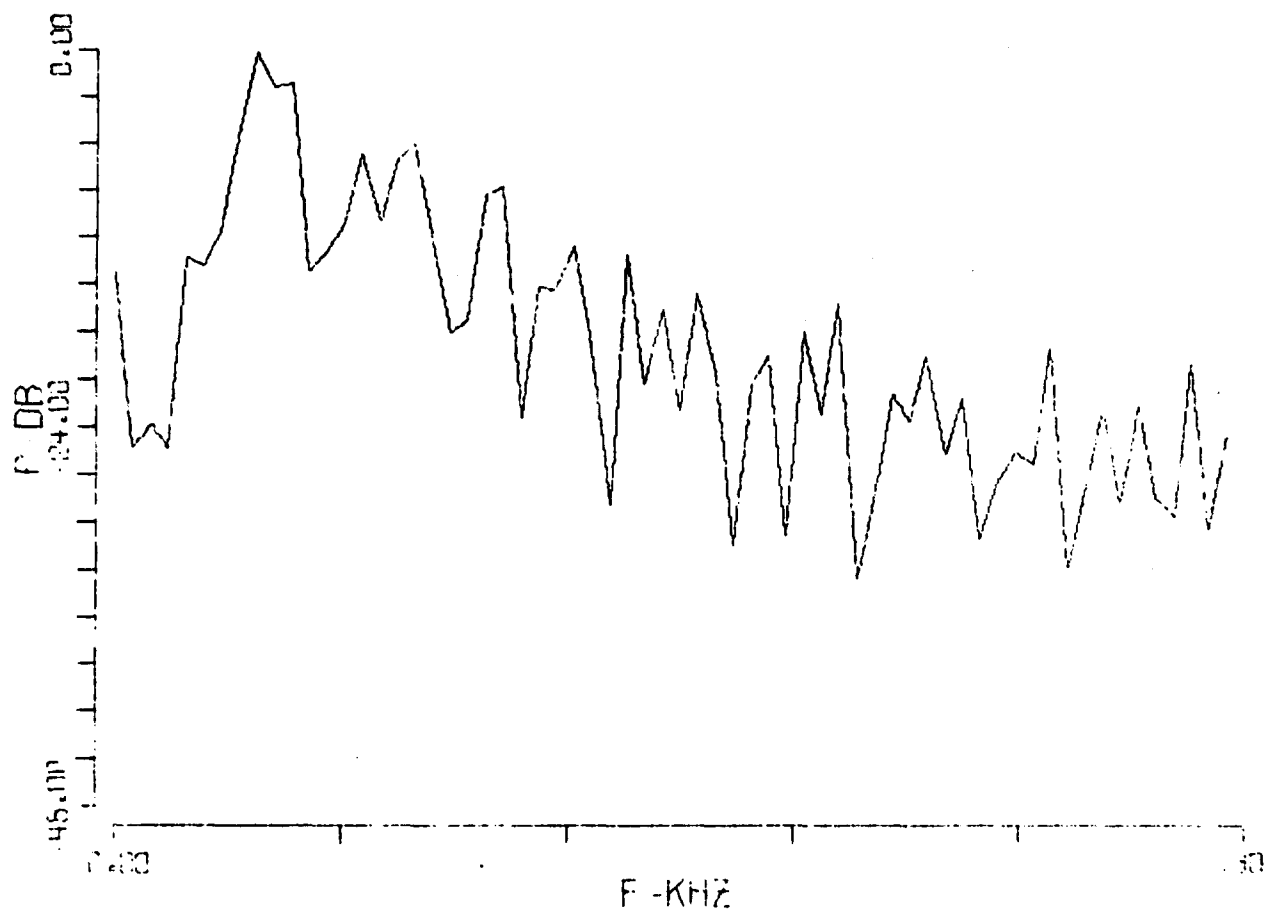
M6-10-800

140<



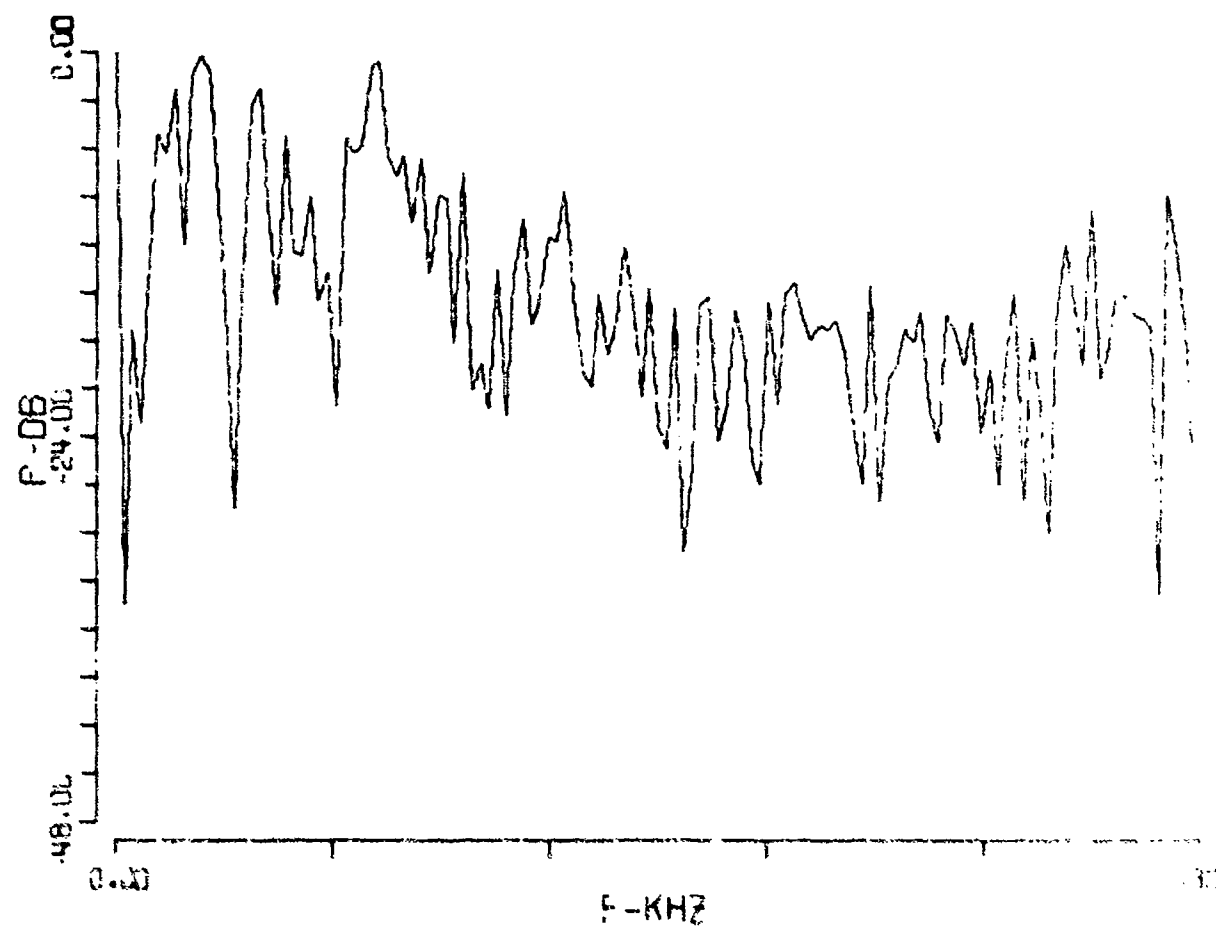
M6-20-300

141<



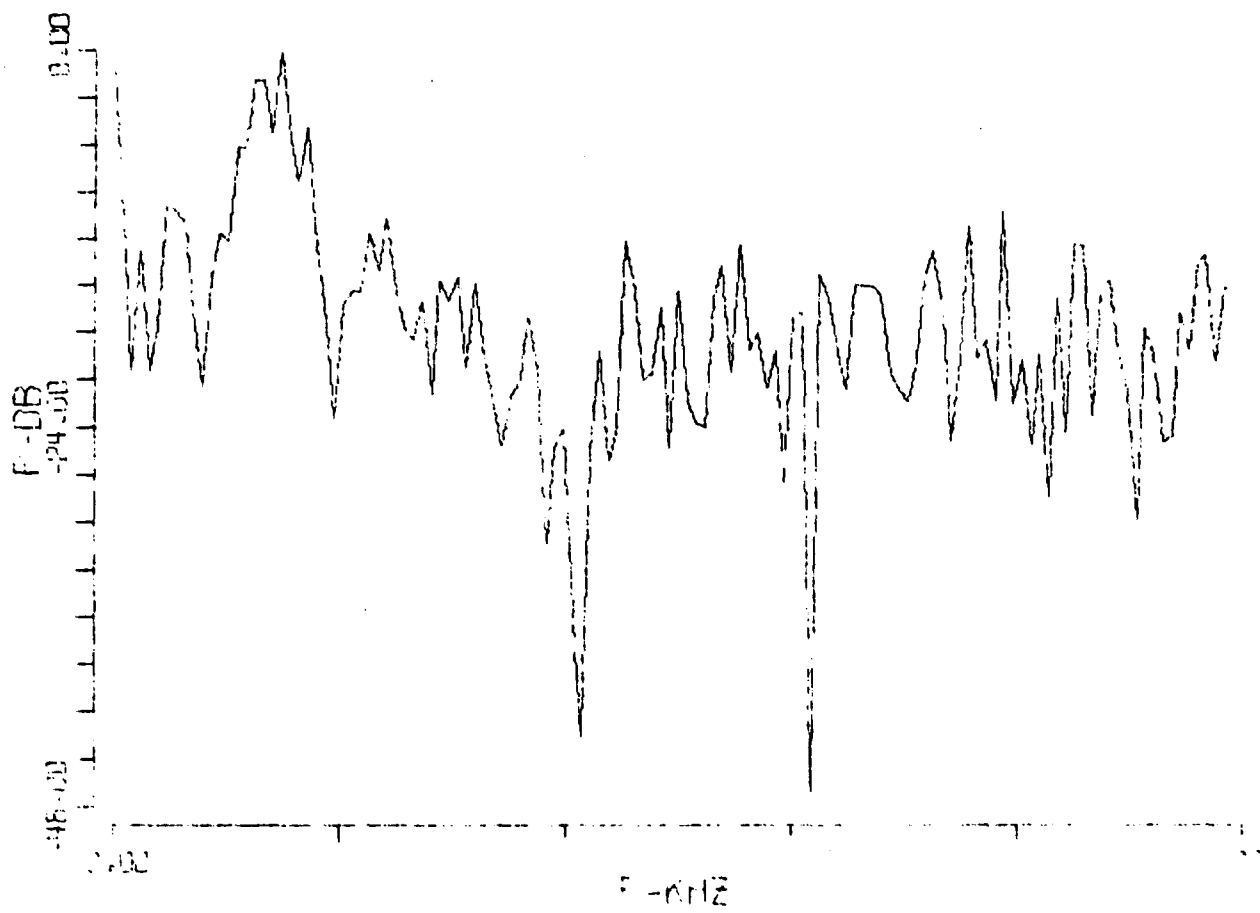
M6-20-800

142<



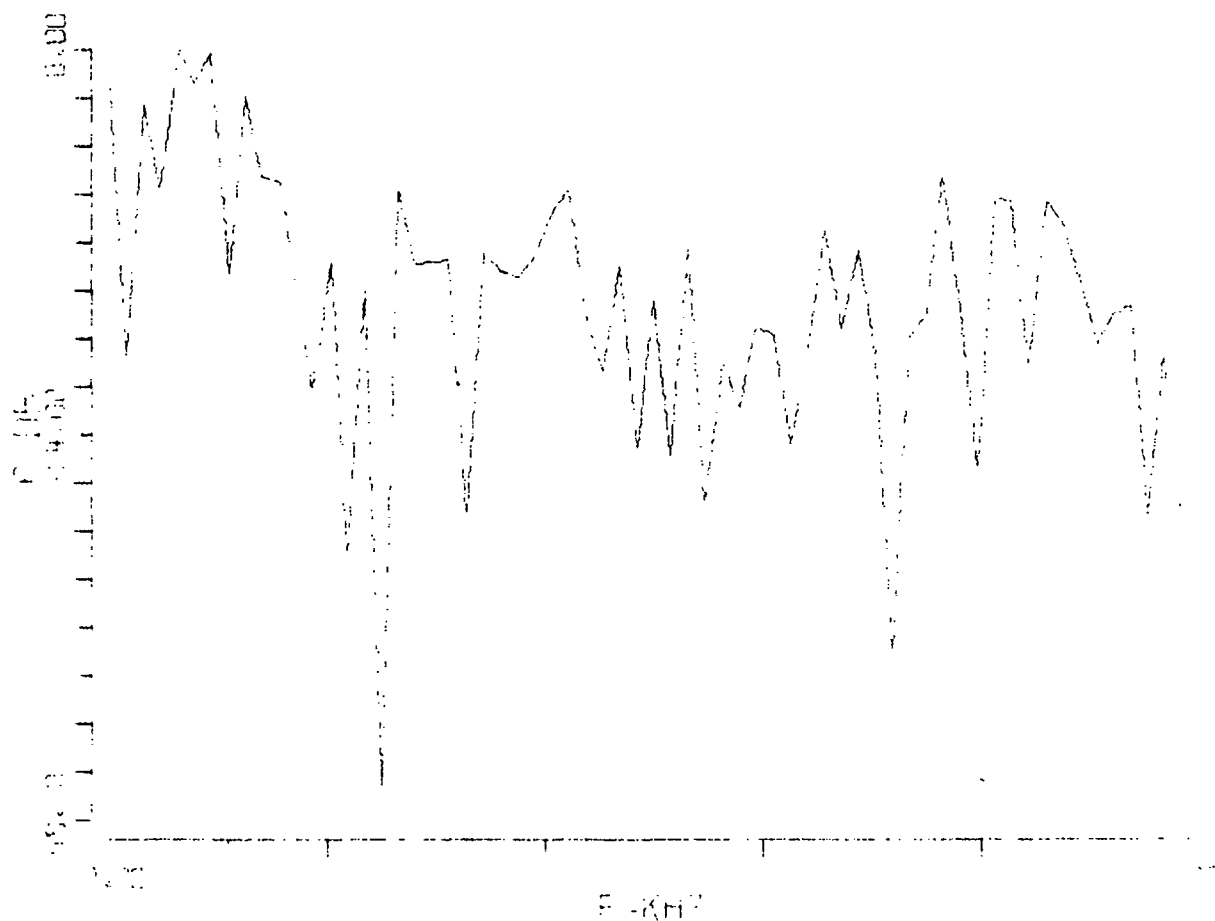
M6-50-300

145-



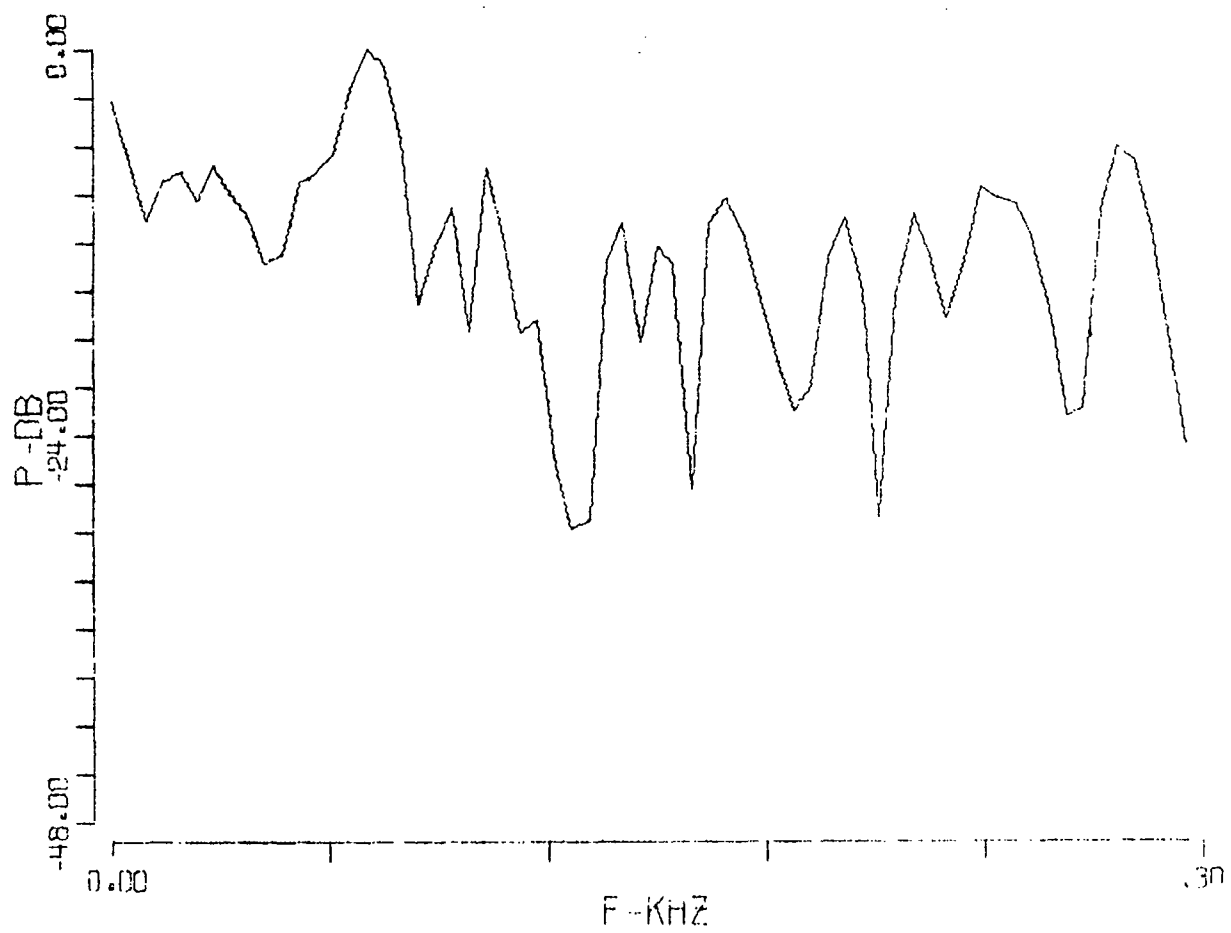
M6-50-800

144<



M6-100-300

145<



M6-100-800

146<



DEPARTMENT OF THE NAVY

OFFICE OF NAVAL RESEARCH
875 NORTH RANDOLPH STREET
SUITE 1425
ARLINGTON VA 22203-1995

IN REPLY REFER TO:

5510/1
Ser 321OA/011/06
31 Jan 06

MEMORANDUM FOR DISTRIBUTION LIST

Subj: DECLASSIFICATION OF LONG RANGE ACOUSTIC PROPAGATION PROJECT (LRAPP) DOCUMENTS

Ref: (a) SECNAVINST 5510.36

Encl: (1) List of DECLASSIFIED LRAPP Documents

1. In accordance with reference (a), a declassification review has been conducted on a number of classified LRAPP documents.
2. The LRAPP documents listed in enclosure (1) have been downgraded to UNCLASSIFIED and have been approved for public release. These documents should be remarked as follows:

Classification changed to UNCLASSIFIED by authority of the Chief of Naval Operations (N772) letter N772A/6U875630, 20 January 2006.

DISTRIBUTION STATEMENT A: Approved for Public Release; Distribution is unlimited.

3. Questions may be directed to the undersigned on (703) 696-4619, DSN 426-4619.

A handwritten signature in black ink, appearing to read "B. F. Link", is positioned above the typed name.

BRIAN LINK
By direction

Subj: DECLASSIFICATION OF LONG RANGE ACOUSTIC PROPAGATION PROJECT
(LRAPP) DOCUMENTS

DISTRIBUTION LIST:

NAVOCEANO (Code N121LC – Jaime Ratliff)
NRL Washington (Code 5596.3 – Mary Templeman)
PEO LMW Det San Diego (PMS 181)
DTIC-OCQ (Larry Downing)
ARL, U of Texas
Blue Sea Corporation (Dr. Roy Gaul)
ONR 32B (CAPT Paul Stewart)
ONR 321OA (Dr. Ellen Livingston)
APL, U of Washington
APL, Johns Hopkins University
ARL, Penn State University
MPL of Scripps Institution of Oceanography
WHOI
NAVSEA
NAVAIR
NUWC
SAIC

Declassified LRAPP Documents

Report Number	Personal Author	Title	Publication Source (Originator)	Pub. Date	Current Availability	Class.
Unavailable	Beam, J. P., et al.	LONG-RANGE ACOUSTIC PROPAGATION LOSS MEASUREMENTS OF PROJECT TRANSLANT I IN THE ATLANTIC OCEAN EAST OF BERMUDA	Naval Underwater Systems Center	740612	ADC001521	U
Unavailable	Cornyn, J. J., et al.	AMBIENT-NOISE PREDICTION. VOLUME 2. MODEL EVALUATION WITH IOMEDEX DATA	Naval Research Laboratory	740701	AD0530983	U
Unavailable	Unavailable	COHERENCE OF HARMONICALLY RELATED CW SIGNALS	Naval Underwater Systems Center	740722	ADB181912	U
Unavailable	Banchero, L. A., et al.	IOMEDEX SOUND VELOCITY ANALYSIS AND ENVIRONMENTAL DATA SUMMARY	Naval Oceanographic Office	740801	ADC000419	U
3810	Unavailable	CONSTRUCTION AND CALIBRATION OF USRD TYPE F58 VIBROSEIS MONITORING HYDROPHONES SERIALS 1 THROUGH 7	Naval Research Laboratory	741002	ND	U
ARL-TM-73-11; ARL-TM-73-12	Ellis, G. E., et al.	ARL PRELIMINARY DATA ANALYSIS FROM ACODAC SYSTEM; ANALYSIS OF THE BLAKE TEST ACODAC DATA	University of Texas, Applied Research Laboratories	741015	ADA001738; ND	U
Unavailable	Mitchell, S. K., et al.	QUALITY CONTROL ANALYSIS OF SUS PROCESSING FROM ACODAC DATA	University of Texas, Applied Research Laboratories	741015	ADB000283	U
Unavailable	Unavailable	MEDEX PROCESSING SYSTEM. VOLUME II. SOFTWARE	Bunker-Ramo Corp. Electronic Systems Division	741021	ADB000363	U
Unavailable	Spofford, C. W.	FACT MODEL. VOLUME I	Maury Center for Ocean Science	741101	ADA078581	U
Unavailable	Bucca, P. J., et al.	SOUND VELOCITY STRUCTURE OF THE LABRADOR SEA, IRMINGER SEA, AND BAFFIN BAY DURING THE NORLANT-72 EXERCISE	Naval Oceanographic Office	741101	ADC000461	U
Unavailable	Anderson, V. C.	VERTICAL DIRECTIONALITY OF NOISE AND SIGNAL TRANSMISSIONS DURING OPERATION CHURCH ANCHOR	Scripps Institution of Oceanography Marine Physical Laboratory	741115	ADA011110	U
Unavailable	Baker, C. L., et al.	FACT MODEL. VOLUME II	Office of Naval Research	741201	ADA078539	U
ARL-TR-74-53	Anderson, A. L.	CHURCH ANCHOR EXPLOSIVE SOURCE (SUS) PROPAGATION MEASUREMENTS (U)	University of Texas, Applied Research Laboratories	741201	ADC002497; ND	U
MCR106	Cherkis, N. Z., et al.	THE NEAT 2 EXPERIMENT VOL 1 (U)	Maury Center for Ocean Science	741201	NS; ND	U
MCR107	Cherkis, N. Z., et al.	THE NEAT 2 EXPERIMENT VOL 2 - APPENDICES (U)	Maury Center for Ocean Science	741201	NS; ND	U
Unavailable	Mahler, J., et al.	INTERIM SHIPPING DISTRIBUTION	Tetra, Tech, BB&N, & PSI	741217	ND	U
75-9M7-VERAY-R1	Jones, C. H.	LRAPP VERTICAL ARRAY - PHASE IV	Westinghouse Electric Corp.	750113	ADA008427; ND	U
AESD-TN-75-01	Spofford, C. W.	ACOUSTIC AREA ASSESSMENT	Office of Naval Research	750201	ADA090109; ND	U